FEMTOSECOND RESOLUTION BUNCH ARRIVAL TIME MONITOR

F. Loehl[#*], Cornell University, Ithaca, New York, USA

Abstract

A need for femtosecond resolution beam arrival time measurements has arisen with the transition from many-picosecond-long bunches in ring-based accelerators to a few femtosecond-long bunches in high-gain free-electron lasers. Here we present an electro-optical detection scheme that uses the signal of a beam pick-up to modulate the intensity of a femtosecond laser pulse train. By detecting the energies of the laser pulses, the bunch arrival time can be deduced. We tested this scheme by distributing a laser pulse train to two locations in the FLASH linac, separated by 60 m, using length-stabilized optical fibers. By measuring the arrival times of the same electron bunches at these two locations, we determined an rms bunch arrival time resolution of 6 fs. This unprecedented monitor resolution allowed us to reduce the beam arrival time jitter from almost 200 fs down to 25 fs with an intra-bunch train feedback. In combination with a beam pick-up with a position dependent time-response, the same electro-optical detection scheme can be applied for micrometer resolution beam position measurements.

INTRODUCTION

High-gain free-electron lasers (FELs) operating in the soft and hard x-ray regimes are capable of generating light pulses with durations below 10 fs [1,2]. Even shorter light pulse durations are envisioned using schemes in which a part of the electron bunch is manipulated using a few cycle laser pulse (see, e.g., [3,4]).

In order to take full advantage of the sub-10-fs light pulses presently available (e.g., in two-color pump-probe experiments), precise measurements and eventually control of the electron bunch arrival time are required. The desired measurement resolution is on the same order as the photon pulse duration–ideally, a small fraction of it. The abovementioned manipulation schemes as well as FEL seeding schemes require a stable longitudinal overlap between the electron bunch and the laser pulse. Many of these schemes require a timing stability between the laser pulses and the electron bunches of around 30 fs or better.

In this work we present electro-optical synchronization schemes which allow for a bunch arrival-time measurement and stabilization with the before-mentioned resolution.

OPTICAL SYNCHRONIZATION SYSTEM

In collaboration with F.X. Kaertner's group at MIT, we developed an optical synchronization system to address the stringent timing requirements of FELs. Figure 1 depicts the schematic principle of the system. A mode-locked laser – the master laser oscillator (MLO) – is used as a time-reference. Its laser pulse train is distributed to the remote locations via length-stabilized optical fibers, where the respective subsystems are synchronized to the time-markers provided by the laser. These subsystems can, for example, be laser systems, which can be synchronized by optical cross-correlation techniques [5,6]; RF systems (for schemes on how to extract stable RF signals from the optical pulse train, see, e.g., [7,8]); or beam diagnostics systems such as the bunch arrival-time monitor discussed in this paper.

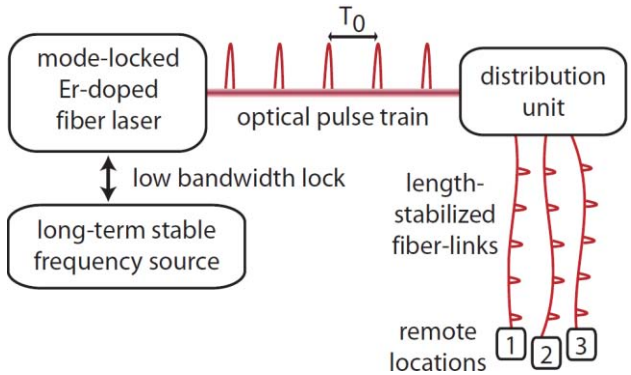

Figure 1: Schematic principle of the optical synchronization system [11].

Master Laser Oscillator

We used an erbium fiber laser operating in the soliton regime as the MLO [9,11]. It produces a train of sub-100 fs long laser pulses and operates at a repetition rate of 216.7 MHz, which is the sixth sub-harmonic of the 1.3 GHz frequency of the superconducting TESLA-type cavities used at FLASH. In order to compensate for length changes of the laser resonator due to thermal expansion or contraction, as well as due to microphonics, the laser repetition frequency is locked to a long-term stable RF oscillator. The phase lock loop (PLL) stabilizes the laser repetition rate up to frequencies of several kHz using a digital feedback loop acting on a fast piezo-mirror inside of the laser resonator. Laser timing changes occurring at frequencies larger than a few kHz are very small–significantly less than 10 fs [11]–and therefore do not need active correction. When all critical timing signals are derived from the MLO, slow timing changes below a few kHz are not critical for most applications, since most subsystems are able to follow these timing changes at a sufficiently high rate. The accuracy of the PLL is therefore not of highest importance. In our case, the timing jitter between the laser and the RF source was around 40 fs. The long-term frequency stability of the RF source is, however, of great importance when fiber links of different lengths are used. The reason is that the electron beam travel time between two locations in the

previously at DESY, Hamburg, Germany
* florian.loehl@cornell.edu

BEAM ARRIVAL-TIME AND POSITION MEASUREMENTS USING ELECTRO-OPTICAL SAMPLING OF PICKUP SIGNALS

K. Hacker,* DESY, Hamburg, Germany

Abstract

By using magnetic chicane bunch compressors, high-gain free-electron lasers are capable of generating femtosecond electron bunches with peak currents in the kilo-ampere range. For accurate control of the longitudinal dynamics during this compression process, high-precision beam energy and arrival-time monitors are required. Here we present an electro-optical detection scheme that uses the signal of a beam pickup to modulate the intensity of a femtosecond laser pulse train. By detecting the energies of the laser pulses, the arrival-time of the pickup signal can be deduced. Depending on the choice of the beam pickup, this technique allows for high-resolution beam position measurements inside of magnetic chicanes and/or for femtosecond-resolution bunch arrival-time measurements. In first prototypes we realized a beam position monitor with a resolution of 3 μm (rms) over a many-centimeter dynamic range and a bunch arrival-time monitor with a resolution of 6 fs (rms) relative to a pulsed optical reference signal.

INTRODUCTION

A beam arrival-time stability of ~30 fs rms (~10 μm at v=c) is desired for pump-probe experiments and is mandatory for laser-based electron beam manipulation at FLASH and the European XFEL [1]. Arrival-time jitter in these FELs is primarily created by energy-dependent path-length changes in the magnetic bunch compressor chicanes. The first bunch compressor of the FLASH linac is shown below in Fig. 1 with the orbit for an R_{16} = 350 mm and R_{56} = 620 ps plotted in green. The locations of beam pickups used for measuring the beam arrival-time and position are indicated with yellow stars.

With the accelerating RF gradient stability of 10^{-4} at FLASH, the transverse position jitter in the dispersive section of the first chicane becomes 35 μm and the longitudinal position jitter becomes 18 μm. A beam-based monitor for an RF gradient feedback system should be able to measure the beam energy by a factor of three better than the desired energy stability of $5*10^{-5}$ and this means that the resolution for a beam position measurement in the chicane must be better than 6 μm and a longitudinal time-of-flight path-length measurement should resolve 3 μm. Each measurement must have a many-centimeter range in order to accommodate different machine configurations.

Devices meeting these requirements were made possible through a technique that involves sampling the zero-crossings of electrical beam pickup signals with short laser pulses. The 20-200 fs pulses from a mode-locked erbium-doped fiber laser are sent over actively length-stabilized fiber links to distant end-stations, whereupon the amplitudes of the laser pulses are modulated by the amplitudes of the beam pickup signals with a commercially available electro-optical modulator. The modulated laser pulses then impinge upon a photodetector, and the amplitude of the photo-detector signal is recorded with an ADC, which is clocked with a signal generated from the very same laser pulse train. These sorts of measurements are vital for the pulsed optical synchronization system at FLASH and the beam-based energy and timing feedbacks upon which it relies.

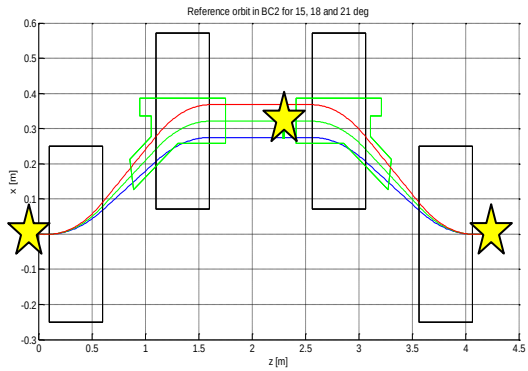

Figure 1: First magnetic bunch compressor chicane at FLASH. Dipoles are drawn in black, the vacuum chamber is drawn in green, and the locations of pickups for beam arrival-time and position measurements are indicated by yellow stars. Higher- and lower-energy particle beams travel a longer or shorter path-length through the chicane, affecting the beam arrival time after the chicane.

This technique has been verified with two types of pickups. Using two sets of broadband, button-like pickups separated by 60 m in a drift section, two independent measurements of the beam arrival-time were conducted, verifying the 6 fs (rms) resolution of the method [2,3]. In another experiment, involving a transversely mounted stripline pickup in the dispersive section of the chicane [4,5], 3 μm (rms) beam position resolution over a 10 cm range was achieved and cross-checked against a synchrotron light-based BPM [6,7]. The arrival-time measurements conducted with this stripline pickup were also cross-checked with a beam arrival-time measurement conducted upstream of the chicane with button-like pickups [7]. A description of how these measurements are locked to an RF reference follows [7].

* kirsten.hacker@desy.de

A WINNING TRADITION: THE FARADAY CUP AWARD

Michelle Wilinski, Brookhaven National Laboratory, Upton, NY 11973, U.S.A.

The Faraday Cup Award is given for an outstanding contribution to the development of an innovative particle beam diagnostic instrument of proven workability. "Like a 'Nobel Prize' for the beam instrumentation community," is how the 2000 winner, Kay Wittenburg of DESY, describes the Faraday Cup Award. It is presented at the Beam Instrumentation Workshop (BIW), a biennial forum for in-depth discussions of techniques for measuring particle beams produced in accelerators. The Faraday Cup winner receives a US $5,000 cash prize, $1,000 for BIW travel expenses, and a certificate of award. An acceptance speech is given at the workshop by the Awardee in the form of a talk on the design and performance of the winning instrument.

Like many other awards, the Faraday Cup Award comes with a storied tradition. The first Beam Instrumentation Workshop was organized by Richard Witkover and held at Brookhaven National Laboratory in 1989 to stimulate interaction among those in the instrumentation field. The idea for an award was conceived during round-table discussions the last day of that meeting as a way to encourage innovation among young engineers and physicists. Agreement on policies for keeping the award fair and non-commercial was reached in 1991 based on nomination and selection procedures written primarily by Bob Shafer. Naming of the award is attributed to Bob Webber. Financial sponsorship of the Faraday Cup Award is donated by Bergoz Instrumentation.

The BIW Program Committee is solely responsible for selecting the Award recipient. The Committee accepts nominations for the award approximately 12 to 18 months in advance of each BIW. Self-nomination is permitted. The award is open to candidates of any nationality for work done at any geographical location. Instrument performance must be proven using a primary charged particle beam; mere concepts or "bench-top" demonstrations are not acceptable. A description of the device, its operation and performance must be published in a journal or conference proceedings that is in the public domain. In the event of deciding between works of similar quality, preference is given to candidates in the early stages of their beam instrumentation career. The award may be shared between persons contributing to the same accomplishment. Complete rules are available at http://www.faraday-cup.com.

Since the first Faraday Cup Award in 1992, fifteen people from laboratories around the world have received the Award (see Table 1) and have gone on to continued career success. Although each prize award is a one-time event, the rewards from the prize have continued for the winners.

Table 1: Faraday Cup Award Winners

	Winner	Diagnostics
1992	Alexander V. Feschenko, INR	"Longitudinal Bunch Shape Measurement "sing Wire Probe Secondary Emission"
1993	Donald W. Rule & Ralph B. Fiorito, NSWC	"Techniques for Measuring Bunch Shapes by OTR"
1994	Edward Rossa, CERN	"Technique for Measuring the 3-D Bunch Shapes"
1996	Walter Barry, LBL and Hung-chi Lihn, SLAC	"Sub-ps e^- Bunch Shape Measurement Techniques"
1998	Andreas Peters, GSI	"Cryogenic Current Comparator"
2000	Kay Wittenburg, DESY	"Beam Loss Monitor Using PIN Diodes"
2002	Andreas Jansson, CERN	"Quadrupole Beam Pickup"
2004	Toshiyuki Mitsuhashi, KEK	"Interferometric Profile Monitor Using Synchrotron Radiation"
2006	Haixin Huang, BNL, and Kazuyoshi Kurita, Rikkyo Univ.	"Innovative Proton Beam Polarization Monitoring System"
2008	Suren Arutunian, YerPhI	"Vibrating Wire Sensor for Beam Instrumentation"
2010	Florian Loehl, CLASSE, & Kirsten E. Hacker, DESY	"Femtosecond Resolution Beam Arrival Time Monitor"

PhD students can have breakout results and winning instruments have emerged from their thesis work. In 1996, Walter Barry of Lawrence Berkeley National Laboratory and Hung-chi Lihn of the Stanford Linear Accelerator Center shared the Faraday Cup Award for development of techniques to measure the bunch shape of subpicosecond electron beams. Lihn, a PhD student at the time, sees the award as a great recognition, by experts in the field, of his years of work and ideas. Now in industry, Lihn still calls upon the skills that he developed building his winning instrument. While he did not personally continue with further development of the device, Lihn's thesis and paper

ACCERATORS AT LOS ALAMOS TODAY

W. Scott Gibbs
Los Alamos National Laboratory, Los Alamos, NM, U.S.A.

Abstract

This keynote address provides a ten minute survey by LANL's Associate Director for Engineering and Engineering Science.

*

LOOKING BEYOND LANSCE: THE MARIE FACILITY

Kevin Jones
Los Alamos National Laboratory, Los Alamos, NM, U.S.A.

Abstract

This keynote address provides a 15-minute look at the future beyond LANSCE by the Los Alamos director of Accelerator Operations and Technology.

*

COMMISSIONING AND FIRST PERFORMANCE OF THE LHC BEAM INSTRUMENTATION

R. Jones, CERN, Geneva, Switzerland.

Abstract

This paper will outline the progress with LHC commissioning to date, detailing the performance achieved with all the main LHC beam instrumentation systems. It will include an overview of the beam loss system and its role in machine protection, along with that of the beam position system and its use for automatic orbit control. Results will be shown from the highly sensitive base band tune system as well as the bunch-by-bunch and DC beam current transformer systems, the synchrotron light monitoring systems, the wire scanner system and OTR screens.

INTRODUCTION

The first beams circulated in the LHC on 10th September 2008 in full view of the world's media. This was a resounding success, and was followed a few days later with RF captured beams circulating for several hours. Nine days on, a poor superconducting splice overheated during a hardware test at high current, creating an arc that pierced the helium containment vessel, with severe consequences. 14 months later, after a major magnet repair and consolidation programme, the LHC was once again cold and ready to take beam. Despite these efforts and the installation of a completely new Quench Protection System (QPS) its energy is currently limited to 3.5 TeV per beam. Further consolidation, requiring a long shutdown in 2012, will be necessary before it can run at its design energy of 7 TeV per beam.

A one month run at the end of 2009 saw the LHC quickly advance with optics, collimation and working point studies at its 450 GeV injection energy. Ramp commissioning to 1.18 TeV followed, ending in collisions at 1.18 TeV per beam in all of its four main experiments.

Further consolidation work was carried out on both the machine and experiments for the first two months of 2010, before the start of a 2 year run at the end of February. To date (late April 2010) the LHC is routinely ramping 2×10^{10} protons to 3.5 TeV and colliding with a β^* of 2 m in all four experiments. The emphasis now is on increasing the total intensity in the machine.

This rapid progress with beam commissioning is in a large part down to the very good beam instrumentation with which the LHC is equipped. These systems and their contributions to this commissioning effort will be the subject of the remainder of this paper.

THE LHC BTV SYSTEM

There are a total of 37 TV beam observation systems (BTV) of 7 different types installed in the LHC. Each BTV station is equipped with two screens; one a 1 mm thick alumina plate (scintillator) and the second a 12 µm thick titanium foil (to produce Optical Transition Radiation or OTR). The alumina plates are very sensitive and can observe single bunches of well below 10^9 particles, but due to their thickness significantly perturb the beam. The number of photons emitted by the OTR is much less than that of the alumina screen; on the other hand the perturbation to the beam is minimal, allowing multiple monitors to be used at the same time, as well as multi-turn observation.

First Results from the LHC BTV System

During initial commissioning the beam was steered through the transfer lines and the different sections of the machine using the alumina screens, most of the time producing very clear but completely saturated images (see Figure 1).

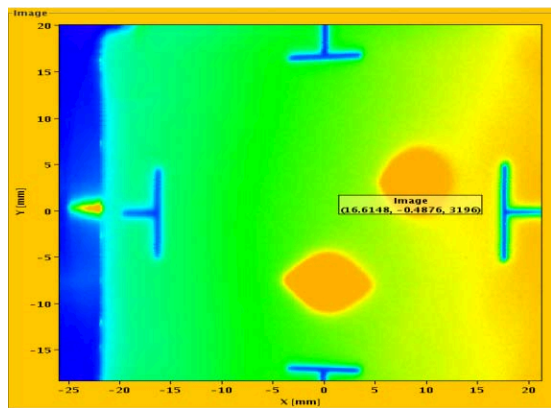

Figure 1 : The first full turn in the LHC as seen by the BTV system (10/9/2008).

After this first step the OTR screens replaced the alumina screens to reduce the blow-up of the beam, reduce the radiation due to beam losses, and produce images well suited for analysis with good linearity and no saturation. There was a possibility of observing OTR emission for even the lowest intensity pilot bunches (2×10^9 protons) due to the high sensitivity of the standard CCD cameras.

All the BTV monitors have performed very well and were extensively used during the synchronization tests and for the first beams in the LHC. The large 1 m diameter alumina screen in the dump line is still continually used to verify the correct functioning of the beam dump system (see Figure 2).

Due to the expected radiation levels in the injection regions, a gradual replacement of the standard CCD cameras with less-sensitive, radiation-hard cameras is foreseen. This will result in the loss of ability to observe pilot bunches in OTR mode.

THE SNS BEAM DIAGNOSTICS EXPERIENCE AND LESSONS LEARNED

A. Aleksandrov
Oak Ridge National Laboratory, Oak Ridge, TN 37830 USA

Abstract

The Spallation Neutron Source accelerator systems are designed to deliver a 1.0 GeV, 1.4 MW proton beam to a liquid mercury target for neutron scattering research. The accelerator complex consists of an H- injector, capable of producing one-ms-long pulses at 60 Hz repetition rate with 38 mA peak current; a 1 GeV linear accelerator; an accumulator ring; and associated transport lines. The accelerator systems are equipped with a variety of beam diagnostics, which played an important role during beam commissioning. They are used for accelerator tuning and monitoring beam status during production runs. This paper gives an overview of our experience with the major SNS beam diagnostics systems.

INTRODUCTION

The SNS accelerator complex consists of an H^- injector, capable of producing one-ms-long pulses with 38 mA peak current, chopped with a 68% beam-on duty factor and a repetition rate of 60 Hz to produce 1.6 mA average current; an 87 MeV Drift Tube Linac (DTL); a 186 MeV Coupled Cavity Linac (CCL); a 1 GeV Super Conducting Linac (SCL); a 1 GeV Accumulator Ring (AR); and associated transport lines. After completion of the initial beam commissioning at a power level below nominal, the SNS accelerator complex is gradually increasing the operating power with the goal of achieving the design parameters in 2011. Results of the initial commissioning and operation experience can be found in [1]. The SNS Power Upgrade Project (PUP) [2] aims at doubling the beam power by 2016. This will be achieved by increasing the SCL and AR beam energy to 1.3 GeV and the peak current in the linac to 59 mA.

The SNS baseline design included a diverse set of beam diagnostics [3], which, for the most part, were brought on line simultaneously with other accelerator systems and which played an important role in the successful SNS commissioning and power ramp-up. As the SNS operation is shifting more and more toward neutron production for users, the roles and requirements for the beam diagnostics are changing as well. This paper describes the status and development plans for the major beam instrumentation systems.

BASELINE SET OF THE SNS BEAM DIAGNOSTICS

The original set of SNS diagnostics included beam current transformers (BCMs); beam position and phase monitors (BPMs); ionization chambers and photomultiplier tubes (BLMs); wire scanners (WS); slit-and-harp emittance scanners; phosphor view screens (VS); and Faraday cups. All of these devices were operational during the initial beam commissioning and their performance characteristics were sufficient for all of the commissioning tasks.

Beam Current Monitors

There are 23 fast beam current transformers in the SNS linac, ring, and transfer lines. They were useful during the initial commissioning until good beam transmission was established. The accuracy of the BCMs, on the order of 5%, is not sufficient for detecting a typical beam loss of .01%. Several of the BCMs are still in use for beam accounting and for protection purposes in the injector, in front of the beam dumps, and in front of the target. A typical result of the BCM measurements is shown in Figure 1.

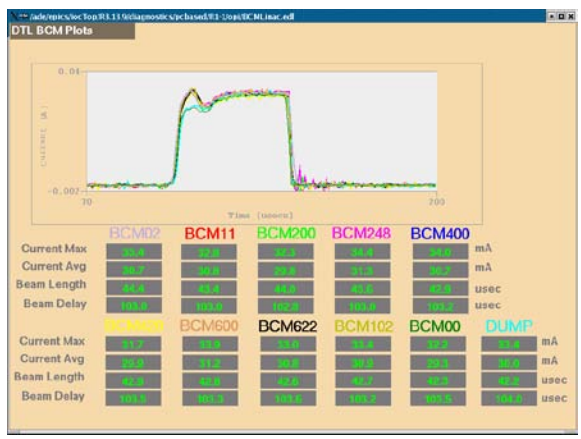

Figure 1. A beam pulse transmission from the injector to the linac beam dump measured by linac Beam Current Monitors.

Beam Loss Monitors

The SNS BLM system consists of 362 detectors measuring the secondary radiation due to beam loss. The BLMs are used as sensors in the machine protection system for shutting off the beam if the integral loss is above a certain threshold. The ionization chamber (IC) is the main detector type in the BLM system due to its simple design and immunity to radiation damage. In addition to the ICs we use several types of photo-multiplier tube based detectors (PMTs). The BLM system has worked quite reliably and typically cause less than ten hours of beam down-time per year. We encountered a few problems with the BLM system during the beam commissioning. The biggest one was significant background from the X-ray radiation produced by the RF

OPERATIONAL PERFORMANCE OF LCLS BEAM INSTRUMENTATION*

H. Loos†, R. Akre, A. Brachmann, R. Coffee, F.-J. Decker, Y. Ding, D. Dowell, S. Edstrom, P. Emma, A. Fisher, J. Frisch, S. Gilevich, G. Hays, Ph. Hering, Z. Huang, R. Iverson, M. Messerschmidt, A. Miahnahri, S. Moeller, H.-D. Nuhn, D. Ratner, J. Rzepiela, T. Smith, P. Stefan, H. Tompkins, J. Turner, J. Welch, W. White, J. Wu, G. Yocky, SLAC, Menlo Park, CA 94025, USA, R. Bionta, LLNL, Livermore, CA 94550, USA

Abstract

The Linac Coherent Light Source (LCLS) X-ray FEL utilizing the last km of the SLAC linac has been operational since April 2009 and finished its first successful user run last December. The various diagnostics for electron beam properties including beam position monitors, wire scanners, beam profile monitors, and bunch length diagnostics are presented as well as diagnostics for the x-ray beam. The low emittance and ultra-short electron beam required for X-ray FEL operation has implications on the transverse and longitudinal diagnostics. The coherence effects of the beam profile monitors and the challenges of measuring fs long bunches are discussed.

INTRODUCTION

The LCLS facility at the SLAC National Accelerator Laboratory [1] is the first free electron laser operating at Ångstrom wavelengths. Since 2006 the last 1 km of the SLAC linac has been upgraded to serve as the electron beam source for the FEL and new construction has been added to house the undulator and the X-ray facilities. The first x-ray operation was achieved in April 2009 [2] and a subsequent user run utilized the soft X-ray beam. After commissioning of the hard X-ray beam transport the second user run later in 2010 will take advantage of the full LCLS capabilities.

Table 1: LCLS accelerator and FEL parameters

	Design	Meas.	Unit
Repetition rate	120	30	Hz
Final energy	13.6	13.6	GeV
Charge	1	0.25	nC
Bunch length	20	8-10	μm
Peak current	3	3	kA
Emittance (injector)	1.2	0.5-1.2	μm
Slice emittance (inj.)	1.2	0.4	μm
Emittance (linac end)	1.5	0.5-1.2	μm
X-ray wavelength	1.5	1.5	Å
X-ray pulse energy	1.5	1.5-3.0	mJ
Photons per pulse	2.0	1.0-2.3	10^{12}

The ultra-high brightness electron beam necessary for the operation of an X-ray FEL requires the accurate measurement of a sub-μm emittance and sub 10 μm long electron beam in both transverse and longitudinal coordinates with state of the art diagnostics. The layout of the LCLS is depicted in Fig. 1 with the location of some of the diagnostics devices indicated. The 250 pC electron beam is generated in a laser-driven photocathode RF gun at 6 MeV and subsequently accelerated in four linac sections (L0-L3) to energies of 135 MeV, 250 MeV, 4.3 GeV, and the final energy of 13.6 GeV. After L1 and L2 the bunches are compressed in two chicanes from 750 μm to 40 μm and 10 μm. The beam is then transported through a dog-leg bend magnet system to the 100 m long undulator consisting of 33 segments and dumped in the main beam dump, whereas the generated X-ray beam enters the X-ray diagnostics, transport, and the various experimental areas (not shown). The main parameters of the electron and X-ray beam are listed in Table 1. The design parameters refer to the high charge mode at 1 nC, whereas the measured ones are given for the medium charge operating mode at 250 nC. Recently, a low charge mode with only 20 pC has been explored [3]. The beam in this mode has a slice emittance of 0.14 μm and can be compressed to an estimated final rms bunch length of about 1 μm giving the same peak current and FEL peak power, but a much shorter X-ray pulse.

Table 2: LCLS Accelerator diagnostics devices

Type	#	Nom. res.	Units
Strip Line BPM	144	5	μm
RF cavity BPM	36	1	μm
Beam current monitor	13	2	%
Phase cavity	5	100	fs
Faraday cup	2	2	%
Wire scanner	17	20	μm
YAG screen	7	15	μm
OTR screen	13	10	μm
Bunch length monitor	2	5	%
Deflecting cavity	2		

A list of all the beam diagnostics devices is given in Table 2 together with their respective highest resolution requirements for each device. In the following sections, the design and operational performance of the various diagnostics for transverse and longitudinal beam parameters, as well as some of the X-ray diagnostics will be discussed.

* Work supported by US DOE contract DE-AC02-76SF00515.
† loos@slac.stanford.edu

MEASUREMENT OF LATTICE PARAMETERS WITHOUT VISIBLE DISTURBANCE TO USER BEAM AT DIAMOND LIGHT SOURCE

G. Rehm, M.G. Abbott, A.F.D. Morgan, J. Rowland, I. Uzun
Diamond Light Source, Oxfordshire, United Kingdom

Abstract

With refined lattice tuning it becomes increasingly important to monitor or feedback on many parameters to keep stable optimum operating conditions. To this end we present techniques to measure betatron tune, chromaticity, betafunction magnitude/phase, and orbit response matrices all in such a way that no disturbance to the stored beam can be observed by the users of the light source. Examples of measurements for the various categories are compared to established methods, and their use in feedback schemes is discussed.

INTRODUCTION

Many measurements of lattice parameters require an excitation or change in setting that typically leads to a change in the beam position or shape. That is not acceptable during user operation in a synchrotron light source, where positional/angular stability to a fraction of a beam size/divergence is paramount (integrated motion of 10% of beam size/divergence up to 100Hz has often been quoted [1] as acceptable, but the demands are often even lower today):

- Measurement of betatron tune requires excitation of beam oscillations with a broadband signal. This is typically a kick, sweep/chirp or broadband noise delivered to the beam through a stripline or similar device. This leads to a blow up of the emittance for the duration of the excitation and following decay of the oscillations.
- Measurement of chromaticity usually requires measurement of the betatron tune at different stored beam energies. This is usually accomplished by changing the main RF frequency, which displaces the beam to a dispersive orbit in addition to the repeated blow up of the emittance from the repeated tune measurements.
- Orbit response matrix measurement requires changing of each corrector magnet one at a time and measuring the resulting differences in orbit. Again, this leads to displacements of the orbit which are many times the beam size. Furthermore, a complete response matrix measurement will take many minutes due to the large number of correctors typically present.
- Measurement of betafunction magnitude and phase is most often derived from a full orbit response matrix measurement.

On the other hand, the demand for regular measurements of all these parameters is increasing as refined tuning of machines requires continuous monitoring or feedback schemes. For example, the precise betatron tune decides the lifetime and injection efficiency, but it will vary with changes in insertion devices (IDs).

We have developed techniques which allow to perform these measurement with no visible disturbance to the user beam by either only exciting a small fraction (one bunch in a train of typically 720) for the tune measurement, or by exciting with small amplitudes (less than beam size) at high frequencies (only leads to an insignificant 'smearing' of the beam) and detecting these small signals with dedicated signal processing of longer durations. The trade off between small amplitude and longer observation time has allowed maintaining resolution at a level comparable to the standard techniques.

Common Principle of Excitation and Detection

The common principle shared by all the discussed applications is the injection of a small, sinusoidal disturbance, which is then measured by digital I/Q detectors which share the same time/frequency base as the excitation. In this way we are able to measure magnitude and phase of the response in a similar way as a lock-in amplifier does. In the following sections we will discuss the technical details of the implementations and show example measurements.

BETATRON TUNE MEASUREMENT

For the betatron tune measurement we excite the beam at a frequency near the nominal tune using a numerical oscillator (NCO) in the transverse multibunch feedback (TMBF) [2]. The beam motion is then detected in the same device by multiplying each bunch position with a

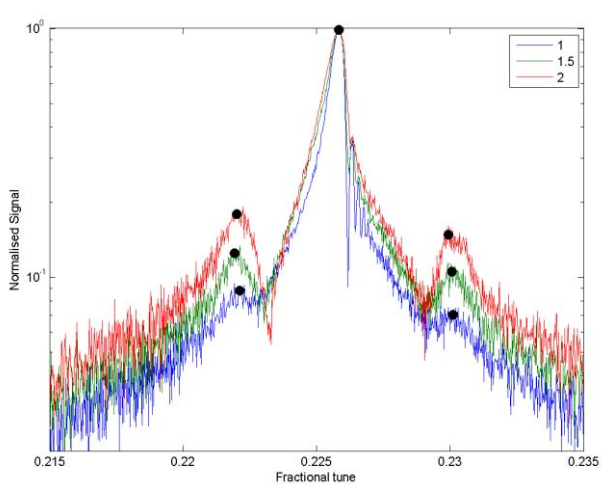

Figure 1: Horizontal betatron tune spectra for chromaticities 1, 1.5 and 2

DIAMOND DETECTORS AS BEAM MONITORS

E. Griesmayer, CIVIDEC Instrumentation, Vienna, Austria
B. Dehning, E. Effinger, CERN BI, Geneva, Switzerland
D. Dobos, H. Pernegger, CERN PH, Geneva, Switzerland

Abstract

CVD diamond particle detectors are already in use in the CERN experiments ATLAS, CMS, LHCb and ALICE and at various particle accelerator laboratories in USA and Japan. This is a proven technology with high radiation tolerance and very fast signal read-out [1]. It can be used for measuring single-particles as well as for high-intensity particle cascades, for timing measurements on the nanosecond scale and for beam protection systems. The radiation tolerance is specified with 10 MGy.

INTRODUCTION

The diamond beam monitor is a solid-state ionization chamber that stands out due to its fast and efficient charge collection and its high radiation tolerance. The diamond technology gives a charge collection time of less than 1 ns and lifetime studies made at CERN showed a 50% decrease in signal ampltude at 10 MGy [2], which make this device particularly well adapted to applications in particle accelerators.

Poly-crystalline CVD diamond beam monitors have been evaluated at the CERN SPS and at LHC accelerators. The read-out was made through 250 m long coaxial cable. Tests were made on the signal-to-noise ratio, the timing resolution and the dynamic range.

A single-crystalline CVD diamond beam monitor was tested for ISOLDE at CERN for the HIE-REX upgrade. This device was used to measure the beam intensity by particle counting and for measuring the beam energy spectrum for carbon ions.

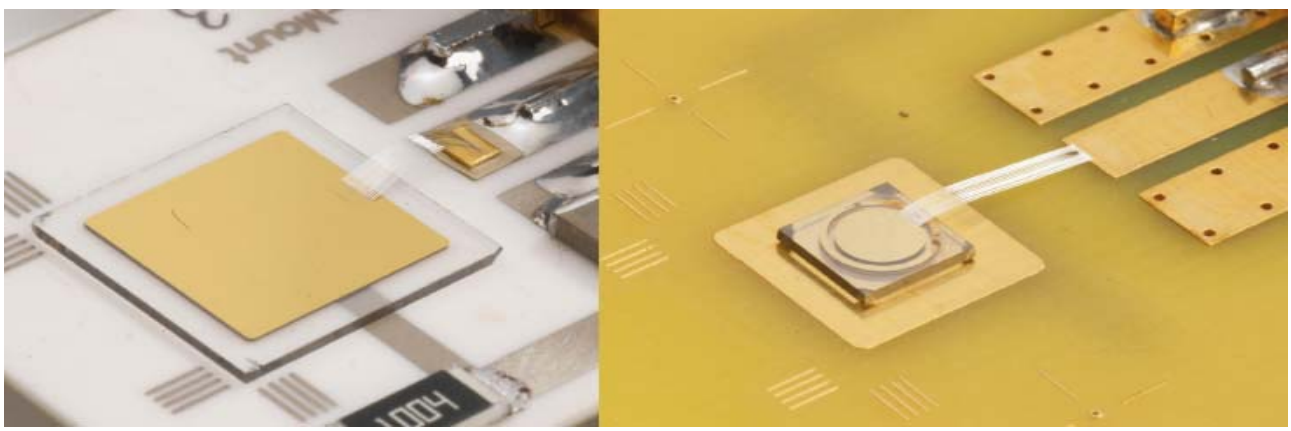

Figure 1: Single-crystalline and poly-crystalline diamond substrates, metalized with gold, are mounted on a ceramics board and a FR72 board, respectively.

TESTS AT ISOLDE

A novel beam instrumentation device for the HIE-REX (High Intensity and Energy REX) upgrade has been developed and tested at the On-Line Isotope Mass Separator ISOLDE, located at the European Laboratory for Particle Physics (CERN) in cooperation with Bergoz Instrumentation [3].

This device is based on a single-crystal CVD diamond detector (Figure 1, right picture) and is used for measuring the beam intensity, particle counting and measuring the energy spectrum of the beam. The detector is located inside the beam pipe in vacuum.

The carbon ions are completely absorbed by the diamond and the deposited energy is

RESIDUAL GAS X-RAY BEAM POSITION MONITOR FOR PETRA-III

P. Ilinski*, BNL, Upton, NY 11973, U.S.A.

Abstract

The development effort is driven by the need for a new type of x-ray beam position monitor, which can detect the centre of gravity of the undulator beam. A residual gas x-ray beam position monitor for the PETRA III storage ring was developed and tested.

INTRODUCTION

Blade type x-ray beam position monitors (XBMP) are currently employed at the third generation synchrotron facilities as "white" undulator beam XBPMs [1, 2]. They provide a micron accuracy resolution and are capable to withstand the high power of the undulator radiation. Nevertheless since the information of the beam position is obtained from the halo of the undulator radiation, the signal depends on the undulator gap and is affected by stray radiation from bending magnets and focusing optics. These can be overcome if XBPM will detect the centre of gravity of the undulator beam. XBPM based on the ionization of a residual gas can be considered a candidate for "centre of gravity white" beam position monitor.

RESIDUAL GAS X-RAY BEAM POSITION MONITOR

Residual gas beam profile monitors were first developed to provide beam profile measurements at charged particles accelerators [3,4]. Development of residual gas x-ray beam position monitor (RGXBPM) for PETRA III undulator x-ray beams was performed at DESY [5]. The profile monitor consists of an ion chamber operated at a residual gas pressure in which ions or electrons are drifted in a parallel electrical field towards the micro channel plate (MCP), which amplifies the signal and produces an image of the beam profile on a phosphor screen, Figure 1.

Spatial Resolution

The resolution of the residual gas beam profile monitors, which are in use at the particle accelerators is in the order of few hundreds of microns. Resolution of RGXBPM has to be substantially improved in order to comply with beam stability requirements at the third generation storage rings. Factors which define the RGXBPM resolution are: quality of the electrical field, initial kinetic energy of ions or electrons, resolution of detection system, and data processing. The electrical field has to be uniform in order to provide aberration free beam profile. Broadening of the beam profile occurs due to electrical field non-uniformity and presence of the transverse component of the electrical field. This broadening should not exceed the broadening of the beam profile, which is caused by the initial transverse kinetic energy of ions or electrons [6]. The resolution of detection system is defined by the MCP, the phosphor screen, optical coupling and signal to background ratio. A proper data processing allows sub-pixel resolution, where pixel characterizes the resolution of the detection system.

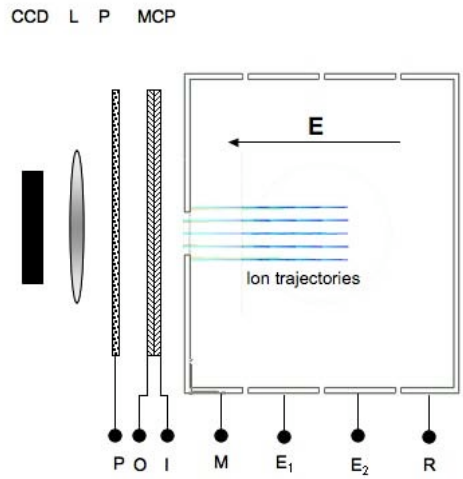

Figure 1: RGXBPM general layout: R - repeller electrode, E_1, E_2 - guide electrodes, M – mesh window electrode, I - MCP input, O - MCP output, P - phosphor screen, L - objective lens, CCD camera.

Signal Level

The signal level of the RGXBPM first of all is defined by the total x-ray cross-section of the residual gas, which depends on gas pressure and composition. Typical pressure at the beamline can be better then 10^{-9} mbar, gas composition of UHV system is mostly hydrogen and may include nitrogen, water vapor etc.

In a typical ion chamber operating at gas pressure of about 10^{3} mbar a primary photoelectron will produce an avalanche of secondary electrons, so the number of created electron ion pairs will be proportional to deposited energy divided by average energy of one electron ion pair creation (35 eV for nitrogen). The upper level of residual gas pressure for RGXBPM is limited by presence of the MCP, and should not exceed $5x10^{-6}$ mbar. At such low pressure primary photoelectrons may not produce secondary electrons before been collected. Two scenarios are presented at Figure 2 for nitrogen and hydrogen at pressure of 10^{-6} mbar, and for detector length of 1 cm. First, when only primary photoelectrons are produced: (dotes) - nitrogen, (dash-dot-dot) - hydrogen, second for high gas pressure, when all secondary electrons were produced: (dashed) - nitrogen, (dash-dot) - hydrogen.

*pilinski@bnl.gov

FEMTOSECOND SYNCHRONIZATION OF LASER SYSTEMS FOR THE LCLS*

J. M. Byrd#, L. Doolittle, G. Huang, J. W. Staples, R. Wilcox, LBNL, Berkeley, CA, USA

J. Arthur, J. Frisch, W. White , SLAC, Menlo Park, CA, USA

Abstract

The scientific potential of femtosecond x-ray pulses at linac-driven free-electron lasers such as the Linac Coherent Light Source is tremendous. Time-resolved pump-probe experiments require a measure of the relative arrival time of each x-ray pulse with respect to the experimental pump laser. To achieve this, precise synchronization is required between the arrival time diagnostic and the laser, which are often separated by hundreds of meters. An optical timing system based on stabilized fiber links that has been developed for the LCLS to provide this synchronization. Preliminary results show synchronization of the stabilized links at the sub-10-femtosecond level and overall synchronization of the x-ray and pump laser of <50 fs. We present details of the implementation at LCLS and potential for future development.

INTRODUCTION

The next generation of accelerator-driven light sources will produce sub-100-fs high brightness x-ray pulses[1]. In particular, pump-probe experiments at these facilities require synchronization of pulsed lasers and x-rays from electron beam on sub-100 fs time scales over distances of a few hundred meters to several kilometers[2,3]. Pump-probe experiments at these facilities plan to use an x-ray "probe" to produce snapshots of atomic positions within a sample some time after it is excited with a laser "pump."

Varying the time between pump and probe enables the recording of a "movie" of the dynamics in the sample, with a time resolution determined by the x-ray pulse length and the relative timing jitter and drift of pump and probe. For experiments that require minutes to hours to collect data, the relative drift of the pump and probe should be less than the x-ray pulse length.

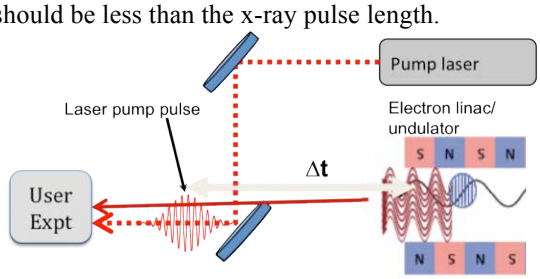

Figure 1: Layout for pump-probe timing.

One of the main challenges in reaching the level of synchronization required for pump-probe experiments is transmission of a timing signal over a relatively large facility. For example, in a facility of a kilometer in length, diurnal temperature variation results in cable length variation from several hundred ps to a nanosecond.

For the next generation of FELs, it is expected that the jitter of the electron beam with respect to the laser pump will be unacceptably large. Therefore, the goal is to measure the arrival time of each electron pulse with respect to the laser pump and allow the proper ordering of the "frames" of the movie. In this case, it is critical to synchronize the electron arrival time diagnostic with the pump laser.

STABILIZED RF SIGNAL DISTRIBUTION

One of the key features in any synchronization scheme is the ability to stably transmit a master clock signal to the remote clients with no uncontrolled relative timing drift between the clients. A schematic view of this distribution is shown in Fig. 2. The master oscillator signal is distributed over the accelerator to remote clients in a star configuration. Each link consists of a stabilized optical fiber with a second fiber carrying the error signal, a receiver for RF signal processing (RX), a synchronization head (S/H), and a remote client. The phase of the master signal is corrected at the end of each fiber link for the length variation of that link. Thus the relative timing drift

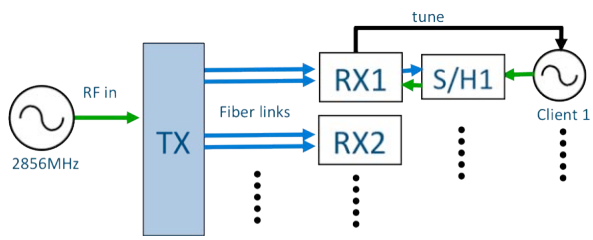

Figure 2: Schematic view of the distribution of the master clock over optical fiber. Each receiver consists of an RF signal processor (RX) and synchronization head (S/H).

of clients locked the master signal on independent fiber links does is minimized over many hours and even days.

Several approaches have been implemented to send stable signals over fiber optic links [4-8]. In our approach, each fiber link is an optical interferometer that precisely

*Work supported by by the U.S. Department of Energy under contract DE-AC02-05CH11231.
#JMByrd@lbl.gov

ADVANCED MODULAR OSCILLOSCOPES AND DIGITIZERS OPTMIZED FOR ACCELERATOR APPLICATIONS

Boyd Shaw, Christopher Ziomek, ZTEC Instruments, Albuquerque, NM 87109, U.S.A.

Abstract

Modular oscilloscopes and digitizers, including those with embedded EPICS IOCs, provide powerful off-the-shelf solutions for accelerator controls and beamline data acquisition applications requiring fast sampling, high resolution and/or tight multi-channel synchronization. This presentation discusses features and capabilities of EPICS and non-EPICS LXI, VXI, PXI/cPCI and PCI oscilloscopes and digitizers as they specifically relate to accelerator and beamline applications. Modular oscilloscopes and digitizers with on-board DSP and FPGAs provide the advanced waveform acquisition and analysis capabilities of benchtop instruments with the size and channel-density advantages of modular instruments. Instruments with on-board processing, such as those from ZTEC Instruments, enable real-time waveform math and waveform parameter analysis. Advanced triggering and multiple acquisition modes are other features found on some of today's advanced modular instruments. Furthermore, instruments with embedded EPICS IOCs save users the time and money of developing their own EPICS drivers and display panels.

ACCELERATOR REQUIREMENTS FOR OSCILLOSCOPES & DIGITIZERS

Accelerator applications often challenge instrumentation manufacturers. In addition to requiring low noise and distortion during data acquisition, responsive remote instrument control and fast screen update rates are important for many machine control applications. And because large amounts of data are often captured, it becomes important to reduce the data to include only the desired information and download the information as quickly as possible so that the instrument is ready for the next acquisition.

Furthermore, it is frequently necessary to tightly synchronize many channels of data acquisition and multiple triggers across numerous instruments and across multiple chassis that may be separated by significant physical distances.

Because of the demanding technical requirements of accelerator applications, it is often necessary for engineers to develop their own custom products to meet specific requirements. However, developing custom instruments adds significant costs and time to most projects. Because of this, engineers and experimenters prefer to purchase off-the-shelf solutions whenever possible.

ATTRIBUTES OF ADVANCED MODULAR SCOPES & DIGITZERS

Advanced instrument functionality that was traditionally found only on benchtop instruments is now available on modular instruments in PXI/cPCI, PCI, LXI and VXI formats. For oscilloscopes and digitizers, this functionality includes input signal conditioning, multiple acquisition modes, advanced triggering, on-board waveform math and analysis and much more. Figure 1 illustrates some of these 'benchtop' functions as they exist in ZTEC modular instruments.

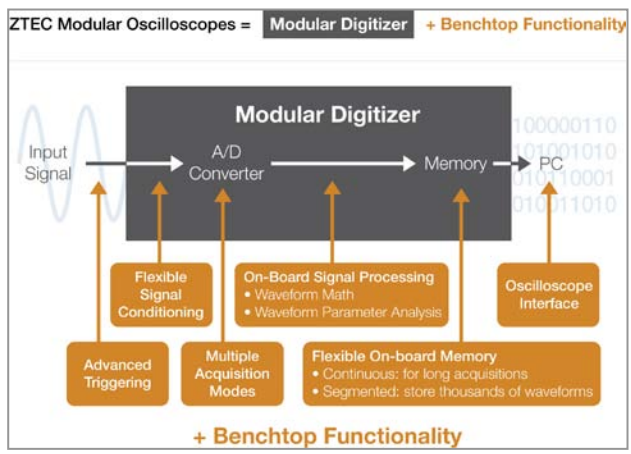

Figure 1: Benchtop functionality

Triggering

Going beyond simple rising/falling edge triggers, advanced modular oscilloscopes and digitizers add the ability to trigger on complex signal conditions, from multiple sources, just like their benchtop counterparts. For example, pulse width triggers can be configured to occur only on pulses that meet certain conditions – e.g., greater than or less than a user-defined pulse width, or inside/outside a specified range of pulse widths.

Pattern triggers are used to acquire waveforms when a user-defined pattern becomes true or false. The pattern is a combination of HIGH/LOW states on a combination of one or more input channels and/or backplane triggers like those found on PXI and VXI. For example, an instrument could be set to trigger and acquire data when Input 1 is HIGH, Input 2 is LOW and Input 3 is HIGH. See Figure 2.

A FUNDAMENTALS OF LOGARITHMIC AMPLIFIERS AND RECENT ADVANCES

B. Gilbert
Analog Devices, Inc., Beaverton, OR, U.S.A.

Abstract

This is a tutorial address. Numerous real-world signals exhibit a large dynamic range (DR)--the ratio of the strongest amplitude to the weakest, usually expressed in decibels. These signals are often handled by high-resolution A/D converters (24 b = 144.5 dB). But these are expensive, especially when fast response is required.

Today, a large family of monolithic integrated circuits can address these needs. They compress the dynamic range of an input on a precise logarithmic scale, and provide an output representing the input expressed in dB with DR capabilities up to 200 dB, bandwidths to over 20G Hz, response times down to 1.5 ns, current-measurement capabilities from 1 pA to 10 mA in one range, and operation from supply voltages as low as 1.5 V. Many are also tiny (sometimes barely visible) and inexpensive.

This talk will present various ways by which a logarithmic response is achieved, starting with strong mathematical foundations that also provides fundamental insights as to how practical logarithmic amplifiers must be designed. The principles are then elaborated by showing several basic circuit forms to address diverse measurement requirements.

*

SUB-NM BEAM MOTION ANALYSIS USING A STANDARD BPM WITH HIGH RESOLUTION ELECTRONICS

M. Gasior, H. Schmickler, J. Pfingstner, M. Sylte, M. Guinchard, A. Kuzmin, CERN, Geneva
M. Billing, Cornell University, Ithaca, New York
M. Böge, M. Dehler, PSI, Villigen

Abstract

In the Compact Linear Collider (CLIC) project high luminosity will be achieved by generating and preserving ultra low beam emittances. It will require a mechanical stability of the quadrupole magnets down to the level of 1 nm_{rms} for frequencies above 1 Hz throughout the 24 km of linac structures. Studies are presently being undertaken to stabilize each quadrupole by means of an active feedback system based on motion sensors and piezoelectric actuators. Since it will be very difficult to prove the stability of the magnetic field down to that level of precision, an attempt was made to use a synchrotron electron beam as a sensor. The beam motion was observed with a standard button Beam Position Monitor (BPM) equipped with high resolution electronics. Beam experiments were carried out to qualify such a measurement at CesrTA (Cornell University) and at SLS (PSI, Villingen), where the residual motion of the circulating electron beams was measured in the frequency range of 5 – 700 Hz. This paper describes the results achieved along with the equipment used to measure both the residual beam motion and the mechanical vibration of machine elements.

MOTIVATION

For all new electron beam based light sources the present "race" is for always smaller beam emittance. The linear collider and FEL projects aim for even smaller beam emittances, such that mechanical vibrations of the quadrupoles start to contribute significantly to the increase of beam emittance during the passage of the beams through the linac. Extensive computer simulations [1] have been carried out for the CLIC project leading to the specifications of the required stability of the magnetic axis of the CLIC main linac quadrupoles listed in Table 1.

The required stability is at least one order of magnitude smaller than what can be achieved by passive damping and shielding of ground motion and technical noise. The present baseline for the CLIC project is an active stabilization system based on motion sensors for 5 degrees of freedom on each quadrupole and piezoelectric actuators in a closed feedback loop for stabilization [2]. It is expected that with this setup the quadrupoles can be mechanically stabilized to the required precision. One point in this approach is left open, namely whether the mechanical stabilization of a quadrupole also assures that the magnetic centre of this quadrupole is stable to the same level. Potentially coil vibrations due to coolant flow or pole tip vibrations might change the magnetic centre. Hence in the framework of the actual R&D program additional instrumentation is being developed, which would allow sensing the stability of a quadrupole down to the required level of precision. For the final experiment the stabilized quadrupole would have to be inserted into that machine, the beam steered through it with a large excursion, whilst the beam in all other quadrupoles would be steered to the minimum possible offset.

Table 1: CLIC project requirements for residual quadrupole stability above the limiting frequencies

Plane	Final focus quads	Main beam quads
Vertical	0.18 nm > 4 Hz	1 nm > 1Hz
Horizontal	5 nm > 4 Hz	5 nm > 1Hz

This paper describes pilot measurements on two synchrotron light sources exploring whether an electron beam could be used as a sensor of the quadrupole magnetic field stability. In simple experiments the residual eigen-motion of the electron beam was observed and beam spectra including the region of interest 5 –100 Hz have been recorded. In order to obtain a noise floor below the nano-meter level an optimized copy of the LHC Base Band Tune (BBQ) measurement hardware [3, 4] was used with observation periods up to many minutes.

The following chapters contain description of the front-end electronics used, results from the beam experiments at CesrTA and SLS and preliminary conclusions whether an electron beam in a synchrotron could be used as a gauge for demonstrating quadrupole stability down to the nano-meter level.

HIGH RESOLUTION BPM ELECTRONICS

Beam signals were taken from standard button BPMs "borrowed" from their native systems (orbit or transverse feed-back) for the time of experiments. The individual button signals were processed with a copy of the LHC BBQ hardware based on the direct diode detection (3D) technique [3, 4]. The principle of the technique is shown schematically in Fig. 1, with the simplified signal waveforms sketched above the characteristic nodes of the circuit.

In this scheme the pick-up electrode signals are processed by diode peak detectors, which can be considered as fast sample-and-hold circuits, with the sampling self-triggered at the bunch maxima and "held" by the parallel capacitors. The purpose of the parallel resistors is to slightly discharge the capacitors so that the next bunch with potentially smaller amplitude

APS BEAM STABILITY STUDIES AT THE 100-NANORADIAN LEVEL*

G. Decker, B.X. Yang, R. Lill, H. Bui, Advanced Photon Source
Argonne National Laboratory, IL 60439, USA

Abstract

Recent developments at the Advance Photon Source (APS) in the area of high-resolution beam position monitoring for both the electron and x-ray beams has provided an opportunity to study beam motion well below the measurement threshold of the standard suite of instrumentation used for orbit control. The APS diagnostics undulator beamline 35-ID has been configured to use a large variety of high-resolution beam position monitor (BPM) technologies. The source-point electron rf BPMs use commercially available Libera Brilliance electronics from Instrumentation Technologies, together with in-house-developed field-programmable gate-array-based data- acquisition digitizing broadband (10 MHz) amplitude-to-phase monopulse receivers. Photo-emission-based photon BPMs are deployed in the 35-ID front end at distances of 16 and 20 meters from the source, and a prototype x-ray fluorescence-based photon BPM is located at the end of the beamline, approximately 39 meters from the source. Detailed results describing AC noise studies will be provided.

INTRODUCTION

Shown in Figure 1 is the experimental arrangement of diagnostics associated with the APS 35-ID undulator source point.

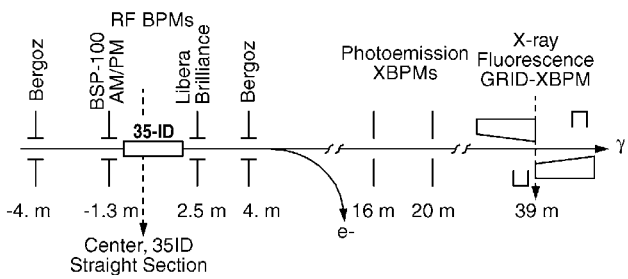

Figure 1: Array of beam position monitoring diagnostics used for beam stability studies at APS 35-ID.

This particular arrangement is unique in that 5 different BPM technologies located at 7 different locations along the beamline are all poised to provide quantitative measurements of beam position and pointing angle with unprecedented resolution. The work described in this paper is an extension of work started in 2009 in collaboration with researchers assessing BPM technologies for the NSLS-II facility now under construction [1].

*Work supported by U.S. Department of Energy, Office of Science, Office of Basic Energy Sciences, under Contract No. DE-AC02-06CH11357.

RF BEAM POSITION MONITORING

Near the source point, both narrowband and broadband rf BPM electronics are used to monitor the electron beam. Closest to the undulator, capacitive button pickup electrodes are mounted on the small-gap insertion-device vacuum chamber in sets of four, each with 4-mm diameter: two buttons above and two below the accelerator mid-plane at each station. The vacuum chamber vertical aperture is 8 mm; these pickup electrodes have very high geometric sensitivity. The upstream electrodes are connected to an in-house-designed data acquisition system: the bunch signal processor BSP-100, a field-programmable gate array (FPGA) module [2] samples a legacy broadband (10 MHz) amplitude-to-phase conversion BPM rf front end at a sample rate of 88 MS/sec, i.e., one fourth the ring's rf frequency. At the downstream station, commercial Libera Brilliance electronics from Instrumentation Technologies (Slovenia) are employed, which have recently been interfaced to the APS control system.

Due to the high sample and processing rates made possible by (FPGA) technology, and AC noise floor approaching 1 nm/√Hz are realizable. Shown in Figure 2 are data showing the performance of commercial Libera Brilliance BPM electronics in contrast to the BSP-100 data acquisition attached to the APS broadband rf BPM front end. By using a four-way splitter from a single button pickup, the noise floor was determined and compared with actual levels of (closed-loop) beam motion in the 35-ID straight section. Horizontal (X) and vertical (Y) data together with the noise floor are plotted as cumulative rms motion by integrating the power spectral density for turn-by-turn data using data sets of 0.5 and 1 second duration for the Libera and BSP-100 module, respectively. The straight lines indicate reference white noise levels.

In addition to the broadband BPMs, located +/- 4 meters from the center of the insertion device straight section, are sets of four 1-cm-diameter pickup electrodes mounted on standard large-aperture (4 cm x 8 cm elliptical) vacuum chambers. Attached to these pickup electrodes are commercial narrowband Bergoz multiplexed BPM electronics which were installed c. 2000.

PHOTOEMISSION-BASED PHOTON BPMS

In the beamline front end at 16.35 and 20 meters downstream of the undulator source point are photo-emission-based photon BPMs [3]. Due to small apertures in the front end, the detector located at 16.35 meters provides both horizontal and vertical position readbacks,

CHERENKOV RING TO OBSERVE LONGITUDINAL PHASE SPACE OF A LOW ENERGY ELECTRON BEAM EXTRACTED FROM RF GUN *

H. Hama#, K. Nanbu, M. Kawai, S. Kashiwagi, F. Hinode, T. Muto, F. Miyahara, Y. Tanaka
Research Centre for Electron Photon Science, Tohoku University
1-2-1 Mikamine, Taihaku-ku, Sendai 982-0826, Japan

Abstract

Particle distribution of the electron beam extracted from a thermionic RF gun in longitudinal phase space is crucial for electron bunch compression. Because space charge effects in the RF gun are not fully understood, an efficient bunch compression scheme employing magnetic chicane or alpha (α-) magnet is not easily designed. In order to measure the distribution in the longitudinal phase space of relatively lower energy electrons (below 2 MeV), we have studied a novel method for direct observation of electron energy employing velocity dependence of opening angle of Cherenkov radiation. Intrinsic energy and temporal resolution are discussed by showing a numerical ray-trace simulation.

ITC-RF GUN FOR FEMTO-SECOND ELECTRON PULSE

An intense terahertz radiation source based on an electron accelerator has been developed at Tohoku University, and is called the t-ACTS project [1]. Coherent THz radiation from an isochronous ring will be provided to multiple users simultaneously as a wide-band short-pulse source. Furthermore, a free electron laser (FEL) in the THz region driven by shorter electron pulses (less than the resonant wavelength) has been studied [2], in which a theoretical simulation suggests that FEL interaction can continuously amplifies the head part of radiation pulse when the cavity length is completely tuned. Stable production of very short electron bunches is a key issue for the t-ACTS project. Photoinjectors have already successfully produced femtosecond pulses with considerable bunch charge. However, we have chosen thermionic cathode for the RF gun because of stability, multi-bunch operation, and cheaper cost. Although the bunch charge will be small (a couple of tens of pC), and then coherent enhancement of the radiation is not so strong, the space charge effect may not be a very serious concern, and the thermionic cathode should have good stability, so excellent beam quality would be expected. Moreover, high repetition operation in multi-bunch mode will open another aspect of application experiments.

The thermionic RF gun consists of two independent cavity cells to manipulate the longitudinal beam phase space (see Fig. 1), so it is named the ITC (Independently-Tunable Cells) RF gun [3]. Particle distribution in longitudinal phase space is very important for the bunch compression including the space charge effect. The ITC-RF gun has been designed so as to produce appropriate longitudinal particle distribution by changing the relative RF phase and field strengths as shown in Fig. 2.

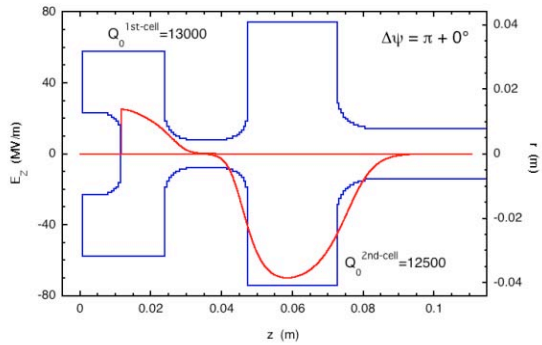

Figure 1: ITC-RF gun. A small size (ϕ = 1.85 mm) cathode of single crystal LaB_6 is employed, which can provide a beam current density of more than 50 A/cm^2.

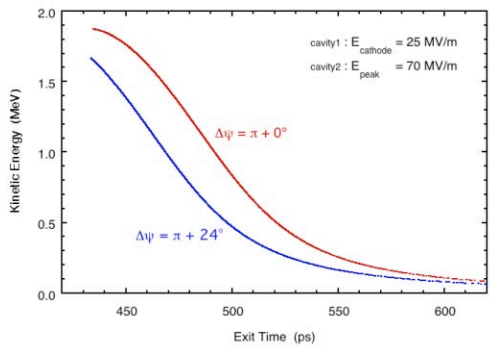

Figure 2: Particle distribution in the longitudinal phase space calculated by an FDTD code [4]. One for the phase difference of π + 0° (usual RF gun) leads higher energy. Meanwhile linear particle distribution results from phase space manipulation performed by phase tuning. Cathode current is 1.34 A for both calculations.

In order to optimize the parameters for the gun, such as field strengths and phase difference between two cells, we have done some numerical simulations of the beam production for the ITC-RF gun. Because a considerable part of the charge is concentrated into the head of the extracted beam, the space charge effect acts to deviate the electron distribution from a simple smooth line. This phenomenon is difficult to understand because different

*Work supported by Grant-in-Aid for Scientific Research (S), the Ministry of Education, Science, Technology, Sports and Culture, Japan, Ccontact No. 20226003.
#hama@lns.tohoku.ac.jp

COTS TECHNOLOGY FOR HIGH ENERGY PHYSICS INSTRUMENTATION

J. Truchard, R. Marawar, A. Veeramani, M. Ravindran
National Instruments, Austin, TX 78759, U.S.A

Abstract

National Instruments (NI) uses Commercial Off-The-Shelf (COTS) semiconductor and computing technology and applies it to measurement, diagnostics and instrumentation needs. NI leverages the rapid technological advancement of the semiconductor and computer industry, while retaining the flexibility and ensuring interoperability between HW & SW. This paper elaborates how general purpose NI products and technology can be applied to specialized instrumentation, measurement and diagnostic needs in High Energy Physics (HEP). In particular we will discuss programming and processing tools, instrumentation platform with custom hardware development using FPGA.

INTRODUCTION

Until recently, most measurement, diagnostic and instrumentation applications in HEP required custom development efforts. Most COTS products did not meet the needs of the community due to high-end specifications, high availability requirements, long term serviceability aspects, closed driver stacks, limited operating system support etc. In recent years NI has led efforts to address these issues by developing state-of-the-art products that meet demanding specifications, making great progress towards reliable and redundant systems, providing long-term replacement and calibration services, support for Linux, providing register maps for open driver development and collaborating on EPICS, Tango and other middleware support. In addition, using COTS products minimizes development costs, reduces unit costs thus focusing limited resources on scientific endeavors.

Reducing Development Time

Many of the HEP applications require development of complex measurement, control and diagnostic systems. In addition, data must be processed real-time to make intelligent decisions about measurement and control parameters. For mathematical computations and simulations it would be desirable to take advantage of COTS technologies such as multicore processors and FPGAs. National Instruments LabVIEW offers scientists and engineers a unique graphical programming environment that combines control and measurement system development along with real-time high performance computing including multicore processors and FPGAs.

LABVIEW GRAPHICAL SYSTEM DESIGN

LabVIEW is a general purpose graphical programming environment used to develop measurement, test, and control systems using intuitive graphical icons and wires that resemble a flowchart. LabVIEW is supported on a variety of platforms including Microsoft Windows (2K, XP, Vista), Linux, and Macintosh. LabVIEW Real-Time, the embedded systems solution for LabVIEW, is supported on VxWorks and Pharlap targets on hardware platforms such as CompactRIO and PXI. LabVIEW offers tight integration with thousands of hardware devices and provides hundreds of built-in libraries for advanced analysis and data visualization. LabVIEW also enables parallel programming targeting Multicore CPUs and FPGAs.

As a COTS product, LabVIEW provides an extensively tested and industry validated product with multiple models of computation, leading data flow architecture and significant R&D investment that is amortized over hundreds of thousands of installations.

LabVIEW on Multicore CPU

To reduce computation time, programmers must divide applications into parallel parts using multithreading. Each of the threads can run in parallel in a multicore system. Applications that take advantage of multithreading have numerous benefits, such as more efficient CPU use, better system reliability, and improved performance. Three techniques to commonly used for reducing computation time include: task parallelism, data parallelism, and pipelining. LabVIEW is an inherently parallel programming language without having to worry about thread management or synchronization between threads. Consider two tasks shown in Fig.1. The two tasks do not have any data dependencies, so the LabVIEW compiler will automatically multi-thread the application.

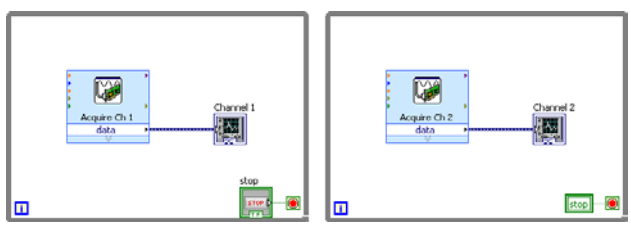

Figure 1: LabVIEW block diagram showing two tasks that will be automatically be executed in parallel.

OTR POLARIZATION EFFECTS IN BEAM-PROFILE MONITORS AT THE FERMILAB A0 PHOTOINJECTOR*

A. Lumpkin#, A. Johnson, J. Ruan, J. Santucci, and R.Thurman-Keup
Fermilab, Batavia, IL U.S.A. 60510

Abstract

Optical transition radiation (OTR) imaging for transverse beam-size characterization is a well-established technique at many accelerators including the Fermilab A0 photoinjector (A0PI) facility. With low beam energies of 14-15 MeV and emittances of 3 mm mrad, one observes beam sizes of 0.8 to 1.5 mm (sigma). However, the use of 50-µm wide slits to sample the beam's transverse phase spaces significantly alters the required resolution of the converter screen and imaging system. Slit-image sizes of about sigma =100 µm or less are observed, depending on drift distance and beam divergence. Moreover, the OTR polarized component perpendicular to the narrow beam dimension systematically gave us ~20-µm smaller projected image sizes than those with the total OTR intensity. This is one of the first reports of this polarization effect at such a low-gamma regime (~30).

INTRODUCTION

The opportunity for a new series of beam characterization experiments at the Fermilab A0 photoinjector (A0PI) was recognized in the last year. There is an ongoing proof-of-principle experiment to demonstrate the exchange of the transverse horizontal and longitudinal emittances [1,2]. This experiment relies on measurements of the transverse emittances and longitudinal emittance upstream and downstream of an emittance-exchange (EEX) beamline. Generally, at the low beam energies of 14-15 MeV and emittances of 3-5 mm mrad, one encounters beam sizes of 0.8 to 1.5 mm (sigma) [2]. Such beam sizes do not present a challenge to standard imaging procedures using scintillator screens or optical transition radiation (OTR) screens as described elsewhere [3]. However, the slits-emittance-measurement technique [4] which involves insertion of 50-µm wide slits to sample the beam's transverse phase spaces significantly alters the required resolution of the converter screen and imaging system. In this case, one deals with slit-image sizes of σ =100 µm or less, and depending on the drift distance one deals with images that can approach the camera resolution limit and/or the converter screen resolution limit. Beam divergence is calculated from the downstream slit image size and the relevant drift distance.

*Work supported by U.S. Department of Energy, Office of Science, Office of High Energy Physics, under Contract No. DE-AC02-07CH1135.
#lumpkin@fnal.gov

In the case of OTR imaging for transverse beam-size characterization, there is empirical evidence for gamma greater than 1000 beams that the utilization of the polarization component orthogonal to the dimension of interest results in a smaller projected image profile [5-7]. This aspect is a small fractional correction for 1-mm sized beam spots, but quite noticeable for 150-µm sized beam spots. While evaluating the slit images for emittance measurements at A0PI, we consistently found that using the OTR polarized component orthogonal to the narrow beam dimension of interest systematically gave us ~20 µm smaller projected image sizes than with the total OTR intensity. For such a low-gamma regime (~30), this is one of the first reports of this polarization effect on observed beam sizes. This correction affects the emittance values through the beam-size-divergence product.

EXPERIMENTAL BACKGROUND

The tests were performed at the Fermilab A0 photoinjector facility which includes an L-band photocathode (PC) rf gun and a 9-cell superconducting radiofrequency (SCRF) accelerating structure which combine to generate up to 16-MeV electron beams [2]. The drive laser operates at 81.25 MHz although the micropulse structure is usually counted down to 1 MHz. Due to the low, electron-beam energies and OTR signals, we typically summed over 50 micropulses with 0.25 nC per micropulse. The tests were performed in the straight-ahead line where energizing a dipole sends the beam into a final beam dump. The setup included the upstream corrector magnets, quadrupoles, the YAG:Ce and/or OTR imaging stations denoted as X3-X6, and the beam dump as schematically shown in Fig. 1. Both the YAG:Ce powder screen and the OTR screens were oriented with the surface normal at 45 degrees to the beam direction and with the viewing port at 90 degrees to the beam direction. The OTR converter was an Al-coated optics mirror that was 1.0 mm thick with a BK7 substrate and was mounted on a stepper assembly. The assembly provided vertical positioning with an option for the YAG:Ce scintillator at X5. The images were obtained with a 10-bit Firewire digital CCD camera with an optical transport consisting of a 150-mm-focal-length field lens, mirror, and a 50 mm C-mount lens on the camera. The images were captured with 8-bit resolution under the DOOCS protocol, and images were processed with MATLAB-based tools for Gaussian curve fitting to the projected profiles.

SNS TARGET IMAGING SYSTEM SOFTWARE AND ANALYSIS*

W. Blokland, T. McManamy, T. J. Shea, ORNL, Oak Ridge, TN 37831, U.S.A.

Abstract

A new Target Imaging System (TIS) has been installed to directly measure the size and position of the proton beam on the Spallation Neutron Source (SNS) mercury target. The proton beam, hitting a luminescent coating on the target nose, produces light that is transferred using a radiation-tolerant optical system to an image acquisition system integrated with the accelerator controls network. This paper describes the software that acquires and analyzes the image, how the system has been integrated with the SNS control system, and compares the TIS results with the indirect methods of calculating the peak densities of the proton beam.

INTRODUCTION

The Spallation Neutron Source at Oak Ridge National Laboratory now commonly operates with approximately one megawatt of beam power on the Mercury target. Each beam pulse, repeating 60 times a second, consists of about 10^{14} 1GeV protons and lasts less than 1 microsecond. The protons hit a stainless steel target filled with mercury to produce the neutrons for the experiments. The protons damage the target and this damage depends on the beam's peak power and transverse profile [1].

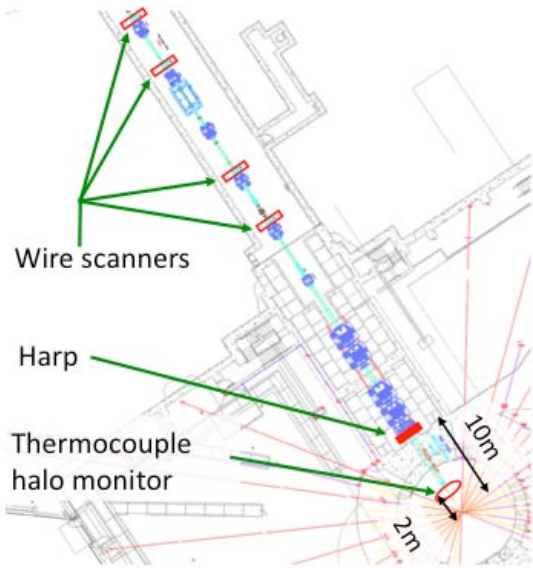

Figure 1: RTBT Instrumentation.

To assure the target lifetime, the operational procedure is to limit the beam's peak density on the target. The RTBT (Ring to Target Beam Transferline) Wizard program combines wire-scanner and harp measurements with the beam-line lattice parameters to calculate the beam size at the target. The harp is the only instrument in the RTBT that measures the transverse profile of the beam during production, see Figure 1. The RTBT Wizard produces scale factors that allow conversion of the measured beam size at the harp to an estimated beam size on the target. The harp program can then calculate the estimated peak densities on the target. If these peak intensities start to exceed the administrative limits, beam power is reduced or the transverse size is increased.

With the TIS, we can now obtain a more direct measurement of the peak intensities and use this system to safeguard the target.

SYSTEM OVERVIEW

A target imaging system was available during the commissioning of SNS and measured the first beam on target. To keep the system simple, it consisted of a fluorescent screen mounted in front of the target and a camera in the target room. It was understood that this system wouldn't last long before the radiation damage would permanently disable the system. The system showed the first beam on the first installed target and its measurements were used to estimate the spread of the beam due to scattering of the protons when passing through the proton window. This success started the drive for a permanent target imaging system. After evaluating various configurations, the choice was made to coat the actual target nose with a layer of Cr:Al2O3 and to use mirrors and a fiber bundle to bring the light out to the camera in a non-radiation environment [2,3].

System Configuration

A radiation resistant aluminum parabolic mirror collects the light from the fluorescent coating of the target. This is followed by a turning mirror and then lenses that focus the image onto a fiber bundle. Figure 2 shows the optical path through the target shielding.

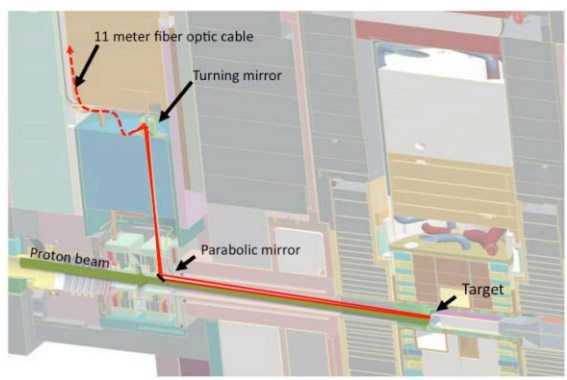

Figure 2: View of optical path with shielding.

The radiation resistant optical fiber bundle is made of 10,000 individual fibers and brings the light out to a non-

* ORNL/SNS is managed by UT-Battelle, LLC, for the U.S. Department of Energy under contract DE-AC05-00OR22725

GAS SCINTILLATION BEAM PROFILE MONITOR AT COSY JÜLICH *

C. Boehme#, T. Weis, Technical University of Dortmund, Germany
J. Dietrich, V. Kamerdzhiev, Forschungszentrum Jülich, Germany
J. L. Conradie, iThemba LABS, South Africa.

Abstract

The interaction of ion beams with the surrounding residual gas leads to photon emission by the excited residual gas atoms and molecules. These photons in the visible spectrum range can be used to monitor the transverse beam profile. We therefore use a multichannel photomultiplier (PMT) together with an optical imaging system. Measurements at COSY synchrotron of the Forschungszentrum Jülich are presented. The usability of the method is discussed by comparing to measurements at the iThemba LABS beamline and the beamline of the JESSICA experiment, a neutron spallation source test setup at COSY.

INTRODUCTION

The knowledge of the beam position and the transverse profile is essential for the successful operation of an accelerator facility. Due to thermal reasons high beam energy and/or high beam currents limit the use of traditional intersecting methods like wire scanners or secondary electron emission (SEM) grids. At synchrotrons non destructive methods are preferred to monitor the circulating beam, as the beam passes the interaction region many times. Even a small influence per turn would add up, leading to possible beam loss. Several kinds of diagnostic devices, using the products of the interaction between the ion beam and the residual gas, are under development or in use. Usually the devices register the ions and/or electrons produced in collisions of the beam particles with the residual gas. A few attempts have already been made to use the emitted light of the excited residual gas particles in order to monitor the beam [1]. This method has the advantage of being insensitive to electric or magnetic fields. Also the spatial and time resolution is high, allowing a single pulse measurement. The principle limitations of this method are the low cross section for light production in the visible range and the small solid angle of the optical setup. This leads to an available count rate about three orders of magnitude lower, compared to profile monitors based on residual gas ionization. Nevertheless, a wide range of applications can still be covered with this method.

MEASUREMENT TECHNIQUE

The light emitted by the residual gas is focused by a glass lens onto a multichannel photomultiplier (PMT) array, as shown in figure 1. A Hamamatsu PMT (7260-type, 32 channels, 0.8×7 mm photocathode size, 1mm pitch size) was used for these measurements. The readout was performed using a 48 multichannel current digitizer, developed at iThemba LABS [3].

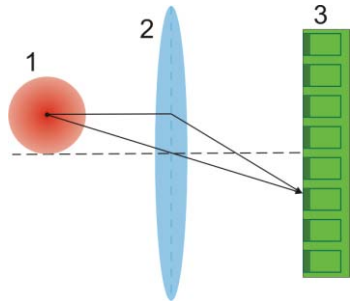

Figure 1: Measurement principle [2] (not to scale): The light from the interaction of the beam with residual gas (1) is focused by a glass lens (2) onto the multichannel photomultiplier (3).

PHOTON YIELD

While measuring the transverse beam profile using photons emitted by residual gas the only controllable parameters to influence the photon yield are the composition and pressure of the residual gas at fixed ion beam parameters. Although the increase of residual gas pressure is normally not standard practice at accelerators, this method has been successfully tested. While the residual gas mixture is given, the gas to be added can be chosen. Two gases are candidates for addition, N_2 and Xe, because both show strong light emission within the visible range and are also easily pumped out of the vacuum system.

Preliminary tests regarding the residual gas scintillation spectra were performed at a test bench [4]. A 20 keV He^+ beam passed an interaction region, where various gases could be added up to a total pressure of 10^{-3} mbar. A grid type monochromator together with a single channel PMT, that has a similar spectral response characteristics compared to the multichannel model, was used to measure the scintillation spectra. Since the ion source of the test bench uses He and H_2 is typically a dominating component of the residual gas in an accelerator, the scintillation spectra of these two gases were measured as well. The spectra are shown in figure 2

The results of the spectral measurements are in good agreement with [5]. The relative intensity at 424 nm (N_2) has been found to be less than expected. The overall results however clearly show that N_2 and Xe are

*Work supported by BMBF and NRF, Project code SUA 06/003
#c.boehme@fz-juelich.de

A NON DESTRUCTIVE LASER WIRE FOR H- ION BEAMS*

C. Gabor#, STFC (RAL), ASTeC, Chilton, Didcot, U.K.
A. Bosco, G. Boorman, G. Blair, RHUL, Physics Department, London, UK
A.P. Lechtford, STFC (RAL) Isis, Chilton, Didcot, UK

Abstract

The Front End Test Stand (FETS) is an R&D project hosted at Rutherford Appleton Laboratory (RAL) with its aim to demonstrate a high power, fast chopped H- ion beam. Possible candidates of applications are Isis upgrade (RAL neutron source), future spallation sources or the Neutrino factory. The high beam power may cause problems due to its thermal power deposition on diagnostics parts introduced into the beam so non-invasive beam instruments are highly preferred to avoid those problems. Diagnostics for H- beams can benefit of laser light where photons with suitable energy are able to detach the additional electron. This method is applied to a beam profile monitor close to the ion source of the FETS beam line. The paper gives a status report of the ongoing process of experimental set-up and provides a detailed discussion of problems and recent changes.

INTRODUCTION

High Power Proton Accelerators (HPPA), capable of producing beams in the megawatt range, have many applications, including drivers for spallation neutron sources, production of radioactive beams for nuclear physics, hybrid reactors, transmutation of nuclear waste, and neutrino factories for particle physics [1,2]. These applications require high quality beams and call for significant technical development, especially at the front end of the accelerator, where beam chopping at an energy of a few MeV and high duty cycle (1…10%) are required in order to minimise beam loss and induced radioactivity at injection into downstream circular accelerators.

The Front End Test Stand (FETS) [3] project, a UK based collaboration involving RAL, ASTeC, Imperial College London, University of Warwick, Physical Department of Universidad del Pais Vasco, and Bilbao, Spain, will test a fast chopper in a high duty factor MEBT line. More recently the project is also supported by Royal Holloway, University of London. The key components of the beamline are an upgraded Isis Penning ion source with 65keV beam energy, a three solenoid Low Energy Beam Transport (LEBT) line, a high duty factor 324 MHz Radio–Frequency Quadrupole (RFQ), a MEBT section including a novel Fast–Slow beam chopper and a comprehensive set of beam diagnostics. The ion source and LEBT are currently being commissioned; the status is described in [4,5,6].

* work supported with a laser loan from Goethe-University Frankfurt, Institute of Applied Physics IAP, Germany
# corresponding author: christoph.gabor@stfc.ac.uk

Photo detachment used for beam diagnostics

For negatively charged particle beams the photo dissociation technique (also called photo detachment) offers an elegant solution to do non destructive diagnosis. Photons with an energy above the threshold for photo dissociation (H- binding energy ~0.75eV) can be used to partially neutralize the beam. For H-, and a photon with an energy of 1.5eV, the maximum cross section for photo neutralization $H^- + \gamma \rightarrow H^0 + e^-$ is about 4.0* 10^{17} cm^2. Calculations of the cross section [7,8,9] and the particle yield [10] respectively in previous experiments [11] have demonstrated that a Nd:YAG laser (2nd harmonic Nd:YAG as well diode pumped solid state (DPSS) Lasers are also possible) can be used as an effective light source.

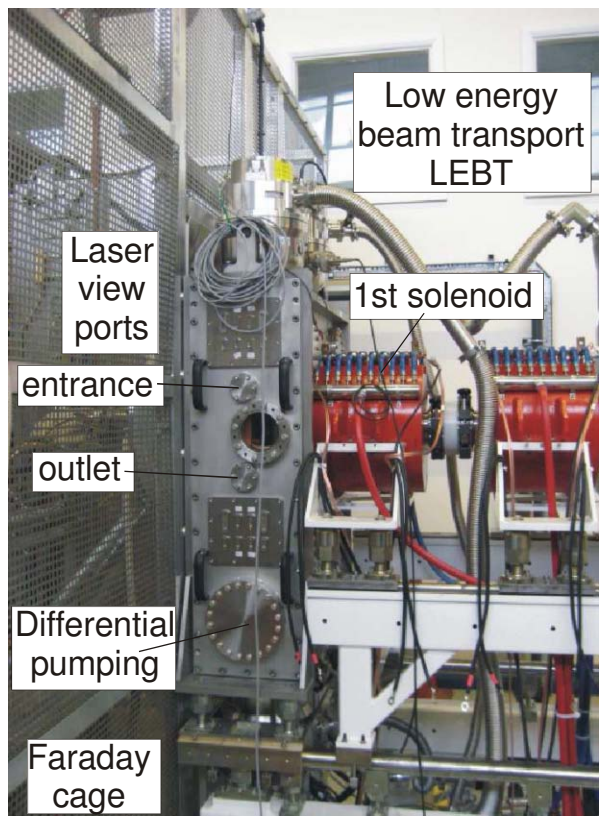

Fig 1: The differential pumping tank housing the detector with the laser mirrors. The first solenoid is as close as possible due to beam transport restrictions.

Behind the laser neutralization number and distribution of either the detached electrons or the neutrals produced in the interaction region can be analysed while the ion beam is still in use. Therefore charge separation, usually achieved using a magnetic dipole field, and a particle detector system are required. As neither the laser photons nor the recoiling photodetached electrons transfer a

MULTI-CHANNELTRON BASED PROFILE MONITOR AT THE ISIS PROTON SYNCHROTRON

S.A. Whitehead, P.G. Barnes, G.M. Cross, S.J. Payne, A. Pertica
STFC, ISIS Facility, Rutherford Appleton Laboratory, UK

Abstract

The gas ionisation beam profile monitor is a well established piece of diagnostic hardware. The use of active devices such as Microchannel Plates (MCPs) and Channeltrons within such a diagnostic can present problems with gain differences between channels. At the Rutherford Appleton Laboratory we have produced a beam profile monitor that uses an array of 40 individually powered Channeltrons; these devices were chosen over the MCP for their robustness and longer lifetimes. These Channeltron devices (like MCPs across their surface) can suffer from large variations in gain at the desired operating voltage. We have successfully shown that an additional in-built calibration system using a single, motorised, Channeltron can overcome these issues. We report on the work to build the calibration system, and the 40 Channeltron array. The PXI (National Instruments) system used to control the motor drive and provide the data acquisition is also covered. Also we report on the new high voltage drift field to reduce space charge effects on the beam profile. Ongoing work on understanding how the drift field as well the beam field affects the measured profile is also discussed.

INTRODUCTION

The ISIS facility at the Rutherford Appleton Laboratory is currently the world's most productive neutron spallation source. The rapid-cycling proton synchrotron operates at 50 Hz and accelerates two proton bunches (total of ~3.5×10^{13} protons) from 70 MeV to 800 MeV within the 10 ms acceleration period, delivering a total beam power of ~0.24 MW to the target. Accurate determination of the beam profile is important for improving injection and acceleration efficiencies as well as helping to reduce beam loss. Recent major upgrades to ISIS, like the 2nd harmonic system and Target Station 2, have resulted in higher beam currents within the accelerator ring. This increase in beam intensity has placed even more emphasis on the need for faster, more accurate profile monitors. This need has led to our current upgrade programme aimed at improving the ISIS profile monitoring systems.

ISIS RING PROFILE MONITORS

The original, and still used, gas ionisation profile monitors installed in the ISIS accelerator ring employ a single electron multiplier (Channeltron) to measure the +ion current produced from the interactions between the proton beam and the residual gas in the beam pipe. The single Channeltron profile monitor (SCPM) measures the beam profile in one plane only. The Channeltron is either stepped horizontally across the top of the proton beam or moved vertically up one side of the monitor. In each case the Channeltron covers a total distance of 240 mm in 5 mm steps. A high voltage drift field (30 kV) sweeps the +ions into the Channeltron device. At present we have five of these SCPMs, three measuring the horizontal plane and two measuring the vertical plane. Using these devices real-time profiles cannot be obtained because the mechanical system takes several minutes to complete each scan. The desire to obtain real-time profiles for setting up the synchrotron and carrying out machine physics studies of the ISIS beam has prompted the development of a new multi-channel profile monitor. This new monitor has an array of 40 fixed Channeltrons spanning 240 mm across the beam thereby allowing it to simultaneously collect beam profile information.

EVOLUTION OF THE MULTI-CHANNEL PROFILE MONITOR

The Channeltrons are manufactured by the company Photonis [1] (previously Burle Industries) and are their standard 4800 series device. These Channeltrons have a collection aperture of 15.75 mm × 4.5 mm and a gain of ~10^4 when biased with -1300 V (our normal operating voltage). An example of a 4800 device is shown in Figure 1.

Figure 1: Channeltron on left is the 4800 series of the Channeltron array. On the right is the 4700 series still used in the old SCPM.

The decision to use Channeltrons rather than a Microchannel Plate was influenced by a number of factors. As the existing single-channel profile monitor already used a Channeltron (Photonis type 4700 device, shown in Figure 1) we already had a good working knowledge of this technology. The 4800 series device is

OPERATIONAL USE OF IONIZATION PROFILE MONITORS AT FERMILAB*

James Zagel, Andreas Jansson, Thomas Meyer, Denton K Morris, David Slimmer, Todd Sullivan, Ming-Jen Yang, Fermilab, Batavia, IL 60439, U.S.A.

Abstract

Ionization profile monitors (IPMs) are installed in the Fermilab Booster, Main Injector and Tevatron. They are used routinely for injection matching measurements. For emittance measurements the IPMs have played a secondary role to the Flying Wires, with the exception of the Booster (where it is the only profile diagnostics). As Fermilab is refocusing its attention on the intensity frontier, non-intercepting diagnostics such as IPMs are expected to become even more important. This paper gives an overview of the operational use of IPMs for emittance and injection matching measurements at Fermilab, and summarizes the future plans.

INSTALLATION LOCATIONS AND OPERATING CONDITIONS

IPMs are used in three accelerators at Fermilab. Booster and Main Injector IPMs are designed to collect a data sample once per machine revolution. The Booster has two electrostatic units that collect ions using an 8 KV clearing field. These units collect data in the Booster throughout its complete operating cycle of about 20,000 turns. At injection (400 MeV) the revolution period is 2.25 µsec. At extraction (8 GeV) this period drops to 1.5 µsec. The Main Injector has two electrostatic units, one horizontal and one vertical, operating at 28 KV, collecting ions and producing data each 11.1 µsec. An additional horizontal unit was installed with a 1 KGauss magnetic field, and 10 KV clearing field which allows the collection of electrons,. The magnetic field confines liberated electrons to orbits smaller than the anode pick-up strips which minimizes the deleterious effect of space charge from the beam. The Main Injector IPMs are limited to the 65K samples of the current digitizer, however by skipping turns during acquisition, the full cycle can be measured. The Tevatron has two magnetic units of 1KGauss and a 10 KV clearing field. As explained later, these units are capable of sampling 36 proton and 36 antiprotons (pbars) bunches, turn by turn, for up to 1000 turns.

FRONT END INTERFACE

LabVIEW was chosen as the environment for the front end program because of its facilities for easily tying together different types of hardware (GPIB, VME, Ethernet) and software (Accelerator Control Network (ACNET), .dlls). The LabVIEW built-in graphical environment has also proved to be a significant help in debugging and commissioning the IPM systems. In normal operation, the system is controlled remotely through ACNET, but the front-end program provides complete functionality for running the system locally. Beam measurements are configured with a set of file based measurement specifications that include trigger and event types, timing delays, high voltage settings, analysis parameters, and logging preference. Measurements are initiated by activating a specification number through ACNET to the front end, which then configures the system hardware and waits for the specified trigger clock event. The triggering phase occurs in two parts. A pre-trigger is generated which initiates the hardware setup. and turns on the micro channel plate high voltage, This is followed by the event trigger, which starts the data acquisition. Data is collected using a beam synchronous clock. After acquisition, the front end analyzes the data using the selected parameters (turn by turn, averaging, start turn for analysis, and number of turns to analyze), and then returns the selected data and measurement parameters through ACNET. Raw data and measurement conditions are saved in binary files on the front end, and can be recalled into the front end program and reanalyzed.

The front-end code makes use of parallelism to take advantage of multi-core processors. There are three major tasks running: an event loop to detect front panel activity and handle ACNET commands, a monitor loop to track high voltage and receive remote commands, and a state machine to execute measurements and all other program functions. State machine functions are driven by a dynamically created command queue which can contain single or multiple commands. After the queued commands are executed, the state machine returns to an idle state. A second state machine was added to one of the IPM systems that does frequent measurements so that the front end could respond to select remote commands while it is waiting for a pre-trigger or trigger. The queue driven state machine design pattern has proved to be very flexible and efficient in operation, as well as easy to diagnose and debug system issues.

A significant benefit of using commercial PC's running LabVIEW is that it has enabled us to retain the front end hardware unchanged while being able to realize overall system performance improvements as faster PCs have become available.

ACNET CONSOLE INTERFACE

The ACNET user interface is comprised of two distinct parts, the console application page, and the pre-existing data collection engines.

*Operated by Fermi Research Alliance, LLC under Contract No. DE-AC02-07CH11359 with the United States Department of Energy.

RESIDUAL-GAS-IONIZATION BEAM PROFILE MONITORS IN RHIC*

R. Connolly, J. Fite, S. Jao, S. Tepikian and C. Trabocchi,
Brookhaven National Lab, Upton, NY, USA

Abstract

Four ionization profile monitors (IPMs) in RHIC measure vertical and horizontal beam profiles in the two rings (yellow and blue). These work by measuring the distribution of electrons produced by beam ionization of residual gas. In 2007 a prototype of a new design was installed in the yellow ring. During the 2007-2008 run it proved to be almost completely free from backgrounds from rf coupling, electron clouds and x-rays from upstream beam loss. In 2009 four new IPMs were built based on the prototype. During the 2009 shutdown two of these IPMs were installed. This paper describes the new IPMs and shows data from the 2010 beam run. The new IPMs have been extremely important in the commissioning of the RHIC stochastic cooling system.

INTRODUCTION

The Relativistic Heavy-Ion Collider (RHIC) at Brookhaven National Laboratory is a pair of concentric synchrotrons in which counter-rotating beams intersect at six points [1]. Beams ranging in mass from protons (E_{max}=250 GeV) to fully-stripped gold (E_{max}=100 GeV/nucleon) are accelerated and stored for several hours. There are detectors at two of the six intersection points for physics experiments with colliding beams.

Transverse beam profiles in RHIC are measured with ionization profile monitors (IPMs)[2,3,4,5]. An IPM collects the electrons in the beamline resulting from residual gas ionization during a bunch passage. The electrons are swept transversely from the beamline and collected on 64 strip anodes oriented parallel to the beam axis. After each bunch passes through the detector, the charge pulses are amplified, integrated, and digitized to give the bunch profile. Four IPMs are installed in RHIC to measure vertical and horizontal profiles in the two rings. Similar detectors are used at Fermi National Lab [6], DESY [7], and CERN [8].

The beam profile is measured primarily to find the transverse beam emittance which is the area occupied by the beam in transverse phase space, ie. (x,p_x) [3]. The beam radius at the IPM is equal to the square root of the betatron function, $\beta(s)$, times the emittance where s is the azimuthal coordinate of the IPM. The value of $\beta(s)$ is either calculated or measured and the beam radius is determined by profile measurements.

DETECTOR

Figure 1 is a schematic of the detector and its associated electronics in the accelerator tunnel. Figure 2 is a cutaway drawing and fig. 3 is a photo of the transducer. The detector chamber is located in a section of 10x15cm rectangular pipe. In an 18-cm-long section of this beam pipe half of the pipe has been removed and a saddle piece inserted. This saddle piece is biased at -6kV producing an accurate transverse electric field of $6x10^4$V/m.

A screen-covered rectangular opening in the grounded half of the beam pipe allows the signal electrons to pass through the image-current path to the detection assembly. The detection assembly is a 8x10cm microchannel plate (MCP) with a 64-channel anode etched on a ceramic circuit board. The collector board with attached MCP is located in an rf enclosure to prevent coupling to the beam. The only opening to this enclosure, which the signal electrons pass through, is a grounded aluminum honeycomb which attenuates rf by 80dB. Between the image-current bypass screen and the rf honeycomb window is a wire-screen control grid for gating the signal electrons off between measurements.

Each channel is connected via vacuum feedthrough to a preamplifier which drives a shielded twisted-pair transmission line to a 10MSPS VME digitizer.

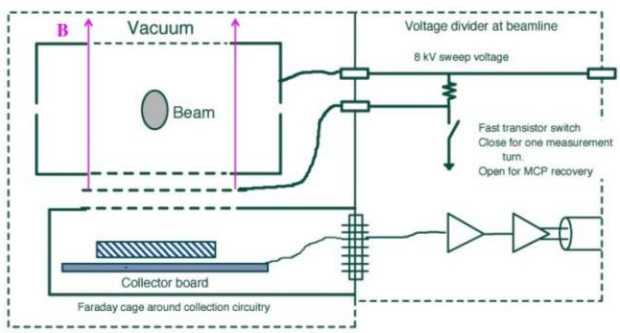

Figure 1: Schematic of detector and electronics located at the beamline.

In routine operation the signal-gating grid is biased at the sweep voltage of -6kV which prevents the signal electrons from passing. It is pulled to ground for a single turn (12μs) for measurement and returned to the off voltage. During this turn the digitizers are triggered. Each channel of an MCP has a dead time of about 1ms after firing. The intense heavy-ion beams of RHIC create such a large signal flux that the MCP becomes charge depleted very quickly. After a single measurement turn the grid is returned to -6kV for about 100 machine revolution periods for the MCP to recover. This is repeated 100 times and the data are averaged.

*Work performed by employees of Brookhaven Science Associates, LLC under Contract No. DE-AC02-98CH10886 with the U.S. Department of Energy.

BEAM-ENERGY AND LASER BEAM-PROFILE MONITOR AT THE BNL LINAC*

R. Connolly, B. Briscoe, C. Degen, L. DeSanto, W. Meng, R. Michnoff, M. Minty, S. Nayak, D. Raparia and T. Russo, Brookhaven National Lab, Upton, NY, USA

Abstract

We are developing a non-interceptive beam profile and energy monitor for H^- beams in the high energy beam transport (HEBT) line at the Brookhaven National Lab linac. Electrons that are removed from the beam ions either by laser photodetachment or stripping by background gas are deflected into a Faraday cup. The beam profile is measured by stepping a narrow laser beam across the ion beam and measuring the electron charge vs. transverse laser position. There is a grid in front of the collector that can be biased up to 125 kV. The beam energy spectrum is determined by measuring the electron charge vs. grid voltage. Beam electrons have the same velocity as the beam and so have an energy of 1/1836 of the beam protons. A 200 MeV H^- beam yields 109keV electrons. Energy measurements can be made with either laser-stripped or gas-stripped electrons.

INTRODUCTION

In 2002 we reported on a project at BNL to develop a beam profile monitor for H^- beams using photoneutralization by a laser beam directed perpendicular to the ion beam [1]. That effort was in support of the Spallation Neutron Source being built at Oak Ridge National Lab [2]. In 2008 we reported on a prototype profile and energy monitor developed at BNL for Fermi National Lab [3] to use on the High Intensity Neutrino Source project [4]. Based on the success of the Fermi device we received funding from the BNL Linac Isotope Producer (BLIP) facility [5] to build a detector to measure beam energy and transverse profiles in the linac HEBT.

An H^- ion has a first ionization potential of 0.75 eV and can be neutralized by the 1eV photons from a Nd:YAG laser (λ=1064nm). To measure beam profiles, a narrow laser beam is stepped across the ion beam, removing electrons from the portion of the H^- beam intercepted by the laser. These electrons are deflected into a Faraday cup by a magnetic field. To measure the energy distribution of the electrons, the laser position is fixed and the voltage on a screen in front of the Faraday cup is raised in small steps.

*Work performed under Contract #DE-AC02-98CH10886 under the auspices of the US Department of Energy.

At the time of this writing, the laser platform is not yet installed. However we found that accurate energy measurements can be made on high-current beams (>5mA) by measuring the electrons stripped from the beam by background gas. Electrons are stripped by the residual gas in the beamline at a rate of ~1.5×10^{-8}/cm at 1×10^{-7} torr. In this detector a 30 mA beam produces about 40 nA of electron current.

In this paper we describe the detector and show results from the gas-stripped energy measurements.

DETECTOR

Figure 1 is a cutaway diagram of the detector from the side showing the signal-electron path. The neutralization chamber is a six-way cross with the laser beam passing through viewports either horizontally or vertically. An optics plate with the laser head and scanning optics is mounted on this chamber. The 100mJ/pulse, Q-switched Nd:YAG laser neutralizes 70% of the beam it intercepts during the 10ns pulse. The laser beam is scanned across the ion beam by reflecting it from a 45° mirror mounted on a linear translation stage.

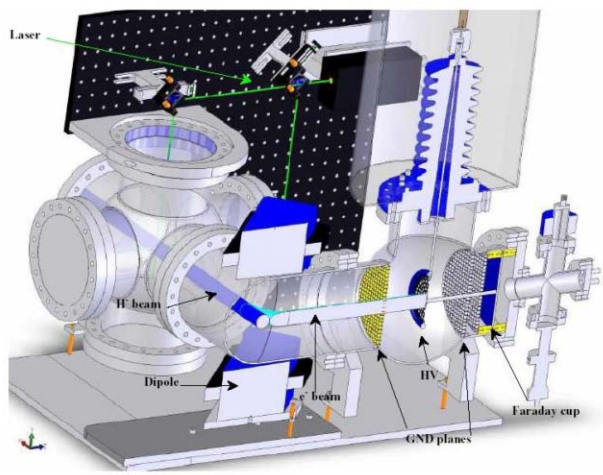

Figure 1: Cutaway schematic. Electrons from the H^- beam are deflected by a magnet through a HV grid into the Faraday collector.

Downstream a dipole magnet deflects the signal electrons 90° into the retarding grid and Faraday cup assembly. A corrector magnet upstream keeps the ion beam straight. A voltage grid in front of the collector

DATA AND ANALYSIS FROM A TIME-RESOLVED TOMOGRAPHIC OPTICAL BEAM DIAGNOSTIC*

Daniel K. Frayer#, Douglas Johnson, National Security Technologies, LLC,
Los Alamos, NM 87544, U.S.A.
Carl Ekdahl, Los Alamos National Laboratory, Los Alamos, NM 87545, U.S.A.

Abstract

An optical tomographic diagnostic instrument developed for the acquisition of high-speed time-resolved images has been fielded at the Dual-Axis Radiographic Hydrodynamic Test (DARHT) Facility at Los Alamos National Laboratory. The instrument was developed for the creation of time histories of electron-beam cross section through the collection of Cerenkov light. Four optical lines of sight optically collapse an image and relay projections via an optical fiber relay to recording instruments; a tomographic reconstruction algorithm creates the time history. Because the instrument may be operated in an adverse environment, it may be operated, adjusted, and calibrated remotely. The instrument was operated over the course of various activities during and after DARHT commissioning, and tomographic reconstructions reported verifiable beam characteristics. Results from the collected data and reconstructions and analysis of the data are discussed.

INTRODUCTION

Kaufman et al. (2006) [1] describe design considerations for the development of a time-resolved diagnostic system for use at the Dual-Axis Radiographic Hydrodynamic Test (DARHT) Facility at Los Alamos National Laboratory. This design was finalized and the diagnostic instrument was fabricated, calibrated, and fielded. Frayer et al. (2008) [2] give the final system description and discuss characterization, qualification, integration, and preliminary experimental results.

In brief, the DARHT facility is designed to record high-speed radiographic images of explosively driven hydrodynamic events. This is accomplished by the illumination of a test object with x-ray pulses that occur within a 2 μs envelope and the recording of the resulting radiographic images. The x-ray pulses are generated by illuminating x-ray converter targets with high-power electron beams along two orthogonal axes.

The tomographic instrument was developed to create time histories of the DARHT electron beam when the DARHT second axis was being commissioned. Four discrete optical subsystems with distinct lines of sight view, through a 6-inch window in a pump cross, Cerenkov light generated by the beam incident upon a inside the vacuum envelope. Each subsystem employs cylindrical optics to image light in one direction and collapse light in the orthogonal direction. Each of the four images and collapses in unique axes, thereby capturing information as a projection. Light along the imaging axes is relayed via optical fiber arrays and is recorded by streak cameras coupled to CCDs, resulting in temporal resolution of 2 ns over a recording window of 2 μs. Computer software then reconstructs a two-dimensional time history of the electron beam from the four optically collapsed one-dimensional (1-D) histories.

Two versions of this diagnostic have been built and fielded: a system with two lines of sight, as described by Bender et al. (2007) [3] and used in early stages of DARHT commissioning [4] and an earlier four-view system [5]. Both systems were fielded at DARHT in easily accessible, low-environmental-risk areas. This third-generation diagnostic was designed to be fielded in an area with restricted access and higher environmental risk, and to have the ability to change optical parameters during experiments. Although the optical design is similar to that of its predecessors, this instrument is necessarily more advanced as it offers remote calibration and remote control of optical magnification, focus, and aperture. This version of the instrument was fielded at DARHT in February, 2008, and has been operational since.

Figure 1: The DARHT tomographic instrument.

We first provide a brief treatment of the methodology used in reconstructing time-resolved images from the individual datasets. We give requirements upon the system for results of such reconstruction, as well as

*This work was done by National Security Technologies, LLC, under Contract No. DE-AC62-06NA25946 with the U.S. Department of Energy.
#frayerdk@nv.doe.gov

LANSCE WIRE SCANNING DIAGNOSTICS DEVICE MECHANICAL DESIGN

Sergio Rodriguez Esparza, Los Alamos National Laboratory, Los Alamos, NM USA

INTRODUCTION

The Los Alamos Neutron Science Center (LANSCE) is one of the major experimental science facilities at the Los Alamos National Laboratory (LANL). The core of LANSCE's work lies in the operation of a powerful linear accelerator, which accelerates protons up to 84% the speed of light. These protons are used for a variety of purposes, including materials testing, weapons research and isotopes production. To assist in guiding the proton beam, a series of over one hundred wire scanners are used to measure the beam profile at various locations along the half-mile length of the particle accelerator. A wire scanner is an electro-mechanical device that moves a set of wires through a particle beam and measures the secondary emissions of electrons from the resulting beam-wire interaction to obtain beam intensity information. When supplemented with data from a position sensor, this information is used to determine the cross-sectional profile of the beam. This measurement allows beam operators to adjust parameters such as acceleration, beam steering, and focus to ensure that the beam reaches its destination as effectively as possible. Some of the current wire scanners are nearly forty years old and are becoming obsolete. The problem with current wire scanners comes in the difficulty of maintenance and reliability. The designs of these wire scanners vary making it difficult to keep spare parts that would work on all designs. Also many of the components are custom built or out-dated technology and are no longer in production.

DESIGN CRITERIA

The first design criterion is that the wire scanner should be constructed with as many commercially available off-the-shelf components as possible. This will facilitate having spare parts that can fit multiple wire scanners. This is similar to the wire scanner design of the Oak Ridge National Laboratory (ORNL) Spallation Neutron Source (SNS) wire scanner. The second criterion is that the wire scanner should be capable of 1mm movements at 4Hz (1mm in 250ms) with a triangular velocity profile as illustrated in Figure 1. Notice that for the area under the curve to be 1mm, the peak velocity must be 8mm/s half way through the motion. This yields an acceleration of 64mm/s² (Note: 1g = 9807mm/s^2). Third, the position of the wires at the end of the "fork" must be known within ±1mm with respect to an external monument. Also, the repeatability of the system must be within ±0.1mm. Fourth, the motor must be powered off while taking a measurement at each bin location. Lastly, the wire scanner should be designed to accommodate as many existing beam structures as possible.

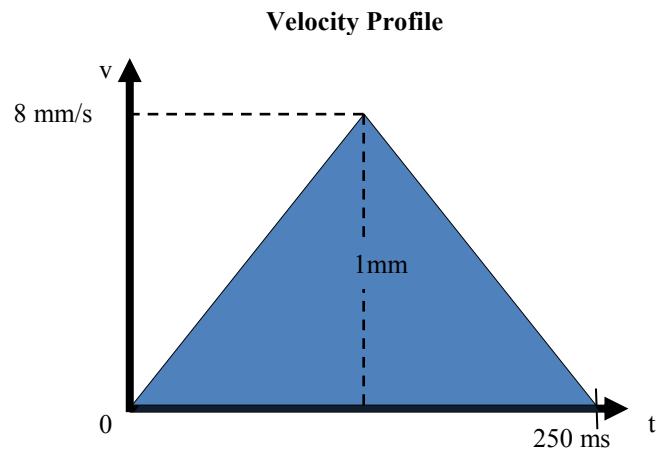

Figure 1: Velocity profile for the wire scanner.

MECHANICAL DESIGN

As mentioned above, the first design criterion resembles that used by ORNL and likewise does so the mechanical design. Figure 2 shows the ORNL wire scanner design.

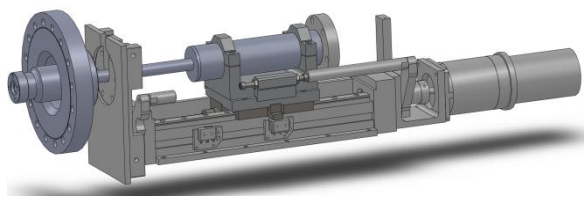

Figure 2: ORNL SNS wire scanner design.

The ORNL SNS wire scanner design has been modified to fit our current beam structures and our design specifications. Figure 3 shows the LANSCE future wire scanner design.

LANSCE HARP UPGRADE: ANALYSIS, DESIGN, FABRICATION, AND INSTALLATION*

J. Douglas Gilpatrick#, Phillip Chacon, Derwin Martinez, John F. Power, Brian G. Smith, Mark A. Taylor, LANL, Los Alamos, NM 87545, U.S.A., and

M. Gruchalla, EG&G Albuquerque Operations, Albuquerque, NM 87107, U.S.A.

Abstract

The primary goal of this newly installed beam profile measurement is to provide the facility operators and physicists with a reliable horizontal and vertical projected beam distribution and location with respect to the proton beam target and beam aperture. During a 3000-hour annual run cycle, 5 μC of charge is delivered every 50 milliseconds through this harp to the downstream TRMS Mark III target. The resulting radioactive annual dose near this harp is at least 6 MGy. Because of this harsh environment, the new harp design has been further optimized for robustness. For example, compared to an earlier design, this harp has half of the sensing wires and utilizes only a single bias plane. The sensing fibers are 0.079-mm diameter SiC fibers. To hold these fibers to a rigid ceramic structure, a collet fiber-clamping device accomplishes the three goals of maintaining a mechanical fiber clamp, holding the sense fibers under a slight tensile force, and providing a sense-fiber electrical connection. This paper describes the harp analysis and design, and provides fabrication, assembly, and some installation information, and discusses wiring alterations.

INTRODUCTION

The Los Alamos Neutron Science Center (LANSCE) facility primary beam target, TRMS Mark III, has been replaced [1]. This target's primary goal is to convert 800-MeV protons to various energetic neutrons. In order to perform this conversion efficiently, the incoming proton beam position and width are measured using a common measurement device known as the "harp" that samples the transverse profile with respect to the beam pipe aperture. The interesting aspect of this particular harp is that due to its location, inside the TRMS Mark III target, it is in a very harsh environment. For a single 3000-hour annual run cycle, this particular harp is expected to receive 6 MGy of absorbed dosage [2]. Since the expected target lifetime is at least 5 years, the harp will receive at least 30 MGy. Therefore, its design should be sufficiently robust to withstand this harsh environment.

1L HARP THEORY

The 1L harp's principle of operation is very basic (Figure 1). Fibers sample the projected beam charge distribution in two orthogonal planes. An intervening plane of fibers between the two signal planes is biased such that secondary electrons emitted from one signal plane are not allowed to impinge on the second signal plane. Generally, a small amount of the proton beam's energy deposited into the fiber and is converted to emitted secondary electrons (SE). The current flow of these SE leaving the fiber is measured by external electronics to produce a series of amplitudes for each projected beam distribution.

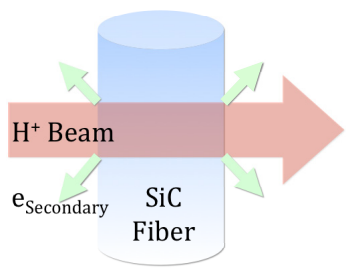

Figure 1: The 800-MeV beam passing completely through the SiC fiber and depositing a small amount of the beam's energy. A subsequent amount of the deposited beam energy is converted to SE emission.

*Work supported by US Department of Energy
#gilpatrick@lanl.gov

RESOLVER-BASED, CLOSED-LOOP POSITION AND VELOCITY CONTROL FOR THE LANSCE-R WIRE SCANNER*

J. Sedillo, LANL, Los Alamos, NM 87545, U.S.A.

Abstract

This study evaluates a technique for the closed-loop position and velocity control of a wire scanner actuator. The focus of this technique is to drive a stepper motor-driven actuator through a 1-mm move using a combination of velocity feedback control and position feedback control. More specifically, the velocity feedback control will be utilized to provide a smooth motion as the controller drives the actuator through a pre-planned motion profile. Once the controller has positioned the actuator within a certain distance of the target position, the controller will transition to position-based feedback control, bringing the actuator to its target position and completing the move. Position and velocity data is presented detailing how the actuator performed relative to its commanded movement. Finally, the layout of, and algorithms employed by the wire scanner control system are presented.

INTRODUCTION

A goal of the LANSCE-R wire scanner design is that it possess the ability to utilize closed-loop feedback for the positioning of the wire scanner actuator. The focus of this study is to describe a controller that utilizes a velocity controller to provide smooth acceleration, cruise, and deceleration motions until finally handing-over control to the position controller to bring the actuator position to within some distance of the desired position.

For this evaluation, a LEDA wire scanner was used. This wire scanner is driven by a Parker OS22B stepper motor coupled to a Moog resolver. A National Instruments compact RIO 9074 was used as the controller. As is typical in general for closed-loop control systems; in order to position the actuator, the controller reads the sensor data of the resolver, compares the resolver data with a commanded set point, and then acts on the drive mechanism (i.e. motor) to drive the actuator to the commanded set point. The drive pulse rate was limited to any frequency within the range of 15.2 Hz to 2.5 kHz.

POSITION AND VELOCITY CONTROLLER

Position Controller

The position controller (algorithm shown in figure 1) reads the actuator position data from the RDK 9314 (resolver-to-digital converter) module and subtracts that position from the commanded position resulting in a position error e(t). This error is then fed into a proportional, integral, and derivative controller. The proportional controller simply multiplies the position error by a constant known as the proportional control constant K_p (unitless). The proportional control constant has the effect of driving the actuator at a higher rate of speed if the position error is large, and a lower rate of speed if the position error is small. The derivative portion of the controller subtracts the present value of the position by the previous position value. This result is then multiplied by the derivative control constant K_d (μseconds).

Generally, the derivative controller is beneficial for command tracking since it detects deviations in the rate of change between the commanded and measured positions (a.k.a. position error). The larger the deviation in the rate of change of the error, the more severely it acts to correct the error. Finally, an integral controller simply sums the position error over time.

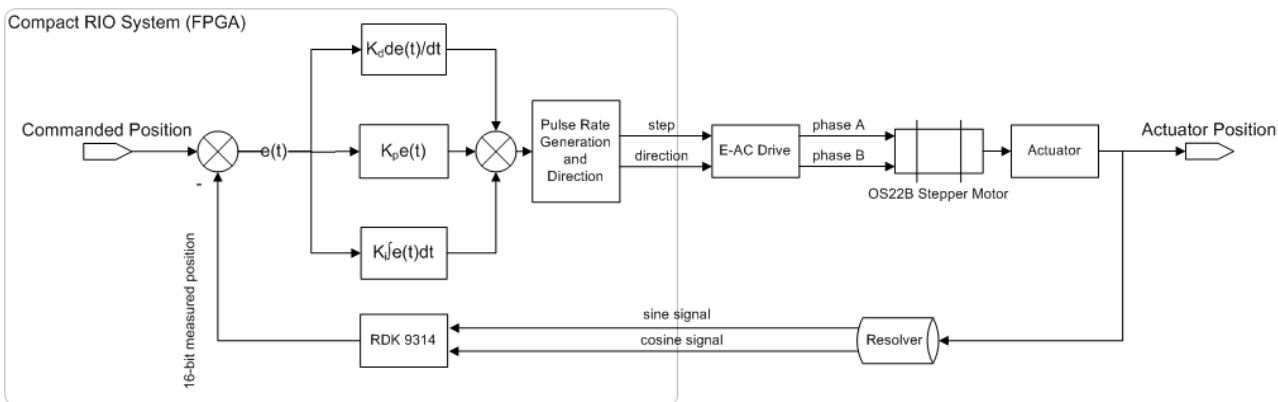

Figure 1: Position Controller Algorithm.

*Work supported by U.S. Department of Energy

LANSCE WIRE SCANNER AFE: ANALYSIS, DESIGN, AND FABRICATION*

M. Gruchalla#, EG&G Albuquerque Operations, Albuquerque, NM 87107, U.S.A.

P. Chacon, J. D. Gilpatrick, D. Martinez, J. Power, B. Smith,

Los Alamos National Laboratory, Los Alamos, NM 87545, U.S.A.

Abstract

The goal of the design LANSCE-R Wire-Scanner Analog Front-end Electronics is to develop a high-performance, dual-axis wire-scanner analog front-end system implemented in a single cRIO module. This new design accommodates macropulse widths as wide as 700μs at a maximum pulse rate of 120Hz. A lossey integrator is utilized as the integration element to eliminate the requirement for providing gating signals to each wire scanner. The long macropulse and the high repetition rate present conflicting requirements for the design of the integrator. The long macropulse requires a long integration time constant to assure minimum integrator droop for accurate charge integration, and the high repetition rate requires a short time constant to assure adequate integrator reset between macropulses. Also, grounding is a serious concern due to the small signal levels. This paper reviews the basic Wire Scanner AFE system design implemented in the cRIO-module form factor to capture the charge information from the wire sensors and the grounding topology to assure minimum noise contamination of the wire signals.

INTRODUCTION

One element of the LANSCE-R task is to replace a number of the aging wire-scanner systems. Both the mechanical components and the electronics are to be replaced.

The National Instruments cRIO system has been selected as the basic platform for the wire-scanner electronics [1]. To the extent feasible, commercial of-the-shelf (COTS) cRIO modules are being utilized with custom modules for specific tasks designed specifically for the LANSCE-R application. The Wire-Scanner Analog Front-end Electronics (WS AFE) is a custom cRIO module.

The WS AFE independently collects and integrates the charge from two orthogonal sensing wires and delivers the processed analog signal to cRIO digitizers. The goal for the LANSCE-R application is to provide the ability to capture macropulses as long as 700μs at a maximum macropulse rate of 120Hz. The long macropulse and the short inter-pulse period present a unique challenge in the design of the integration function of the WS AFE.

The small signal levels expected at the extremes of the beam distribution require careful attention to minimizing noise encroachment into the WS AFE signal paths. It is reasonably expected that there will be a substantial potential difference between the beam-line equipment ground and the electronics equipment ground. This represents a nuisance potential that could corrupt the wire-scanner data. Therefore, management of the grounding between the beam line and the instrumentation is critical.

DESIGN STRATEGIES

The LANSCE accelerator is a production system, as compared to a purely experimental accelerator, and the wire scanners are diagnostic tools used to manage system operation. In comparison to typical experimental venues, the magnitude and spectrum of the wire-scanner signals expected in the LANSCE accelerator are very-well bounded. This relieves some of the complexity of the WS AFE by allowing functions typically required in the wire scanner to be moved into other elements of the system. Several of the more critical design challenges are reviewed below.

Measurement Dynamic Range

The maximum total collected charge in a macropulse is a function of the wire-scanner location in the LANSCE accelerator. The dynamic range of collected charge across all locations at the distribution center is less than nominally 100. The dynamic range required in the measurement at any specific position has been set at nominally 100. Therefore, a total dynamic range of 10,000 is required in the WS AFE system so that any WS AFE unit may be utilized at any position [2].

Normally, the WS AFE would include analog gain switching to accommodate a very wide operational dynamic range. Since only a nominal 10,000 dynamic range is required in the LANSCE-R application, this may be totally provided in the cRIO digitizers. A National Instruments NI 9205 cRIO digitizer is utilized to digitize the WS AFE analog signals. The NI 9205 is a 16-bit plus sign digitizer and provides four full-scale sensitivities: ±10V, ±5V, ±1V and ±200mV. This unit provides a theoretical dynamic range of 3e6 with a basic precision of 3μV.

Measurement Sensitivity

The measurement sensitivity required is a function of how far down in the distribution data is desired at the position in the accelerator providing the lowest signals.

*Work supported by US Department of Energy

#gruch@lanl.gov

A STATISTICAL ANALYSIS OF THE BEAM POSITION MEASUREMENT IN THE LOS ALAMOS PROTON STORAGE RING*!

J. Kolski#, R. Macek, R. McCrady, LANL, Los Alamos, NM 87545, U.S.A.

Abstract

The beam position monitors (BPMs) are the main diagnostic in the Los Alamos Proton Storage Ring (PSR). They are used in several applications during operations and tuning including orbit bumps and measurements of the tune, closed orbit (CO), and injection offset. However, the BPM data acquisition system makes use of older technologies, such as matrix switches, that could lead to faulty measurements. This is the first statistical study of the PSR BPM performance using BPM measurements. In this study, 101 consecutive CO measurements are analyzed. Reported here are the results of the statistical analysis, tune and CO measurement spreads, the BPM single turn measurement error, and examples of observed data acquisition errors.

INTRODUCTION

A PSR BPM is a collection of four stripline electrodes located in the beam pipe and situated top, bottom, left, and right. The BPM diameters are 4″ and 6″. They are tuned to the 201.25 MHz longitudinal structure of the beam and are a 201.25 MHz quarter wavelength long, ~37 cm. A mechanical relay matrix switch (MUX) selects the BPM for measurement. There are four MUXs to interface with each of the four BPM electrodes. Beam signals from the selected BPM pass the MUX to the analog front end (AFE) where the signals are converted from AM to PM. The AFE outputs a voltage proportional to the power ratio deposited on opposing BPM electrodes [1]. The voltages are digitized by a 12-bit analog to digital converter (ADC). The intrinsic BPM resolutions (defined as the BPM diameter divided by 2 to the power of the bit depth, $d/2^b$) are .0124 mm and .0186 mm for the 4″ and 6″ BPMs respectively. The ADC is triggered to digitize data by a beam present trigger. The digitized voltages are read to the input/output controller (IOC) where they are converted back to beam positions using geometric coefficients and AM-PM theory [2, 3]. The position data is lastly read by EPICS.

There are 18 real and two "missing" BPMs in the PSR. The missing BPMs do not exist, but data is still collected. The missing BPMs are included in the analysis because they possess information about the data acquisition errors. For the convenience of analysis, an orbit response matrix (ORM) BPM naming convention is employed. This convention distinguishes the two dimensions of a single BPM, dividing a bi-directional BPM into two different BPMs, a horizontal and vertical BPM. The convention then gathers all BPMs of the same direction and numbers them consecutively. Thus, the 20 BPMs in the PSR are divided into 40 different BPMs. BPMs 1-20 are the horizontal BPMs and BPMs 21-40 are the vertical BPMs such that BPM 1 and BPM 21 are the horizontal and vertical division of SRPM01, BPMs 2 and 22 are the horizontal and vertical parts of SRPM02, and so on. The missing BPMs are indexed as BPMs 10, 15, 30, and 35.

MEASUREMENT SETUP AND DATA ANALYSIS

The PSR was set up for single turn injection and after ~1800 turns, extraction to the tune up beam stop (TUBS) at 20 Hz. The vertical bump magnets and the harmonic buncher that respectively allow phase space painting in the vertical and keep the beam bunched longitudinally were turned off. The CO was centered. The beam was injected near-on-axis ([-0.72 mm, 0.31 mradian] in the horizontal and [1.99 mm, -0.168 mradian] in the vertical) to avoid scraping and BPM saturation. Injecting near-on-axis allowed for 40 turns of turn-by-turn beam positions to be collected before the 201.25 MHz longitudinal structure of the beam washed out due to momentum variation in the mircopulses. The energy of the beam was corrected using the time of flight for 1100 turns.

One hundred one consecutive CO measurements were taken for the same PSR configuration. Each CO measurement consists of 40 turns of turn-by-turn beam position data at each BPM. Since a MUX is employed to select the BPMs, data from only one BPM can be recorded per machine cycle. The CO is measured at each BPM on a different pulse with slightly different central momentum (different CO) due to the pulse-to-pulse momentum variations in the linac. It took 7.5 minutes to take 101 CO measurements.

As the beam circulates around the ring, it performs harmonic (betatron) oscillation about the CO. Thus, the turn-by-turn BPM data is then fit to a cosine wave,

$$y_n = A\cos(2\pi\nu n + \phi) + O_{offset} \qquad (1)$$

where y_n is the turn-by-turn BPM data, n ranges from 1 to 40; A, ν, ϕ, and O_{offset} are the amplitude, betatron tune, phase, and CO respectively. A nonlinear least squares fitting routine was used to fit for A, ν, ϕ, and O_{offset}. The sum of squares of residuals per degree of freedom (SSR/DOF) was used as the goodness of fit quality factor. A maximum likelihood (ML) error analysis was applied to calculate the fitting error on the fitting parameters, the single turn BPM measurement error, and the covariance and correlation matrices relating the fitting parameters. Aside from the tune and the phase, the fitting parameters were found to be uncorrelated. The tune and the phase

*Work supported by the US DOE under contracts DE-AC52-06NA25396 and DE-FG02-92ER40747 and the NSF under contract NSF PHY-0852368.
! LA-UR 10-02364
jkolski@lanl.gov

LIGHT YIELD, IMAGING PROPERTIES AND SPECTRAL RESPONSE OF INORGANIC SCINTILLATORS UNDER INTENSE ION IRRADIATION

E. Gütlich, W. Ensinger, Technical University Darmstadt, Germany
P. Forck, R. Haseitl, B. Walasek-Höhne, GSI Helmholtz Centre for Heavy Ion Research GmbH, Darmstadt, Germany

Abstract

Scintillating screens are widely used for transverse beam profile monitoring and pepper-pot emittance measurements at accelerator facilities.
For high current beam operations at the GSI heavy ion UNILAC, several inorganic scintillators were investigated under different ion beam conditions. The imaging properties of various materials were studied with respect to light yield and imaged beam width.
The measured properties show a strong dependence on the scintillating material and change significantly with screen temperature. The spectral response of the materials was mapped for different temperature levels, using a spectrometer in the visible and near UV range. The results clearly demonstrate that their temperature behaviour and scintillating properties are critical issues for high current operations and have to be taken into account for correct beam profile reading.

INTRODUCTION

Scintillating screens are a direct but intercepting method to observe an ion beam. Profile measurements are important for controlling the spatial distribution of the ion beam, as well as the matching of the different parts of the accelerator from the ion source to the experimental area. Depending on beam current and energy, a large variety of scintillating materials can be used.
Additionally scintillating screens are an essential part of a single shot pepper-pot emittance measurement system used for the determination of the width of 'beamlets' created by a plate with several small holes. The realization at GSI used for the high current operation of UNILAC is described in [1]. The angular distribution within the phase space can be calculated from the intensity distribution of the 'beamlets'. The precise measurement of the spot's light distribution requires a linear light output without saturation effects from the scintillating material and has to match the optical sensitivity of the CCD camera. To observe possible (time dependent) variations of the beam size a short decay time is necessary. The scintillating material has to be radiation hard and it is necessary to ensure that the material is not destroyed by ion beam irradiation during high current operation (see Fig. 1). For precise profile reading the heating of the scintillating material due to the energy loss has to be considered [2].

Several scintillating materials (Table 1) were investigated with different ion beams from protons up to Uranium at energies between 4.8 and 11.4 MeV/u and different beam currents as delivered by the GSI linear accelerator. Standard scintillators like YAG:Ce or BGO could only be used for low beam currents in the range of some nA [4]. For the high intensity ion beams, ceramic materials and quartz glass have to be applied [2].

Table 1: Investigated materials

Type	Material	Supplier
Crystal scintillator	YAG:Ce, BGO, $CdWO_4$, CaF_2:Eu	Saint Gobain Crystals
Powder	ZnS:Ag	HLW
Ceramics	ZrO_2:Al, ZrO_2:Y (YSZ), ZrO_2:Mg, BN, SiN, SiC, AlN, Al_2O_3, Al_2O_3: Cr	BCE Special Ceramics
Quartz glass	Herasil 102, SiO_2:Ce (M382)	Heraeus Quarzglas

EXPERIMENTAL SETUP

For systematic measurements a movable target ladder (see Fig. 1) with six different scintillating materials was used. This experimental setup allowed to test different materials under identical beam conditions without breaking the vacuum (typical $5 \cdot 10^{-7}$mbar).

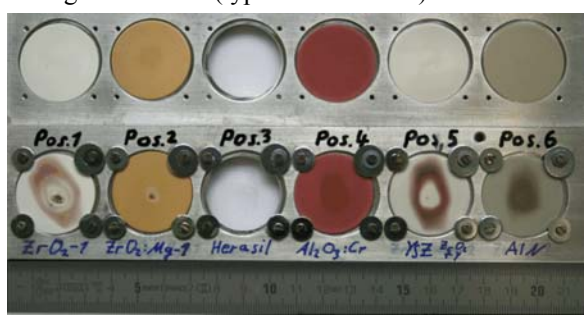

Figure 1: Target ladder with six different scintillating materials before (upper row) and after 100 pulses of U^{28+} ion beam (lower row). Beam parameters: $5.2 \cdot 10^{10}$ particles per pulse (ppp) at 4.8 MeV/u, 0.8 ms pulse length and 0.5 Hz repetition rate. Target modifications after irradiation are visible.

The scintillating screens were monitored with a monochrome CCD camera (AVT Stingray F033B, 8-bit ADC and VGA resolution). Due to the material dependent light yield a lens system with remote controlled iris (Pentax, 25 mm focal length) was implemented. With this experimental setup a resolution of 10 px/mm was achieved. The software BeamView [5] was used for data acquisition. The camera was connected to a PC which runs the server part of BeamView. The images were

BEAM INDUCED FLUORESCENCE MONITOR - SPECTROSCOPY IN NITROGEN, HELIUM, ARGON, KRYPTON AND XENON GAS

F. Becker*, P. Forck, T. Giacomini, R. Haseitl, B. Walasek-Hoehne, GSI, Darmstadt, Germany

F.M. Bieniosek, P.A. Ni, LBNL, Berkeley, California, D.H.H. Hoffmann, TU-Darmstadt, Germany

Abstract

As conventional intercepting diagnostics will not withstand high intensity ion beams, Beam Induced Fluorescence (BIF) profile monitors constitute a pre-eminent alternative for non-intercepting profile measurements [1]. This diagnostic technique makes use of the optical fluorescence emission of beam-excited gases. Recently BIF became an important diagnostic tool for transversal beam profile measurements with applicability in beam tuning over a wide range of beams and accelerator conditions [2]. In this paper optical VIS-spectroscopy with an imaging spectrograph for 5 MeV/u proton, S^{6+} and Ta^{24+} beams in nitrogen, Xe, Kr, Ar, Ne and He at 10^{-3} mbar gas pressure is presented. Atomic physics processes are a major performance issue, since they determine transition intensities and lifetimes of excited states. Further investigations are required to improve the detector performance and increase its range of application.

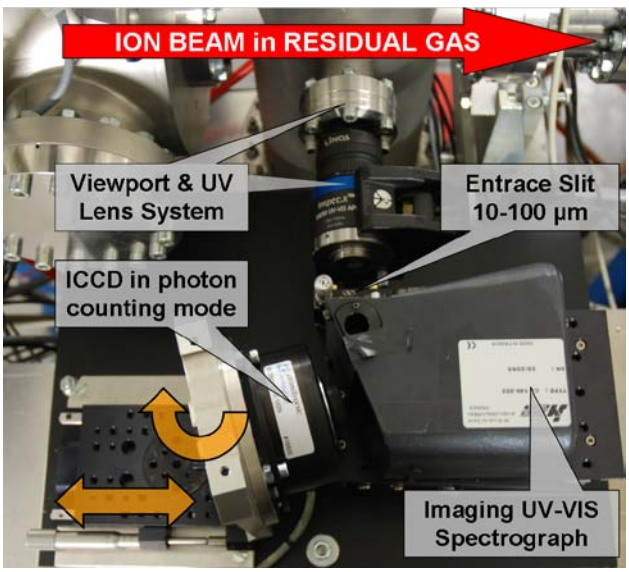

Figure 1: Top-view of the optical setup looking onto the diffractive plane. Length of spectrum in the image plane is 10 mm. 1:1 imaging from slit to image plane. All refractive optics adapted to UV-VIS [4]. ICCD performs single photon detection including a Ø 25 mm UV-enhanced photocathode with a V-stack MCP [5] and digital VGA 8-bit greyscale camera [6].

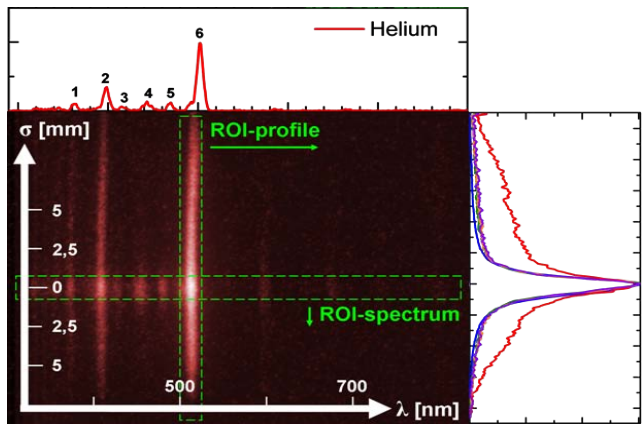

Figure 2: Spectrographic average image of n=2000 pulses of $3{\cdot}10^{11}$ S^{6+} ions @ 5.16 MeV/u in 10^{-3} mbar helium gas, σ_w=1.8 mm. Log colour-scale for better illustration. Projections yield either spectra (upper) or profiles (right).

EXPERIMENTAL SETUP

Key issue of this experimental layout using an imaging spectrograph with an area scan intensified CCD (ICCD) camera (Fig. 1) was to have both, the spectral information of specific beam induced gas transitions along the diffraction axis and the spatial information about the beam profile width, transition wise along the imaging axis, see Figure 2. For 150 mm object distance, a chromatically corrected UV-lens of f = 50 mm and f/2.8 was chosen. A CCD height of 4.9 mm and a total reproduction scale β_{tot} = 0.42 yield a 19.5 mm field of view, covering ~ $5{\cdot}\,\sigma_w$.

Imaging Spectrograph & Gas Composition

The spherical mirror (Ø 70 mm) with 140 mm focal length is holographically etched and astigmatism corrected. 140 sinusoidal grooves per mm produce a spectral dispersion of 50 nm/mm and an image field of 8x12 mm on the vertical imaging axis and the horizontal dispersive axis, respectively. With an optical resolution of 33 lp/mm the ICCD limits the spectral resolution to 1.5 nm for an entrance slit ≤ 30 µm. The total spectral system efficiency includes all single component efficiencies as a convolution, see Fig. 3 (upper plot). Most limiting factors for increasing wavelength ≥ 600 nm are the tri-alkali $(Na_2KSb)Cs$ photocathode and the decreasing grating-efficiency. Investigation of optical gas spectra relies on a

* Frank.Becker@gsi.de

PHOTON BEAM POSITION MEASUREMENTS BY LIBERA PHOTON USING COPPER BLADE SENSORS AT SOLEIL SYNCHROTRON

P. Leban, D.Tinta, Instrumentation Technologies, Solkan, Slovenia
N. Hubert, J.C. Denard, SOLEIL Synchrotron, Gif-sur-Yvette, France

Abstract

Libera Photon is the new Photon Beam Position processor (PBPM) from the Instrumentation Technologies. First measurements on real beam have been done at SOLEIL Synchrotron. The module was connected to a PBPM installed on the DIFFABS bending magnet beam line. Three different beam position experiments were done: measurement of position at beam bump (+/- 500 µm), beam current dependence and filling pattern dependence. Measurements were done with internal BIAS voltage source set to -70 V. Measured current was in the range up to 250 µA on the sensor. Measurements were done on standard 100 kS/s, 10 kS/s and 10 S/s data flows with different bandwidths. The article discusses the results and consequential improvements of the device.

INSTRUMENTATION

Libera Photon is a photon beam position processor, which features current-to-voltage conversion, digitalization and signal processing. The output data flows are delivered with different rates (100 kS/s, 10 kS/s and 10 S/s) and can be accessed simultaneously. The acquisition can be performed using Matlab, Tango or EPICS clients.

Input currents were in the range up to 200-250 µA per input. Libera Photon features Automatic Range Control (ARC) with 7 ranges: ±2 nA, ±20 nA, ±200 nA, ±2 µA, ±20 µA, ±200 µA and ±1,85 mA. ARC adapts the I/U converter values automatically according to the input signal level. During our tests, the measurement range was set manually.

Blade sensors were copper type. It requires BIAS voltage to extract the photons. BIAS voltage was supplied by the Libera Photon unit and was set to -70 V. There were 2 XBPM sensors placed in the storage ring front-end: Libera Photon unit was connected to the first one (XBPM1), whereas Soleil analog device was used on the second one (XBPM2) to be used as a comparison. XBPM1 sensor is placed 4,7 metres from the source point, XBPM2 is placed 7,73 metres from the source point.

MEASUREMENTS

The following measurements were done on the beamline: beam bump measurement, beam current dependence measurement, filling pattern dependence measurement and noise measurement. Beside tests in the beamline, beam current dependence and noise measurements were done also under laboratory conditions.

All data, presented in this paper, were acquired at 10 kS/s (DD buffer) or at 10 S/s (SA) data rates.

Beam bump measurement

Slow orbit feedback and Fast orbit feedback in the storage ring were disabled in order to be able to displace the photon beam. Transverse feedback was enabled all the time. Filling pattern was multi bunch 4/4. Photon beam was displaced from -500 µm to +500 µm by steps of 100 µm using correctors to create a bump on the electron beam. Position was read by Libera Photon on XBPM1 and analog device on XBPM2 and compared to the position at source point using electron BPM. Results are presented in Figure 1.

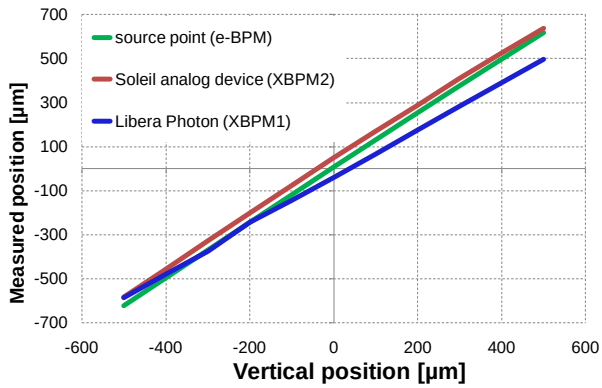

Figure 1: Beam bump measurement.

The analog device shows good correlation with the source point. Libera Photon, however, shows different slope in the measurement. There was no calibration or compensation used in Libera Photon. The slope and the offset can be set for each input channel individually. This must be done during instrument set up and then saved to the configuration file.

Beam current dependence measurement

With orbit feedbacks ON, the current in the storage ring was increased from 0 to 400 mA by steps of 50 mA (injections) and then scrapped down to 0. Measuring range used on Libera Photon was ±200 µA.

Both instruments (Libera Photon and Soleil analog device) measured changes in the position for several microns. The beam was really moving because of the machine current dependence (thermalization, eBPM beam current dependence,...). So this method could not be used to measure the beam current dependence of the Libera Photon electronics.

The current dependence measurements were done also under laboratory conditions. Both centered and off-

THE DIAGNOSTICS' BACK END SYSTEM BASED ON THE IN HOUSE DEVELOPED A|DA| AND A|D|O BOARDS

A. O. Borga#, R. De Monte, M. Ferianis, L. Pavlovic, M. Predonzani, ELETTRA, Trieste, Italy

Abstract

Several diagnostic instruments for the FERMI@Elettra FEL, among them the Bunch Arrival Monitor (BAM) [1] and the Cavity Beam Position Monitor (C-BPM), require accurate readout, processing, and control electronics integrated within the main machine control system. The back end platform, based on the MicroTCA standard [2], provides a robust environment for accommodating such electronics, including reliable infrastructure features. Two types of Advanced Mezzanine Cards (AMC) had been developed in-house and manufactured for meeting the demanding performance requirements. The first is a fast (160 MSps) and high-resolution (16 bits) Analog to Digital and Digital to Analog (A|D|A) Convert Board, hosting 2 A-D and 2 D-A converters controlled by a large FPGA (Virtex-5). The FPGA is also responsible for service and host interface handling. The latter board is Analog to Digital Only (A|D|O) Converter, derived from the A|D|A, with an analog front side stage made of four A-D converters. The overall systems' architectures, together with the specific AMCs' functionalities, are described. Results on performance measurements are also presented.

BACK END OVERVIEW

Figure 1 shows a block diagram of the general architecture of the high-bandwidth, real-time diagnostics back end. Three sub-systems can be identified according to their installation location:

Tunnel area: hosting the *monitors* and the monitors' *front-end electronics* responsible for signal pick-up, conditioning, and transmission to the back-end.

Service area: *back-end* and *A|D|A* and *A|D|O boards*, the system fulcrum where further signal conditioning, data processing, analysis, and computations are performed before data are sent back to users in the control room.

Control room: the users' control and monitor Linux/Tango PC, for data storage, further off-line analysis, and visualization.

The sub-systems are interfaced through transmission media chosen according to the different sections' specific needs. From the tunnel area to the service area the **A-B interface** carries signals via shielded coaxial or optical cables, for noise immunity. The cabling of the A-B interface is a task left to the monitors and front-end designers. The **E-F interface** connects the back-end crates to the control room's PC through standard Ethernet CAT6 cables and doesn't require particular attention. In the service area inside the back-end system, flexibility is more of a concern, so boards are connected through the **C-D interface** with SMA coaxial cables (for analog signals) or flat ribbon cables (in the case of digital signals).

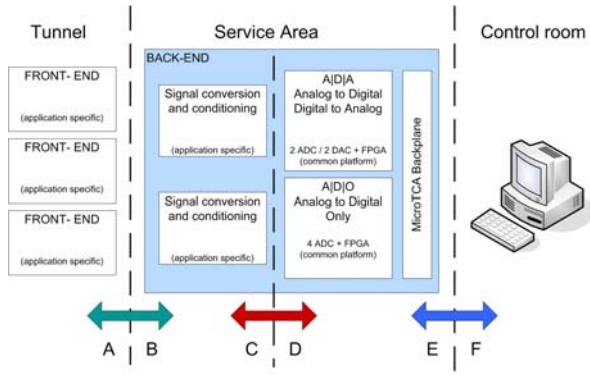

Figure 1: Block diagram of a diagnostic system based on µTCA and A|D|A and A|D|O AMCs

The C-D interface inside the back-end system's crate is used to interface three types of modules:

A|D|A and A|D|O AMCs: Advanced Mezzanine Cards (AMCs) for digital processing; FPGA based.

Custom Passive AMCs: interface transition cards that adapt front-end signals to the inputs of A|D|A and A|D|O.

Custom Active AMCs: standalone modules, for application-specific tasks not strictly related to diagnostics, that might not require an interface with A|D|A or A|D|O (e.g. timing and trigger cards, storage devices, processor cards, etc).

The whole electronics is based on the Micro Telecommunications Computing Architecture, which is beyond the scope of this paper but is described in, for example, [2]. For the C-BPM diagnostics case a 3D mock-up of a hypothetical system is shown in Figure .

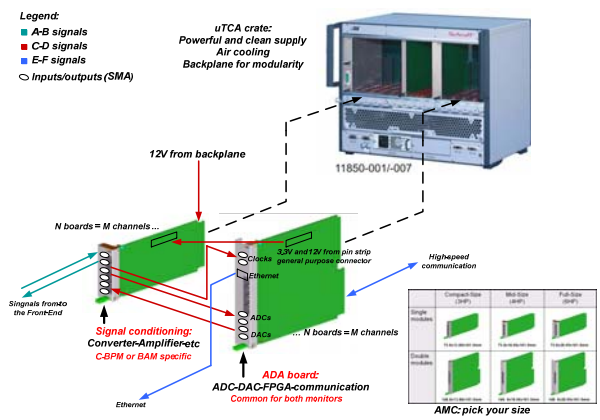

Figure 2: Example 3D mock-up of a system

SIMULATION OF A CAVITY BPM FOR HIGH RESOLUTION SINGLE-PASS BEAM POSITION MEASUREMENTS

A. Morgan, G. Rehm, Diamond Light Source, UK
A. Lyapin, University College London , UK
S. Boogert, N. Joshi, S. Molloy, Royal Holloway University London, UK

Abstract

This paper describes the design of a cavity BPM for use in single pass machines. The design was modelled using a number of different EM codes to allow cross comparison of the simulation results. Furthermore, in addition to existing designs, the geometry has been modified to introduce a frequency separation between the horizontal and vertical dipole signals, as well as a reduction of the sensitivity of the position monitor to the monopole sum signal. The next stage of this project will be the manufacture of a prototype for tests in the transfer path at Diamond Light Source.

DESIGN REQUIREMENTS

Modern and future single-pass machines such as Free Electron Lasers and Linear Colliders require fast and sensitive beam position monitors (BPMs) able to do precision beam position measurements of individual bunches.

Cavity BPMs have been shown to provide nanometre level resolutions [1], while stability studies resulted in micrometre and even sub-micrometre drifts over a few hours [2].

Several methods of improving the time resolution of cavity BPMs allow for bunches separated by 10s of nanoseconds to be resolved.

Basing on the previous works we wanted to take advantage of the simple cylindrical geometry and the inherent filtering effects of the slot-coupled design in order to better select out the desired dipole mode, while simultaneously suppressing the signals from the unwanted modes.

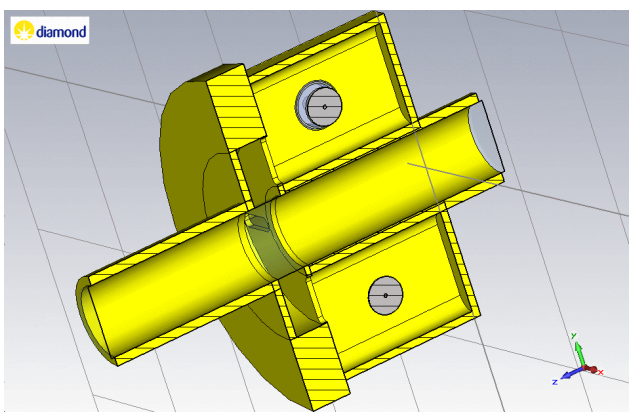

Figure 1: Full cavity BPM geometry

We also aim at simplifying the design flow, making the BPM easy and hence inexpensive to manufacture, and also fixing the remaining problems of cavity BPMs, such as the cross-coupling of the horizontal and the vertical signals.

As with many other recent cavity BPMs[3,4,5], this design comprises of a resonant cavity with coupling slots leading into waveguides. Each waveguide has a pickup in it to transmit the signal down a coaxial line for signal processing. (See figure 1)

Resonant cavity

The radius of the resonant cavity is determined by the frequency we are interested in. In the longer term we want to use the Diamond RF system (running at 499.654 MHz) to deliver local oscillator (LO) signals for down conversion. We chose the 13th harmonic, which gave us an initial target of 6.495 GHz. The dipole mode frequency has to be slightly offset from the peak so once the signal is down converted it sits near the centre of the IF bandwidth. A 100Msample ADC gives 50MHz bandwidth so a 20 MHz offset downwards was included, bringing the target to 6.475 GHz.

The longer the cavity the stronger it couples to the beam. On the other hand, the cavity becomes sensitive to the beam incline while the sensitivity increase with the length drops due to the signal in the cavity and the beam becoming asynchronous. 8 mm length was found to provide enough coupling while keeping the timing effects to a minimum.

Waveguide

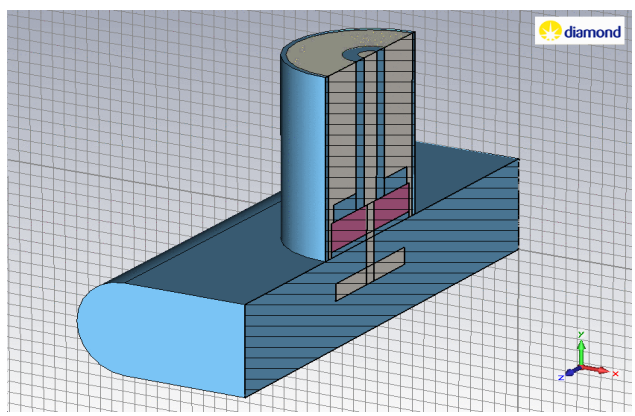

Figure 2: waveguide and coaxial port geometry

The dimensions of the waveguides are such that the first monopole mode is below the waveguide cut-off for the lowest odd mode TE_{01}, so that the monopole mode signal leaking due to asymmetries is suppressed, while the dipole mode is the first mode transmitted by the TE_{01}.

Although the other modes can be present near the slots they do not propagate. Therefore the length of the

NEW BEAM MONITORING INSTRUMENTATION AT ATF2, KEK*

E. Medvedko, R. Johnson, S. Smith, G. White
SLAC National Accelerator Laboratory, Menlo Park, CA 94025, U.S.A.

Abstract

A new stripline beam position monitoring (BPM) readout and processing system was installed and successfully tested over a two-week period at the Accelerator Test Facility (ATF2), at KEK, Japan during February 2010. The core analog processing board used in the system is a duplicate of that developed for, and in use at, the Linac Coherent Light Source (LCLS) at SLAC. The digitization, processing and control front-end were custom designed for ATF2 using a 14-bit 100-MHz VME digitizer and an EPICS Input / Output Controller (IOC) running on the VME controller. Control of the analog boards is via EPICS, which controls a serial-over-TCP / IP port server. Hardware for the readout of up to 14 BPMs with 3 spare analog boards was delivered. The goal of this installation was to provide better than 10 microns resolution, non-charge-dependent readout of the ATF2 electron beam with long-term gain stability compensation. These criteria were tested and successfully met. This design was found to be highly effective and to have many advantages, especially that it required minimal installation effort at ATF2.

INTRODUCTION

Twelve analog processing chassis are connected with cables to ATF2 stripline electrodes (Fig. 1). Each chassis has four inputs from Y+/- and X+/- striplines.

The 140 MHz output signals go to the VME 14-bit digitizers which have a 100 MHz sampling frequency. An EPICS IOC on a VME controller (Motorola MVME3100) receives and analyses the digitizer data, controls the analog processor gain, and calibrates signal power and calibration tone pulse width.

The port server communicates with the analog processing board via RS232 protocol. One trigger pulse initiates the calibration cycle in the time gap between the beam pulses. Another trigger synchronizes the digitizer's data conversion.

REQUIREMENTS

The main requirements:

- Resolution better than 10 microns.
- The measured beam position independent of beam charge. Operational ranges are ~ 0.15-1.5 nC (single bunch) with a dynamic range of +/- 3mm.
- Long-term gain stability 5%-10% over month timescales. The actual gain stability performance is still to be assessed.

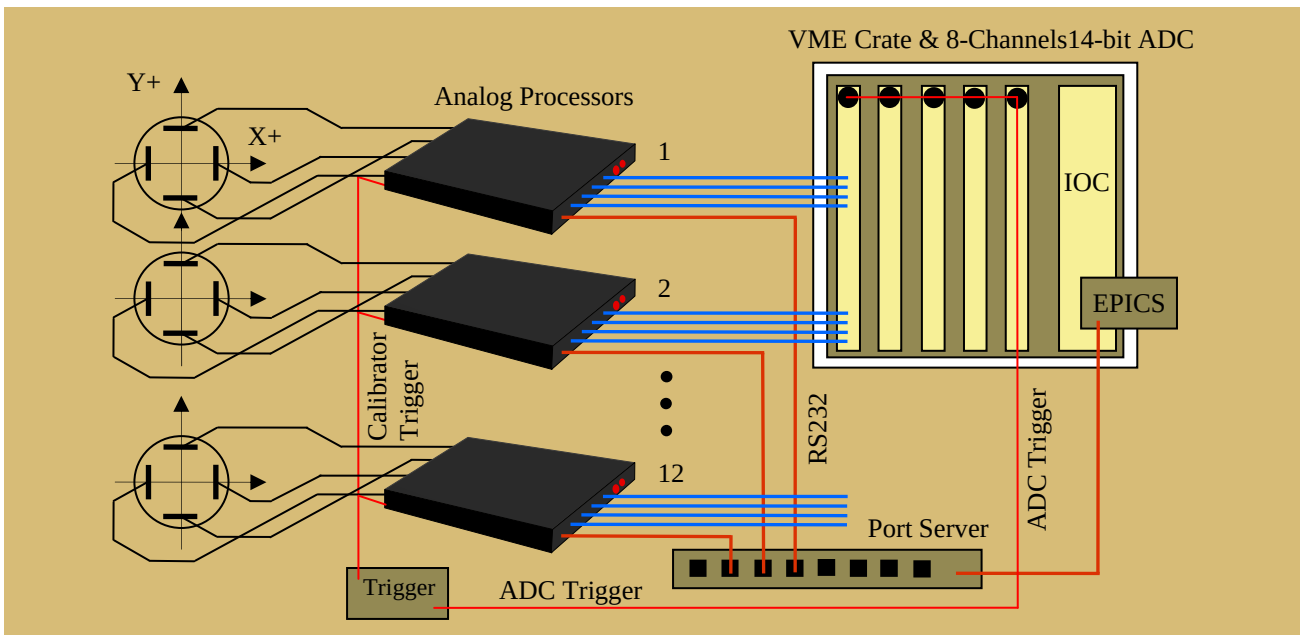

Figure 1: The ATF2 BPM processing system block diagram.

* Work supported by U.S. Department of Energy contract DE-AC02-76SF00515

LCLS RESONANT CAVITY BEAM POSITION MONITORS *

Andrew Young, Ronald G. Johnson, Stephen Smith
SLAC National Accelerator Laboratory, Menlo Park, CA 94025, U.S.A.
Robert M. Lill Argonne National Laboratory, Argonne, IL 60439, U.S.A.

Abstract

The Linac Coherent Light Source (LCLS) is a free-electron laser (FEL) at SLAC producing coherent 1.5 Å x-rays. This requires precise, stable alignment of the electron and photon beams in the undulator. We describe construction and operational experience of the beam position monitor (BPM) system which allows the required alignment to be established and maintained. Each X-band cavity BPM employs a TM_{010} monopole reference cavity and a single TM_{110} dipole cavity detecting both horizontal and vertical beam position. The processing electronics feature low-noise single-stage three-channel heterodyne receivers with selectable gain and a phase-locked local oscillator. Sub-micron position resolution is required for a single-bunch beam of 200 pC. We discuss the specifications, commissioning and performance of 36 installed BPMs. Single shot resolutions have been measured to be about 200 nm rms at a beam charge of 200 pC.

FEL COMMISSIONING

LCLS photocathode RF gun and injector systems were commissioned in 2007, followed by linac and bunch compressor systems in 2008. Beam was first taken through the undulator beamline (with no undulators installed) in December, 2008. After aligning each undulator segment individually, 21 undulator magnets were inserted in April 2009. We observed lasing at 1.5 Angstroms essentially immediately [1].

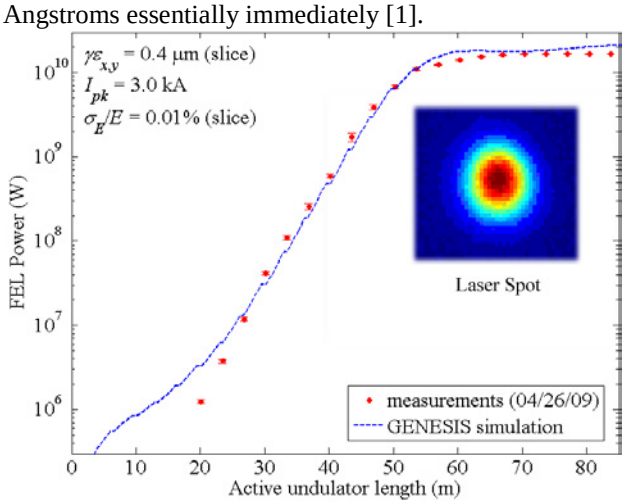

Figure 1: FEL gain length measurement at 1.5 Å made by kicking the beam after each undulator sequentially (red points), prediction (blue line) and YAG screen laser spot.

*Work supported by U.S. Department of Energy under Contract Numbers DE-AC02-06CH11357 and DE-AC02-76SF00515.

BPM REQUIREMENTS

Laser saturation in the LCLS FEL requires the electron and photon beams be collinear in the 131 meter-long undulator to about 10% of the 37 μm rms transverse beam spot size over scales of the FEL amplitude gain length (~4m) [2,3]. BPM system requirements include centering accuracy, reproducibility, small physical size, radiation hardness, and sub-micron resolution at 200 pC.

SYSTEM DESIGN

The major subsystems for the LCLS undulator BPM system are the cavity BPM, receiver, and data acquisition components. The cavity BPM and downconverter reside in the tunnel while the analog-to-digital converters (ADC) and processing electronics are in surface buildings.

Thirty-four BPMs are installed on undulator girders while two are placed in the linac-to-undulator (LTU) transport line. The BPMs provide stable and repeatable beam position data for both planes on a pulse-to-pulse basis for up to a 120-Hz repetition rate.

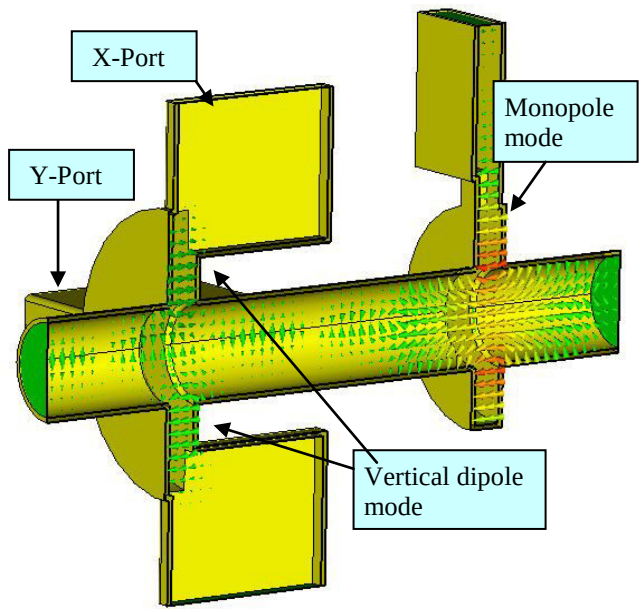

Figure 2: BPM Cavity schematic with electric fields of position (dipole) and reference (monopole) cavities.

X-Band Cavity

Figure 2 shows the electric field vectors in the cavity BPM simulated when the beam is offset[4,5]. Beam passes through the monopole reference cavity on the right, exciting the TM_{010} monopole mode signal resonant

DESIGN AND PERFORMANCE OF SSRL BEAM POSITION ELECTRONICS*

J. Sebek#, D. Martin, T. Straumann, J. Wachter, SSRL/SLAC, Menlo Park, CA 94025, U.S.A.

Abstract

SSRL designed and built beam position electronics for its SPEAR storage ring. We designed the electronics, using digital receiver technology, for highly accurate turn by turn measurements of both the position and arrival time of the beam, allowing us to use this system to measure the betatron and synchrotron tunes of the beam. The dynamic range of the system allows us to measure the properties of the beam at currents ranging from those of single bunch injection to those of the full SPEAR stored beam. This paper discusses the architecture of the electronics, presents their performance specifications, and shows a range of applications of this system for accelerator physics experiments.

SPEAR PARAMETERS

SPEAR is a 3 GeV electron storage ring used for synchrotron radiation. The operational beam current is now 200 mA; the ring will run at 500 mA after all of the beamline optics have been commissioned. The beam emittance is 10 nm, the vertical beam size is 30 μm, and the bunch length is 5 mm. The radio frequency (RF) of the SPEAR klystron is 476.316 MHz and the ring circumference is 234.3 meters; the harmonic number of SPEAR is 372 and its revolution frequency is 1.28 MHz.

ORBIT FEEDBACK BPM ELECTRONICS

We use a modified version of the Bergoz MX-BPM processor [1] to measure the beam position monitor (BPM) signals for our orbit feedback system. We use 60 BPM processors to monitor the beam position and 60 steering magnets to correct the orbit. Our feedback algorithm updates at a rate of approximately 4 kHz. Our target orbit stability is 3 μm in a 1 Hz bandwidth, 10% of the nominal vertical beam size. Our orbit feedback system achieves a stability of a few hundred nm, an order of magnitude better than our requirements.

SINGLE TURN BPM ELECTRONICS

We also wanted a high performance BPM processor that was optimized for machine physics applications. Therefore it needed to produce highly accurate turn by turn data of the beam from which we could extract the dynamics of the machine. We have 18 of these electronics, one for each sector of the ring.

Machine physics use requires the electronics to work over a large dynamic range, from injected beam to stored beam at full current and it needs to work for all potential fill patterns, ranging from the standard fill pattern, when almost all buckets are full, to single bunch studies. In particular we need to be able to use this processor to measure the betatron and synchrotron oscillations of the beam, both when we are driving the beam and the oscillations are strong, as well as when the beam is quiet.

*Work supported by the U.S. Department of Energy under contract number DE-AC02-76SF00515

#sebek@slac.stanford.edu

BEAM SPECTRUM

Ideal Bunch

In order to motivate our system architecture, we first briefly review the properties of a relativistic beam in a storage ring. The ideal beam circles the ring at the revolution period T. If the bunch were ultra-relativistic, a point particle, and the BPM button had infinite bandwidth, the signal would be a series of delta functions

$$i(t) = \sum_{n=-\infty}^{\infty} Q\delta(t - nT),$$

where Q is the bunch charge. Because of its periodic nature the current can be expressed in a Fourier series

$$i(t) = \sum_{k=-\infty}^{\infty} Qe^{ik\omega_0 t},$$

where $\omega_0 = 2\pi/T$, showing that the spectrum consists only of the harmonics of the revolution frequency. Even though there are an infinite number of harmonics, they all carry the same information about the bunch. Finite size of the bunch and finite bandwidth of the pickup give Q a dependence on the frequency ω.

The ring may have up to h bunches, where h is the harmonic number of the ring. The beam spectrum is still composed of the harmonics of ω_0, but now the amplitude of the various harmonics depends on the fill pattern of the ring. For example, if h is even, and every other bunch is equally filled, only the coefficients of the even harmonics are non-zero; one cannot distinguish between this situation and one in which the ring is half as large (with twice the revolution frequency) but in which every bunch is filled. But even though there are an infinite number of harmonics, the number of independent terms is finite. In fact, since there are h bunches, there are only h independent coefficients Q_k. The coefficient corresponding to the klystron RF frequency ω_{RF}, and all of its multiples, is the same as the DC coefficient. In order to obtain a signal independent of bunch pattern, one needs to process the signal at a harmonic of ω_{RF}.

Dynamic Bunch

We can see what happens to a dynamic bunch by making a slowly varying approximation to the Fourier expansion. A beam executing transverse motion about its nominal trajectory will have a time-varying amplitude; a

A WIRE POSITION MONITOR SYSTEM FOR SUPERCONDUCTING CRYOMODULES AT FERMILAB*

D. Zhang#, N. Eddy, B. Fellenz, J. A. Fitzgerald, O. Lysenko, P. Prieto, A. Saewert, A. Semenov, D. C. Voy, M. Wendt, FNAL, Batavia, IL 60510, U.S.A.

Abstract

Fermilab is jointly developing capabilities in high gradient and high Q superconducting accelerator structures. Based on the 1.3 GHz INFN/TESLA design [1-4], a wire-position-monitor (WPM) system is integrated to monitor cavity alignment and cold mass vibrations. The system consists of a reference wire carrying a 325 MHz signal, 7 stripline pickups (per cryomodule, 12-m long), and read-out electronics using direct digital signal down-conversion techniques. We present technical details of the system, and preliminary results on resolution and stability measured at a mock-up test stand.

Figure 1: The first cryomodule being moved to the cave.

WPM PRINCIPLE

Fermilab is building up a SCRF test facility. It consists 3 INFN/TESLA style cryomodules (see Figure 1), each incorporates 7 WPMs, at each end, at the three posts and between the posts.

Figure 2: Picture of the WPM at one end.

As shown in Figure 2, a WPM is a coaxial tube with four 50-Ω microstrip pickups spaced 90° apart. The IF wave on the center wire induces signals on the pickups through space coupling. While the wire's position in space is determined by its two ends, a WPM may move or vibrate with the cryomodule body. This relative displacement (in the transverse plane) between a WPM and the center wire manifests as imbalances between the strengths of the four induced signals, and can be deducted by iterations according to:

$$I_x = \frac{V_B - V_D}{V_B + V_D}, I_y = \frac{V_A - V_C}{V_A + V_C}$$

$$x = a_{10} I_x + a_{30} I_x^3 + a_{12} y^2 I_x + \ldots, y = a_{01} I_y + a_{03} I_y^3 + a_{21} x^2 I_y + \ldots$$

where A through D denote the pickups at the top, left, bottom and right.

READOUT SYSTEM

The readout electronics is housed in a VME crate. It includes a MVME-5500 PPC processor board, a timing board and a few digital receiver boards. The timing board generates a 325 MHz CW signal and 8 clock signals, using either an external RF or an internal oscillator. The 325 MHz CW is amplified and feed to the center wire. The 8 clock signals are divided down from the 325 MHz by either 4, 8, 16 or 32. They are used to clock the digital receiver boards and can be individually phase adjusted at 8.6 ps steps. Each digital receiver board has 8 channels, handling 2 WPMs. The digital receiver boards sample the induced signals from the pickups at 40.625 MHz. Every 9918 samples are grouped to get one average making the data output rate of 4096.09 Hz. For each cycle, the system takes 16384 data samples in about 4 seconds. It then processes the data and self trigger again.

The frequency of 325 MHz is chosen for good coupling between the center wire and the pickups, and for easy handling.

The DAQ software is in C++ under VxWorks. It incorporates a client-server tool to communicate with host machines. A LabVIEW package is used to control the system and visualize the results.

TEST STAND

A test stand is set up to test the readout electronics and DAQ software (see Figure 3). It uses a thinner CuBe alloy wire, 0.5 mm diameter, about 1.1 m long. The tension is 9.07 kg. The fundamental vibrating frequency of the wire is calculated to be 104.5 Hz.

To verify the long term stability of the electronics, one average position was recorded every ~ 4 seconds over a period of about 8 hours, with the inputs to the digital receiver boards connected to test signals. It showed that the system is stable to within ~ 1 um. Over another similar period, the system clearly showed the instability of the amplifiers for the test signals (see Figure 4).

To verify the capability of the system as a detector for microphonic vibrations, the support table were struck, and

*Operated by Fermi Research Alliance, LLC under Contract No. DE-AC02-07CH11359 with the United States Department of Energy.
#dhzhang@fnal.gov

A HIGH-RESOLUTION CAVITY BPM FOR THE CLIC TEST FACILITY*

N. Chritin, H. Schmickler, L. Soby, CERN, Geneva, Switzerland
A. Lunin, N. Solyak, M. Wendt#, V. Yakovlev, Fermilab, Batavia, IL 60510, U.S.A.

Abstract

In frame of the development of a high resolution BPM system for the CLIC Main Linac we present the design of a cavity BPM prototype. It consists of a waveguide loaded dipole mode resonator and a monopole mode reference cavity, both operating at 15 GHz, to be compatible with the bunch frequencies at the CLIC Test Facility. Requirements, design concept, numerical analysis, and practical considerations are discussed.

INTRODUCTION

The next high energy physics (HEP) lepton collider, operating at the energy frontier (CM > 500 GeV) needs to accelerate the particles along a straight line, to avoid too high losses caused by synchrotron radiation. For both concepts, the superconducting RF technology based International Linear Collider (ILC) [1], as well as for the two-beam acceleration Compact LInear Collider (CLIC) [2], generation and preservation of beams with ultra-low transverse emittance is mandatory to achieve the luminosity goals. A "golden" trajectory path has to be established, steering the beam with sub-micrometer precision through the magnetic centres of the quadrupoles, avoiding a beam blow-up due to non-linear fields.

Table 1: CLIC / CTF Main Linac BPM specifications.

	CLIC	CTF CALIFES
Nominal bunch charge [nC]	0.6	0.6
Bunch length (RMS) [μm]	44	225
Batch length [nsec]	156	1-150
Bunch spacing [nsec]	0.5	0.6667
Beam pipe radius [mm]	4	4
BPM time resolution [nsec]	<50	<50
BPM spatial resolution [nm]	<50	<50
BPM stability [nm]	<100	<100
BPM accuracy [μm]	<5	<5
BPM dynamic range [μm]	±100	±100
BPM resonator frequency [GHz]	14	14.98962

To discover and minimize unwanted dispersion effects along the Main Linac beam-line, an energy chirp modulation within the bunch train is proposed for the CLIC beam commissioning. Therefore the beam position monitors (BPM) have to have both, high spatial and high time resolution. We propose a low-Q waveguide loaded TM_{110} dipole mode cavity as BPM, which is complemented by a TM_{010} monopole mode resonator of same resonant frequency for reference signal purposes.

Table 1 gives the basic requirements for the BPM, however, as the bunch frequencies at the CLIC Test Facility (CTF) are different from the proposed CLIC linear collider, the nominal resonant frequencies (f_{110} for the dipole mode cavity, f_{010} for the reference cavity) are not the same for the CTF prototype BPM, and the CLIC Main Linac BPMs:

- CLIC: 14 GHz
- CTF: 15 GHz

Choosing a rather high operating frequency $n\ f_{\text{bunch}}$ has several advantages, e.g. most higher-order modes (HOM) are damped by the beam pipe cut-off frequency, and higher shunt impedances can be achieved (better sensitivity, higher resolution potential). However, as dipole mode and reference cavity operate at the same frequency, we have to ensure that they do not couple by evanescence fields leaking into the beam pipe.

With a time resolution of <50 nsec we will be able to acquire three beam position samples within the 156 nsec long bunch train (batch). Because of dynamic range limitations in the read-out system, the high 50 nm spatial resolution can only be accomplished within a small range of ±100 μm beam displacement from the BPM center, however a moderate resolution (some μm) will be achievable over the full aperture (±4 mm).

Each of the two ~20 km long CLIC Main Linacs will be equipped with ~2000 BPMs, therefore a simple, cost-effective design with minimum maintenance and calibration requirements is important. The longitudinal expansion of the two BPM resonators should not exceed 95 mm, including flanges. A simple analog down-converter has to be placed in close proximity to the BPM detector; no external reference or timing signals are required.

CAVITY BPM PRINCIPLE

A cylindrical "pillbox" having conductive (metal) walls of dimensions radius R and length l resonates at eigenfrequencies:

$$f_{\text{mnp}} = \frac{1}{2\pi\sqrt{\mu_0\varepsilon_0}}\sqrt{\left(\frac{j_{mn}}{R}\right)^2+\left(\frac{p\pi}{l}\right)^2} \qquad (1)$$

This resonator can be utilized as passive, beam driven cavity BPM by assembling it into the vacuum beam pipe. A subset of these eigenmodes is excited by the bunched

*Work supported by the Fermi National Accelerator laboratory, operated by Fermi Research Alliance LLC, under contract No. DE-AC02-07CH11359 with the US Department of Energy.
#manfred@fnal.gov

ROGUE MODE SHIELDING IN NSLS-II MULTIPOLE VACUUM CHAMBERS*

A. Blednykh#, B. Bacha, A. Borrelli, M. Ferreira, H.-C. Hseuh, B. Kosciuk, S. Krinsky, O. Singh, K. Vetter, BNL, NSLS-II, NY 11973-5000, U.S.A.

Abstract

Modes with transverse electric field (TE-modes) in the NSLS-II multipole vacuum chamber can be generated at frequencies above 450MHz due to its geometric dimensions. Since the NSLS-II BPM system monitors signals within 10 MHz band at RF frequency of 500 MHz, frequencies of higher-order modes (HOM) can be generated within the transmission band of the band pass filter. In order to avoid systematic errors in the NSLS-II BPM system, we introduced frequency shift of HOMs by using RF metal shielding located in the antechamber slot.

INTRODUCTION

A new 3GeV NSLS-II storage ring is under construction at Brookhaven National Laboratory. The ring has a 30 cell double-bend achromatic (DBA) lattice [1]. Six beam position monitors (button type) per cell are going to be located on multipole vacuum chambers to control electron beam trajectory. Each vacuum chamber in each cell is numerated in according to girder location. Five types of multipole vacuum chambers are going to be used in the NSLS-II storage ring [1]. They have the same cross-section profile and differ mostly in length. Multipole vacuum chambers S2, S4 and S6 are shown in Figure 1 with location of BPM Buttons.

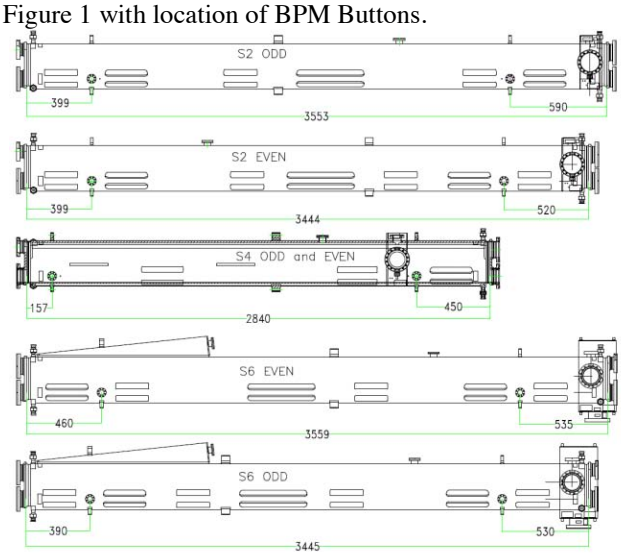

Figure 1: Types of NSLS-II multipole vacuum chambers.

The NSLS-II multipole vacuum chamber profile is shown in Figure 2. The full horizontal and vertical aperture of the beam channel is *76mm* x *25mm* respectively. The antechamber slot with a gap of 10mm is extended up to a trapezoidal area with a vertical aperture of 44mm. The NSLS-II cross-section profile has a complex geometry and looks similar to APS chamber design, except a difference in geometric dimensions. There is a concern that existence of rogue modes observed in vacuum chambers with antechamber slot [2] can affect precision of the NSLS-II BPM diagnostic system. As in APS, the NSLS-II BPM buttons are located on top and bottom of multipole vacuum chambers, which have an antechamber slot (Fig. 2). Rogue modes, which are classified as modes with Transverse Electric field (H-mode) in a ridged waveguide, can couple to the BPM buttons at frequencies near to the RF. It can produce a noise in BPM system and difficulties in monitoring of beam position in the ring.

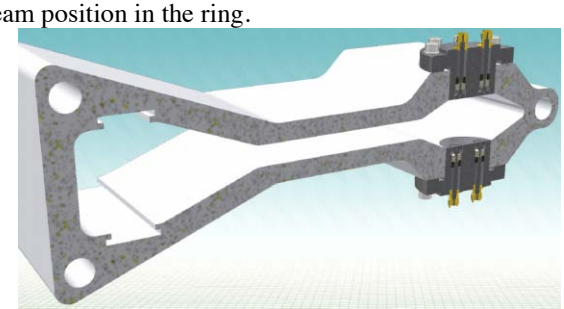

Figure 2: NSLS-II multipole vacuum chamber profile.

Since the NSLS-II multipole vacuum chamber profile has a complex geometry, the cutoff wavelength has been simulated numerically using the GdfidL code [3]

$$\lambda_c = 0.695m\,.$$

Since the cutoff wave length is known a set of resonance modes can be generated in a chamber at frequencies

$$f^H_{mnp} = \frac{c}{2\pi}\sqrt{\left(\frac{2\pi}{\lambda_c}\right)^2 + \left(\frac{p\pi}{L}\right)^2}\,,$$

where c is the velocity of light, λ_c is the cutoff wavelength, $p=1,2,..k$ and L is the chamber length. Based on Maxwell's equations the first lowest mode like in a ridged cavity depends on the structure length (H_{101}-mode). Index p cannot be equal zero ($p \neq 0$). For a length of $L=3553mm$ (length of the S2-chamber), the first resonant frequency is $f^H_{101} = 434MHz$. It agrees well with the frequency of the dominant mode obtained due to numerical simulations and microwave measurements (Table 1). Frequencies of the first six H_{mnp}-modes are shown in Table 1. The frequency of H_{106}-mode is almost equal to the RF frequency. In order to avoid interference of H-modes (TE-modes) with the BPM signal, the RF shielding is required.

*Work supported by DOE contract No: DE-AC02-98CH10886
#blednykh@bnl.gov

OPTIMIZATION OF SMALL APERTURE BEAM POSITION MONITORS FOR NSLS-II PROJECT*

I. Pinayev #, A. Blednykh, B. Kosciuk, O. Singh, BNL, Upton, NY 11973, U.S.A.

Abstract

The NSLS-II Light Source is being built at Brookhaven National Laboratory. It will provide users with ultimate brightness beam and full realization of its capabilities requires corresponding stability of the beam orbit. The small aperture beam position monitors (BPMs) will provide better sensitivity to the beam position but also requires thorough design. In this paper we present the results of the optimization including signal power levels and button heating.

INTRODUCTION

The standard beam position monitors for the NSLS-II storage ring is be mounted on an aluminum multipole vacuum chamber [1, 2]. The vertical gap is 25 mm and the distance between the button centers is 16 mm.

Small aperture BPMs will be installed in the straights around the insertion devices (ID). The ID beamlines are the most demanding for the beam stability, therefore, most of the small aperture BPMs will be installed on the special supports providing high mechanical stability [3]. The vertical gap is expected to be around 15 mm. Therefore the design of the small aperture BPMs will differ from the regular assemblies.

GEOMETRY OPTIMIZATION

The MATLAB script similar to [4] was used for optimization of the distance between centers of the buttons.

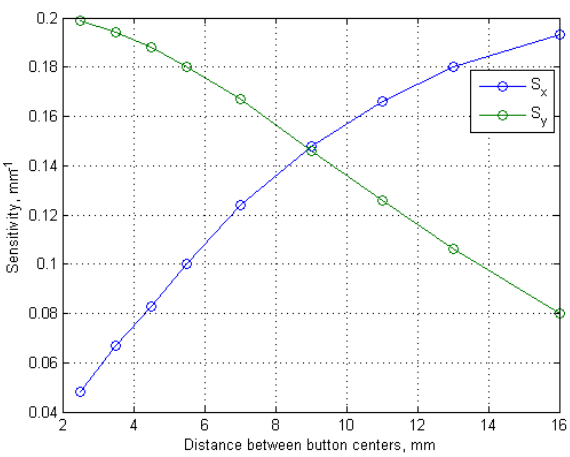

Figure 1: Dependence of sensitivity coefficients on the distance between the centers of the 4.5 mm buttons.

The results of the simulations are shown in Fig. 1. Based on the numerical the calculations we specified 4.5 mm separation between the button centers. In this case sensitivity to the vertical motion doubles in comparison with the standard BPMs when horizontal is not changed. The rational for such choice is that the vertical beam size is much smaller and requirement for beam stability in the vertical plane are stricter. The dependence of difference over the sum signal for the chosen button separation is shown in Fig.2.

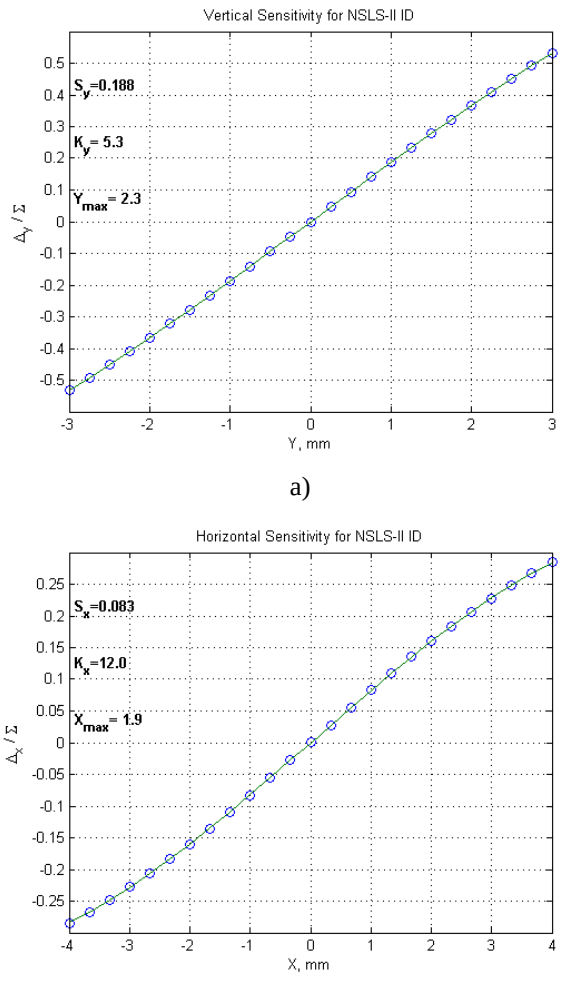

Figure 2: Dependencies of difference over sum signal for the geometry with 4.5 mm distance between button centers: a) for the vertical plane, b) for the horizontal plane.

The standard BPMs has separation of 16 mm and it is possible to reduce the distance down to the 9.6 mm. Further reduction is limited by the size of the SMA connector. However, it is possible to reduce the effective

*Work supported by U.S. Department of Energy, Office of Science, Office of Basic Energy Sciences, under Contract No. DE-AC02-98CH10886.

#pinayev@bnl.gov

CONCEPT OF BEAM POSITION MONITOR WITH FREQUENCY MULTIPLEXING*

I. Pinayev#, P. Cameron, BNL, Upton, NY 11793, U.S.A.

Abstract

Two most widely used beam position monitor (BPM) systems (manufactured by Bergoz [1] and Instrumentation Technologies [2]) implement switching technique to eliminate errors associated with drifts in the channel gains. High stability is achieved by an alternative routing of signals from all pick-up electrodes (PUE) through the same chain. Such an approach creates problems with turn-by-turn acquisition as well as measurement noise. In this paper, basing on the advances of digital signal processing that allow identical gains for the wide frequency ranges, we propose separating signals in the frequency domain. The experimental set-up and test results are presented. Practical realization of the beam position monitors is also discussed.

INTRODUCTION

Development of ultra-bright synchrotron radiation sources and high luminosity colliders requires unprecedented levels of beam stability. To achieve needed steadiness one can use a channel switching technique [1, 2] or utilize a pilot tone [3, 4]. The channel switching produces very low drifts but also manifests itself as narrow band measurement noise at the switching frequency. Another disadvantage is lack of the turn-by-turn (TbT) capabilities. Pilot tone technique can provide both stable long-term beam position monitoring and TbT data: however it requires extra hardware to be placed inside an accelerator tunnel.

In this paper we propose a new approach based on the separation of the signals from different pick-up electrodes (PUE) in the frequency domain combined with digital processing. Processing in the digital chain is a key element, because it provides stable and equal gain in the wide frequency range.

EXPERIMENTAL SETUP

The proposed signal processing scheme is shown in Fig. 1. For simplicity the scheme with two pick-up electrodes, A and B, is used (four-PUE implementation will be discussed later). Signal from each pick-up is divided into the two channels with equal amplitudes by splitters S_1 and S_2. Two local oscillators Osc 1 and Osc 2 set the intermediate frequencies (IF). Signals from each PUE are down-converted with mixers M_1-M_4 and cross combined with combiners C_1-C_2. The first analog-to-digital converter (ADC) processes signal A at the first intermediate frequency and signal B with the second IF; the second ADC processes signal A at the second IF and signal B with the first IF.

Due to symmetry of the processing chain the first-order errors from the splitters and combiners (such as inequality of division and summation) and the amplitude variations of the local oscillators are cancelled; only the second-order terms remain. For the analysis purpose the variation of mixers insertion losses are included into the corresponding errors in splitters and/or combiners.

Components characterization

The tests were performed utilizing a LeCroy WavePro 7300A digital oscilloscope, ZFSC-2-4-S+ splitters/combiners, ZX05-10-S+ mixers by Mini-Circuits, two N5181A RF signal generators by Agilent were used as local oscillators, and an RF and Clock Generator by Instrumentation Technologies for the signal source. The carrier frequency was suppressed by the low-pass filters with cut-off frequency depending on the chosen IF. The carrier frequency was set to 481.57 MHz to minimize the effect of reflected wave from the mixers.

First, the splitters and ADC were verified with two measurements in which signal after splitter goes directly and then is crossed to the two channels of the oscilloscope. The measured waveforms were fit with sine, and obtained amplitudes were used to calculate unevenness of the splitters and the gain inequalities of the ADCs. The channel gains were different by 6×10^{-3} and the splitter was found to have 1.4×10^{-3} unbalance.

Beam offset was simulated by insertion a 1 dB attenuator (theoretical transmission of 0.8913) into position A or position B. The measured transmission was 0.885.

Tests with Low IF

The initial measurements were performed with low IF, where the reduced sampling rate allows ADCs to have less noise and more effective bits. The local oscillators were set to 478.93 MHz (IF_1=2.64 MHz) and 478.01 MHz (IF_2=3.56 MHz). The SLP-5+ low-pass filters by Mini-Circuits have cut-off frequency of 5 MHz. The sequence of 10 μs duration was recorded with 1 Gs/sec rate. The recorded signals ware fitted with a two-tone sine waveform:

$$y = y_0 + A\cos\omega_1 t + B\sin\omega_1 t + \\ + C\cos\omega_2 t + D\sin\omega_2 t \quad (1)$$

The obtained amplitudes were used to calculate the ratio of levels:

*Work supported by U.S. Department of Energy, Office of Science, Office of Basic Energy Sciences, under Contract No. DE-AC02-98CH10886.

#pinayev@bnl.gov

NSLS-II RF BEAM POSITION MONITOR*

Kurt Vetter#, Al Joseph Della Penna, Joseph DeLong, Bernard Kosciuk, Joe Mead, Igor Pinayev, Om Singh, Yuke Tian, Kiman Ha BNL, NSLS-II, NY 11973, U.S.A.

Abstract

An internal R&D program has been undertaken at BNL to develop an RF BPM to meet all requirements of both the injection system and storage ring. The RF BPM architecture consists of an Analog Front-End (AFE) board and a Digital Front-End board (DFE) contained in a 1U 19" chassis. An external passive RF signal processor has been developed that will be located near the RF BPM pickups. The partitioning into two boards enables a flexible Software Defined Instrument. A model-based design flow has been adopted utilizing AWR VSS, Simulink, and Xilinx System Generator for algorithm development and AFE impairment performance analysis. The DFE architecture consists of a Virtex-5 with MicroBlaze embedded processor. An optional Intel Atom SBC is also supported. The AFE is based on a bandpass sampling architecture utilizing 16-bit ADCs. Long-term drift is corrected by inclusion of an out-of-band calibration tone. An RF BPM Calibration Tool is being developed for removal of systematic errors and performance verification. In this contribution we will present a detailed overview of the architecture, then compare simulation results to laboratory performance.

INTRODUCTION

An internal R&D program was started in August 2009 to develop an RF BPM for the 3GeV NSLS-II currently under construction at Brookhaven National Laboratory for the Injection System and Storage Ring. Since the start of the BPM R&D program was after the Critical Decision 3 award, the development timeline is aggressive. The development schedule mandates a proof-of-principle demonstrated August 2010.

As a state-of-the-art 3rd generation light source designed to deliver world-leading intensity and brightness, beam stability will be of utmost importance. The most stringent BPM stability requirement [1] is for the multi-bunch stored beam condition where vertical resolution, horizontal resolution, and long-term stability must be less than 200nm rms. It is well known that the most challenging requirement is the sub-micron long-term stability. The sub-micron horizontal, and vertical resolution correlate to the intrinsic signal-to-noise (SNR) of the pickup geometry [4] which can be met by proper analysis and design of the analog and digital processing.

The NSLS-II RF BPMs utilized in the Storage Ring are housed in thermally stabilized racks, regulated to +-0.1° C of the preset operational temperature. Based on tests of existing BPM technology in the NSLS-II thermally controlled racks it is possible to achieve sub-micron long-term gain drift without calibration. However, a dynamic calibration scheme has been incorporated to achieve long-term (i.e., 8 h) gain stability to meet the required 200 nm objective [4] over the operational range of 50-500 mA.

SYSTEM ARCHITECTURE

The NSLS-II RF BPM architecture consists of a passive RF Processor box located in the tunnel, the AFE, and DFE. Shown below in Figure 1 is the prototype BPM consisting of both AFE and DFE.

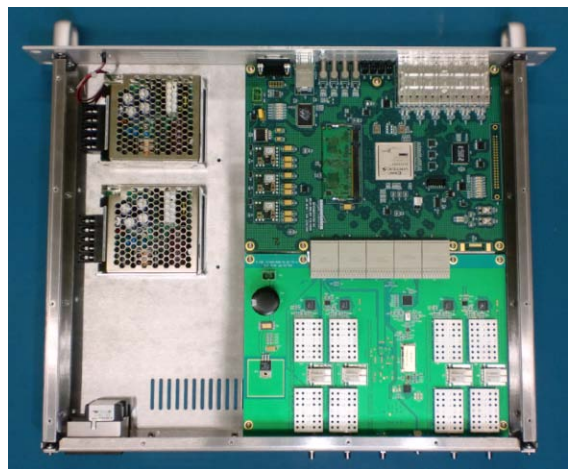

Figure 1: NSLS-II Prototype RF BPM.

The RF Processor box consists of a custom Diplexer designed by K&L Microwave, isolator, and 4-way power splitter. An illustration of the Passive RF Processor is illustrated below in Figure 2. The RF Processor is shown located on the girder directly below the BPM pickups. Four 1 m SiO_2 cables are connected from the pickup assembly to the RF Processor.

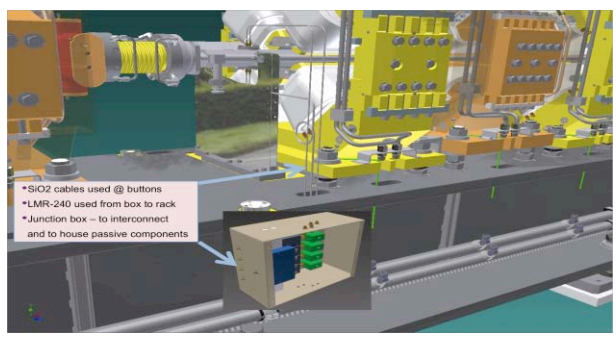

Figure 2: Passive RF Processor.

A detailed illustration of the RF Processor is illustrated below in Figure 3. One m of SiO_2 is used to connect the BPM pickup to the RF Processor. The RF Processor consists of an isolator and custom diplexer. The isolator presents a return loss of 18 dB over a 150 MHz

*Work supported by DOE contract No: DE-AC02-98CH10886
#kvetter@bnl.gov

STATUS OF THE RE-ENTRANT CAVITY BEAM POSITION MONITOR FOR THE EUROPEAN XFEL PROJECT

C. Simon#, O. Napoly, CEA-Saclay/DSM/Irfu, Gif sur Yvette, France
J-P. Prestel, N. Rouvière, CNRS-IN2P3-IPN, Orsay, France.

Abstract

The European XFEL is a research facility, currently under construction in Germany. It is based on a superconducting electron linac including about 100 cryomodules based on the TESLA technology. Each cryomodule is equipped with a beam position monitor connected to a quadrupole at the high-energy end of the cavity string. Around one third of cold BPMs will be re-entrant RF cavities. This contribution describes the present status of the cold re-entrant cavity BPM and presents the measurements performed with BPM pickup and electronics prototypes.

INTRODUCTION

The European XFEL (E-XFEL) is a project to construct an X-ray Free-Electron-Laser international user facility close to DESY in Hamburg [1]. This machine, which is based on the TESLA superconducting RF technology, will accelerate electron beams up to 17.5 GeV at a repetition rate of 10 Hz. The first beam is expected in 2014.

To provide position and charge information along the linac, about 450 Beam Position Monitors (BPM) will be installed. Depending on the BPM location and the performance requirements, different BPM types will be used. In the accelerator modules, two types of BPMs will be installed: button BPMs [2] and re-entrant cavity BPMs. These latest represent 30 % of the cold BPMs. Independent of the type of BPM, they will have a common mechanical interface and the same specifications shown in table1.

Table 1: Cold BPM parameters

Parameter	Value
Beam pipe diameter	78 mm
Length	170 mm
Single bunch resolution (RMS)	50 µm
Operation range for maximum resolution	± 3 mm
Transverse Alignment Tolerance (RMS)	300 μm

One re-entrant BPM is already installed in a warm section of the FLASH linac [3], and achieves 4 µm resolution over a dynamic range of ± 5 mm [4].

In this paper, the status of the XFEL cold re-entrant BPM is presented. A prototype has been manufactured to be installed in an XFEL prototype cryomodule and an electronics based on a Printed Circuit Board (PCB) will be discussed.

#claire.simon@cea.fr

RE-ENTRANT BPM MECHANICS

The length of the re-entrant cavity is 170 mm to respect the constraints imposed by the cryomodule and its aperture is 78 mm (see Fig. 1). It is composed of two parts, in stainless steel, welded together by an electron beam. Flanges are manufactured in the same blocks to get the alignment tolerances. The alignment of the BPM is done by dowel pins with respect to the cold magnet.

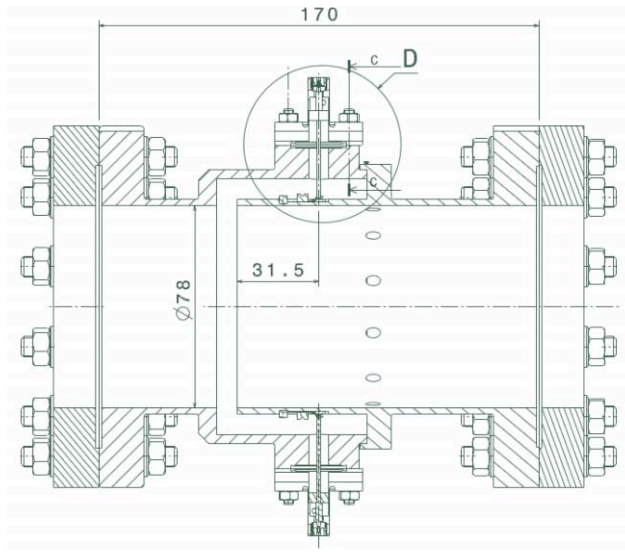

Figure 1: Drawing of the re-entrant cavity BPM.

In order to avoid hydrogen out-gassing, a heat treatment at 950 °C for 2 hours is applied to the BPM cavity. Since it is connected to a cold magnet, the BPM will be at a temperature close to the 4 K level and will be mounted in a clean room. For an effective cleaning, twelve holes of 5 mm diameter are drilled at the end of the re-entrant part.

To reduce the cryo-losses, a 12 µm thick copper coating is deposited on the inner beam pipe. Then, a heat treatment at 400 °C is done to check the copper surface and test the contact of copper and steel.

Each antenna, which is a combination of stainless steel, molybdenum and alumina Al2O3 ceramic brazed, is mounted on the cavity via a CF16 flange. They have to pass cryogenic shocks and to fulfil the conditions of Ultra High Vacuum (UHV). Four copper-beryllium radio-frequency contacts are also welded in the inner cylinder of the cavity to ensure the electrical conduction between the feedthrough inner conductors and the cavity.

MAGNETIC COUPLED BEAM POSITION MONITOR FOR THE FLASH DUMP LINE

N. Baboi, A. Brenger, D. Lipka#, J. Lund-Nielsen, K. Wittenburg, DESY, Hamburg, Germany.

Abstract

To measure the beam position at the entrance of the FLASH dump a position monitor has been installed outside of the vacuum in a nitrogen atmosphere. When a charged particle travels through the gas it ionizes the atoms. Therefore the signal from a capacitive button BPM would be contaminated by high backgrounds. To avoid this a magnetic coupled monitor has been designed. The monitor consists of four longitudinal loops symmetrically arranged in the pipe wall. An analytical expression of the signal for this monitor is derived and compared with simulations. Measured data are compared with predictions.

INTRODUCTION

A new diagnostics section before the beam dump has been installed at FLASH [1]. A major component is a new beam position monitor (BPM). The beam exits the vacuum system through a special window before reaching the dump. Its position must be measured here to verify the proper absorption of the beam in the dump. A beam-pipe here connects the exit window to the dump.

The charged particles of the beam ionize the N_2 gas volume between the window and the dump. A 1 GeV electron has an ionization loss of 3 keV/cm in nitrogen. The effective ionization length is the distance between the window and the dump (l = 15 cm). The energy loss over this length is 45 keV. According to the production yield [2] this corresponds to about 1300 electron-ion pairs per beam-electron. In the absence of an electric field most of the pairs recombine but some would reach the electrodes of a BPM. In this case the signals of an electric coupled button or stripline BPM would be strongly influenced by the electron-ion pairs [3]. The influence can be drastically reduced by measuring not the electric but the magnetic field of the fast moving charge.

The coupling has been realized with a thin metallic wire forming an electric loop in the pipe. The normal direction of the area of the loop is parallel to the magnetic field of the beam to maximize the signal amplitude. In Figure 1 a sketch of the magnetic coupling is shown. This paper discusses the derivation of analytic expressions for the signal of this BPM and the results are compared with simulations and with measured signals.

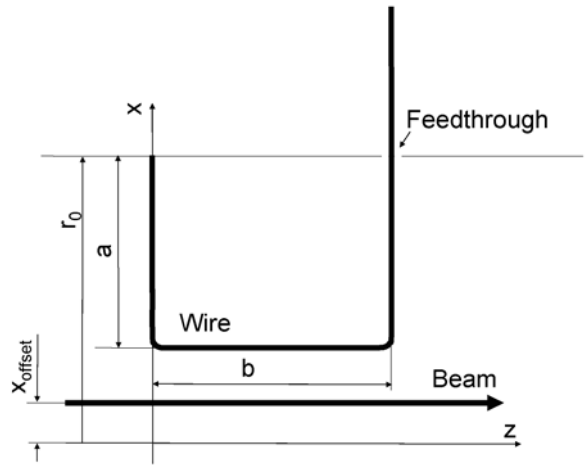

Figure 1: A sketch of one quarter of the detector. A wire forms a loop in the pipe with radius r_0=61.5 mm in the y plane and surrounds an area $A = a \times b$, with a=12 mm and b=10 mm. The signal is transferred with a feedthrough.

ANALYTICAL SOLUTION

The magnetic field of a beam with current $I(t)$ is given by the Biot-Savart rule as

$$\vec{B}(\vec{r},t)=\frac{\mu_0 I(t)}{2\pi\rho}\vec{e}_\phi ,$$

with μ_0 the vacuum permeability and ρ the distance to the z-axis in cylindrical coordinates. The beam current can be expressed as

$$I(t)=q_0\frac{1}{\sigma\sqrt{2\pi}}e^{-\frac{1}{2}\frac{t^2}{\sigma^2}},$$

with q_0 the beam charge and σ the bunch length in units of time. In Cartesian coordinates the magnetic field is

$$\vec{B}(x',y',t)=\frac{\mu_0 I(t)}{2\pi\left(x'^2+y'^2\right)}\begin{pmatrix}-y'\\ x'\\ 0\end{pmatrix}.$$

The magnetic field with a horizontal offset can be described by a coordinate transformation: $x'=x_{offset}-x$, $y'=y$, $z'=z$, resulting in

$$\vec{B}_1(x_{offset},x,y,t)=\frac{\mu_0 I(t)}{2\pi\left(\left(x_{offset}-x\right)^2+y^2\right)}\begin{pmatrix}-y\\ x_{offset0}-x\\ 0\end{pmatrix}.$$

This field is valid without the beam pipe. To include it a second current is introduced with $I_2(t)=-I(t)$. The direction

#dirk.lipka@desy.de

COMMISSIONING RESULTS AND IMPROVEMENTS OF THE MACHINE PROTECTION SYTEM FOR PETRA III

T. Lensch#, M. Werner, DESY, Hamburg, Germany

Abstract

PETRA III is a high brilliant synchrotron light-source operating at 6GeV. The commissioning of the machine had started in April 2009 [1]. In the first months of operation the Machine Protection System (MPS) ran on basic MPS requirements to protect absorbers and vacuum chambers in the damping wiggler section and the undulator section against synchrotron light. Therefore several alarms distributed along the machine are identified and within 100µs a dump command is created. The beam is dumped within 400µs by switching off the RF system [2]. Prior to the first user runs different improvements increasing the reliability and availability were planned and partly implemented in the MPS. This paper presents commissioning results of the system and gives an overview of these new implementations as well as a more detailed discussion of some alarm conditions and the dump procedure. Additionally some key aspects of the Temperature Interlock as one major alarm deliverer are described.

INTRODUCTION

Starting in June 2007 the former preaccelerator PETRA II was rebuilt to a high brilliant 3rd generation synchrotron light source operating at 6 GeV. In seven eights of the 2.3km long accelerator tunnel all installations were removed, modernized and reinstalled. In one eight an experimental hall was built which houses 14 undulator beamlines, experimental hutches and laboratories. In two straight sections of the machine damping wigglers are installed to reduce the horizontal emittance to the designed value of 1 nm rad [1]. A Machine Protection System (MPS) is required to protect absorbers against too high impact of synchrotron light and wigglers and undulators against losses of the electron beam. The MPS needs to dump the beam within several hundreds microseconds in case of unsafe conditions, detected from several alarm deliverers located around the machine [2].

The commissioning of the PETRA III machine as well as the MPS started in March 2009, the first beam was stored in April 2009. In the first months of operation with low beam currents the MPS ran on basic requirements to prevent the machine from damage. Since then diverse functionalities for increasing the availability and reliability of the system were implemented as well as upgrades for diagnostic purposes.

timmy.lensch@desy.de

MPS CONFIGURATION

The MPS is distributed in nine PETRA III halls in 19” crates. A connection to the control system is made via the in-house fieldbus SEDAC. At one position (east hall) the beam current (DC) is measured and digitally distributed by a redundant optical fibre loop which transmits both beam current information and dump information to all crates in the system. 24 alarm modules are shared in 10 crates. Each alarm module features 16 inputs for several alarm deliverers (e.g. beam position monitors (BPM), temperature interlock, etc.).

Every alarm input can be masked by an individual beam current threshold. There are three types of alarms connected to the MPS:

- To protect the machine against damaging by synchrotron radiation or the electron beam about 170 alarms can create a trigger which dumps the beam.
- Further 16 alarms are used to mask other inputs.
- Additionally 50 alarms from magnet power supplies, the RF system and kickers are connected to the MPS which are not triggering a dump but allow a first alarm detection. This can help operators finding the reasons of beam losses and dumps [2].

Figure 1 shows the connections of the MPS; figure 2 shows the topology of the MPS.

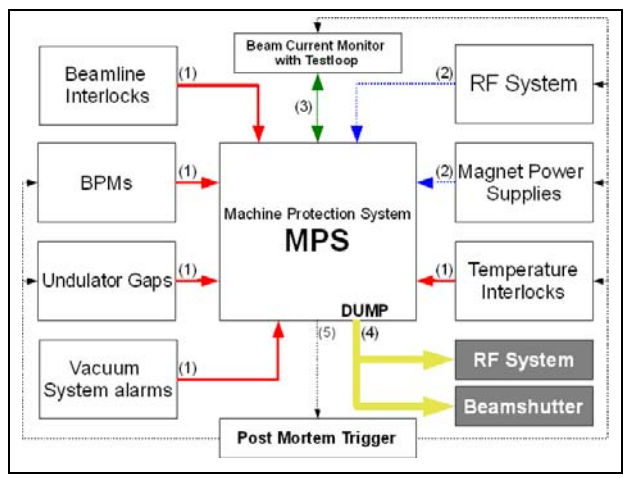

Figure 1: Connections of the MPS. Diverse alarm deliverers are connected to the MPS: red (1) Alarms generate a beam dump; blue (2) alarms are used for the first alarm detection. The MPS compares the measured beam current (green, 3) with an individual beam current threshold for each alarm input. The RF system and beam-stoppers are used for a beam dump (yellow, 4). A post mortem trigger (black, 5) is sent to several systems (e.g. RF system, BPM system).

DEVELOPMENT OF BUTTON ELECTRODES FOR SUPERKEKB RINGS

M. Tobiyama*, H. Fukuma, K. Shibata, M. Tejima, S. Hiramatsu, K. Mori, H. Ishii, T. Obina
KEK Accelerator Laboratory, 1-1 Oho, Tsukuba 305-0801, Japan

Abstract

Button-type beam position monitors for SuperKEKB rings have been designed. The RF characteristics such as beam response, trapped modes or wake functions have been simulated using 3-D E-M codes such as GdfidL and HFSS. The estimated instability threshold from the trapped modes was much higher than the radiation damping time. The prototype units have been tested in the prototype-antechambers installed in KEKB rings. The mechanical reliability and the beam responses are also reported.

INTRODUCTION

The KEKB B-Factory has been operating since 1998, keeping the world highest luminosity and accumulating integrated luminosity more than 1 ab^{-1} up to now. To investigate the flavour physics with the aid of huge integrated luminosity, improvement of the KEKB to SuperKEKB has been proposed. In SuperKEKB rings, we almost double the stored current, reduce the emittance about 1/10, squeeze betatron functions at the interaction point to achieve about 40 times larger luminosity. To reduce the beam size of the injected beam, we will construct a positron damping ring. Most of vacuum chambers around arc sections will be replaced with new antechambers to reduce the electron cloud effect in LER (4 GeV positron ring), and to overcome huge heat load from SR in HER (7 GeV electron ring). In the positron ring, the inner surface will be coated with TiN to reduce secondary emission yield (SEY) of electron clouds. The interaction region (IR) will be completely re-designed with much more complicated structure. Since all of the modifications shown above change the requirements for beam position monitors, it is necessary to evaluate and re-design the BPM electrodes.

We have designed N-type feedthroughs (FTs) with the button electrode of diameter of 12 mm for KEKB rings[1]. Those FTs were brazed to a vacuum chamber of Cu directly with good precision except several special region such as IR or a monitor test section which are made of aluminium vacuum chambers. Up to now, no major trouble was found on the FTs. However, for the SuperKEKB, the original N-type BPM will have the following difficulties:

- Since the FTs are already assembled under blazing process, the second blazing process to the vacuum chamber needs to be controlled with great care not to break the FTs with exceed temperature. We will need huge trials before establishing the final procedure.
- It is fairly difficult to repair the electrodes even if the case of the FT are fairly suspicious to such as shorted circuit or deformed output. The minimum unit of replacement is a quadrupole vacuum chamber unit; not realistic in most cases.
- Because of the large structure, a center frequency of the trapped mode (HOM) around a button-head stays rather lower frequency, around 5 GHz. The threshold beam current of the longitudinal coupled bunch instability caused by this HOM is estimated to be near the present maximum beam current of KEKB[2].

We have developed a BPM electrode with a vacuum flange-connection which will be used for most of a new vacuum chamber and the new damping ring, and an IR special electrode capable for very tight space and large beam power. The RF characteristics, beam response, wake function and beam impedance have been evaluated using 3D electromagnetic codes such as HFSS[3] and GdfidL[4]. The trial pieces of the electrodes have been installed in a vacuum chamber as a position monitor and been checked with the beam. The main parameters of SuperKEKB rings including damping ring are shown in Table 1.

Table 1. Main parameters of SuperKEKB rings (HER: electron, LER: positron, DR: positron damping ring)

	LER	HER	DR	
Energy	4.0	7.0	1.05	GeV
Circumference	3016		135	m
RF frequency		508.886		MHz
Beam current	3.8	2.6	0.08	A
Bunch number	2503		4	
Bunch length	6	5	5	mm
No. of BPM	~450	~450	84	
H emittance	3	5	13	nm rad
Coupling	0.4	0.3	10	%

NORMAL BPM ELECTRODE

Mechanical structure

A button electrode for SuperKEKB rings needs to have enough mechanical precision, at least the position error of the BPM to the level comparable to the errors coming from the gain or loss error of other components such as cables. Also the structure should be capable to the beam power much larger than KEKB. An RF connector should have full reliability on long term operation. Longitudinal coupling impedance of the BPM needs to be reduced lower enough not to cause coupled bunch instability with maximum beam current. Since the vacuum chambers of the LER and the damping ring (DR), including monitor section will be coated with TiN to reduce the SEY, it is necessary to assemble the BPM heads after the coating

*makoto.tobiyama@kek.jp

BEAM MEASUREMENTS OF A LARGE SOLID-ANGLE BEAM LOSS MONITOR IN THE APS*

B.X.Yang, W. Berg, J. Dooling, A. Pietryla, A. Brill, and L. Erwin
Advanced Photon Source, Argonne National Laboratory, Argonne, IL 60439, USA.

Abstract

For reliable radiation dosimetry of undulator magnets, a beam loss monitor (BLM) covering a large solid angle from the point of beam losses is highly desirable. A BLM that uses a Cherenkov radiator plate wrapping around the beam pipe is utilized in the Linac Coherent Light Source (LCLS) undulators, and a similar BLM geometry has been tested for the Advanced Photon Source (APS) undulators. We report on measurements made with these BLMs recently installed in the APS storage ring and the booster-to-storage-ring transfer line. A two-order-of-magnitude variation in the relative sensitivity of the Cherenkov detector is observed as a function of incident electron position in the quartz radiator. A factor of 10 variation in signal sensitivity was observed with the change of particle entry angle. The introduction of tungsten and lead shields enhances count rates by 30 – 40%. When the detector is moved along the insertion device chamber, the signal intensity peaks 1 m from the chamber entrance. The measured data are compared with numerical simulation of the beam loss processes.

INTRODUCTION

At the APS, a large area beam loss monitor (BLM) was developed for the LCLS to measure radiation dose rates at the FEL undulator magnets [1]. The BLM detects Cherenkov radiation generated by high-energy electrons in an aluminum-coated, quartz radiator. The radiator is placed just upstream of each LCLS undulator magnet. Ray-tracing analyses and numerical simulations show that the optical efficiency varies by at least 2 orders of magnitude as a function of electron position in the radiator [2]. In this work, we present detector efficiency measurements using APS high-energy radiation beams.

BEAM LOSS MONITOR DESIGN

Figure 1 shows the tuning-fork-shaped LCLS-BLM radiator design. The electron beam passes into the paper at the location of the small cross in the figure. The radiator wraps around the beam pipe and covers the entire area of the undulator magnets. Shower particles from high-energy, lost electrons are expected to deviate only slightly from the incoming beam direction and enter the radiator approximately normal to the surface of the paper.

Figure 2 shows the enlarged top view of the coupling area between the radiator and the photomultiplier tube (PMT). The Cherenkov radiation is emitted in a cone with a half cone angle determined by $\cos\theta_C = 1/n\beta \approx 1/n$, where $n \approx 1.47$ is the refractive index of the radiator material. In our case, where the PMT is mounted 90º from the direction of the electron beam, $\theta_{PMT} = \pi/2 - \theta_C$, and $\sin\theta_{PMT} \approx 1/n$, which is the same condition of total internal reflection at the PMT coupling surface, implying a very low coupling efficiency with the PMT. We note that the condition of total internal reflection can be broken if the radiator is rotated.

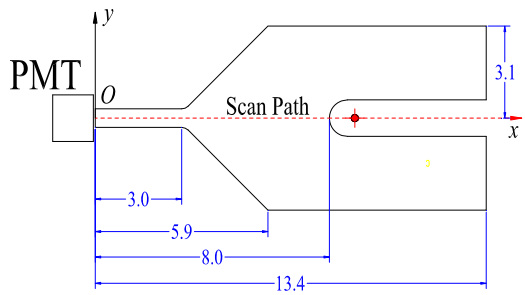

Figure 1: BLM radiator (units in cm). The dashed line shows the scan path of the gas bremsstruhlung beam.

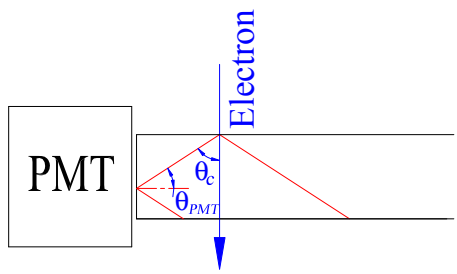

Figure 2: Top view of the radiator showing the Cherenkov radiation cone and the total internal reflection.

GAS BREMSSTRUHLUNG SOURCE

Undulators occupy many long straight sections in synchrotron radiation sources. As stored electrons traverse through the residual gas in these straight sections, gas bremsstruhlung (GB) photons are generated with energies up to the electron energy of the machine [3-6]. During normal operations, the GB photon beam is stable with a well-defined direction, size, and intensity. Accessibility to experimental stations makes it possible to perform experiments with high-energy, gamma-ray and electron detectors with great flexibility and convenience. We hope to demonstrate the advantages of this gamma-ray source for testing radiation detectors using, for example, pair-production electrons and photoneutrons.

Simulated Angular Distribution

To characterize the GB radiation in the 35-IDA hutch, realistic beamline geometry is simulated using the

* Work supported by U.S. Department of Energy, Office of Science, Office of Basic Energy Sciences, under Contract No. DE-AC02-06CH11357.

HIGH-POWER HARD X-RAY BEAM POSITION MONITOR DEVELOPMENT AT THE APS*

B.X.Yang, G. Decker, S. H. Lee, and P. Den Hartog
Advanced Photon Source, Argonne National Laboratory, Argonne, IL 60439, USA

Abstract

Accurate and stable x-ray beam position monitors (XBPMs) are key elements in a feedback control system for good x-ray beam stability. For the low-emittance mode of operation of the Advanced Photon Source (APS), the cross sections of the undulator x-ray beams are not upright ellipses, and the effective beam sizes in the horizontal and vertical planes depend on the undulator gaps. These beam characteristics introduce strong gap dependence in photo-emission blade-type XBPMs designed for upright elliptical beams. A center-of-mass XBPM will significantly reduce the gap dependence of the BPM readings. We report the development status of a high-power center-of-mass XBPM at the APS. We note that users often discard more than 50% of the undulator beam power outside of the monochromatic beam. These photons can be intercepted by the limiting aperture of the beamline, and their x-ray fluorescence footprint can be imaged onto a detector. The position of the x-ray beam can be read out using position-sensitive photodiodes. Thermal analyses show that the XBPM can be used for the measurement of beam with a total power up to 21 kW for the 7-GeV APS beam.

INTRODUCTION

X-ray beam stability is an important requirement from the Advanced Photon Source (APS) users. X-ray beam position monitors (XBPMs) are at the heart of the control system delivering the required stability. As the stability requirements become increasingly demanding, XBPMs are asked to deliver increasingly precise information about the x-ray beam. In this work, we propose a design concept that combines the function of a high-heat-load photon collimator and the beam position monitor. We will present a thermal analysis of the collimator, an optical design of the readout detector, and the results of preliminary tests.

XBPM Challenge

Table 1 shows properties of typical APS undulator sources, as well as the beam stability currently achieved and planned for the future upgrade [1].

Since its commissioning, the APS has used the photoemission blade-based XBPM [2]. It is located well away from the undulator beam core and does not have to handle the full power of the undulator under normal conditions. The thermal distortion of its blades has not been measured experimentally. The dependence of its calibration on undulator gap is its main weakness. To understand the gap dependence, let us consider a vertical XBPM using Gaussian beam approximation: We assume that the spatial distribution of the photoelectron is given by:

$$J_{PE}(y) = J_{PE0} e^{-(y-y_0)^2/2\sigma_y^2}, \quad (1)$$

where y_0 is the center of the x-ray beam. We further assume that the upper blade covers b to $+\infty$, and its signal is given by $I_{PE+} = \int_b^{\infty} J_{PE}(y)\,dy$. A similar expression can be written for the lower blade, $I_{PE-} = \int_{-\infty}^{-b} J_{PE}(y)\,dy$.

Table 1: XBPM Characteristics

Location (m)	Current	Planed
Maximum beam current	100	200
No. of Undulator A	1	2
Maximum power	6 kW	21 kW
Maximum power density	183 kW/mr^2	630 kW/mr^2
RMS stability, Horizontal (0.1 – 200 Hz) Vertical	5 μm/0.85μr 2 μm/0.8 μr	3 μm/0.53μr 0.4 μm/0.2 μr

The BPM ratio signal is defined as the ratio of the difference over sum of these two signals,

$$R_{PE}(y_0) = \frac{erfc\left(\frac{b-y_0}{\sqrt{2}\sigma_y}\right) - erfc\left(\frac{b+y_0}{\sqrt{2}\sigma_y}\right)}{erfc\left(\frac{b-y_0}{\sqrt{2}\sigma_y}\right) + erfc\left(\frac{b+y_0}{\sqrt{2}\sigma_y}\right)}, \quad (2)$$

where $erfc(u) = \frac{2}{\sqrt{\pi}} \int_u^{\infty} e^{-t^2} dt$ is the complementary error function. The readout of the BPM is given by $Y = l_y R_{PE}$, where the calibration length,

$$l_y = \sqrt{\frac{\pi}{2}} \sigma_y e^{\frac{b^2}{2\sigma_y^2}} erfc\left(\frac{b}{\sqrt{2}\sigma_y}\right), \quad (3)$$

is chosen so $Y \approx y_0$ for small displacement. Figure 1 plots the calibration length l_y as a function of the beam size σ_y, for b = 2, …, and 6 (mm). For fixed blade spacing, l_y depends on beam sizes: the larger the beam size, the larger is l_y, and the less sensitive the XBPM becomes.

When undulator harmonic energies are away from Au absorption edges, the broadband excitation can be approximated using bend magnet (BM) spectra. The total electron yield (TEY) from the gold surface can be estimated using Henke approximation [3] with x-ray spectra calculated with XOP [4]. We found that, as shown in Figure 2, the vertical TEY profile fits well to a pseudo-Student distribution function,

$$S_e = S_{e0}\left(1 + \frac{1}{\nu}\left|\frac{y_0}{\sigma_s}\right|^m\right)^{-\frac{\nu+1}{2}}, \quad (4)$$

* Work supported by U.S. Department of Energy, Office of Science, Office of Basic Energy Sciences, under Contract No. DE-AC02-06CH11357.

BUNCH-BY-BUNCH DIAGNOSTICS AT THE APS USING TIME-CORRELATED SINGLE-PHOTON COUNTING TECHNIQUES*

B. X. Yang, W. E. Norum, S. Shoaf, and J. Stevens
Advanced Photon Source, Argonne National Laboratory, Argonne, IL 60439, USA.

Abstract

Time-correlated single-photon counting (TCSPC) techniques have been used for bunch purity measurement since the Advanced Photon Source (APS) started operations. Recent improvements of the monitor have increased the signal-to-noise ratio and dynamic range to about 100 billion. Resolution improvements of commercial TCSPC components to under 50 ps FWHM allowed us to measure the longitudinal profile of individual bunches in the APS storage ring using a single-photon avalanche photodiode and a PicoHarp 300 TCSPC unit. Due to its robustness, the system operates continuously and measures the average longitudinal profile of the stored beam, updating the process variables for bunch phases and bunch lengths every 8 seconds. In a third application, using a TCSPC x-ray detector with an x-ray wire scanner in the monochromatic beam of the diagnostics undulator, measurements of transverse profiles of individual bunches can be completed in less than 4 minutes. It showed that, due to energy losses to the storage ring impedance, the high-current bunch clearly travels a different trajectory from low-current bunches. These bunch-by-bunch diagnostics provide valuable beam information to users performing timing experiments.

INTRODUCTION

Time-correlated single photon counting (TCSPC), a technique for measuring arrival time of the photon pulses against a clock pulse train, is a well-established technique for studying time-resolved phenomena in physics, chemistry and biology [1,2]. At the Advance Photon Source (APS), this technique has been used for bunch purity measurement since 1999 [3].

Figure 1 shows a conventional TCSPC instrument. It uses a time-to-amplitude converter (TAC) to produce a pulse with its amplitude proportional to the interval of time between the signal pulse (START) and the clock pulse (STOP), and an analogue-to-digital converter (ADC) to measure the pulse height. Since only one signal pulse can be processed during the interval between two clock pulses, the dead time may be as long as a clock period, and obtaining a high count rate and long time-scale at the same time is difficult. Modern TCSPC instrument, however, digitizes the event time using time-to-digital converters (TDC). Figure 2 shows the timing diagram of a TDC: A high-frequency clock and one or more lower-frequency timing signals establish a timing grid. Internally, the TDC generates higher-frequency ticks to make finer timing divisions. When a signal pulse (event) triggers the counter, the number of ticks since the last clock pulse, $\tau(k)$, the number of clock pulses since the last timing marker, $t(j)$, and the number of timing markers since the instrument are enabled, $T(i)$, are recorded by the internal circuitry, giving the complete timing information of the event. In the time-tagged time-resolved (TTTR) mode, the complete set of event timing information, (i, j, k), is recorded for user processing. In histogram mode, these events are collected and made into frequency of occurrence within designated intervals by an internal program. Using the TDC, more than one event can be recorded between two clock pulses, and a high count rate of several Mc/s is not in conflict with a long time scale of μs or even ms. In the following examples, we will show how the TDC-based TCSPC techniques are used at the APS for accelerator diagnostics.

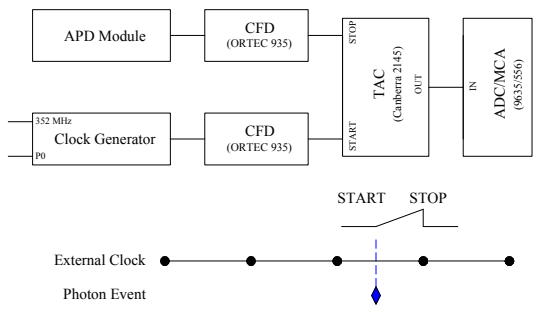

Figure 1: Conventional TCSPS and timing diagram.

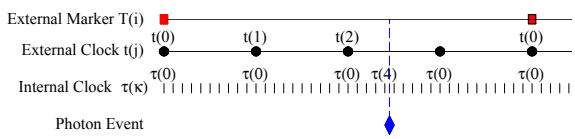

Figure 2: Digital TCSPS timing diagram.

BUNCH PURITY MONITOR UPGRADE

The original APS bunch purity monitor used the conventional TAC-ADC technique. It was used 2–3 times daily and provided bunch purity data typically at the 10^{-6} – 10^{-7} level [3]. Our upgrade effort included redesign of the fluorescence-target; improvement of the detector and analogue electronics operations, and implementation of an field-programmable gate array (FPGA) based TDC [4].

Redesign of the fluorescence target chamber

Figure 3 shows the redesigned fluorescence target

* Work supported by U.S. Department of Energy, Office of Science, Office of Basic Energy Sciences, under Contract No. DE-AC02-06CH11357

NUMERICAL STUDIES OF CURTAIN GAS JET GENERATION FOR BEAM PROFILE MONITORING APPLICATIONS IN THE ULTRA LOW ENERGY STORAGE RING*

M. Putignano†, C.P. Welsch, Cockcroft Institute and University of Liverpool, UK.

Abstract

For beam profile monitoring applications where low beam perturbation together with bi-dimensional imaging is required, ionization monitors based on neutral gas-jet targets shaped into a thin curtain are an interesting option. When integrated in ultra-high vacuum systems, such as in the Ultra-low energy Storage Ring (USR), where local vacuum preservation is of primary concern, such systems present severe difficulties linked to the creation and proper shaping of a high quality gas-jet curtain. In this contribution, investigations into the generation and evolution of the jet with the Gas Dynamics Tool (GDT) software and purpose-written C++ analysis modules are presented. By means of extensive numerical analysis the advantages of a novel nozzle-skimmer system in terms of curtain quality are summarized when compared to traditional axisymmetric gas-jet creation and curtain shaping by means of scrapers. It is also shown that variable nozzle-skimmer geometries allow for modifying the gas-jet characteristics in a wide range, including jet splitting and local density modulation. Finally, the layout of a test stand that will be used for an experimental benchmark of these studies is shown.

INTRODUCTION

Low-energy physics and storage rings are recently attracting growing interest in the scientific community, as remarkable characteristics of quantum systems are most conveniently studied at low projectiles energies in the keV range [1,2]. Development of low-energy storage rings causes widespread beam diagnostic technologies to become obsolete. In particular preservation of the beam lifetime causes perturbing profile monitoring, like e.g. interceptive foils, to be ruled out [3]. Furthermore, existing non-perturbing techniques such as residual gas monitors can take up to about 100 ms [4] to make meaningful measurements, due to the low residual gas pressure, at the expected operating pressure of around 10^{-11} mbar. A possible solution around these limitations is constituted by a neutral supersonic gas jet target shaped into a thin curtain and bi-dimensional imaging of the gas ions created by impact with the projectiles. If the curtain is kept at a 45° angle from the impinging direction of the projectiles, and the ions extracted perpendicularly to this direction on a position sensitive detector, an image of the projectile beam transverse section is formed on the detector, much like a mirror reflection [5], as shown in Fig. 1.

Such monitor, as compared to those based on residual gas, allows injection of additional gas, in order to increase the ionization rate, together with efficient evacuation to keep the required vacuum level elsewhere in the storage ring, due to the high directionality of the supersonic jet [6]; furthermore, it allows simultaneous determination of both transversal profiles and beam imaging. At the same time, it is possible to use it also as a current and beam position monitor.

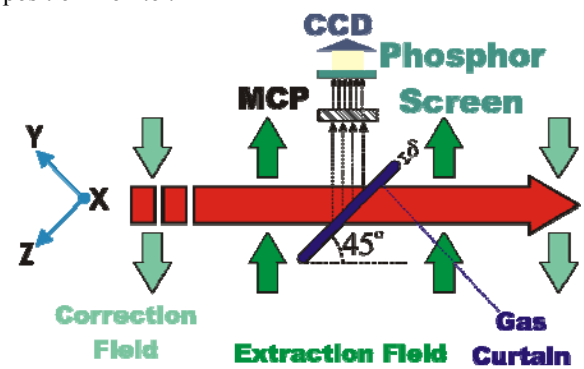

Figure 1: Jet-curtain profile monitor operation principle: the large horizontal arrow shows the projectiles path.

This monitor becomes hence the monitor of choice for multi-pass, low-energy, ultra-high vacuum storage rings such as the Ultra-Low Energy Storage Ring (USR), to be installed at the Facility for Low Energy Antiproton and Ion Research (FLAIR), in the FAIR facility planned to be built at GSI, Darmstadt, Germany.

Crucial to such monitor is the generation and control of the gas-jet in terms of achieved density and directionality. In order to prove that optimization of the jet performance can be obtained through suitable engineering of the nozzle-skimmer system for the jet generation, we have run a detailed numerical study of the fluid dynamic system.

NUMERICAL SIMULATIONS

Software Description

The software used for our simulations was a well-established commercial code, the Gas Dynamic Tool, GDT, developed by the CFD group of A. Medvedev in Tula, Russia. The code has been widely benchmarked against known flows, proving very reliable in dealing with high compressibility effects such as shock waves.

*Work supported by the EU under contract PITN-GA-2008-215080, by the Helmholtz Association of National Research Centers (HGF) under contract number VH-NG-328 and GSI Helmholtzzentrum für Schwerionenforshung GmbH.
†corresponding author: massimiliano.putignano@quasar-group.org

INFLUENCE OF DARK COUNT ON THE PERFORMANCE OF SILICON PHOTOMULTIPLIERS

A. Intermite#, M. Putignano, C.P. Welsch, The Cockcroft Institute, Warrington WA4 4AD, UK,
Department of Physics, University of Liverpool, Liverpool L69 7ZE, UK

Abstract

The introduction of Silicon Photomultipliers (SiPMs) as single photon sensitive detectors represents a promising alternative to traditional photomultiplier tubes. This is especially true in applications in which it is compulsory to attain magnetic field insensitivity, low photon flux detection, quantum efficiency in the blue region that is comparable to standard photomultipliers, high timing resolution, dimensions comparable to the dimensions of an optical fiber diameters, and low costs. The structure of the SiPM is based on an array of independent Avalanche Photodiodes (APDs) working in Geiger-mode at a low bias voltage with a high gain. The output signal is proportional to the number of pixels "fired" by impacting photons. The detection efficiency for state-of-the-art devices is in the order of 20% at 500 nm. In this contribution, the measured dark count rates of different SiPMs are compared and the signal shape and statistical spectrum of this noise analyzed. A characterization of the effects on the noise of the bias voltage is performed as part of the study to determine the optimized working parameters for a future beam loss monitor at CTF3/CLIC.

INTRODUCTION

Sensors capable of detecting single photons have found different applications in fields as astronomy [1] laser ranging [2], Optical Time Domain Reflectometry (OTDR) [3] and beam loss detection [4], replacing in such applications the former use of photomultiplier tubes (PMTs). The need to reduce the detector dimensions and to produce marketable nanotechnology applications require the use of small area, highly sensitive detectors that combine integrated readout circuitry functionality in a cheap fabrication process. In addition, small area detectors can be easily integrated in a dense array, be coupled with optical fibers, and reach high sensitivities.

Due to their high quantum efficiency, magnetic field immunity, robustness, low costs, possibility to operate at non-cryogenic temperatures and single photon detection capability, SiPMs are considered a suitable candidate for the readout of optical fibers in a beam loss detection system [4].

In this contribution, the operation principle of the beam loss monitor that will be used at CLEX/CLIC is introduced before a noise study for the SiPM, providing both a theoretical description and a set of experimental data, is described in detail. Within the analysis the behaviour of the noise with respect to the bias voltage applied to the SiPM by the user and to the quality of the manufacturing features dependent on the supplier are explored.

BEAM LOSS DETECTION

For detecting and localizing beam losses in an accelerator, it is possible to exploit the generation of Cerenkov light inside optical fibers generated by impinging charged relativistic particles. At the locations where particles are lost from the main beam in the accelerator, these are likely to generate secondary particles through interaction with material, such as the beam pipe. These secondary charged particles are typically moving at relativistic velocities, hence, when they cross a medium with high enough dielectric constant, such as an optical fiber, they generate photons by the so-called *Cerenkov Effect* [5]. In such a configuration the fiber can be used to guide these photons to a SiPM, optically coupled to the fiber end [6]. In order to detect the beam losses at CTF3/CLIC, a system consisting of two parallel fibers connected to two identical SiPMs with an active surface matched to the fiber core of 1 mm^2 is under consideration.

The first fiber is used to carry a reference signal, and is chosen to be a low attenuation multimode fiber with a large core diameter. This maximizes the length of interaction with the escaping particles and thus the production of Cerenkov photons. The second arm is instead a composite sensor, realized by separating equally long sections of a fiber identical to the one in the first arm by splicing in between them equally long section of a different fiber with larger attenuation. This way, the number of Cerenkov photons reaching the SiPM at the end of the second arm will be smaller than the number reaching the SiPM in the first arm by a factor depending on how many section of the more attenuating fiber were crossed and, therefore, on the position of the loss.

Simulation studies indicate that this sensor has the ability to achieve a resolution of down to a few centimeters, depending mainly on the length of the spliced fiber sections in the second sensor. In addition, each signal is read independently and the absolute position is then calculated from the intensity ratio in the two branches. This guarantees that there is no overlap of the signals and it becomes possible to detect multiple signals without using clock triggers.

The high spatial resolution of the monitor is particularly relevant when there is the need to monitor losses in narrow spaces as for example in the CLIC Experimental

#Corresponding author : angela.intermite@quasar-group.org

BEAM POSITION MONITOR DEVELOPMENT FOR THE USR*

J. Harasimowicz#, C. P. Welsch, Cockcroft Institute, Warrington WA4 4AD, UK,
and Department of Physics, University of Liverpool, Liverpool L69 7ZE, UK.

Abstract

Capacitive pick-ups for closed-orbit measurements are presently under development for an Ultra-low energy Storage Ring (USR) at the future Facility for Low-energy Antiproton and Ion Research (FLAIR). Low-intensity, low-energy antiprotons impose challenging demands on the sensitivity of the monitoring system. The non-destructive beam position monitors (BPMs) should be able to measure about 10^7 particles and give sufficient information on the beam trajectory. This contribution presents the status of the BPM project development. Main goals of the investigation include optimization of the mechanical design and preparation of a narrowband signal processing system.

INTRODUCTION

A diagonal-cut capacitive pick-up (PU) is a device of choice for beam diagnostics in hadron machines due to its highly linear response and large sensitivity. This beam position monitor (BPM) consists of four isolated and equally distributed metal plates formed to surround the beam. It provides information on beam offset by means of non-destructive measurements of electric field produced by passing bunches: by comparing the signals generated at each electrode, it is possible to determine the position of the beam centre. PU linearity, important for beams of non-negligible diameter, is assured by a diagonal cut of the plates. Their length is typically of 10-20 cm per plane, but still much less than the bunch longitudinal profile, and results in high signal strength. On the other hand, bulky dimensions might be a problem when only limited space is available. Also the capacitive coupling between the large electrodes should not be neglected and its reduction may lead to a complex mechanical design. Nevertheless, an optimised diagonal-cut PU can be a powerful tool for a variety of measurements, like beam position, Q-value or closed orbit determination [1].

The application of BPMs for low intensity, low energy beam diagnostics requires additional considerations. The signal-to-noise (S/N) ratio drops down with the decreasing beam current and becomes a dominating problem for beams with only few particles per bunch. In order to improve PU sensitivity, the signal U_S has to be amplified while the noise U_N needs to be significantly reduced. Since U_N is proportional to $\sqrt{(\Delta f)}$, where Δf is the bandwidth of the system, a narrowband signal processing is required for low intensity beam diagnostics. Further complications can be caused by low velocities. For $\beta < 0.1$, the beam can no longer be approximated by a TEM wave and deviations from a relativistic case should be taken into account. The field distribution becomes dependent on the beam displacement and the PU response may be affected [2].

* Work supported by the EU under contract PITN-GA-2008-215080, by the Helmholtz Association of National Research Centers (HGF) under contract number VH-NG-328, and GSI Helmholtz Centre for Heavy Ion Research.
#Janusz.Harasimowicz@quasar-group.org

BEAM PARAMETERS

The boundary conditions of a novel electrostatic Ultra-low energy Storage Ring (USR) [3] at the future Facility for Low-energy Antiproton and Ion Research (FLAIR) [4] put challenging demands on its beam instrumentation. The USR will store and decelerate antiproton beams from 300 keV to 20 keV, corresponding to β values of only 0.025 and 0.006 respectively. At such low energies the total number of particles is restricted by space charge limitations to about $2 \cdot 10^7$ antiprotons. With the ring circumference of 42.6 m, their revolution frequency f_{rev} will vary from 178 kHz to 46 kHz in the given energy range. To achieve bunch lengths of the order of 100 ns required in the standard operation of the USR, an RF field $f_{RF} = h \cdot f_{rev}$ with harmonic number $h = 10$ will be applied. The resulting frequencies and related beam parameters are summarized in Table 1. Since bunches will be at least 1 m long, a diagonal-cut capacitive pick-up will be an ideal tool for beam position monitoring. However, few particles per bunch as well as low β values have to be considered when designing the BPM system.

Table 1: USR beam parameters

Energy	300 keV → 20 keV
Relativistic β	0.025 → 0.006
Revolution frequency	178 kHz → 46 kHz
Revolution time	5.6 µs → 21.8 µs
RF frequency (h = 10)	1.78 MHz → 459 kHz
Bunch repetition time (h = 10)	560 ns → 2.2 µs
RF bucket length (h = 10)	4.4 m
Charge per bunch (h = 10)	0.3 pC ($2 \cdot 10^6$ pbars)

MECHANICAL DESIGN

The initial proposal for the diagonal-cut capacitive pick-up for the USR was already discussed in [5], but its final design includes several important modifications.

In order to avoid distortion of the electric field in the vicinity of the monitor edges, the inner diameter of the cylindrical PU is the same as of the straight section vacuum pipe of the USR. Initially, it had been assumed to

FARADAY CUP FOR LOW-ENERGY, LOW-INTENSITY BEAM MEASUREMENTS AT THE USR*

J. Harasimowicz#, C. P. Welsch, Cockcroft Institute, Warrington WA4 4AD, UK,
and Department of Physics, University of Liverpool, Liverpool L69 7ZE, UK.

Abstract

For destructive beam intensity measurements, electrostatic Faraday cups will be incorporated into the Ultra-low energy Storage Ring (USR) and its transfer lines at the Facility for Low-energy Antiproton and Ion Research (FLAIR). This multi-purpose machine will offer both slow and fast extracted beams resulting in a wide range of intensities and varying time structure of the beam. In this contribution, we present the particular challenges of measuring the beam intensity in the USR, results from numerical optimization studies, as well as the design of the cup.

INTRODUCTION

Faraday cups are commonly used for beam intensity monitoring due to their simplicity and reliability. Despite a destructive character of the measurements, they can provide accurate information on the beam current in a very straightforward manner: a conductive beam stopper is introduced in the beam path and the total charge carried by the particles is collected and measured by means of an ammeter connected to the device.

A number of issues need to be considered when designing a Faraday cup: the heat load together with a proper cooling system, a suitable current meter, and finally, the emission of secondary charged particles which could escape from the cup and affect the results. This is normally not a problem for most accelerators, but very important when an existing design needs to be optimised to specific beam parameters.

BEAM INTENSITIES AT THE USR

A novel electrostatic Ultra-low energy Storage Ring (USR) [1], being under development for the future Facility for Low-energy Antiproton and Ion Research (FLAIR) [2], will require ultra-sensitive instrumentation for its proper operation. The USR will store antiprotons and decelerate them from 300 keV to 20 keV. Due to the space charge limitations at such low energies, the expected total number of single-charge particles is about $2 \cdot 10^7$ corresponding to only 3.2 pC. In order to make a wide range of external experiments possible, the beam will be extracted in two modes: in a single shot lasting a few microseconds and in a quasi-DC manner with the particles released over a longer time scale [3]. The latter will result in as few as $5 \cdot 10^5$ - 10^6 particles per second. Consequently, a Faraday cup planned for the USR will have to cover intensities from about 1 μA down to the fA range.

* Work supported by the EU under contract PITN-GA-2008-215080, by the Helmholtz Association of National Research Centers (HGF) under contract number VH-NG-328, and GSI Helmholtz Centre for Heavy Ion Research.
#Janusz.Harasimowicz@quasar-group.org

SECONDARY PARTICLES

Whilst antiprotons are of the main interest at the USR, other particles, like protons or H^- ions, will be used for the initial commissioning of the machine. Ideally, all beams would be monitored with one device, but this may not be possible. Given that the Faraday cup accuracy will depend on the collection efficiency of the total charge carried by the beam, the secondary charged particles emission processes need to be well understood and no charge should be allowed to escape the detector.

In the case of a proton beam, only secondary electrons will be emitted from the surface of the beam stopper. The total electron yield varies proportionally to the inelastic stopping power of the projectiles in the target material. It increases with increasing proton energy, then reaches a maximum in the 100 keV range and decreases thereafter. The yield scales with the incident angle α, measured with respect to the surface normal, by a factor $1/\cos(\alpha)$ for protons [4]. The energy spectrum of the secondary electrons has a peak at a few eV with a spread at half height of the same order of magnitude, thus about 85% of emitted particles are below 50 eV [4]. The emission of these low energy electrons is a result of a cascade process, while the higher energy tail of the spectrum is due to direct energy transfer from the impinging particle to an electron of a solid body. However, the most energetic δ-electrons are expected to be emitted mostly in the forward direction. Electrons emitted backwards can be stopped by means of an electric field applied at the entrance of the monitor.

In the case of an antiproton beam, the use of the Faraday cup will be strongly limited. The reason for this is the creation of highly energetic charged particles being able to escape the device very easily. Following the annihilation of antiprotons on protons or neutrons, various combinations of pions will emerge at 100-MeV-scale energies. Due to momentum conservation, a nuclear recoil of a few tens of MeV, depending on the target material, will be also observed. In addition, a fraction of annihilations will induce the production of an unstable nucleus; the nuclear breakup will result in fragments emitted in all directions and ionizing surrounding atoms. All in all, many annihilation products will have energy hundreds of times higher than the primary keV beam, thus their stopping in the detector will be extremely difficult. Consequently, the MeV-scale pions and recoiling ions will leave the monitor and the charge measured will not reflect the absolute beam current. Despite this limitation, the cup

MEASUREMENT, SIMULATION, AND SUPPRESSION OF APS STORAGE RING VACUUM CHAMBER TE MODES IMPACTING VERTICAL BPM READINGS *

R. Lill, G. Decker, J. Hoyt, X. Sun
Advanced Photon Source, Argonne National Laboratory, Argonne, IL 60439
J. Wang
CST of America, Inc., 492 Old Connecticut Path, Framingham, MA 01701

Abstract

The Advanced Photon Source (APS) storage ring rf beam position monitors (BPMs) are impacted by the presence of beam-excited transverse electric (TE) modes. These modes are excited in large-aperture vacuum chambers and become trapped between the bellow end flanges. The TE modes are vertically oriented and are superimposed on the TEM beam position signals, corrupting the BPM measurements. Erroneous step changes in beam position measurements and systematic intensity dependence in the vertical plane have been traced to these modes, placing a fundamental limitation on vertical beam position stabilization. Experiments were conducted suppressing these modes on a test vacuum chamber. These experiments were simulated with Mafia [1] and Microwave Studio [2], confirming experimental results. We will describe the measurements, simulations, and prototype test results.

INTRODUCTION

As the Advanced Photon Source (APS) prepares for a large-scale upgrade, many of the fundamental limitations on beam stability are being studied. The APS storage ring vacuum chambers presently suffer from transverse electric (TE) longitudinal resonances trapped in the beam vacuum chamber. These TE-like modes are excited in the large-aperture sections of the vacuum chambers and become trapped between the bellow end flanges. The modes are vertically oriented and are superimposed on the beam position signals. These modes were identified and reported in 1998 when a network analyzer was used to measure the transmission of rf power from one beam position monitor (BPM) to an adjacent BPM on the same vacuum chamber section [3].

VACUUM CHAMBER DESCRIPTION

The Advanced Photon Source (APS) storage ring has 40 sectors each having 5 sections of vacuum chambers for a total of 200 individual sections. There are 80 curved and 120 straight sections of vacuum chambers that make up the 1104-meter-diameter APS storage ring. The storage ring vacuum chamber geometry shown in figure 1 has an oval beam chamber (left), connected to the antechamber by a small gap in the area between the two sections. The 0.426-inch gap section between the beam and antechamber sections shown in figure 1 introduces large capacitive loading that effectively lowers the cut-off frequency for TE01-like modes of the chamber.

The wavelength in a hollow waveguide satisfies the relationship:

$$F = \frac{c\sqrt{\left(1+\left(\lambda_g/\lambda_c\right)^2\right)}}{\lambda_g} .$$

Where c is the speed of light in free space, λ_c is the cut-off wavelength, and λ_g is waveguide wavelength. Using chamber length L = 4.81 m and λ_g = 2L/N (N=1, 2, 3….), the resonance frequencies can be estimated. The first resonance is the one closest to the cutoff frequency of the waveguide. The waveguide wavelengths for these lower-order modes are much longer than free space wavelengths.

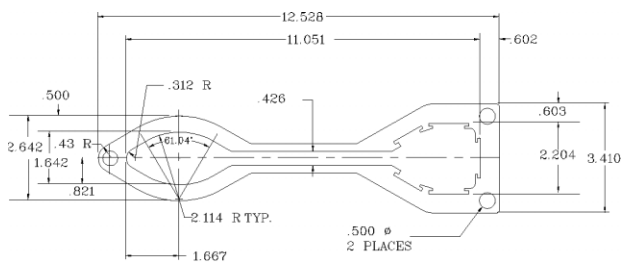

Figure 1: Storage ring vacuum chamber cross section (dimensions shown are inches).

MEASUREMENTS

Figure 2 illustrates the measurements that led to the discovery that these TE-like modes were corrupting

*Work supported by U.S. Department of Energy, Office of Science, Office of Basic Energy Sciences, under Contract No. DE-AC02-06CH11357.

STUDIES OF APS STORAGE RING VACUUM CHAMBER THERMAL MECHANICAL EFFECTS AND THEIR IMPACT ON BEAM STABILITY*

R. Lill, B. Yang, G. Decker, L. Erwin, J. Xu, J. Collins
Advanced Photon Source, Argonne National Laboratory, Argonne, IL 60439 USA

Abstract

As the Advanced Photon Source (APS) prepares for a large-scale upgrade, many of the fundamental limitations on beam stability have to be identified. We report on measurements of thermal mechanical effects of both the water, and air-handling systems impacting insertion device vacuum chambers (IDVCs). Mechanical stability of beam position monitor pickup electrodes mounted on these small-gap IDVCs places a fundamental limitation on long-term x-ray beam stability for insertion device beamlines. Experiments conducted on an insertion device vacuum chamber indicates that the beam position monitor blocks are moving with water temperature cycles at the level of 10 microns / degree C perpendicular to the beam direction. Measurements and potential engineering solutions will be described.

INTRODUCTION

The Advanced Photon Source (APS) is preparing for a large-scale upgrade and many of the fundamental limits on beam stability are being studied. One of the most critical locations for beam stability is at the insertion device (ID) points. The insertion device vacuum chambers (IDVC) are extruded aluminum with integrated beam position monitors (BPM) electrode housings machined out at each end of the IDVC. Three different versions of the vacuum chamber have vertical apertures of 12 mm, 8 mm, and 5 mm. The chambers are fabricated by extruding 6063 aluminum alloy to form a tube with the desired internal shape shown in figure 1. The exterior details, such as the BPM electrode housing, are machined to the finished dimensions. The IDVC have a pumping antechamber with non-evaporable getter strips. The wall thickness of the completed chamber at the beam orbit position is 1 mm. The design uses a rigid strongback that limits deflection of the chamber under vacuum despite the thin wall. Alignment of the vacuum chamber on its support is routinely accomplished with a precision of 75 microns over the entire surface, allowing minimum ID pole gaps.

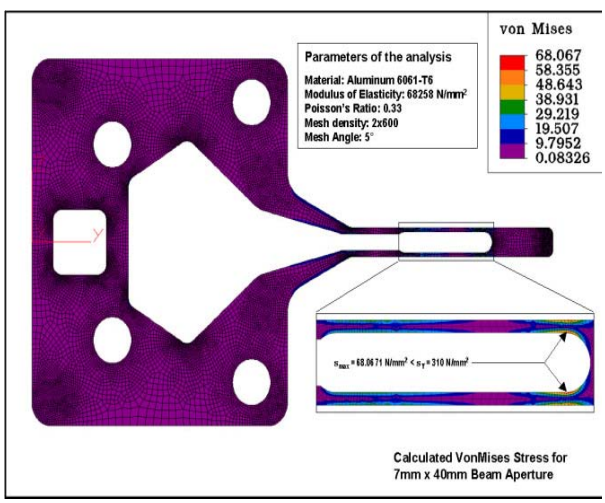

Figure 1: Storage ring IDVC cross section

ID BPM MEASUREMENTS

The IDVC BPMs provide the critical steering data necessary to maintain beam stability through the ID. The BPMs are machined in precise platforms on each end of the IDVC. In figure 2 the BPM is shown on the far left of the picture. The BPM button electrodes mounted in the machined platforms have a 4 mm diameter. There are two button electrodes mounted on a single miniature vacuum flange. The horizontal separation of the buttons is 9.6 mm center-to-center, with vertical apertures of 12 mm, 8 mm, and 5 mm. The button signals are cabled out to the electronics racks located above the tunnel. Narrowband Bergoz switching-type receivers are connected to the IDVC buttons. Narrow-band (300 Hz) BPM electronics are used to reduce beam intensity dependence and long-term drift. The long-term (one week) drift associated with the BPMs at this time is 7 microns horizontally and 5 microns vertically peak-to-peak. Plans to improve this will also include upgrading the electronics in the future.

BPM Measurements

As the noise sources are eliminated and BPM improvements are made, new noise sources can be discovered. During the operations period October 2009, an elevated noise level was reported on several IDVC BPMs. The plot in figure 3 shows beam position and vacuum chamber water temperature as a function of time. It was determine at this time that the beam position measurement was correlated to the water cycle of the aluminium vacuum chamber. The period of the water cycle is about 15 minutes with a 2.8 microns/degree Fahrenheit (5.2 microns/degree Celsius) change in the vertical position.

*Work supported by U.S. Department of Energy, Office of Science, Office of Basic Energy Sciences, under Contract No. DE-AC02-06CH11357.

THE LHC FAST BCT SYSTEM: A COMPARISON OF DESIGN PARAMETERS WITH INITIAL PERFORMANCE

D. Belohrad#, L. K. Jensen, O. R. Jones, M. Ludwig, J. J. Savioz, CERN, Geneva, Switzerland

Abstract

The fast beam current transformers (FBCTs) for the Large Hadron Collider (LHC) were designed to provide bunch to bunch and turn by turn intensity measurements. The required bunch to bunch measurements together with a large machine circumference call for stringent control of the transmission bandwidth, droop and DC offsets in the front-end electronics. In addition, two measurement dynamic ranges are needed to achieve the required measurement precision, increasing the complexity of the calibration. This paper reports on the analysis of the measurement and calibration methods, discusses theoretical precision limits and system limitations and provides a comparison of the theoretical results with the real data measured during the LHC start-up.

INTRODUCTION

The FBCT measurement system (Fig. 1) is composed of the measurement device [1], front-end electronics, an acquisition system [2], and a software control system. The system was designed to comply to the measurement specification [3].

The beam current is measured using 1:40 toroid transformer from Bergoz Instrumentation. The signal is split in the RF distributor into two dynamic ranges, each of them providing measurements in two bandwidths: 200 MHz for bunch by bunch measurements and ~2 MHz for turn based measurements. The four measurement signals are independently integrated using the LHCb2002 analogue integrator ASIC, and sampled using 14 bit ADCs clocked synchronously with the beam. The entire measurement process is driven in the hardware by two Digital Acquisition Boards (DABs) [4]. Each DAB processes two integrated signals of the same bandwidth using an FPGA. The measured data are stored either in the FPGA on-chip memory, or in the external synchronous SRAM for large-volume measurements. The real-time software running in the front-end controller (FEC) provides the necessary system control, calibration procedure, conversion of the stored measurements to the number of charges, and a data publishing.

Four measurement modes are provided:

- **Capture** – a snapshot of the intensity measurement in each bunch slot for a specified number of turns
- **Turn Sum** – a total intensity measured over single LHC turn (3564 bunch measurement slot)
- **Slot Sum** – a sum of bunch slot intensities measured over specified number of turns
- **Sum Sum** – a measurement of *Turn Sum* over specified number of turns.

Each FBCT system is calibrated by 5 µs long current pulses of specific amplitudes. The calibration pulses are generated in a calibrator, implemented into a VME64x 6U board, and they are transported to the calibration circuit installed in the measurement device using 7/8" Heliflex cables.

MEASUREMENT ERROR

According to [3], the measurement error is specified in terms of absolute accuracy and resolution. Two LHC operational modes relevant to the measurement error are discussed in this article: the LHC pilot bunch injection, and the LHC ultimate SPS batch injection. The required turn-based measurement precision for both scenarios is summarised in Tab. 1.

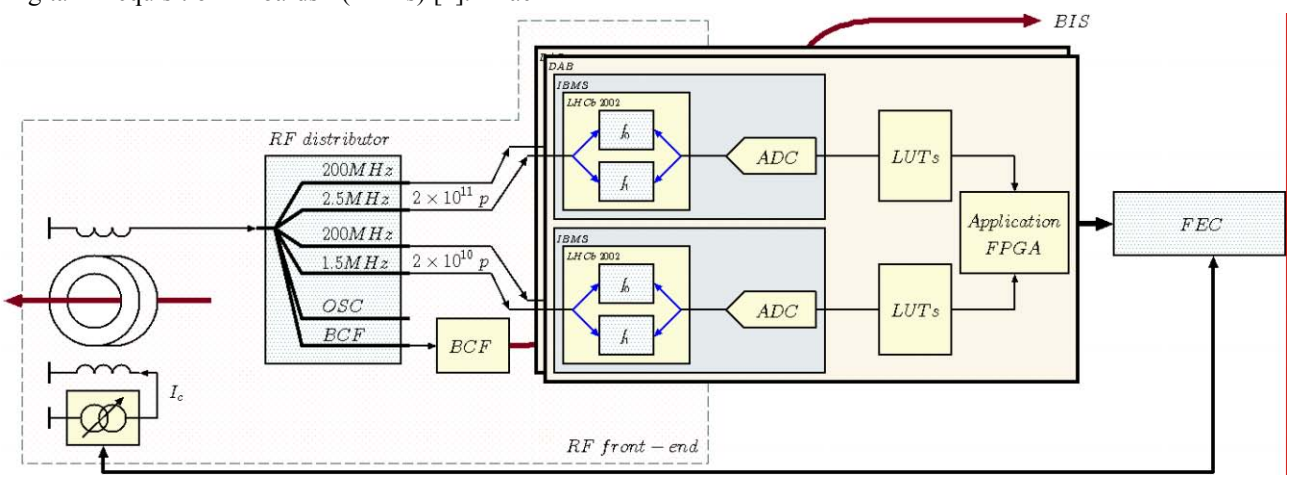

Figure 1: Block schematic of the FBCT measurement system

#david.belohrad@cern.ch

ANALYTICAL METHOD FOR DETERMINING ERRORS IN CURRENT MEASUREMENTS WITH A ROGOWSKI COIL

M. J. Hagmann, NewPath Research L.L.C., P. O. Box 3863, Salt Lake City, UT 84110, U.S.A.

Abstract

Algebraic expressions are derived for the open-circuit voltage induced on a toroidal coil with unevenly spaced turns, by a sinusoidal current through its aperture. The derivation requires that the winding layer is thin, the number of turns is large, and the cross-section of the winding is rectangular. These expressions are used to determine the effects of the gap between the ends of the coil and other irregularities in the spacing of the turns on the position sensitivity, defined as the dependence of the induced voltage on the location of the current. This technique may be used to define the criteria to meet a specified upper limit for the positional sensitivity.

INTRODUCTION

A Rogowski Coil [1] is a non-ferrous current probe in which a uniformly wound helix with a constant cross-sectional area follows a closed curve of arbitrary shape. Faraday's law of induction, with Ampere's law [2], requires that the open circuit voltage V induced on the coil is given by

$$V = \mu_0 N' A \frac{dI}{dt} \qquad (1)$$

where N' is the number of turns per unit length of the helix, A is the cross-sectional area of the helix, and dI/dt is the rate of change of the current passing through the area enclosed by the closed curve.

An ideal Rogowski coil would provide equal sensitivity to currents that are located anywhere within the aperture and would not be sensitive to currents outside of the aperture. However, the derivation of Eq. (1) requires that (1) The winding is uniform; (2) The radius of the winding is much less than the distance from the current to the coil; (3) N' is large so the helix may be approximated by a large number of evenly-spaced coils that are each normal to the curved axis of the helix; and (4) The frequency is low enough that displacement current and transit time may be neglected.

Measurements show that Rogowski coils have "position sensitivity" in that the induced voltage depends on the location of the current within the aperture [3]. Conventional methods of winding coils generally cause a positional sensitivity greater than 1%. A position sensitivity of less than 0.1% has been obtained by machining coils to a precision of 25-50 μm and reducing the gap where the two ends of the coil are adjacent to each other.

In the following sections of this paper we examine the effects of unevenly spaced turns in a toroidal Rogowski coil on the induced voltage when the cross-section of the winding is uniform and rectangular with arbitrary size. However, it is necessary to assume that the winding has zero thickness, so the present analysis does not show changes in the sensitivity when the distance of the current to the coil is comparable to the thickness of the winding. The number of turns per unit length is assumed to be large enough that the winding may be approximated by a group of closely-spaced coils in planes having constant θ (azimuthal coordinate about the axis through the center of the aperture). Otherwise the incremental advancement of each turn would create an undesirable one-turn loop to cause the coil to be sensitive to magnetic fields parallel to the axis. However, the latter effect may be mitigated by adding a one-turn return loop [4] or other methods which are not considered here. The present analysis is limited to frequencies that are low enough so the current probe is much smaller than a wavelength.

Our objective is to provide a tool to determine limits for the nonuniformity in the winding to satisfy a specified upper limit for the positional sensitivity. Others have used numerical integration to model these effects [5], but we have derived algebraic expressions that are intended to be simpler to implement and provide greater understanding.

ANALYSIS

Figure 1 shows the configuration used for the analysis of induction with a non-ferrous toroidal coil that may have a nonuniform winding. We consider the induction in an incremental winding of length $R_1 d\theta$, centered at (R_1,θ) that is caused by current I intersecting the plane at point $P(R_2,\Phi)$. Lines L_1 and L_2 are normal to the plane of the incremental winding, and parallel to the magnetic field caused by the current, respectively, and the angle between these two lines is α.

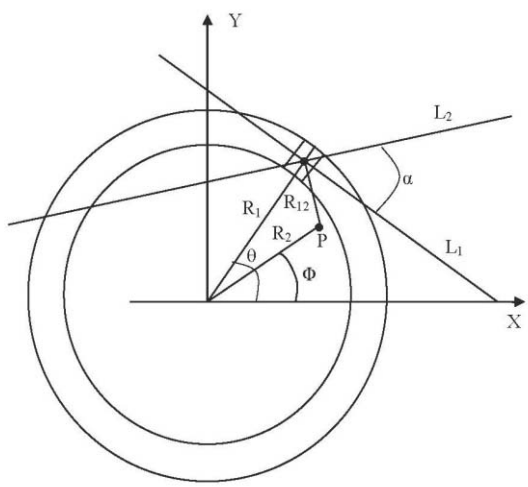

Fig. 1. Diagram for analysis.

The increment of winding has $dN = N'(\theta)R_1 d\theta$ turns, where $N'(\theta)$ is the turn density, defined as the number of turns per unit length of the toroid. Thus, the open-circuit voltage induced on the coil is given by

MONITORING TRANSVERSE BEAM PROFILE WITH NONUNIFORMLY-WOUND TOROIDAL COILS

M. J. Hagmann, NewPath Research L.L.C., P. O. Box 3863, Salt Lake City, UT 84110, U.S.A.

Abstract

Others have shown that the voltages induced on one uniformly-wound toroidal coil and two sinusoidally-wound toroidal coils may be used to determine the current in a single filament and its coordinates. We have extended this technique to show that the voltages measured on a group of sinusoidally-wound toroidal coils may be used to approximate the transverse distribution of the current that passes through their common aperture. This is possible because each measured voltage is proportional to the product of unique functions of the radial and azimuthal coordinates of each increment of the current. We have developed matrix methods to determine the transverse distribution of the current and determined the sensitivity of these calculations to measurement errors. Shielded sinusoidally-wound coils with a precision of 0.02 cm have been prepared using rapid prototyping, and methods to prepare the next generation of these coils, which will have a precision of 0.001 cm, by using an engraving tool with the 4th axis of a vertical milling machine have been defined.

INTRODUCTION

A number of different techniques have been used to monitor the transverse distribution of the beam current in accelerators, including secondary emission monitors, wire scanners, multi-wire chambers, gas curtains or jets, residual gas monitors, scintillator screens, scrapers and measurement targets, synchrotron radiation, and Laser-Compton scattering [1], as well as optical transition radiation [2] and the deflection of a probe beam of electrons [3].

A Rogowski Coil is a non-ferrous current probe which is generally wound as a toroid, but may also be made by bending a uniformly wound helical coil to follow a closed curve having arbitrary shape [4-6]. A time-dependent current passing through the aperture of a Rogowski Coil induces a voltage on the coil, and for an ideal coil this voltage would be independent of the location of the current within the aperture, and zero for currents outside of the aperture.

Great care is taken to limit the deviations from a perfectly uniform winding because these errors cause a Rogowski Coil to have "position sensitivity" so that the induced voltage depends on the location of the current within the aperture and may be non-zero when the current is outside of the aperture [7-8]. However, others have shown that the position sensitivity of non-uniformly wound coils may be used advantageously to determine the location of a single current that passes through the aperture [9-11].

SUMMARY OF THE ANALYSIS

We have previously derived exact closed-form expressions for the open-circuit voltage that is induced on a non-ferrous toroidal coil by a time-dependent current passing through the aperture when the turn density of the coil varies sinusoidally as a function of θ, which is the angle about the axis of the toroid [12-13]. To illustrate the configuration, Fig. 1 is a design drawing that was used in fabricating one of our toroids which has a total of 268 turns in which N'(θ), the number of turns per unit length at the mean radius R_1, is proportional to sin(θ). Thus, it may be seen that there is a reverse in the direction of the winding at the midpoint of the coil.

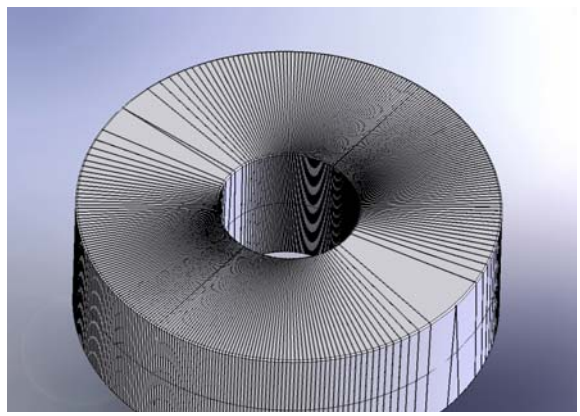

Fig. 1. Design drawing for sin(θ) toroid.

Each coil has a rectangular cross-section with height h, inner radius r_1, and outer radius r_2. To begin with we determine the open-circuit voltage induced on the coil by a filament of current I_0 which is located at the coordinates (R_2, Φ) where $R_2 < r_1$ to be inside of the aperture. The current is assumed to have harmonic time-dependence of $e^{j\omega t}$, but Fourier analysis may be used to extend the analysis to pulses or other functions of time. If the turn density is given by N_0', $N_{JC}\cos(J\theta)$, or $N_{JS}\sin(J\theta)$, it may be shown that the open-circuit voltage is given respectively, by the following three expressions:

$$V_{oc} = j\omega\mu_0 h R_1 N_0' I_0 \ln\left(\frac{r_2}{r_1}\right) \qquad (1A)$$

$$V_{oc} = \frac{j\omega\mu_0 h R_1 N_{JC}' I_0 \cos(J\Phi)}{2J}\left[\left(\frac{R_2}{r_1}\right)^J - \left(\frac{R_2}{r_2}\right)^J\right] \qquad (1B)$$

$$V_{oc} = \frac{j\omega\mu_0 h R_1 N_{JS}' I_0 \sin(J\Phi)}{2J}\left[\left(\frac{R_2}{r_1}\right)^J - \left(\frac{R_2}{r_2}\right)^J\right] \qquad (1C)$$

For the special case of a thin toroid, where $r_2 - r_1 << R_1$, these three expressions simplify to give those which were

EMITTANCE MEASUREMENT WIZARD AT PITZ

A.Shapovalov(1) and L.Staykov(2), DESY, Zeuthen, Germany

Abstract

The Photo Injector Test Facility at DESY, Zeuthen site (PITZ) develops electron sources of high brightness beams, required for linac based free electron lasers (FELs) like FLASH or the European XFEL. One of the key issues in electron beam optimization is the minimization of the transverse emittance. The main method to measure emittance at PITZ is a single slit scan technique, implying local beam divergence measurement by insertion of the slit mask at a definite location within the beam and measurements of the transmitted beamlet profile downstream of the slit station. "Emittance Measurement Wizard" (EMWiz) is the program used by PITZ operators for automated emittance measurements. EMWiz combines an acquisition program for beam and beamlet image recording and a postprocessing tool for the analysis of the measured transverse phase space of the electron beam. It provides a way to execute the difficult emittance measurements in an automatic mode and to get a calculated emittance result.

INTRODUCTION

At the PITZ facility, the electron source optimization process is conducted. The goal is to reach the XFEL specifications of 0.9 mm mrad at a bunch charge of 1 nC. The research activities at PITZ include the production, optimization and characterization of electron sources with a small normalized projected transverse emittance. The transverse emittance is a key property of high brightness electron sources and the key value for the measurements at PITZ [1]. This task of emittance measuring is organized at PITZ through the emittance measurement wizard (EMWiz) software. This advanced high-level software application interacts through a Qt [2] graphical user interface with the DOOCS [3] and TINE [4] systems for machine control and ROOT [5] for data analysis and visualization. For communication with the video system and acquiring images from cameras at several screen stations, a set of video kernel libraries have been created [6]. In this paper, details about the Emittance Measurement System for both hardware and software parts are described.

shapovalov.mephi@yandex.ru
[1] On leave from NiYaU MEPhI, Moscow Russia

lazaraza@ifh.de
[2] On leave from INRNE, Sofia, Bulgaria

EMITTANCE MEASUREMENT HARDWARE

The transverse emittance and phase space distribution are measured at PITZ using the single slit scan technique [7, 8]. The Emittance Measurement SYstem (EMSY) consists of horizontal and vertical actuators with 10 and 50 μm slits masks and YAG/OTR screens for the beam size measurement. The slit mask angle can be precisely adjusted for the optimum angular acceptance of the system (Figure 1). Three EMSY stations are located in the current setup as shown in Figure 2. The first EMSY station (EMSY1) behind the exit of the booster cavity is used in the standard emittance measurement procedure. It is at 5.74 m downstream of the photocathode corresponding to the expected minimum emittance location. For this technique, the local divergence is estimated by transversely cutting the electron beam into thin slices. Then, the size of the beamlets created by the slits is measured at the YAG screen at some distance downstream the EMSY station. The 10 μm slit and a distance between the slit mask and the beamlet observation screen of 2.64 m are used in the standard emittance measurement. Stepper motors are applied to move each one of the four axes separately. They give the precise spatial positioning and orientation of the components. On each of the actuators, either a YAG or OTR screen is mounted to observe the beam distribution. A single and a multi slit masks are mounted consecutive to take samples from the transverse phase space of the electron beam. A CCD camera is used to observe the images on the screens (see Figure 1).

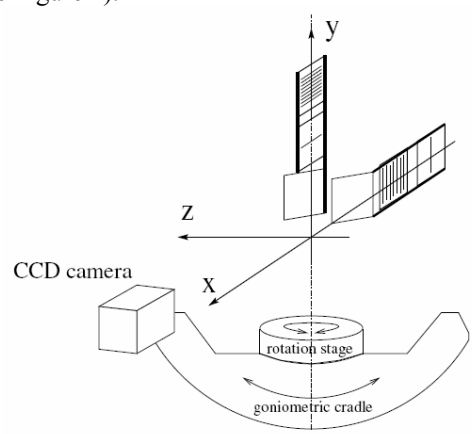

Figure 1: Layout of the Emittance Measurement System.

COMPARISON OF EXTRACTION AND BEAM TRANSPORT SIMULATIONS WITH EMITTANCE MEASUREMENTS FROM THE ECR ION SOURCE VENUS*

D. Winklehner#, D. Todd, LBNL, Berkeley, CA 94704, USA
D. Grote, LLNL, Livermore, CA 94551, USA
D. Leitner, J. Benitez, M. Strohmeier, LBNL, Berkeley, CA 94704, USA
F. Aumayr, Vienna University of Technology, Vienna, Austria

Abstract

The versatility of ECR (Electron Cyclotron Resonance) ion sources makes them the injector of choice for many heavy ion accelerators. However, the design of the LEBT (Low Energy Beam Transport) systems for these devices is challenging, because it has to be matched for a wide variety of ions. In addition, due to the magnetic confinement fields, the ion density distribution across the extraction aperture is inhomogeneous and charge state dependent. In addition, the ion beam is extracted from a region of high axial magnetic field, which adds a rotational component to the beam. In this paper the development of a simulation model (in particular the initial conditions at the extraction aperture) for ECR ion source beams is described. Extraction from the plasma and transport through the beam line are then simulated with the particle-in-cell code WARP. Simulations of the multispecies beam containing Uranium ions of charge state 18+ to 42+ and oxygen ions extracted from the VENUS ECR ion source are presented and compared to experimentally obtained emittance values.

INTRODUCTION

The superconducting Versatile ECR ion source for NUclear Science (VENUS) [1, 2], was developed as the prototype injector for the Facility for Rare Isotope Beams (FRIB) and as injector ion source for the 88-Inch Cyclotron at Lawrence Berkeley National Laboratory [3, 4]. Like most ECR ion sources VENUS operates in a minimum B field configuration which means that a magnetic sextupolar field for radial confinement is superimposed with a magnetic mirror field for axial confinement. Consequently:

- Ions are extracted out of a region with high axial magnetic field (in VENUS typically 2 T) which then continuously decreases as the ions move along in axial direction, adding a rotational component to the beam.
- Due to the sextupolar field, the total magnetic field inside the source is not rotationally symmetric and thus the spatial distribution of ions at extraction resembles a triangle rather than a circle. This is also confirmed by beam imaging of single- or few-species ion beams (e.g. Figure 1) [4].

Furthermore, the extracted beam often consists of more than 30 different ion species with different mass-to-charge ratios which makes modeling even more complicated. At the moment, several groups are developing versatile extraction codes that are able to handle the complex initial conditions presented by ECR ion source plasmas. The main goals are:

- To better understand the underlying plasma physics that leads to these initial conditions.
- To create a design tool for future ECR injection systems.

The work described here represents the current status of a long-term effort to create a highly adaptable, advanced simulation code utilizing the well-established PIC (particle-in-cell) code WARP [5].

Figure 1: Tantalum imaging of a triangular He^+ beam, 80 cm after extraction [4].

Many of the issues regarding the extraction simulation and the beam transport through the beam line have been addressed in earlier work by D. Todd et al. [4, 6] and will be reviewed briefly in the following sections respectively. Results of a Uranium beam simulation using an improved way to obtain the initial conditions will then be presented and compared to emittance measurements.

SIMULATIONS

The simulation of a multispecies ion beam from plasma extraction to the position of the diagnostics box can be divided into three separate simulations (see Figure 2), each employing different simulation methods which are discussed in the following subsections.

* This research was conducted at LBNL and was supported by the U.S. Department of Energy under Contract DE-AC02-05CH11231.
# dwinklehner@lbl.gov

ESTIMATION OF PROFILE WIDTH IN HYBRID ION BEAM TOMOGRAPHY

H.Reichau*, O. Meusel, U. Ratzinger, C. Wagner, IAP, JWG University, Frankfurt, Germany

Abstract

In beam diagnostics, optical techniques had become increasingly important as they provide information with the advantage of minimal effect on the beam. The planned Frankfurt Neutron Source will consist of a proton driver linac providing beam energies up to 2.0 MeV. The rotatable diagnosis tank hybrid ion beam tomography tank HIBTT will be placed at the end of the low energy beam transport section (LEBT) to provide beam tomography based on the visible radiation of the ion beam in front of the RFQ. The beam energy in this section will be 120 keV and the current 200 mA. Additional to the CCD camera that takes optical data for the tomography, other non-interceptive devices could be used to gain additional information. The question behind this hybrid approach to non invasive beam diagnostics is: what and how much information can be extracted from an ion beam without disturbing or destroying it? The actual contribution deals with the information of profile width in beam profile measurements. The presentation introduces a definition and an information sensitive method for profile width determination and verifies them using experimental and numerical data.

INTRODUCTION

Beam diagnosis systems that provide knowledge about beam properties and behavior of an ion beam serve as a source of potential controllability through attained information. What one could actually learn about an ion beam, or rather, which and how much information can be extracted from it without disturbing or destroying it, essentially influences the extent of possible control over the beam. Based on a theory of information, an extended diagnosis pipeline was derived that forms the basis for a beam diagnostic system for HIBT (hybrid ion beam tomography), consisting of a flexible measurement device and an associated, modular software agent. The hardware device is the hybrid ion beam tomography tank (HIBTT) that was developed to serve as a multi-measurement device (Figure 1). It consists of a rotatable vacuum chamber with four 100 mm adapter flanges sthat everal non-invasive measuring equipment could be plugged into. HIBTT rotates within a maximum angle of 270 degrees in >5000 steps of angle encoding driven by a pecking motor and drive belts. The seal was constructed to resist vacuum pressures up to 10^{-7}mbar. Accordingly the software agent for data analysis has to be built in a modular manner. This permits analysis of data from several measurement devices without adjusting the basic structure. To analyze the measured data, an interface module for the software agent might be implemented if not contained in the default assembly. Furthermore, collective phenomena that arise from intense beams or non neutral plasma can be identified. In the first section of this contribution a suitable theory of information for beam diagnostics will be introduced. The second section deals with an information sensitive approach to profile width in optical beam measurements by giving a general definition of profile width, an error estimation and a first algorithm that will be implemented and proved in relation to the introduced error estimation.

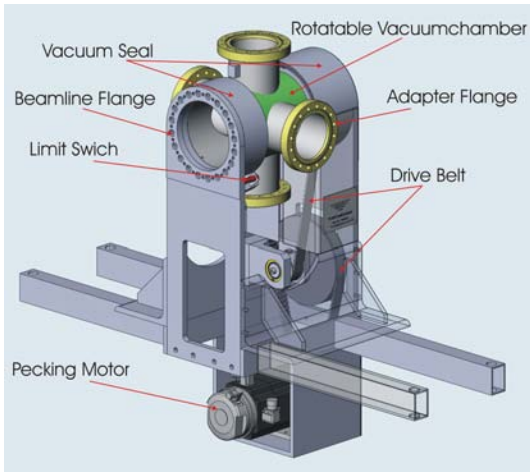

Figure 1: HIBTT is designed to serve as a multi measurement device for non- invasive beam diagnostics.

INFORMATION AND BEAM DIAGNOSTICS

Unfortunately no consistent theory of information in general exists, so one has to specify what has to be understood by the term *information* as the case arises. Consider a definition for beam diagnosis:

Let the term beam diagnosis be considered as ascertainment of distinctive properties called information for the evaluation of beam quality.

Then one has to point out the meaning of *information* in this context. In [1] three dimensions of information are introduced. The syntactical dimension of information, where the information theory of Shannon [2] resides, deals with relations between individual symbols, e.g., single particles or a beam in this case. Around this dimension lies the semantical dimension of information, which assigns a

* reichau@iap.uni-frankfurt.de

A LOW ENERGY ION BEAM PEPPER POT EMITTANCE DEVICE

M. Ripert, A.Buechel, A. Peters, J.Schreiner, T.Winkelmann, HIT, Heidelberg, Germany

Abstract

The transverse emittance of the ion beam at the Heidelberg Ion Therapy Center (HIT) will be measured within the Low Energy Beam Transport (LEBT) using a pepper-pot measurement system. At HIT, two ECR sources produce ions (H, He, C and O) at an energy of 8keV/u with different beam currents from about 80 µA to 2mA. The functionality and components of the pepper-pot device is reviewed as well as the final design and the choice of the scintillator. For that, results from recent beam test at the Max Planck Institute für Kernphysik at Heidelberg are presented. The material investigation was focused on inorganic doped crystal, inorganic undoped crystal, borosilicate glass and quartz glass with the following characteristics: availability, prior use in beam diagnostics, radiation hardness, transparency, fast response, spectral matching to CCD detectors.

PEPPER POT DEVICE

Location

The Pepper-Pot Scintillator Screen system should fit within the existing beam line components (vacuum boxes already used with beam diagnostics equipment like Faraday cups, profile grids and slits). The N1DK1 vacuum box will be equipped with a fast iris shutter, a pepper-pot mask and a scintillator screen. The N1DK2 vacuum box will contain a 45 degrees tilted mirror inside and a CCD camera outside. (Figure 1)

The pepper-pot principle

The pepper-pot mask, which is perpendicular to the beam and contains a regular array of identical holes, splits the beam into beamlets. The scintillator is used to create a photographic image of the beamlets with pixel intensity corresponding to the charge concentration of beam particles striking the transparent scintillator. A CCD camera with a mirror placed behind at 45 degrees will record single and multi-shots.

Why use a pepper-pot device?

We want to measure both x-y components of the beam emittance simultaneously in one shot and to obtain data in real time. Four methods [1-2] can be used and all utilize a slit or mask to select a portion of the beam for analysis:

1. The two-slit scanner method uses a second slit which can be scanned through the direction parallel to the first. The cut out beam current is normally measured by a Faraday cup.
   However, this method is really slow because the second slit has to be scanned through the range for every position of the first slit.
2. With the multi-wire collector method, each wire collects the beam particles that pass through the slit. The disadvantage of this method is that it requires an amplifier for every wire in the collector.
3. The Allison-type emittance scanner is faster than the multi-wire collector method but slower than the pepper –pot method [2]
4. The Pepper-pot.

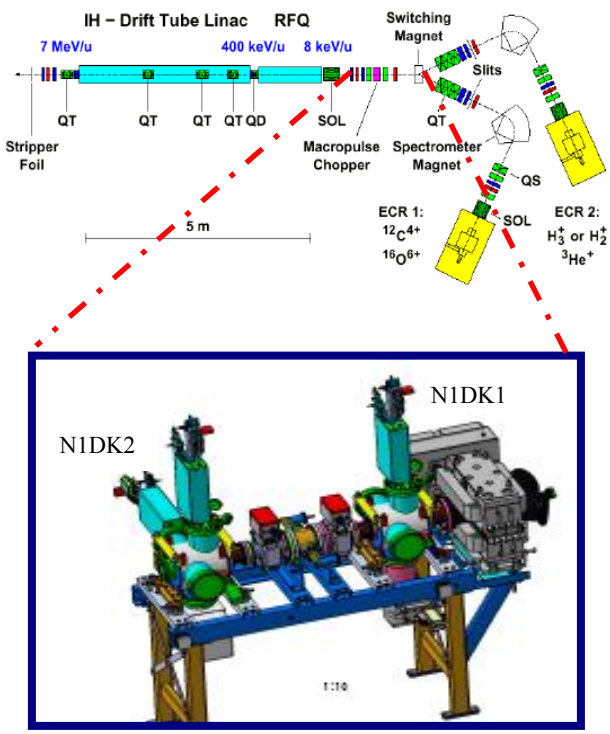

Figure 1: The Low Energy Beam Transport at HIT and the position of the Pepper-Pot Scintillator Screen device within the LEBT (Low Energy Beam Transfer).

EMITTANCE MEASUREMENTS AT THE LBNL ECR AND AECR-U ION SOURCE USING A PEPPER-POT EMITTANCE SCANNER *

M.Strohmeier#,1,2, J.Y.Benitez[1], D.Leitner[1], D.Winklehner[1], D.S.Todd[1], C.M.Lyneis[1], M.Bantel[2]

[1] Lawrence Berkeley National Laboratory, 1 Cyclotron Road, Berkeley, CA, 94720, U.S.A.
[2] University of Applied Science Karlsruhe, Moltkestrasse 30, 76133 Karlsruhe, Germany

Abstract

Two Electron Cyclotron Resonance (ECR) ion sources are currently available to inject beams into the 88-Inch Cyclotron at Lawrence Berkeley National Lab (LBNL). Ion beam emittances for various ion species of both sources were measured using a recently commissioned pepper-pot emittance scanner[1] and are discussed in this paper. Pepper-pot scanners[1,2,3] are capable of extracting the full four-dimensional transverse phase space of the beam, allowing for the calculation of the cross coupled emittances xy' and yx'. This is especially of interest for ECR ion sources, where asymmetric beams are extracted in the presence of a strong solenoidal field. The axial field adds a rotational momentum to the extracted beam resulting in a transverse emittance growth, which depends on the magnetic stiffness of the extracted species. In this paper, the pepper-pot software is described and emittance data from both LBNL ECR sources are presented and compared. The data confirm a strong mass dependence of the normalized emittance for ions with the same mass-to-charge-state ratio, as previously also observed by other groups. This dependence indicates different particle distributions at the extraction aperture for different ion species.

INTRODUCTION

Electron cyclotron resonance (ECR) ion sources are widely used in the particle accelerator community because they are capable of producing high current beams of highly charged ions. Their operation relies on magnetically confined plasmas in which the electrons are resonantly heated with microwave radiation. They can reach energies of several hundred keV and ionize the gas in a step-by-step ionization process. In order to achieve high charge states, long confinement times (milliseconds) are needed which are achieved by the superposition of an axial mirror field and a radial multi-pole field, resulting in a minimum B-field configuration. Since the extraction aperture of most ECR sources is located near the center of the extraction solenoid coil, particles are extracted and accelerated in a decreasing magnetic field, which increaes the transverse emittance. Two different types of emittance scanners are currently in operation at LBNL to measure the beam emittance: an Allison type slit scanner[4] and a pepper-pot scanner[1]. The slit scanner can provide a better spatial and angular resolution than the pepper-pot, but measurements take a few minutes. Additionally, the slit scanners can only extract one-dimensional data sets, since the intensities are integrated over the whole slit while stepping through the beam. Scintillator based pepper-pot scanners capture the image data in just a fraction of a second, making it less vulnerable to emittance changes caused by plasma instabilities or other transitions. Furthermore, the image array of a pepper-pot scanner provides two dimensional data sets from which the xx' and yy' as well as the cross coupled xy' and yx' phase spaces can be extracted.

The principle of the pepper-pot scanner[1,2,3] is to image the beam as it passes through a hole mask and creates a light pattern on a scintillator behind the mask. By knowing the absolute locations of the holes in the mask and relating them to the light pattern on the scintillator, one can obtain the transverse angular distribution of the particles in the ion beam. Since the pepper-pot scanner uses a camera (typically a CCD camera) to capture the light pattern on the scintillator, it is important to investigate the influence of the optical parameters on the emittance. These parameters can greatly influence the final emittance values and have to be chosen carefully in order to minimize and define the induced error stemming from the respective parameters[2]. For the scintillator, the absolute light yield, its linearity and the lattice degradation as a function of the integrated beam exposure are crucial parameters [1, 2]. Camera settings that influence the emittance value are the exposure time of the charge coupled device CCD chip to the scene, the gain and the brightness.

NOISE PROCESSING

The noise treatment consists of the following three steps, which are described in this section in detail:

1. Detecting faulty pixels.
2. Smoothing the data.
3. Threshold cut of the data.

1) Detecting fault pixels

As CCD cameras age, the pixel array degrades, and the number of faulty pixels increases. If the camera is additionally mounted in a radiation environment, this degradation is even more accelerated. Unfortunately, the gray scale values of these damaged pixels show a random distribution rather than a constant value of “255” or “0”. Neglecting these pixels for the emittance evaluation would introduce a large error in the calculation. Therefore, before calculating the emittance value the analyzing software needs to locate and replace those pixels with approximated values. In order to locate the faulty pixels, a reference image without beam has to be

* This research was conducted at LBNL and was supported by the Director, Office of Energy Research, Office of High Energy and Nuclear Physics, Nuclear Physics Division of the U.S. Department of Energy under Contract No. DE-AC02-05CH11231.
# MMStrohmeier@lbl.gov

BUNCH-LENGTH MEASUREMENTS AT SCSS TEST ACCELERATOR TOWARD XFEL/SPRING-8

Y. Otake#, S. Matsubara, H. Maesaka, K. Tamasaku, T. Togashi, K. Togawa, and H. Tanaka
RIKEN/SPring-8, 1-1-1, Kouto, Sayo-cho, Sayo-gun, Hyogo, 679-5148, Japan
M. Goto, Hamamatsu Photonics K.K., 812 Joko-cho, Higashi-ku, Hamamatsu-shi,
Shizuoka, 431-3196, Japan

Abstract

The SCSS test accelerator, which was constructed to check the feasibility of XFEL/SPring-8, is being operated for user experiments using stable EUV (Extreme Ultra-violet) SASE. This accelerator provides a high-quality electron beam with parameters, such as a bunch length of 300 fs and a peak current of 700 A, for power saturation of the EUV SASE. Evaluating the parameters is very important to ensure the stable generation of SASE. Bunch-length measurement systems to evaluate the parameters have been developed. The systems use the rf zero-phase crossing method, the EO sampling method with temporal decoding and an 800 nm laser, and a method for observing OTR (near the infrared region) by a streak camera (fesca-200), which is mature technology. All of the measured bunch lengths were about 300 fs (FWHM), which is consistent with the individual methods. The most important result is that the streak camera with optimum tuning directly measured the temporal structure with femto-second resolution, and the reliabilities of these systems were mutually checked.

INTRODUCTION

Constantly keeping the peak currents of the electron bunches of a free electron laser at SPring-8 (XFEL/SPring-8) [1] and the SCSS test accelerator to check the feasibility of the XFEL/Spring-8 [2.3], which are used to generate coherent and extremely intense x-rays and extreme ultra-violet (EUV) light, respectively, is one of the most important points to ensure stable generation of their lasers. In the present technology, the charge amount of a bunch can only be reliably measured by a current transformer with a reasonable accuracy of 1~5%. Therefore, measurements of the bunch shape, which determines the peak current, are very important. Furthermore, we introduced the SCSS concept [2] for the XFEL and the SCSS test accelerator. The SCSS concept employs a velocity bunching process using multi sub-harmonic bunchers (SHB) for an injector and a magnetic bunching process using a chicane bunch compressor (BC) comprising four bending magnets after the injector. For the SCSS test accelerator, a single BC is used, and for the XFEL three-stage BCs are employed after the injector. For this reason, the individual bunch compression processes have different bunch lengths; the bunch width of the velocity bunching is from 1 ns to 10 ps (1~20 A in peak current), the bunch length after the 1st BC is 2~3 ps (~70 A), the bunch length after the 2nd BC is around 150 fs (~600 A), and the bunch width after the 3rd BC is about 30 fs (~3 kA). Since the stability of the laser is extremely dependent on their bunch lengths, evaluating and properly adjusting the bunch lengths at each process are very important to ensure a stable laser. To establish the measurement reliability and adapt measurements with the different bunch lengths, different kinds of bunch-length measurement methods are employed for the XFEL and the SCSS test accelerator, even through the methods almost cover the same temporal resolution and range. Because the temporal accuracy of the individual bunch length methods in the case of a measurement with a resolution under 1ps, such as a streak camera for observing optical transition radiation (OTR) and an rf zero-crossing [4], still has some ambiguity caused by measurement errors. For example, the errors are sensitivity dependent on the wavelength, where the streak camera is used [5], and the aberration of an electron beam optical system, where rf zero-crossing is employed. Therefore, we think that the reliability on the temporal resolution of the bunch-length measurements in a femto-second region is not yet established at the present time.

Six kinds of bunch-length measurement systems, as mentioned below, to guarantee the reliability of the beam-monitor system of the XFEL have been developed, or are under development. In this paper, we report on the already developed bunch-length measurement systems using a streak-camera method, an rf zero-phase crossing method, and an EO sampling method [6] selected from the bunch-length monitors for the XFEL, which are described blow. These methods cover a temporal measurement range of several hundred femto-seconds. This time range can adapt observing the electron bunch of the 1st BC and the 2nd BC.

To check the reliability of the developed methods, and to evade any ambiguity of the measurement accuracy, the electron bunch length of the SCSS test accelerator was measured by the developed systems, and the data taken by the systems were compared. The test accelerator uses multi- SHBs of 238 MHz and 476 MHz for velocity bunching and a BC for magnetic bunching. A schematic layout of the test accelerator is illustrated in Fig. 1. The electron bunch length of the accelerator is compressed from 1 ns to a spiky lasing part of 300 fs with the 750 A peak current by the bunching process, while the final whole compressed bunch length is about 1ps, including the spiky lasing part. These bunch compression processes were numerically simulated, and their performances were experimentally confirmed by measurements.[3]

otake@spring8.or.jp

BEAM LIFETIME MEASUREMENTS WITH LIBERA BRILLIANCE

A. Kosicek, P. Leban, Instrumentation Technologies, Solkan, Slovenia
B.K. Scheidt, ESRF, Grenoble, France.

Abstract

The lifetime of the electron beam in a Synchrotron Light Source is an important parameter. Its precise measurement within a short time is an essential tool to evaluate properties and stability of a storage ring. In some cases, for example during short gas outbursts in the UHV vacuum chamber leading to rapid lifetime drops, it can be used as a useful diagnostic tool as well. Traditionally, dedicated PCTs (Parametric Current Transformers) are mostly used for this purpose. The idea to use Libera Brilliance Beam Position Processor instead came after the excellent quality of its sum signal was observed. Moreover, the measurement accuracy is greatly increased by averaging the lifetime measurements of all the individual stations, bearing in mind that there are typically more than hundred BPMs positioned around the ring. First measurements were performed on ESRF, showing very good performance potential. The article discusses the measurements, their results, the comparison with more classical methods, and the implementation of this feature in the Libera Brilliance software.

INSTRUMENTATION

Libera Brilliance is widely used as a beam position processor at third generation synchrotron light sources around the world. Its flexibility allows very fast wideband measurements on one side, fast feedback operation, and narrowband monitoring of the signals on the other. All this data is available simultaneously, enabling complete characterization of the accelerator system.

The native purpose of such instrumentation is of course the beam position measurement at different bandwidths. It was however noticed that the sum signal is very useful as well as it is proportional to the stored current in the ring. Specifically, the Slow Acquisition (SA) dataflow is used for slow monitoring of the position and comes at 10 Sps. It consists of four amplitudes, the derived Δ/Σ position and the derived sum value of four amplitudes.

MEASUREMENTS

All measurements were performed in the ESRF storage ring, where a total of 224 Libera Brilliance units are routinely used for the beam position monitoring. The injection at ESRF is scheduled twice a day, at 9 AM at 9 PM. The typical current in the ring is ~200 mA immediately after the injection, decreasing to a minimum value at ~150 mA before the next injection. A typical graph of sum value of one Libera Brilliance can be seen in Figure 1.

It can be assessed immediately that a single Libera Brilliance unit is already capable of a precise and reproducible beam lifetime measurement. Theoretically, all Libera Brilliances around the storage ring should of course measure the same beam lifetime.

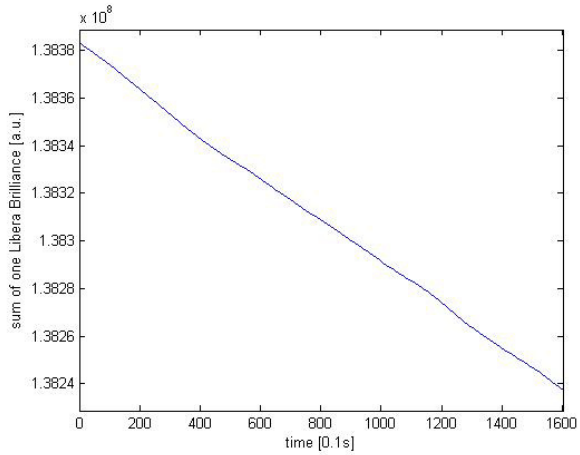

Figure 1: Decrease of the sum value on one Libera Brilliance through 160 s.

However, when reading the data from all units around the storage ring at the same time, few random units reported significantly different beam lifetime from time to time. Jumps in the lifetime value are just short spikes and are not really related to the beam lifetime change. The most frequent reason for them is a change in the fans speed due to temperature control loop inside Libera Brilliance. This phenomenon is depicted in Figure 2.

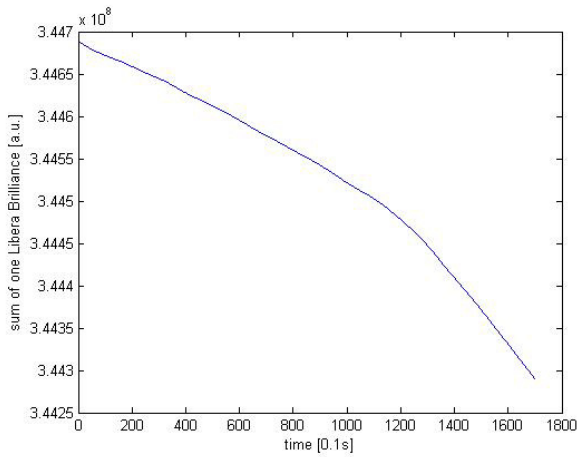

Figure 2: Decrease of sum value on this Libera was affected by the fans speed change.

This actually shows how sensitive the beam lifetime measurement is. The effect of the fans speed change can be even better observed on Figure 3. Six Libera Brilliances lifetime calculations are directly compared to recorded fans speed. Same colour denotes the same

AN FPGA-BASED BUNCH-BY-BUNCH TUNE MEASUREMENT SYSTEM FOR THE APS STORAGE RING*

C.-Y. Yao#, Y.-C. Chae

Advanced Photon Source, Argonne National Laboratory, Argonne, IL 60439, USA

W.E. Norum

Lawrence Berkeley Laboratory, Berkeley, CA 94720, USA

Abstract

A bunch-by-bunch tune measurement system was developed for beam diagnostics and machine studies of Advanced Photon Source (APS) storage ring. It can be applied to such machine physics studies as characterization of transverse impedance, observation and identification of coupled-mode instabilities, and electron cloud effects. The system has a single-bunch and a multibunch operation mode. In single bunch mode tunes are processed with FFT. In multibunch mode the system excites a set of driven bunches with a frequency sweep signal, samples a set of monitored bunches, and extracts amplitude and phase information from sampled data using digital demodulation method. We report its hardware and software design, performance, and recent experimental results on the APS storage ring beam.

SYSTEM DESCRIPTION

The bunch-by-bunch tune measurement system was originally developed as a diagnostics tool for a transverse feedback system at the APS [1]. It now serves as an alternative of the original storage ring tune measurement system that uses spectrum analyzers.

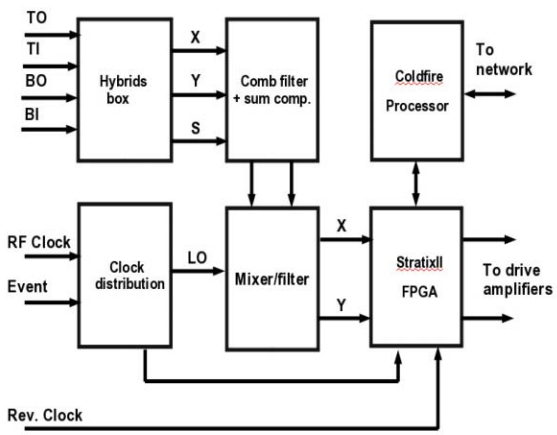

Figure 1: Block diagram of the tune measurement system.

Figure 1 shows a diagram of the system. The front-end circuit consists of a hybrid input box, a 3-tap comb filter and sum compensation circuit, and a down converter mixer. The LO input of the mixer is a 352 MHz clock signal directly derived from main rf source. The front-end and pickup stripline are shared by the tune measurement system and a transverse feedback system [2]. The tune measurement module consists of a StratixII DSP development board [3] for data conversion and processing, a ColdFire uCDIMM card as EPICS IOC, and a small daughter card for receiving timing synchronization signals from the APS even system. Other than this small daughter card, all components are commercial, off-the-shelf.

Two 12-bit 125 MHz ADCs on the FPGA board are used for beam position acquisition, one for each transverse plane. Two 14-bit 175 MHz DACs are used for generating chirp signals for both planes. Two trigger output channels provide synchronization with external excitation sources.

FIRMWARE PROCESSES

Figure 2 shows a block diagram of the tune measurement firmware. The ADC block acquires input beam signals at a rate of 117 MHz, or 1/3 of the storage ring rf frequency.

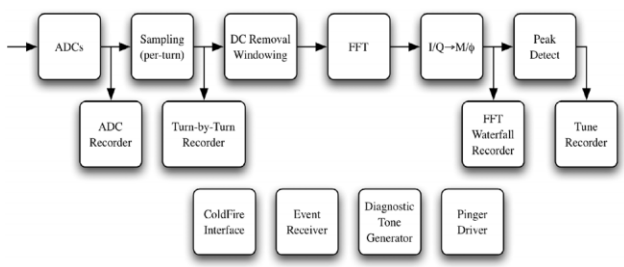

Figure 2: Block diagram of the tune measurement firmware.

The system has two operations modes: a single-bunch mode that provides tune measurement of any single bunch of the storage ring, and a multibunch mode that chirps a train of selected driven bunches and acquires tune data on another train of monitored bunches.

*Work supported by U.S. Department of Energy, Offices of Science, Office of Basic Energy Sciences, under contract No. DE-AC02-06-CH11357

#cyao@aps.anl.gov

INJECTION BEAM DYNAMICS IN SPEAR3*

J. Corbett[1], W. Cheng[2], A.S. Fisher[1], X. Huang[1], W. Mok[3], J. Safranek[1] and S. Westerman[1]
[1]SLAC National Accelerator Laboratory, Menlo Park, CA 94025
[2]Brookhaven National Laboratory, Upton, NY 11973
[3]Life Imaging Technology, Palo Alto, CA 94301

Abstract

For the top-off operation it is important to understand the time evolution of charge injected into the storage ring. The large-amplitude horizontal oscillation quickly filaments and decoheres, and in some cases exhibits non-linear x-y coupling before damping to the stored orbit. Similarly, in the longitudinal dimension, any mismatch in beam arrival time, beam energy or phase-space results in damped, non-linear synchrotron oscillations. In this paper we report on measurements of injection beam dynamics in the transverse and longitudinal planes using turn-by-turn BPMs, a fast-gated, image-intensified CCD camera and a Hamamatsu C5680 streak camera.

INTRODUCTION

SPEAR3 is a 3rd generation, 3GeV storage ring light source with nominal emittance ε_x=10nm-radian. Single-bunch top-off injection occurs at either 8 hr or 10 min intervals with photon beamline shutters open [1]. Since the injector and BTS transport line were not specifically designed for top-off, it is particularly important to measure and understand dynamics of the injected beam in order to minimize perturbations seen by the users and to protect sensitive ID magnets in the lattice.

The injection system consists of a 10Hz booster synchrotron with single-bunch filling capability. Under nominal I=200mA operating conditions each stored bunch contains ~550pC (700uA) and each injected pulse contains ~30pC (40uA). The contrast makes measurement of the injected pulse difficult. A vertically-deflecting Lambertson septum brings the beam to SPEAR3 with the injected beam at x=-13mm. Several key parameters related to injection are listed in Table 1.

A number of diagnostic instruments are used to measure the injected beam dynamics. Centroid motion is monitored with fast turn-by-turn BPMs developed specifically for SPEAR3 [2]. Optical imaging of the charge distribution is possible at a diagnostic beam line which directs 3.5 x 6mrad of unfocused visible/UV light to an optical bench. After passing through a 6" diameter, f=2m collection lens the light is relayed to one of several diagnostic stations. An intensified, fast-gated camera can image the transverse beam profile at each turn [3] but the light intensity is low and in most cases must be averaged over consecutive injection events [4]. Similarly, in the longitudinal direction, a dual-axis streak camera can be used to image the injected beam profile by integrating over a series of injection pulses [5]. For a detailed analysis of the transient response of the injected beam into a storage ring see references [6,7].

*Work sponsored by U.S. Department of Energy Contract DE-AC03-76SF00515 and Office of Basic Energy Sciences.
[1]corbett@slac.stanford.edu

Table 1: SPEAR3 injection parameters

Injection amplitude	x=-13 mm
Stored beam size	310x20 μm, 20 ps
Stored beam, dp/p	0.1%
Damping times	4.2, 5.1, 2.8 ms
Injected beam size	~1.0x0.8 mm at SLM
Injected dp/p	0.07%

BTS TUNING AND TURN-BY-TURN BPMS

As reported in [8], a systematic program was carried out to optimize electron beam steering and lattice optics through the booster-to-SPEAR (BTS) transport line. Important elements of this work included removal of stainless steel windows intercepting the beam path and application of response-matrix analysis to correct the beam optics.

The injection kicker waveforms were then carefully matched and 6-D phase-space coordinates of the incoming beam adjusted by monitoring the bunch centroid motion on turn-by-turn BPMs. For these measurements, specially-designed Ecotek BPM receivers [2] mix the raw BPM signals down to an intermediate frequency $f_{IF} = 13f_0$ that is band-pass filtered and allowed to electronically ring several times while being digitized by high quality commercial digitizers. In order to monitor and compensate for changes in gain, a low-level calibration signal at $f_{cal} = f_{RF} - f_0/2$, is combined into the BPM long haul cables. Parallel digital receivers tuned to both f_{RF} and f_{cal} respectively allow for the calibration. The resulting digitally-processed data yields low-distortion, highly-accurate measurements of beam position on a turn-by-turn basis. For nominal stored-beam conditions the beam centroid resolution is of order 1μm.

For injected-beam measurements, the incoming single-bunch charge is only ~30pC so the BPM signals are relatively weak, -85dBm after cable loss, and the position resolution is only about 1mm. As a result, horizontal injection oscillations can be resolved but small amplitude vertical motion and synchrotron oscillations require averaging. In order to measure individual injection pulses, at each injection cycle injection kicker #3 (downstream of the injection septum) is triggered at the nominal injection time while injection kickers #1 and #2 (upstream of the septum) are mismatched and triggered 50ms late to kick out the stored beam [8].

Of particular interest, the synchrotron oscillation component was extracted via FFT processing and the initial phase-space coordinates of the motion used to match injected beam energy and timing. An example

LHC BEAM STABILITY AND PERFORMANCE OF THE Q/Q' DIAGNOSTIC INSTRUMENTATION

R.J. Steinhagen, A. Boccardi, M. Gasior, O.R. Jones, S. Jackson (CERN, Geneva, Switzerland)

Abstract

The BBQ tune (Q) and chromaticity (Q') diagnostic systems played a crucial role during the LHC commissioning while establishing circulating beam and first ramps. Early on, they allowed to identify issues such as residual tune stability, beam spectrum interferences and beam-beam effects – all of which may impact beam life-times and thus are being addressed in view of nominal LHC operation. This contribution discusses the initial beam stability in relation to the achieved instrumentation sensitivity, corresponding tune frequency and Q' resolution.

INTRODUCTION

The LHC requires excellent control of particle loss which – with the tunes being in the vicinity of third-order resonances – implies an excellent control of tune, coupling and chromaticity effects. Relying on the Base-Band Tune meter (BBQ, [1]), the base-line Q/Q' diagnostics chain was widely considered to be a 'work-horse' from Day 1 of LHC commissioning and could since be operated with no hardware-, minimal software- and only a few beam-dynamics related issues. While the general system overview is given in [2], this contribution focuses on the system's performance and issues that arose during initial beam operation.

BBQ PERFORMANCE

Due to the BBQ's nm-level sensitivity, most of the tune and corresponding chromaticity measurements could be done with residual beam excitation using one of the two Fourier analysis-based systems per beam. Figure 1 shows a typical non-excited LHC beam oscillation magnitude spectrum that has been calibrated against the LHC BPM system. The spectrum is based on an acquisition of 8192 turns (corresonding bin bandwidth is about 0.72 Hz) and normalised so that the spectral amplitude has a one-to-one relation with the r.m.s. amplitudes in time-domain for single-tone frequencies. The corresponding amplitude of broad-band perturbations require an integration over the given bandwidth using this scheme. Thus, the residual tune oscillations at $q_h \approx 0.292$ and $q_v \approx 0.277$ have r.m.s. oscillation amplitudes between 0.1 and 1 μm in the time domain. The vertical tune oscillations being typically ten times stronger than the horizontal ones are typically also visible in the horizontal plane. A number of additional lines and a broad-band excitation around 0.31 f_{rev} are also visible in the spectrum.

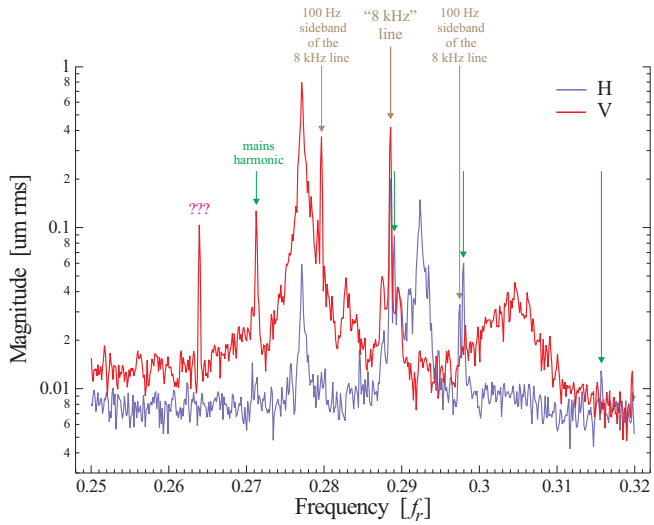

Figure 1: Typical LHC beam spectrum zoomed-in around the tune working points.

Based on this measurement, the BBQ turn-by-turn resolution is estimated to be better than 1 μm. Nevertheless, a full set of tune beam exciters (tune kickers, transverse damper exciters and an experimental strip-line based, low-amplitude and low-noise exciter) were commissioned.

FFT-based Q-Tracking

The BBQ oscillation data is typically processed using Fourier-analysis (FFT) and Phase-Locked-Loop (PLL) based systems described in [3, 4]. Figure 2 shows an exemplary FFT-based measurement of the tune and intensity evolution during the third LHC ramp with the tune feedback being switched 'off'.

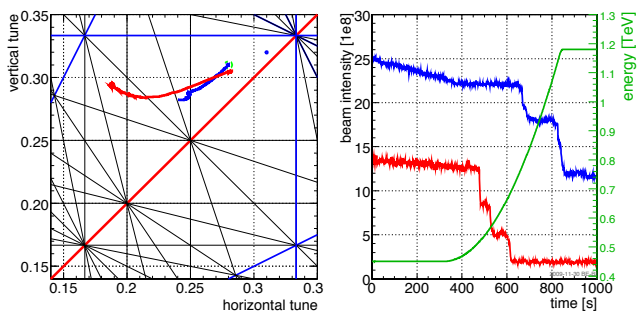

Figure 2: Tune and intensity evolution during the third ramp (2009-11-30).

HIGH RESOLUTION BEAM ORBIT MEASUREMENT ELECTRONICS BASED ON COMPENSATED DIODE DETECTORS

M. Gasior, R. J. Steinhagen, CERN, Geneva, Switzerland

Abstract

A high resolution beam position monitor (BPM) electronics based on diode peak detectors has been developed at CERN. The circuit processes the BPM electrode signals independently, converting the short beam pulses into slowly varying signals which can be digitized with high resolution ADCs operating in the kHz range or even measured with a DC voltmeter. For signals with peak amplitudes larger than some hundred mV the non-linear forward voltage of the diodes is compensated by a simple network using signals from two peak detectors, one with a single and the second with two diodes in series. This contribution presents results obtained with the first prototype in the laboratory and with the CERN-SPS beam. Ongoing development and possible future applications of the technique are also discussed.

INTRODUCTION

Diode peak detectors have been used at CERN for processing BPM signals in tune measurement systems [1] and recently for observing beam motion of very small amplitude [2]. For these applications the detector DC components related to beam position are rejected and only AC beam motion signals are processed. Diode detectors allow direct conversion of the fast beam pulses from BPM electrodes to signals in the kHz range, which can be efficiently digitised with high resolution ADCs. These benefits allow a very high amplitude resolution to be achieved with simple and robust hardware.

The main difficulty in using a similar scheme for measuring beam position is the diode forward voltage. This voltage causes the detector output voltage to be smaller than the true peak of the input signal, introducing an important error. In the ideal case the beam position p_{AB} in the plane of BPM electrodes A and B can be evaluated from the electrode peak voltages V_A and V_B as

$$p_{AB} = c_{AB}\frac{V_A - V_B}{V_A + V_B} \qquad (1)$$

where c_{AB} is the BPM conversion factor, for simplicity assumed to be a constant equal to the BPM half aperture. If beam position is estimated from the output voltages of the diode peak detectors of electrodes A and B, which are smaller than V_A and V_B by the diode forward voltage V_d, then (1) can be rewritten as

$$p_{AB} = c_{AB}\frac{V_A - V_B}{V_A + V_B - 2V_d} \qquad (2)$$

Thus, V_d causes large beam position errors for small V_A and V_B. In reality V_d is not a constant, but varies with the detector input signal amplitude, its slew rate, temperature, making the beam position error a complex function.

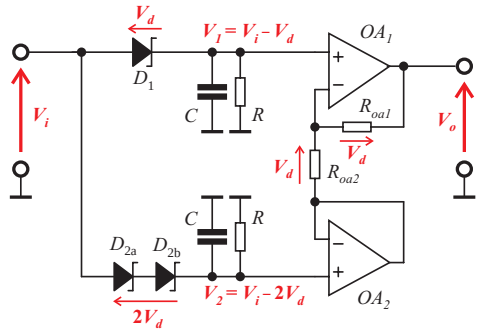

Figure 1: A compensated diode detector

The dream of the authors was to find a circuit with self-compensation of the diode forward voltage, in order to profit from the benefits of the peak detector scheme also for beam orbit measurement. The simplest and most promising scheme found is shown schematically in Fig. 1. Such a circuit diagram was published in [3], and mentioned in a popular electronics textbook [4].

The compensation scheme is based on two peak detectors, one with a single and the second with two diodes in series. The signals from two such detectors are processed with a simple network with two operational amplifiers, allowing the input peak voltage to be restored. The voltage values at circuit nodes explain the compensation scheme. The difference of the output voltages from both peak detectors is equal to the drop on one diode, V_d. As the voltage between the inverting and non-inverting inputs of the operational amplifiers is practically zero, V_d is converted into current V_d/R_{oa1} and, as the current of the non-inverting input of OA_1 is practically zero, the current V_d/R_{oa1} is converted again into V_d with $R_{oa2} = R_{oa1}$. In this way $2V_d$ is added to the output of OA_2, compensating the $2V_d$ drop on the two diodes D_{2a}, D_{2b}.

Identical voltage drops across each diode require the diode currents for both detectors to be equal, also during transients when the parallel capacitors are being charged. This is not possible with small input signal amplitudes, for which the current of the two-diode detector is smaller. Hence, the compensation mechanism does not work for small input signals. This limitation cannot be removed for pulse signals by biasing the diodes with DC current, as the symmetry of the detector pulse currents is required.

THE PROTOTYPE

The first prototype of the diode orbit measurement electronics was built as a simple circuit to test the performance of the compensated diode detectors. It was built using the PCB, power supply and mechanical parts of a diode tune measurement front-end [5]. For simplicity

IMPROVEMENTS FOR OPERATIONAL BASEBAND TUNE AND COUPLING MEASUREMENTS AND FEEDBACK AT RHIC*

M. Wilinski, W.C. Dawson, C. Degen, A. Marusic, K. Mernick, M. Minty, T. Russo, BNL, Upton, NY, USA

Abstract

Throughout RHIC Run-9 (polarized protons) and Run-10 (gold), numerous modifications to the Baseband Tune (BBQ) system were made. Hardware and software improvements resulted in improved resolution and control, allowing the system to overcome challenges from competing 60Hz mains harmonics, other spectral content, and other beam issues. Test points from the Analog Front End (AFE) were added and connected to diagnostics that allow us to view signals, such as frequency spectra on a Sr785 dynamic signal analyser (DSA), in real time. Also, additional data can now be logged using a National Instruments DAQ (NI-DAQ). Development time using tune feedback to obtain full-energy beams at RHIC has been significantly reduced from many ramps over a few weeks, to just a few ramps over several hours. For many years BBQ was an expert-only system, but the many improvements allowed BBQ to finally be handed over to the Operations Staff for routine control.

INTRODUCTION

Tune measurement and feedback [1, 2, 3] in RHIC was first begun during the 2004 RHIC gold run as part of the US LHC Accelerator Research Program (LARP). Development of the system has continued since then with the present installation consisting of a pickup and kicker in each of the 1 and 2 o'clock sectors in the RHIC tunnel. The remainder of the system is installed in Service Building 1002A and consists of direct diode detection (3D), and analog front end (AFE), a kicker chassis, various VME/controls modules (such as Numerically Controlled Oscillators (NCO), digitizers, and timing), and several diagnostics packages including Stanford Research Systems Sr785 Dynamic Signal Analyzers and National Instruments PCI-6143S Multifunction DAQ PCI cards.

From the 2004 run through the 2008 run, a good amount of progress was made, but an expert was still required to operate the BBQ system. Various problems were encountered [4] such as mains interference, 'anomalous' beam transfer functions, and 'tune scalloping' which often interfered with acquiring a successful tune lock on the beam. Prototype boards and chassis were fabricated to try to help solve some of these problems.

Prior to the 2009 run (Run-9), a new team of people took over responsibility for BBQ [5]. During this time, nearly 50 issues involving tune measurement hardware items were addressed, along with numerous software enhancements that significantly improved resolution of the measured tunes. Modifications were also made to allow for exploration of near integer working points, as well as working points near 1/3.

*Work performed by employees of Brookhaven Science Associates, LLC under Contract No. DE-AC02-98CH10886 with the U.S. Department of Energy

HARDWARE MODIFICATIONS

General Modifications for Operations

Among the first major tasks were massive cleanups of the tunnel areas and Service Building 1002A. Both areas contained a great deal of clutter (old cables, connectors, clamps, etc). A number of old, unused prototype chassis were still installed in the racks, some with cables connected only at one end. Once all of the extraneous equipment was removed, the remaining equipment was adjusted such that the racks for the blue and yellow rings were identical in layout. Blank panels were added to racks as needed to cover up empty areas and improve shielding.

Next, attention was focused on improving the AFEs. Several voltage under-rated capacitors were replaced with properly rated capacitors. Transfer functions of the AFE were simulated and measured, and upon comparison of the results were found to match well. A driver board was added to each AFE to get the pickup +/- signals into the controls system so a dB-to-mm position calculation would be available. The addition of the test signals allow the BBQ pickups to be easily centered on the beam, rather than the beamline.

The most significant effort on the AFE was adding additional test points to observe internal signal levels. Small daughter cards were added to monitor the following signals: +/- input signals from the pickups, the input difference signal, and the filtered signal. All of these signals can be observed via several methods: a local scope, an Sr785 DSA, or the NI-DAQ. Two, 2-channel DSA units are installed, one each for the blue and yellow rings. Typically the difference signals of the blue horizontal (BH), blue vertical (BV), yellow horizontal (YH), and yellow vertical (YV) planes are monitored and logged through the controls system, but signals can be changed locally if necessary. The NI-DAQ system consists of two computers, each with two 8-channel PCI-6143S cards that sample at 250kSamples/second. All four test point signals from each plane (BH, BV, YH, and YV) along with several kicker diagnostic signals are input into the cards. The DAQ is triggered automatically at the start

DYNAMICALLY TUNED HIGH-Q AC-DIPOLE IMPLEMENTATION*

P. Oddo, M. Bai, W. C. Dawson, W. Meng, K. Mernick, C. Pai, T. Roser, T. Russo, Brookhaven National Laboratory, Upton, NY 11973, USA

Abstract

AC-dipole magnets are typically implemented as a parallel LC resonant circuit. To maximize efficiency, it's beneficial to operate at a high Q. This, however, limits the magnet to a narrow frequency range. Current designs therefore operate at a low Q to provide a wider bandwidth at the cost of efficiency. Dynamically tuning a high Q resonant circuit tries to maintain a high efficiency while providing a wide frequency range. The results of ongoing efforts at BNL to implement dynamically tuned high-Q AC dipoles will be presented.

INTRODUCTION

Work on a new spin flipper for RHIC (Relativistic Heavy Ion Collider) incorporating multiple dynamically tuned high-Q AC-dipoles has been developed for RHIC spin-physics experiments. A spin flipper is needed to cancel systematic errors by reversing the spin direction of the two colliding beams multiple times during a store [1]. The spin flipper system currently consists of four DC magnets and three AC-dipoles and will go to five AC-dipoles. Multiple AC-dipoles are needed to localize the driven coherent betatron oscillation inside the spin flipper. Having multiple AC-dipoles that require precise control over amplitude and phase makes it necessary to implement them as dynamically tuned high-Q resonant circuits. One of the major challenges was to design of a new magnet and the proper topology to drive it. The topology is required to be both efficient and serviceable.

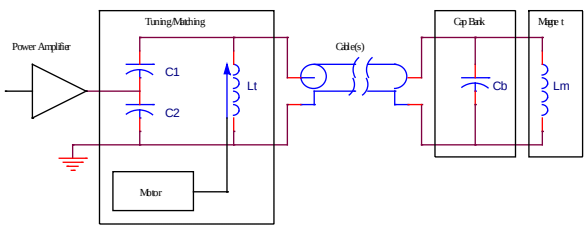

Figure 1: RHIC High-Q AC-dipole simplified schematic.

HIGH-Q AC-DIPOLE SYSTEM

Figure 1 is a simplified schematic of the present implementation. This topology places the bulk of the capacitance at the magnet. A pair of heliax coaxial cables connects the capacitor bank to the tuning chassis in the service building. Tuning is accomplished via a motor driven variable air-gap inductor. A servo loop adjusts the air gap to maintain the system at resonance.

This topology was initially chosen to support solid state (switched capacitor) tuning which required the tuning to be done outside of the ring in order to protect the semiconductor (MOSFET) switches from radiation damage. However, due to scheduling and concerns over switching distortion, solid state tuning was not implemented.

Existing AC-dipole systems

For comparison, figure 2 is a simplified schematic of the existing RHIC AC-dipoles [2] and figure 3 of the CERN LHC [3] and the FNAL Tevatron [4] AC-dipoles. For clarity, these schematics only illustrate the location of major components. In all cases the transmission line is the dividing line between the components in the service building and in the ring. The placement and use of the transmission line is a key difference between approaches.

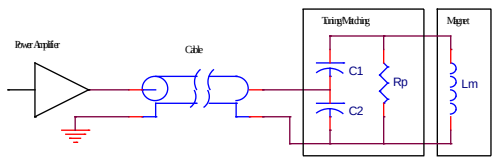

Figure 2: RHIC AC-dipole simplified schematic.

RHIC AC-dipoles

The RHIC AC-dipoles matches and tunes the AC-dipoles at the magnet. This approach tries to terminate the transmission line with its characteristic impedance. Although the magnet was designed as a high-Q air-core, the Q is deliberately spoiled (Rp). Since the resonant impedance is greater than amplifier/transmission line impedance, a capacitive step-up matching network was used (C1, C2).

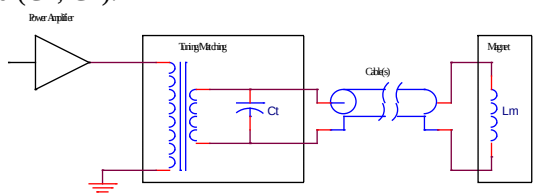

Figure 3: LHC/Tevatron AC-dipole simplified schematic

LHC and Tevatron AC-dipoles

The LHC/Tevatron approach does the tuning and matching at the service building. For this approach the transmission line current is the magnet current. Furthermore, since low impedance kicker magnets are used, the transmission line is terminated with an impedance that's much lower than its characteristic impedance; the transmission line therefore forms a parasitic series inductance. This inductance increases the peak energy stored.

DIGITAL BASE-BAND TUNE DETERMINATION

P. Kowina [1], U. Springer [1,2], P. Forck [1], P. Hülsmann [1,2] and P. Moritz [1]

[1] GSI, Darmstadt Germany, [2] Goethe University, Frankfurt, Germany

Abstract

To avoid beam losses of intense beams stored at the GSI heavy ion synchrotron SIS18 a precise tune measurement during a whole acceleration cycle is required. This contribution presents a sensitive method of tune determination using data of Beam Position Monitor (BPM) measured in bunch-by-bunch manner. The signals induced in the BPM electrodes were digitized by 125 MS/s and integrated for each individual bunch. The tune was determined by Fourier transformation of the position data for typically 512 subsequent turns. Coherent betatron oscillations were excited with bandwidth-limited white noise. The presented method allows for tune measurements with satisfactory signal-to-noise ratio already at relatively low beam excitation i.e. without significant increase of transverse beam emittance. In parallel the evolution of transverse beam emittance was monitored by means of an Ionization Profile Monitor. The system for online tune measurement is an integral part of the new digital BPM System, presently under commissioning.

INTRODUCTION

Unlike other beam parameters, e.g. beam current, position, transversal beam profile etc., the tune is a crucial beam parameter that can not be obtained in a single individual measurement. A most fundamental technique is based on the excitation of coherent transversal beam motions with a known perturbation source and post-processing of the beam response using beam position monitors (BPM).

The GSI heavy ion synchrotron SIS18 has some particular machine parameters, which make tune diagnostics challenging. Namely the comparatively long bunches, the injection at non-relativistic velocity β = 15.5% and the fast ramping of the acceleration frequency from 0.8 to 5 MHz within 400 ms. Since tune measurement during a whole acceleration cycle is required, other methods of tune determination using e.g. passive monitoring of the residual beam oscillation (like observation of Schottky noise) or active techniques based on phase-locked-loop systems are either to slow or require a lot of manpower during implementation. For an overview see e.g. [1] and references therein.

On the other hand, a new data acquisition system for BPMs at SIS18 presently under commissioning [2] opens new possibilities for tune determination. Since the beam position is measured in bunch-by-bunch manner it was evident to investigate if the tune can be determined by appropriate post-processing of anyhow existing beam position data. The results of these investigations are presented and discussed in the following sections.

For a stable beam consisting of a large but finite number of particles a movement of the centre-of-mass is the incoherent sum of individual particle oscillations effected by random phases and frequency spread. This so called *Landau damping* [3] makes the betatron motions of individual particles inaccessible. Usually the residual coherent particle motions are too weak to be detected and the beam needs to be slightly excited. There are three methods of the beam excitation available at SIS18:

- One-turn kick-type excitation using a pulsed magnet that applies its full power within a single revolution period. However, the transversal motions decay within some hundreds of turns due to Landau damping which excludes the possibility of tune observation over the whole acceleration cycle.
- Frequency sweep excitation: generated using a sinusoidal-type signal with time-varying frequency. However, for fast ramping accelerators like SIS18 the increase of the SIS rf frequency is faster compared to the sweeps performed by the exciter which does not allow for tune diagnostics on the acceleration ramp.
- Noise excitation which considers an excitation with a broadband noise covering the expected frequency range.

For the investigation presented in this contribution the last method was used.

METHODS AND RESULTS

Fig.1 shows schematically the detection setup. The beam was excited using a noise applied to the exciter plates installed at SIS18. The noise signal with adjustable bandwidth around the side bands of the carrier frequency

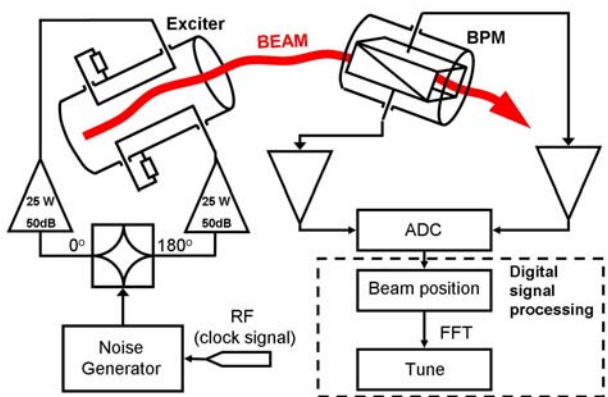

Figure 1: Detection setup (see description in text).

A SHIELDED PICK-UP DETECTOR FOR ELECTRON CLOUD MEASUREMENTS IN THE CESR-TA RING*

J. Sikora#, Y. Li, M. Palmer, Cornell University, Ithaca, NY 14850, U.S.A.
S. De Santis, D. Munson, LBNL, Berkeley, CA 94720, U.S.A.

Abstract

The experimental study of the electron cloud dynamics and mitigation techniques is one of the main objectives of the CESR Damping Ring Test Accelerator (Cesr-TA) program. Shielded pick-up buttons are a relatively simple diagnostic device for obtaining time-resolved information on the electron cloud density. They have been already successfully employed on the SPS at CERN [1], although with different resolution parameters due to the different type of beams. We present the initial results obtained using such a detector in the Cesr-TA electron/positron ring. By carefully designing the read-out electronics we were able to resolve the individual bunch contribution to the electron cloud formation process along a bunch train and gain useful information on its decay time. Alternatively, by increasing the electronics integration time, we could use our device as a sensitive detector of the average electron cloud density level generated by the passage of a bunch train.

INTRODUCTION

One of the leading R&D issues for the positron damping ring of a future linear collider is to ensure that the density of electron cloud (EC) build-up in the vacuum chambers can be kept below the levels at which beam instabilities and incoherent emittance growth will occur. In the present ILC damping rings (ILCDR) design, the presence of the EC in the positron ring limits the maximum current that can be stored and hence the minimum circumference of the ring that can be employed. As such, it is a significant cost driver for this accelerator system as well as being a major source of concern for whether the design can reach its performance goals.

Characterization and mitigation of the electron cloud effect constitutes one of the main activities in the Cesr-TA research program [2]. Several methods have been developed to experimentally study electron clouds such as retarding field analyzers (RFA) [3], TE wave based method [4], tune shift measurements with a witness bunch [5]. All these methods complement each other in that each one of them is best suited to study some particular aspects of the electron cloud dynamics.

Shielded pickups (SPU) are especially useful for measuring the time properties of the electron cloud formation and decay process at a given location in the accelerator. Their small size and relatively simple electronics also makes them a good choice as monitoring devices for the electron cloud density at multiple points around the accelerator ring. The SPU voltage V_{PU} is a function of the electron cloud density in the beampipe region close by. An estimate is given by the following formula [1]:

$$\lambda_{EC} = \frac{V_{PU}}{F_g t \cdot f_b \cdot Z_{PU} G_{sys}} \qquad (1)$$

where λ_{EC} is the electron cloud linear density, F_g a geometric factor that takes into account the SPU electrode and the beampipe size, t the shielding grid transparency, f_b the bunch frequency and Z_{PU} the pickup input impedance, and G_{sys} the system's gain.

In this paper we present our studies of the electron cloud in the Cesr-TA synchrotron ring using SPUs discussing their hardware and showing experimental results with both positrons and electrons beams.

HARDWARE DESCRIPTION

An SPU is conceptually an electrode placed on the beampipe wall, which collects low-energy electrons present in that portion of vacuum chamber and is shielded from the beam wakefield. By applying a DC bias voltage to the electrode, with respect to the pipe ground, it is

*Work supported by the US National Science Foundation, the US Department of Energy, and the Japan/US Cooperation Program.

TUNE MEASUREMENT SYSTEM AT THE ALBA BOOSTER

U. Iriso*, F. Pérez, and A. Salom.
CELLS, Ctra BP-1413 Km 3.3, Cerdanyola - 08290 (Barcelona), Spain

Abstract

The ALBA Booster synchrotron is designed to ramp electron beams of 5 mA from 100MeV to 3GeV in a 3Hz cycle. The Booster is equipped with two common $\lambda/4$ striplines for tune excitation and precise beam position measurement. Beam excitation along the cycle requires the amplitude kick to increase in synchronism with the energy ramp. This paper shows the excitation and measurement system at the ALBA Booster, including both mechanical and hardware instrumentation. First results during the 2 weeks of Booster pre-commissioning are shown.

INTRODUCTION

ALBA is a third generation light source whose injection system is composed by a 100MeV Linac followed by a full energy Booster synchrotron, which ramps the electron beams up to 3GeV in a 3Hz cycle. More details about the Booster are given in Table 1 and Ref. [1].

Table 1: Booster design main parameters.

Parameter	Injection	Extraction
energy, E [GeV]	0.1	3.0
hor. emittance, ε_x [nm-rad]	150	9
max. current, I [mA]	5.0	
circumference, C [m]	249.6	
rf freq., $f_{\rm rf}$ [MHz]	499.6	
hor / ver tunes, ν_x/ν_y	12.42 / 7.38	

In order to properly monitorize the betatron tunes along the ramp, two identical $\lambda/4$ stripline BPMs are installed. The first stripline is devoted to excite the beam, while the second one is used to precisely measure the beam position. Their acronyms are SEXC and SMES, respectively.

Horizontal and vertical beam excitation are done with an electrick kick whose amplitude increases in synchronism with the energy ramp. An excessively strong kick will induce beam losses at low energy, while a too weak one will not allow the measurement at full energy [2]. Two weeks of Booster pre-commissioning were scheduled during January 2010 [3]. This paper present as well the first results obtained during this pre-commissioning.

MECHANICAL DESIGN

Two pictures of the Booster stripline are shown in Fig. 1. The same setup is used for excitation and measurements, and so we used $\lambda/4$ electrodes, matched to 50Ω for tune excitation, and shorted for tune measurements (being $\lambda = c/f_{\rm rf}$ the rf wavelength).

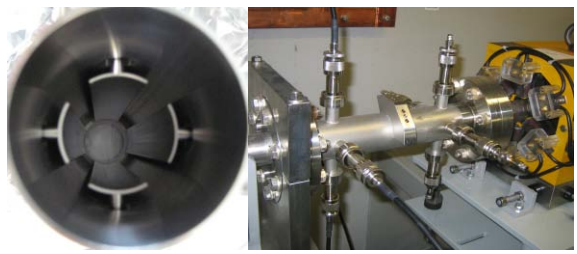

Figure 1: Picture of the stripline transverse geometry (left), and stripline as installed in the ALBA Booster. The electrode covering angle is 60°.

The electrode surface has been maximized as much as possible to increase kick efficiency when used as excitation device, and pick-up detection when used as measurement device. SUPERFISH simulations have been carried out to match the electrodes to 50 Ω. Figure 2 shows the S-parameters measured with the NA, which shows optimum results for both reflection (S11) and electrodes coupling (S12).

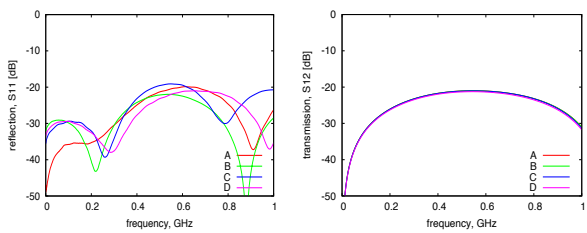

Figure 2: Stripline S-parameters as measured with the Network Analyser (NA): S11 (left) and S12 (right).

TUNE EXCITATION LAYOUT

The shunt impedance $Z_{\rm sh}$ of a kicker made out of two electrodes of length l and spaced with a distance d is [4]

$$Z_{\rm sh} = 2Z_0\left(\frac{2g\beta c}{d\omega}\right)^2 \sin^2\left(\frac{\omega l}{c}\right), \qquad (1)$$

where Z_0 is the vacuum impedance, ω refers to the kick angular frequency, c is the speed of light, and g is the geometrical factor. Assuming a pessimistic case of a flat electrode of $w = R \times (\pi/3)$ spaced by a distance $d = 2 \times R$ (with R the chamber radius), this is inferred as [4]:

$$g = \tanh\frac{\pi w}{2d}. \qquad (2)$$

* ubaldo.iriso@cells.es

DIAGNOSTICS DURING THE ALBA BOOSTER COMMISSIONING

U. Iriso*, M. Alvarez, R. Muñoz, A. Olmos, and F. Pérez.
CELLS, Ctra. BP-1413 km 3.3, Cerdanyola - 08290 (Barcelona), Spain

Abstract

The ALBA Booster is a synchrotron designed to accelerate electron beams from 100 MeV to 3GeV in a 3Hz cycle. The maximum pulse coming from the ALBA Linac provides 5 mA in the Booster. In order to check all the Booster sub-systems, a Booster pre-commissioning took place during two weeks in January 2010. This paper presents the Diagnostics elements installed in the ALBA Booster and our experience during the Booster pre-commissioning.

INTRODUCTION

The ALBA Booster installation finished in November 2009. In order to find out unexpected problems at an early stage, a short Booster pre-commissioning was scheduled for January 2010. It lasted only two weeks so as not to interfere excessively with the installation of the Storage Ring and beamlines.

The electron beam at the Booster comes from the Linac, which can work in Single and Multi Bunch Mode and was commissioned in Autumn 2008 [1]. The maximum Linac pulse charge is 4 nC, which represents a current of 5 mA at the Booster. The beam is then accelerated in the Booster synchrotron from 100 MeV to 3 GeV in a 3Hz cycle. The Booster consists of a 4-fold symmetry FODO lattice with 40 combined function dipoles [2]. The basic parameters of the ALBA Booster are listed in Table 1.

Table 1: Booster design main parameters.

Parameter	Injection	Extraction
energy, E [GeV]	0.1	3.0
hor emittance, ε_x [nm-rad]	150	9
max. current, I [mA]	4.0	
circumference, C [m]	249.6	
rf freq., f_{rf} [MHz]	499.6	
hor / ver tunes, ν_x/ν_y	12.42 / 8.37	
dipole field, B [T]	0.168	0.873
hor size (at dipole), σ_x [mm]	< 1.8	< 0.3
ver size (at dipole), σ_y [mm]	< 1.8	< 0.10

In order to properly check the Booster synchrotron performance, the set of Diagnostics equipment described in Fig. 1 is installed in the machine. Next, we present the Diagnostics elements installed in the Booster and our experience during the pre-commissioning.

SCREEN MONITORS

The FSOTR is the acronym used to describe the setup that allows to insert either a Fluorescent Screen (YAG:Ce) or an Optical Transition Radiaton plate. The YAG screen is used for moderate intensity beams, the OTR is devoted for high intensity beams (which typically saturate the YAG emission). The setup includes a manually controled focus and zoom optics got *off-the-shelf* from EHD-Imaging and a Gigabit Ethernet CCD camera (Basler Scout, 12-bit resolution, 1034x779 pixels, with a square pixel size of 4.65μm). More information about this setup is shown in [3].

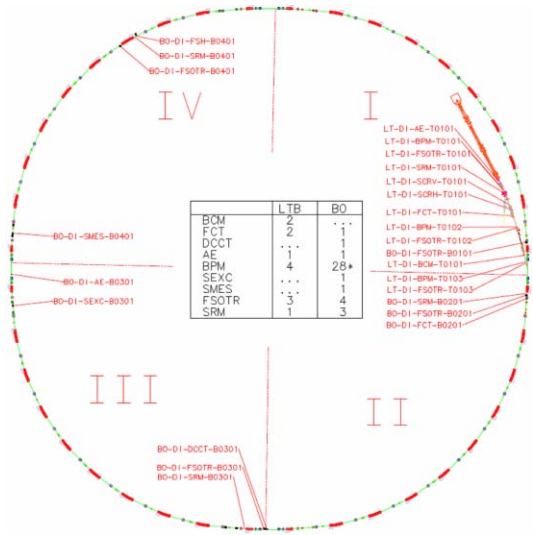

Figure 1: Linac, LTB, and Booster sketch with the location of the Diagnostics components.

We placed 3 FSOTRs to monitor the beam path along the transfer line from the Linac to Booster (LTB), while 4 more are installed in the Booster to ease the first commissioning goals (first injection, first quadrant, first turn).

In order to avoid undesirable image reflections with the YAG screen, it is convenient to make YAG plates optically non-transparent. We did so by attaching a sandblasted plate downstream the YAG. Moreover, reference marks have been added to this plate to provide in-situ calibration and centering position. Figure 2 shows an example of an image taken with the YAG screens.

BPM SYSTEM

The Booster is equipped with 44 hor and 28 ver correctors, and 44 button type BPMs. For economical reasons, it was decided to equip only 28 BPMs with the read out electronics (I-Tech Libera Brilliance). Simulations showed that the horizontal orbit correction with 28 BPMs allows an rms residual of 0.5 mm at BPMs, with a maximum of 4.5 mm

* ubaldo.iriso@cells.es

BEAM POSITION MONITORS CHARACTERIZATION FOR ALBA

A. Olmos*, M. Álvarez and F. Pérez. ALBA-CELLS, Cerdanyola del Vallès, Barcelona, Spain

Abstract

Beam position monitors (BPM) characterization has been widely studied at ALBA Synchrotron Light Source. Special care has been taken on the analysis of their electrical offset in order to achieve submicron beam stabilities. This paper shows the results of the BPM offset study for Booster and Storage Ring. The electrical effect of the different vacuum vessels housing the BPMs is also reported.

INTRODUCTION

Beam position monitoring at ALBA synchrotron will be performed using a total of 177 button type BPMs, 172 of them dedicated to pure orbit measurements; 3 will be used to do machine studies and 2 for multi-bunch instabilities measurement.

Table 1: BPM Distribution at ALBA

# BPMs	Machine	Purpose
1	Linac	Position
3	LTB	Position
44	Booster	Position
2	Booster	Machine Studies
4	BTS	Position
120	Storage Ring	Position
1	Storage Ring	Machine Studies
2	Storage Ring	Multi-Bunch

Intensive measurements of the feedthroughs during their manufacturing process have been done at the factory on the Booster and Storage Ring BPMs. Electrical tests have been done at ALBA for final manufacturing checking and electrical offset calculation of the BPMs.

BUTTONS CHECKING AND SORTING

Feedthrough capacitance has been measured at different stages during the manufacturing process of the BPM blocks in order to analyze their deviation from specifications. These tests also allow tracking of the BPM quality during the manufacturing. ALBA BPM blocks are directly welded on the vacuum chamber and any defect on the BPM block will require complete chamber replacement. For that reason, intense checking of the feedthrough quality at each stage was almost mandatory.

Measurement of button capacitance

Capacitance was measured using a TDR device [1,2]:

- After button manufacturing
- After button welding on the BPM block
- After BPM block bake-out

The plots in Figure 1 show the results of the capacitance measurement of the 204 buttons of Booster and Booster to Storage Transfer line (BTS) before and after the manufacturing process of the complete vacuum chamber. Design capacitance value was 3.2 pF. The buttons capacitance deviation from specs remained in all cases below +-10% (the tender requirement), with an absolute average value of 3.2%, maximum change on a button of +8% and -5.3%.

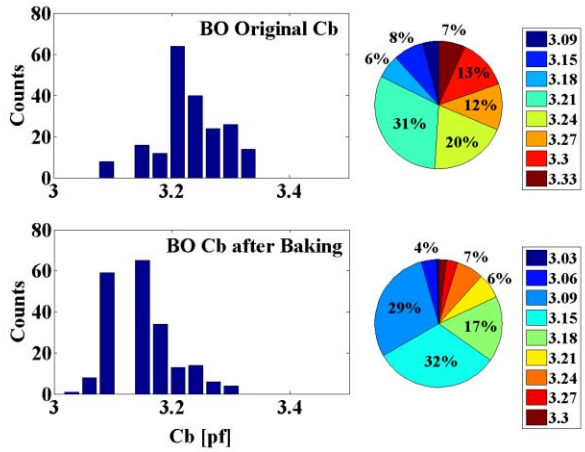

Figure 1: Capacitance deviation on Booster and BTS buttons after vacuum chamber manufacturing.

All these variations of capacitance led to an electrical offset effect on the BPMs (only due to the buttons difference). An extra effect was introduced by the relative positioning of each button on the BPM block (measured later using a network analyzer test).

Button sorting

A sorting of all buttons was done before welding in order to reduce their effect on the electrical offset of the BPMs. Figure 2 shows the calculated offset on the Storage Ring BPMs before and after welding. Buttons were sorted for closer capacitance, so the obtained offset before welding is negligible. Offset after manufacturing remains well below +-50 μm.

ELECTRICAL OFFSET MEASUREMENTS

Once the BPMs were welded and baked on the vacuum chambers and delivered to ALBA, an electrical offset measurement on all of them was performed before installation.

Electrical offset must be known in order to improve the absolute beam position readings, especially on the first days of the accelerator commissioning and operation.

*angel.olmos@cells.es

FIRST BEAM MEASUREMENTS OF THE FNAL HINS RFQ*

V. Scarpine#, R. Webber, J. Steimel, S. Chaurize, D. Wildman, B. Hanna, D. Zhang, FNAL, Batavia, IL 60510, U.S.A.

Abstract

The High Intensity Neutrino Source (HINS) is a research project to address accelerator physics and technology questions for a new-concept, low-energy, high-intensity, long-pulse H^- superconducting linac. HINS will consist of a 50 kKeV ion source, a 2.5 MeV Radiofrequency Quadrupole (RFQ), and a 10 MeV room temperature spoke resonator acceleration section, followed by superconducting spoke resonator acceleration sections. To date a proton ion source and the RFQ module have operated with beam. This paper presents the results of first beam measurements through the HINS RFQ.

INTRODUCTION

The HINS accelerator project is a DOE approved and funded avenue to pursue advanced low-energy linac technologies. HINS has undergone various changes, as its development is vital for the testing and design of Project-X [1]. Details of the HINS program can be found in [2].

The HINS project has identified four basic goals [2]:

1. Demonstrate beam acceleration using superconducting spoke type cavity structures.
2. Demonstrate the use of high power RF vector modulators to control multiple RF cavities by a single high power klystron for acceleration of a non-relativistic beam.
3. Demonstrate beam halo and emittance growth control by the use of solenoidal focusing.
4. Demonstrate a fast 325 MHz bunch-by-bunch beam chopper.

Figure 1 shows an early block diagram of a 60 MeV version of the HINS accelerator. This version of HINS consists of an ion source, a 2.5 MeV RFQ, a medium energy beam transport (MEBT), a room temperature acceleration section and a series of superconducting single spoke resonator cyromodules. For this paper, only a proton ion source and RFQ have operated with beam.

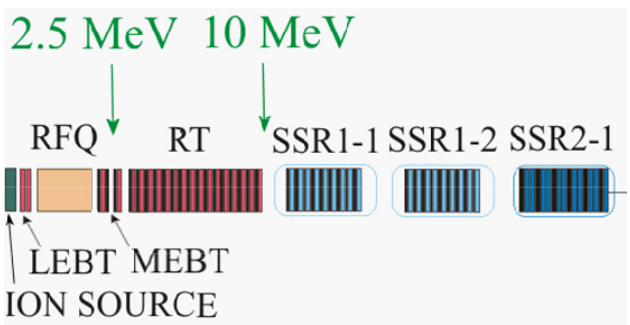

Figure 1: An early proposed HINS layout for a 60 MeV beam line and three superconducting cryomodules.

RFQ BEAMLINE

Figure 2 shows a block diagram of the present HINS beamline with its 2.5 MeV diagnostics section. This section consists of a pair of BPMs, a toroid, three transverse wire scanners and a water cooled beam dump. Figure 3 is a photograph of this 2.5 MeV diagnostic section used for the measurements in this paper.

Ion Source

The present HINS ion source is a 50 keV proton source and a low energy beam transport line (LEBT) with solenoid focusing. This proton source is capable of up to 30 mA beam in 3 ms pulses at a rate of 5 Hz [3].

RFQ

The HINS RFQ is designed to accept 50 keV beam and accelerator it to 2.5 MeV. The RFQ operates at 325 MHz and has been tested to a peak power of 450 kW, without beam, for up to 1 ms [2]. Details of the RFQ design can be found in [4].

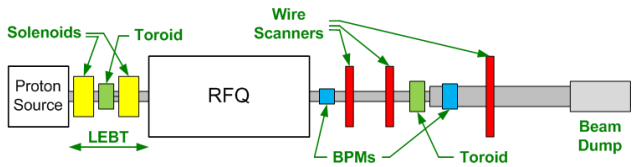

Figure 2: Original HINS proposal from 2006 showing a 90 MeV beam line and four cryomodules.

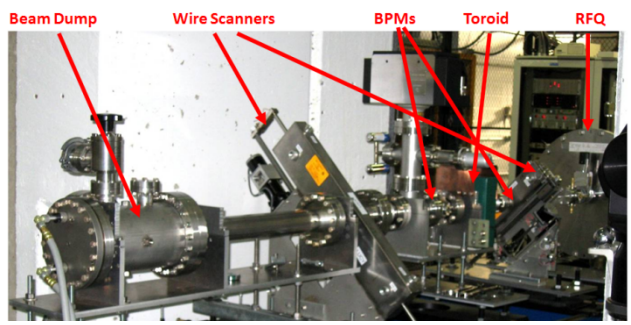

Figure 3: Original HINS proposal from 2006 showing a 90M eV beam line and four cryomodules.

RFQ BEAM MEASUREMENTS

RFQ Beam Current and Transmission Efficiency

RFQ beam current measurements were taken with a toroid in the 2.5 MeV diagnostic line. The maximum current measured was 4 mA for an input source current of 20 mA. However, these current values cannot give a measure of the RFQ transmission efficiency for two

BUNCH-BY-BUNCH DETECTION OF COHERENT TRANSVERSE MODES FROM DIGITIZED SINGLE-BPM SIGNALS IN THE TEVATRON*

G. Stancari#†, A. Valishev, and A. Semenov, FNAL, Batavia, IL 60510, U.S.A.

Abstract

A system was developed for bunch-by-bunch detection of transverse proton and antiproton coherent oscillations based on the signal from a single beam-position monitor (BPM) located in a region of the ring with large amplitude functions. The signal is digitized over a large number of turns and Fourier-analyzed offline with a dedicated algorithm. To enhance the signal, the beam is excited with band-limited noise for about one second, and this was shown not to significantly affect the circulating beams even at high luminosity. The system is used to measure betatron tunes of individual bunches and to study beam-beam effects. In particular, it is one of the main diagnostic tools in an ongoing study of nonlinear beam-beam compensation studies with Gaussian electron lenses. We present the design and operation of this tool, together with results obtained with proton and antiproton bunches.

INTRODUCTION

In the Tevatron, 36 proton bunches collide with 36 antiproton bunches at the center-of-momentum energy of 1.96 TeV. Each species is arranged in 3 trains of 12 bunches, circulating at a revolution frequency of 47.7 kHz. The bunch spacing within a train is 396 ns, corresponding to 21 53-MHz rf buckets. The bunch trains are separated by 2.6-μs abort gaps. The synchrotron frequency is around 30 Hz, or 7×10^{-4} times the revolution frequency. The machine operates with betatron tunes near 20.58.

The betatron tunes and tune spreads of individual bunches are affected by the head-on and long-range beam-beam interaction. These phenomena are among the limiting factors of modern colliders. For optimal machine performance, knowledge of bunch-by-bunch tune distributions is crucial. Three systems are currently used in the Tevatron to measure incoherent tune distributions: the 21.4-MHz Schottky detectors, the 1.7-GHz Schottky detectors, and the direct diode detection base band tune (3D-BBQ). The latter two can be gated on single bunches.

Detection of transverse coherent modes can complement these three systems. The relationship between coherent oscillation frequencies and betatron tunes is indirect, and therefore a systematic uncertainty arises from the beam-beam model when extracting the lattice tunes and the beam-beam parameter. Still, the method is appealing because of its high frequency resolution.

*Work supported by the United States Department of Energy under contract No. DE-AC02-07CH11359.

#stancari@fnal.gov

†On leave from Istituto Nazionale di Fisica Nucleare, Sezione di Ferrara, Italy.

Another motivation for measuring coherent modes is our study of nonlinear beam-beam compensation with Gaussian electron lenses [1-3]. Due to their high brightness compared with protons, an improvement in antiproton lifetime from beam-beam compensation is not foreseen. The goal of this project is a proof-of-principle observation of tune shifts induced by the electron lens and the associated changes in tune spread and beam-beam parameter. This may benefit the Relativistic Heavy Ion Collider, where electron lenses are being built, and possibly the Large Hadron Collider. Also in the case of beam-beam compensation, the spectrum of coherent modes complements the observation of Schottky signals in terms of frequency resolution.

In this paper, we present the detection technique and the measured spectra of proton and antiproton bunches under various experimental conditions.

TRANSVERSE COHERENT MODES

Transverse coherent modes carry information about lattice tunes and the beam-beam parameter [4-8]. In the simplest case, when two identical bunches collide head-on in one interaction region, two modes appear: a σ-mode at the lattice tune, where bunches oscillate transversely in phase, and a π-mode, separated from the σ-mode by a shift slightly larger than the beam-beam parameter, in which bunches are out of phase.

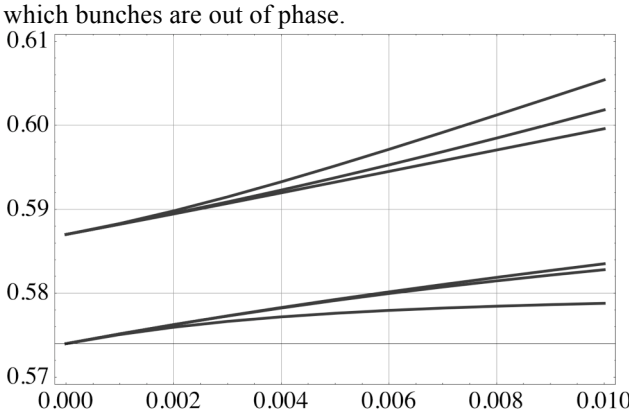

Figure 1: Sample calculation of coherent mode frequencies vs. beam-beam parameter per interaction point for 3×3 rigid round bunches with different lattice tunes.

In general, the frequency and number of these modes depend on the number of bunches and interaction regions, on the tune separation between the two beams, on beam sizes and relative intensities. Figure 1 shows how the mode frequencies evolve as a function of the beam-beam parameter, in the case of 3 rigid round bunches colliding with 3 bunches with different lattice tune at 2 head-on

11.424 GHZ STRIPLINE TRANSVERSAL FILTER FOR SUB-PICOSECOND BUNCH TIMING MEASUREMENTS*

D. Van Winkle, A. Young, J. D. Fox SLAC National Accelerator Laboratory, Menlo Park, CA

Abstract

Measurement of time-of-arrival or instantaneous longitudinal position is a fundamental beam diagnostic. We present results from a stripline transversal periodic coupler structure which forms the heart of a sub-ps beam timing detector. This filter structure approximates a sinx/x response in the frequency domain which corresponds to a limited pulse length response in the time domain. These techniques have been used extensively in beam feedback systems at 3 GHz center frequencies with operational single-shot resolutions of 200 fs [1]. We present a new design, based on a 11.424 GHz center frequency, which is intended to offer a factor of four improvement in time resolution. Two-dimensional electromagnetic simulation results are shown, and the design optimization approach leading to the final circuit implementation is illustrated. The prototype circuit has been fabricated on 64mil Rogers 4003 and lab frequency domain and time domain data are compared to the 2-D simulation results. Performance of the prototype circuit is shown with applicability to sub-ps beam measurements in LINAC and FEL applications.

INTRODUCTION

In this paper, we discuss the general application of using these transversal filters for longitudinal position and phase detection in comparison to other potential schemes, followed by a brief discussion of why increasing the frequency could potentially increase the resolution, we then move on to details regarding the design of the filter and discussion of simulated vs. Measurement results. We finally discuss a demo phase detection system we simulated and have preliminarily built and close with conclusions and potential follow on work.

Application

Techniques to measure time-of-arrival or relative phase of a particle bunch are fundamental diagnostics. A bunch can be detected from the signals it generates in pick-up devices, though direct measurements in the time domain can be limited in time resolution due to the difficultly of processing very wideband signals. Some techniques use the bunch passing to resonate a high-frequency resonator as part of the beam vacuum structure, or an external resonator driven from a wideband BPM. This resonator can be a high frequency (GHz), and a phase detection technique can give high resolution in the measurement of the arrival phase. These external resonator techniques [2], [3] require adequate separation of bunches so that the excitation can decay away before the next measurement (a high-Q resonator also offers a narrower measurement bandwidth which can help improve resolution). Another approach samples the beam signals in an electro-optic sampler, which allows very high-resolution time measurements [4], [5]. However this approach is limited to sampling rates of the sampling mode-locked laser, which is typically in the 100 MHz range.

For measurements of closely spaced bunches, these resonator or electro-optic techniques are not useful (for example in bunch-by-bunch longitudinal feedback systems sampling at 500 MHz rates). For these measurement needs, a technique using short periodic coupled microwave circuits was developed [6]. The heart of this technique is a microwave circuit with a sin(x)/x frequency response, so that in the time domain the excited signal has a rect(t) envelope, and ends cleanly after a few cycles of a defined frequency. Systems of this sort have been developed at 1 - 3 GHz in several applications with resolutions of 160 - 200 fs [1]. This paper extends the technique to 11.424 GHz, and potentially improves the measurement resolution by a factor of 4.

Higher Resolution

As timing requirements become more and more stringent for various accelerator facilities, the resolution requirements for timing detection systems continue to increase. It follows logically that to detect finer and finer time scales (sub-ps), the bandwidths and frequencies of the detection electronics need to increase.

The idea for extending this technique to higher frequencies comes from the fact that if we do phase comparisons at X-Band instead of S-Band, we should see a four times increase in phase sensitivity by comparing to a frequency 4 times previous. In the case of the PEP-II longitudinal feedback system receiver noise analysis shows an effective resolution of 200 fs at 2856 MHz [6]. Extrapolation to 11.424 GHz could imply resolutions on the order of 50 fs.

In the real world, things simply don't scale quite so easily, so the authors set out to begin work on an actual demonstration system which could potentially show the aforementioned resolutions. The first step in the process is to design the transversal filter. At this stage, we are still working on the estimation of the actual resolution.

TRANSVERSAL FILTER DESIGN

General Considerations

The basic structure of this filter is that of microwave couplers connected together by quarter wave transmission

*Work supported by Department of Energy contract DE–AC03–76SF00515 and the US-Japan High Luminosity Collaboration

STABLE TRANSMISSION OF RADIO FREQUENCY SIGNALS ON FIBER LINKS USING INTERFEROMETRIC DELAY SENSING*

R. Wilcox, J. M. Byrd, L. R. Doolittle, G. Huang#, J. W. Staples,
Lawrence Berkeley National Laboratory, One Cyclotron Road, Berkeley, CA 94720, USA

Abstract

We demonstrate distribution of a 2850 MHz radio frequency signal over stabilized optical fiber links. For a 2.2 km link we measure an RMS drift of 19.4 fs over 60 hours and for a 200 m link an RMS drift of 8.4 fs over 20 hours. RF signals are transmitted as amplitude modulation on a continuous optical carrier. Variations in the delay length are sensed using heterodyne interferometry and used to correct the RF phase. The system uses standard fiber telecommunications components.

INTRODUCTION

The next generation of accelerator-driven light sources will produce sub-100 fs high brightness x-ray pulses [1]. Pump-probe experiments at these facilities require synchronization of pulsed lasers and RF accelerating fields on sub-100 fs time scales over distances of a few hundred meters to several kilometers. Several approaches have been implemented to send stable signals over fiber optics, with average uncertainties of a few hundred femtoseconds to under 10 fs[2, 3, 4, 5, 6].

We describe a system for stable radio frequency distribution which has demonstrated less than 20 fs RMS jitter and drift over 2.2 km of optical fiber for 60 hours, and less than 10 fs over a 200 m fiber, using common fiber telecommunications components and microwave electronics

The system is easily manufacturable and low cost. It is straightforward to expand to many channels, because all delay control is done electronically in the receiver rather than by mechanical delays at the transmitter. Eliminating commonly-used mechanical delays also improves reliability and provides an arbitrarily large delay correction range, limited only by software. Because delay sensing is done using a continuous optical carrier, rapid delay changes beyond the control bandwidth are tracked continuously without jumping fringes. Standard fiber is used, requiring no dispersion compensation. Signal processing in the receiver is done digitally, so all key parameters are inherently controllable. Any frequency or combination of frequencies can be transmitted, in contrast to a fixed set of harmonics available in pulsed schemes.

A schematic diagram of a single-channel RF transmission and delay stabilization link is shown in Fig. 1 (a dual-channel variant is shown in Fig. 2). In our scheme, the optical phase delay through a fiber is precisely measured using a heterodyne interferometer. This measurement is used to correct the phase error of an RF signal which is transmitted on that fiber. We can derive simplified equations for propagation of optical and RF signals through the link, assuming that the small and constant delays within the temperature controlled boxes are zero.

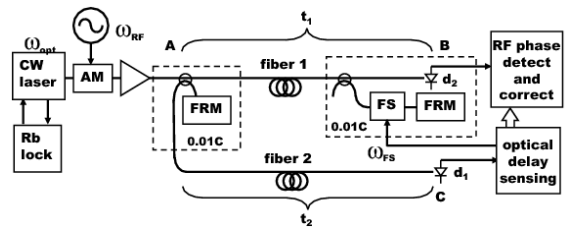

Figure 1: Schematic layout of a single channel RF transmission over an optical link. RF frequency is 2850 MHz. AM: Amplitude modulator; FRM: Faraday rotator mirror; FS: optical frequency shifter. Dotted rectangles indicate components temperature controlled to ±0.01° C.

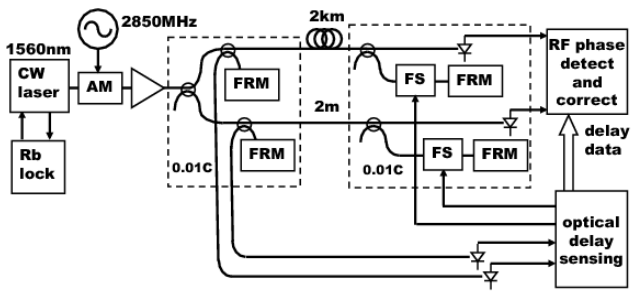

Figure 2: Dual channel RF transmission experiment. RF frequency is 2850 MHz.

To understand the operation of the interferometer, consider an optical wave starting at A and propagating through fiber 1 with delay t_1. At B, it is shifted in frequency by ω_{FS} by the optical frequency shifter (FS), retroreflected by the Faraday rotator mirror (FRM) and shifted in frequency again. It goes back through fiber 1 with delay t_1 to A, through a directional coupler, and through fiber 2 with delay t_2 to C. This is the "long" path. A second path through the interferometer is from A to the Faraday rotator mirror in the box at A, back through the directional coupler, and through fiber 2 to C. This is the "short" path. These two waves can be represented by their electric fields at C, which contain information as to the phase shifts each has encountered along its path. The fields can be expressed as

$$E_{long} = \cos(\omega_{op}((t - t_1 - t_1 - t_2) + 2\omega_{FS}(t - t_1 - t_2) + \phi_{FS})) \quad (1)$$

$$E_{short} = \cos(\omega_{op}((t - t_2)) \quad (2)$$

*Work supported by the U.S. Department of Energy under Contract No. DE-AC02-05CH11231
#ghuang@lbl.gov

SIGNAL PROCESSING FOR HIGH PRECISION PHASE MEASUREMENTS*

G. Huang#, L.R. Doolittle, J. W. Staples, R. Wilcox, J.M. Byrd,
LBNL, Berkeley, CA 94720, U.S.A.

Abstract

High precision phase measurement is important for many areas of accelerator operation. In a heterodyne digital receiver, one source of phase error is the thermal variation of the input stage. We have developed a technique to calibrate this drift. A CW calibration signal is sent through the same components together with the RF signal to measure and compensate the component drift. At intermediate frequency (IF), we use FPGA based digital signal processing to measure and reconstruct the RF signal after applying appropriate correction. Using this technique, we can measure the phase of a 2856 MHz signal with an accuracy of 15 milli-degrees. We describe how this approach is applied to the femtosecond timing distribution system.

INTRODUCTION

We developed a high precision phase measurement technique by using a live calibration signal to compensate for the thermal effect on the input stage of heterodyne receiver. This technique can be applied in a timing system, a low-level RF controller, and potentially other accelerator subsystems. We used this technique in a femto-second timing distribution system and achieved ~20 fs timing jitter and drift between two RF receivers[1].

A simplified block diagram of the femtosecond timing distribution system is given in Figure 1.

An RF signal is distributed as a phase reference over the fiber link. At each end station, a receiver reconstructs the RF signal and maintains the jitter between two end stations at the tens-of-fs level.

At the transmitter side, we amplitude modulate the RF source onto the carrier light, which is from a CW laser in our case. The modulated light is transmitted through a single-mode fiber link to the end station. The phase delay variation of the signal on the fiber is measured by a frequency shifted Michelson interferometer.

At the receiver side, the RF signal is detected by a photodiode. As soon as the RF signal is peeled off from the light and enters components, including cables, mixers, etc., the thermal variation effect becomes significant.

We measure the RF signal phase by downconverting it to IF, then digitize the IF signal, and process it with an FPGA based signal process board. The LLRF4 board we are using was developed for the SNS low level RF system[2]. We describe the signal processing for the phase measurement in this paper.

A CW double sideband suppressed carrier (DSB-SC) signal is added onto the RF signal as a common mode

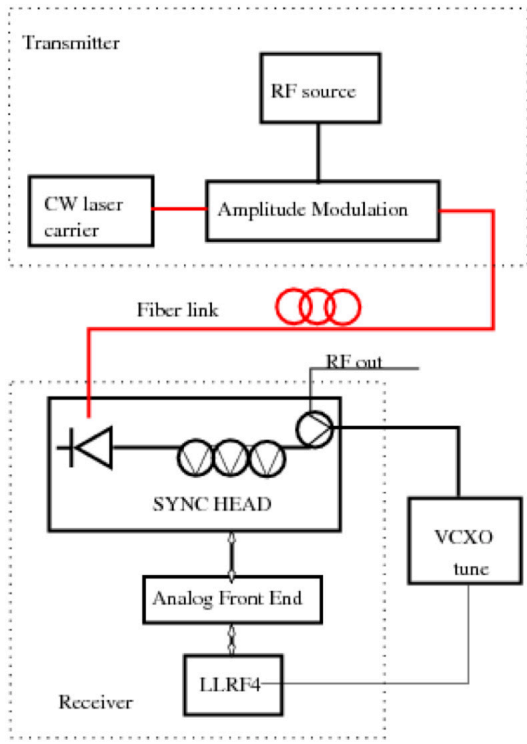

Figure 1: Simplified block diagram of the timing distribution system.

among both channels; we call it the calibration signal. The cable from the photodiode to the combiner is not included in the calibrated path, so that part needs to be temperature stabilized.

Physically, we split our receiver into a sync head, close to the device under control, and a stabilizer chassis, in a rack. The variation of the cable between them can be calibrated out. In the stabilizer chassis, an analog front end circuit downconverts the RF signal and upconverts the calibration signal. There is another bandpass filter on the LLRF4 board in front of the fast ADC.

After the signal is digitized, we measure the phase of each spectrum line in the signal and calculate the corrected RF phase accordingly.

We set up a simplified experiment to evaluate the out-of-loop error of our phase measurement, and the result was 15 mdeg at a 250 kHz sample rate.

ANALOG FRONT END CIRCUITS

We measure the phase difference between two signals: reference (REF) and signal (SIG).

THE LCLS TIMNG EVENT SYSTEM*

J. Dusatko#, S. Allison, M. Browne, P. Krejcik,
SLAC National Accelerator Laboratory, Menlo Park, CA 94025 U.S.A.

Abstract

The Linac Coherent Light Source requires precision timing trigger signals for various accelerator diagnostics and controls at SLAC-NAL. A new timing system has been developed that meets these requirements. This system is based on COTS hardware with a mixture of custom-designed units. An added challenge has been the requirement that the LCLS Timing System must co-exist and "know" about the existing SLC Timing System. This paper describes the architecture, construction and performance of the LCLS timing event system.

INTRODUCTON

The Linac Coherent Light Source (LCLS) at the SLAC National Accelerator Laboratory is a fourth generation X-ray light source. It uses the last 1/3rd of the SLAC Linac to create 4.6 to 13.6 GeV, electron bunches at a nominal charge of 0.05 to 1.0 nC which are sent into a single-pass permanent magnet undulator FEL. Through the Self-Amplified Spontaneous Emission (SASE) process, the undulator produces tuneable 1.5 to 15 Angstrom hard X-rays. A precision timing system is required to coordinate the acceleration process, as well as the triggering of diagnostics to measure beam performance. In addition, experimental data acquisition systems require precision timing reference and triggers to properly coordinate their measurements in coincidence with the LCLS beam.

The comprehensive LCLS Timing System consists of three levels of timing and synchronization, correlating to three different, but interlinked timing subsystems [1]. The first is a precision RF phase reference generation and distribution system needed to drive the injector gun and acceleration klystrons as well as the gun laser system and keep the phase within few fractions of a degree of S-band. The second is an ultra-stable timing phase reference distribution system that is used to synchronize the LCLS electron beam with experiment pump-probe laser systems to a level of 10fs at the photon end of the machine [2]. The third is the timing trigger generation and distribution system which produces precision timed triggers for use by acceleration, diagnostic and experimental DAQ subsystems. This has been designated the Timing Event System to distinguish it from the other two timing subsystems, and is the focus of this paper.

SYSTEM OVERVIEW AND DESIGN

The Timing Event System was developed to meet the requirements of the LCLS [3]; table 1 lists these requirements. It should be noted that the original trigger jitter requirement was specified as 2ps rms. This requirement was driven by the bunch length measurement. The requirement was later relaxed to the 10-ps value after it was determined that level of trigger jitter was not needed and would require a larger effort in the system design to achieve.

Table 1: LCLS Timing Trigger System Requirements

Requirement	Value
Maximum trigger rate	360 Hz
Clock frequency	119 MHz
Clock Precision	20 ps
Coarse step size	8.4 ns ± 20 ps
Delay range	>1 sec
Fine step size	20 ps
Maximum timing jitter (w.r.t. clock)	10 ps rms
Differential error, location to location	8 ns
Long term stability	20 ps

The previous generation SLAC Linac timing trigger system is CAMAC based and developed in the 1980s for the Stanford Linear Collider (SLC) [4]. This system had served the machine well for many years, but was not extensible for LCLS from a requirements, HW obsolescence and SW development point of view. It was not practical to replace the entire SLC timing system (where existing system requirements were sufficient) for LCLS from a cost and retrofitting effort standpoint. Thus, the LCLS Timing Event System had to be layered on top of and function alongside the SLC Timing System; at least for the initial running of LCLS. Because of this, certain architectural tradeoffs were made and the LCLS event timing system was slaved to the SLC system, receiving reference and synchronization signals from it, which are ultimately used to form the LCLS timing triggers.

During the design phase of the LCLS Timing System, several timing trigger solutions were considered including COTS (Commercial Off The Shelf) units. COTS was emphasized as a implementation solution for LCLS controls as a way of cost savings by leveraging industrial solutions that could meet system requirements. An accelerator timing component supplier, MicroResearch Finland (MRF) [5], was identified and selected. MRF had developed the Event System, originally for the Swiss Light Source and later commercialized it. The MRF Event

*Work supported by U.S. Department of Energy under Contract Nos. DE-AC02-06CH11357 and DE-AC02-76SF00515.
#jedu@slac.stanford.edu

THE LCLS UNDULATOR BEAM LOSS MONITOR READOUT SYSTEM*

J. Dusatko#, M. Browne, A. S. Fisher, D. Kotturi, S. Norum, J. Olsen
SLAC National Accelerator Laboratory, Menlo Park, CA 94025, U.S.A.

Abstract

The LCLS Undulator Beam Loss Monitor System is required to detect any loss radiation seen by the FEL undulators. The undulator segments consist of permanent magnets which are very sensitive to radiation damage. The operational goal is to keep demagnetization below 0.01% over the life of the LCLS. The BLM system is designed to help achieve this goal by detecting any loss radiation and indicating a fault condition if the radiation level exceeds a certain threshold. Upon reception of this fault signal, the LCLS Machine Protection System takes appropriate action by either halting or rate limiting the beam. The BLM detector consists of a PMT coupled to a Cherenkov radiator located near the upstream end of each undulator segment. There are 33 BLMs in the system, one per segment. The detectors are read out by a dedicated system that is integrated directly into the LCLS MPS. The BLM readout system provides monitoring of radiation levels, computation of integrated doses, detection of radiation excursions beyond set thresholds, fault reporting and control of BLM system functions. This paper describes the design, construction and operational performance of the BLM readout system.

INTRODUCTION

SLAC National Accelerator Laboratory's Linac Coherent Light Source (LCLS) is a Free Electron Laser which produces tuneable hard X-Rays in the 1.5 to 15 Angstrom range. The X-rays are produced by passing 4.6 to 13.6 GeV, 0.05 to 1.0 nC single bunches of electrons from the last third of the SLAC Linac through a newly constructed undulator line. The undulator line consists of 33, 3.42 meter long permanent magnet segments. Each segment contains 226 NdFeB magnets with vanadium permendur poles arranged with 30mm period [1]. These materials can be demagnetized by radiation induced by beam loss. The Beam Loss Monitor (BLM) system has been developed based on system requirements [2] to detect this loss before it reaches an appreciable level.

The BLM system was developed in collaboration with Argonne National Laboratory. ANL had the responsibility of developing the BLM detectors and detector signal conditioning electronics. SLAC had the responsibility for developing the readout electronics system, integration into the LCLS Machine Protection System, and system commissioning.

The system design requires 33 BLM detectors, one for each undulator segment. Due to initial budget limitations, only five ANL BLM detectors and associated electronics were produced. As a interim solution, re-purposed PEP-II BLM detectors, available after the shutdown of the B-factory, were installed on the remaining 28 undulators plus some additional locations.

BEAM LOSS DETECTORS

The ANL BLM detectors consist of a fused silica Cherenkov radiator optically mated to a PMT [3]. The complex geometry of the radiator was chosen in order to cover the undulator magnets, while propagating the resultant output light to a single PMT. Signal conditioning, high voltage and a test signal are provided by a local BLM Interface Module (BLM-IM) on a per detector basis. The detectors are mounted at the upstream end of each undulator segment, with the companion BLM-IM mounted nearby on the undulator girder in the undulator hall tunnel. The BLM-IM contains an adjustable high-voltage power supply with a range of 0…-1KV, as well as a charge-sensitive preamp which converts the PMT charge pulse into a time-shaped (tc=50μs) voltage signal with a maximum output voltage of -1.5V in 50 ohms. Additionally, the BLM-IM contains an LED pulse generator whose 600ns light signal is optically connected to the detector head. This allows the detector and electronics chain to be stimulated with a test pulse during non-beam time as a built-in self check.

The PEP-II detectors [4] are similar in their materials (quartz Cherenkov radiator mated to a PMT) but have a different geometry: cylindrical radiator mounted in a cylindrical housing. The housing contains a lead shield to attenuate the storage ring synchrotron radiation and enhance beam-loss showers, and also the dynode resistive divider chain. The PEP-II detectors are mounted near the original locations of the ANL units, but a 10cm away due to their incompatible geometry. High voltage is supplied to a string of PEP-II tubes from one of two supplies, serving approximately 15 tubes each. The raw charge pulse from the PMTs is sent directly, following a 1dB attenuator, to the readout system. Thus the readout system has to accommodate mixed-mode detector signals. Note that the PEP-II units have no provision for an LED test signal input. In addition to the undulator, additional PEP-II BLM detectors were installed near upstream collimators and the Undulator tune-up dump in the Linac-To-Undulator beamline.

SYSTEM OVERVIEW AND DESIGN

The original system design accommodated the ANL detector systems exclusively. This design was modified in

*Work supported by U.S. Department of Energy under Contract Nos. DE-AC02-06CH11357 and DE-AC02-76SF00515.
#jedu@slac.stanford.edu

MICROWAVE LINK PHASE COMPENSATION FOR LONGITUDINAL STOCHASTIC COOLING IN RHIC*

K. Mernick#, M. Blaskiewicz, J.M. Brennan, B. Johnson, F. Severino, BNL, Upton, NY 11973, U.S.A.

Abstract

A new microwave link has been developed for the longitudinal stochastic cooling system, replacing the fiber optic link used for the transmission of the beam signal from the pickup to the kicker. This new link reduces the pickup to kicker delay from 2/3 of a turn to 1/6 of a turn, which greatly improves the phase margin of the system and allows operation at higher frequencies. The microwave link also introduces phase modulation on the transmitted signal due to variations in the local oscillators and time of flight. A phase locked loop tracks a pilot tone generated at a frequency outside the bandwidth of the cooling system. Information from the PLL is used to calculate real-time corrections to the cooling system at a 10 kHz rate. The design of the pilot tone system is discussed and results from commissioning are described.

INTRODUCTION

In the Relativistic Heavy Ion Collider (RHIC), intra-beam scattering (IBS) is a primary cause of emittance growth of the gold beam. The stochastic cooling system is a wide band feedback loop designed to combat IBS and reduce the emittance of the beam.

A longitudinal stochastic cooling system was commissioned in the Yellow ring at RHIC in 2007 [1] and used during the FY07 and FY08 runs. The pickup for this system was in the 12 o'clock straight section, and the kicker was in the 4 o'clock straight section. As the beam travelled counter-clockwise, the pickup signal was transmitted on an analog fiber optic link through the tunnel. The pickup to kicker delay was 2/3 of a turn.

Prior to the FY09 run, a new longitudinal system was installed in the Blue ring. This system had the pickup located in the 2 o'clock region and the kicker at 4 o'clock. A microwave link connected them, with the transmitter installed on the berm above the beamline and the receiver located on the roof of the RF service building. The Blue beam travels clockwise, so the delay from pickup to kicker is 1/6 of a turn. The FY09 run was dedicated to polarized protons, so while important R&D work was completed, the new longitudinal cooling system was not made operational.

During the 2009 summer shutdown, the existing longitudinal cooling system in the Yellow ring was removed, and an upgraded system using the microwave link was reinstalled. The pickup was now located in the 2 o'clock straight section, with the kicker in the 12 o'clock region. Systems for vertical cooling were also installed in both rings. The vertical cooling systems use fiber optic links to transmit the signal from the pickups to the kickers.

The Blue and Yellow longitudinal stochastic cooling systems were both successfully commissioned during the FY10 100 GeV/nucleon gold run. Blue cooling was used in routine operation. Yellow cooling was successfully tested, but a series of mechanical problems with the kicker prevented routine operation. A schematic representation of the locations of the system components, along with the links between them, is shown in figure 1.

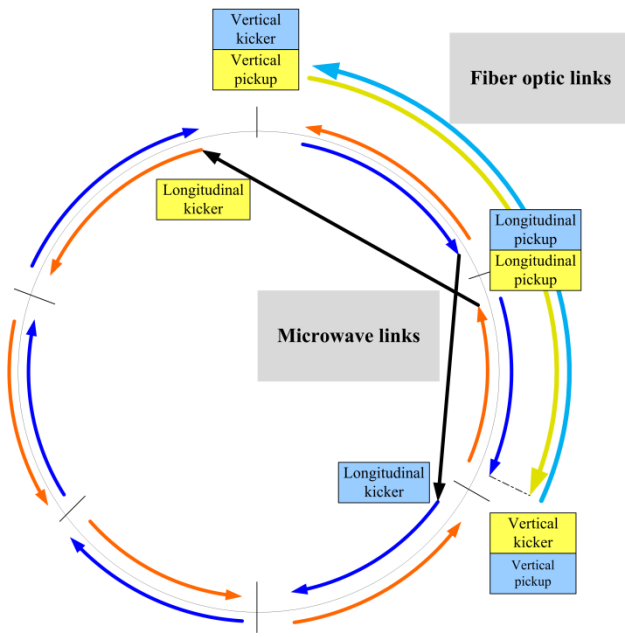

Figure 1: Locations of pickups and kickers (blue and yellow boxes), longitudinal system microwave links (black arrows), and vertical system fiber optic links (light blue and yellow arrows). The dark blue and orange arrows indicate the direction the beams travel.

EFFECT OF PICKUP TO KICKER DELAY

The longitudinal cooling system uses a one-turn delay notch filter to determine the kick necessary for cooling. The signal from the previous turn is subtracted from the current signal. This filter has the transfer function $G_1(f) = [1 - \exp(2\pi i \Delta f T_0)]\exp(2\pi i \Delta f T_d)$, where T_0 is the revolution period, T_d is the pickup to kicker delay, and Δf is the difference between the drive frequency and the nearest revolution line.

With the 2/3 of a turn delay of the fiber optic link and the one-turn filter, the cooling force has the correct sign for $|\Delta f| \leq 16.5$ kHz [2]. For gold beam with γ = 107 and 4 MV on the RF storage cavities at h = 2520 the

*Work performed by employees of Brookhaven Science Associates, LLC under Contract No. DE-AC02-98CH10886 with the U.S. Department of Energy.
#kmernick@bnl.gov

BUNCH ARRIVAL MONITOR AT FERMI@ELETTRA

L. Pavlovic, University of Ljubljana, Ljubljana, Slovenia
A. O. Borga, M. Ferianis, M. Predonzani, F. Rossi, Sincrotrone Trieste ELETTRA, Trieste, Italy

Abstract

The bunch arrival monitor (BAM) for the IV generation synchrotron light source FERMI@Elettra is presented. It is based on an original idea developed at FLASH/DESY, specifically designed and built in-house for FERMI@Elettra. Each BAM station consists of a front-end module, located in the machine tunnel, and of a back-end unit located in the service area. It makes use of the pulsed optical phase reference along with the stabilized fiber link. The front end converts the bunch arrival times into amplitude variations of the optical phase reference pulses distributed over the link. The analogue signal is generated at the e-beam's passage in a broadband pick-up and is sent to the modulation input of an electro-optical modulator (EOM). The back end acquires, synchronously, the amplitude modulated pulses, using a broadband photodiode and a fast analog-to-digital converter. The digitized data is sent to the machine control system for further processing. The dedicated analog-to-digital conversion, processing and communication board, part of the monitor back end, is also briefly described.

INTRODUCTION

New 4th Generation Light Sources (4GLS) currently in operation, construction or design at several National Laboratories are posing demanding requirements on the associated Timing and Synchronization (T&S) systems, identified as femto-second (fsec) T&S systems. 4GLS are typically Free Electron Lasers (FEL) driven by single pass Linear Accelerators (LINAC). Such demanding requirements on jitter (<10fsec$_{RMS}$), and drift, originate from the adopted scheme for the generation of the electron beam and the FEL radiation.

The typical bunch length (τ_B<50fsec$_{FWHM}$), achievable in single pass accelerators thanks to the beam longitudinal manipulation techniques, the required beam quality (6-D emittance) and the radiation generation (seeding) and exploitation (time resolved / pump-probe experiments) schemes call for an ultimate jitter of <10fsec$_{RMS}$. This ultra-low jitter value is typically required either between the electron bunch and the seed laser pulse or between the FEL pulse and the User laser pulse. To achieve this goal, the whole accelerator components need to share a Phase Reference with <10fsec$_{RMS}$ jitter and drift.

BUNCH ARRIVAL MONITOR

In 4GLS, the time position of the bunch is identified by the combination of the timing pulse (as a reference) and the slope of the electrical signal produced by the bunch passage through the pick up mounted on the beam line. This scheme was first proposed by the Desy group [1]. The pick up signal is fed to an Electro-Optical Modulator (Mach-Zehnder modulator - MZM) and modulates the optical pulses of the optical master oscillator (OMO) as a reference. The timing jitter of the bunch shifts the temporal position of the slope and thus amplitude modulates the optical pulses. Therefore the amplitude variations correlate to the timing jitter of bunches. The BAM system consists of two main parts, the front end installed in the tunnel close to the beam pick up and the back end installed in the service area for the readout of the modulated pulses and further processing.

BAM Front End

The BAM front end does the timing comparison between the reference's optical pulses and the electron bunches in the accelerator. Due to the very high resolution requirement, the BAM front end is mainly an optical system. The time comparison is done by a MZM, which converts the time difference into an amplitude difference. The modulated optical pulses from the MZM are fed to the photodiode in the BAM back end. The front end is shown in Figure 1.

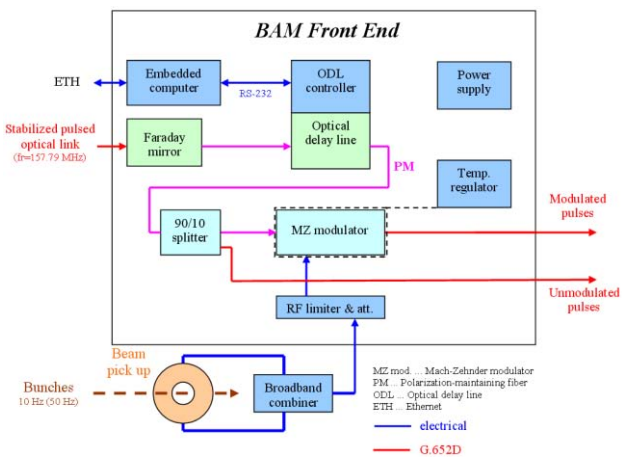

Figure 1: Block diagram of the BAM front end.

The front end has two inputs, the optical pulses from the OMO, distributed via a stabilized link, and the electrical signal from the pick up. The Faraday mirror is part of the stabilized link and needs to be close to the MZM, since short pulses provide better timing resolution. The optical delay line compensates slow drifts of the link and enables the calibration of the system at the beginning of the operation. The splitter passes 90% of the optical power to the MZM, while the 10% is left un-modulated for the ADC clock extraction at the back end. The polarization from the stabilized link needs to be controlled. Optionally, there is a need for a limiter after the pick up for the protection of the MZM's RF input. Since the MZM's transfer characteristic is temperature dependent, the MZM is temperature stabilized by a

THE COPPER FREE FERMI TIMING SYSTEM: IMPLEMENTATION AND RESULTS

M. Ferianis, A. Bucconi, G. Gaio, G. Mian, M. Predonzani, F. Rossi
Sincrotrone Trieste S.C.p.A. ELETTRA, Trieste, Italy

Abstract

With respect to its timing system, FERMI@Elettra is the first "copper free" FEL facility. Having been conceived during the FERMI Technical Optimization Study (TOS), the FERMI timing system is based on the original ideas developed at MIT/DESY and at LBNL, which have been demonstrated also with the significant support of Sincrotrone Trieste. Since then, at FERMI, a young though strong team has been growing in time and is now running the system on the facility. As for the trigger distribution we have adopted the COTS solution by Micro-Research Finland Oy, the main original contribution to the Community is found in the phase reference generation and distribution. The huge engineering effort afforded by the FERMI@Elettra project in the last twelve months has produced a unique system that is now ready to assure a stable seeded FEL operation. The current system implementation is presented here along with the obtained performances, at the few tens of femto-second (fs) level (jitter and drifts).

INTRODUCTION

FERMI@Elettra is the fourth generation synchrotron light source currently under commissioning in Trieste [1,2], Italy. Being based on a seeded Free Electron Laser (FEL), it requires state of art timing and synchronization.

Given the electron bunch length and seed laser pulse duration, both in the tens of fs range, the specifications of the timing system are very demanding as the whole machine stability requirements are. When the FERMI@Elettra project officially started, back in 2006, there were laboratory experiments on optical timing systems showing possible solutions to meet these challenging small values, jitter having been addressed first. It was common believe that only newly developed optical techniques could meet the target jitter (<<100fs).

Collaborations were started in 2006 and 2008, with the Research Laboratory of Electronic (RLE) at MIT [3], Cambridge MA-USA, and with the Center for Beam Physics at the LBNL, Berkeley CA-USA, respectively.

Furthermore, a European expert group on fs timing systems [5] also grew during the FP6 EUROFEL Design Study [6], coordinated by DESY. In this joint effort, 16 European organisations developed some of the key technologies required for the design and construction of next generation free electron laser (FEL) sources.

After having analyzed the timing system specifications for a single bunch FEL, the *hybrid* timing system has been proposed for FERMI@elettra, adopting both the *pulsed* and *continuous wave* (CW) optical timing [2].

The rationale for this original approach is in that the synchronization schemes, adopted to phase lock different systems, are some based on an optical pulsed phase reference (like an optical cross-correlator or an electro-optical bunch arrival monitor) and some based on a CW one (like the low level radio frequency system). A fs jitter measurement laboratory has been also set-up as well as demonstrators of both pulsed and CW systems.

THE FERMI TIMING SYSTEM

In figure 1, the basic block diagram of the FERMI@elettra timing system is presented.

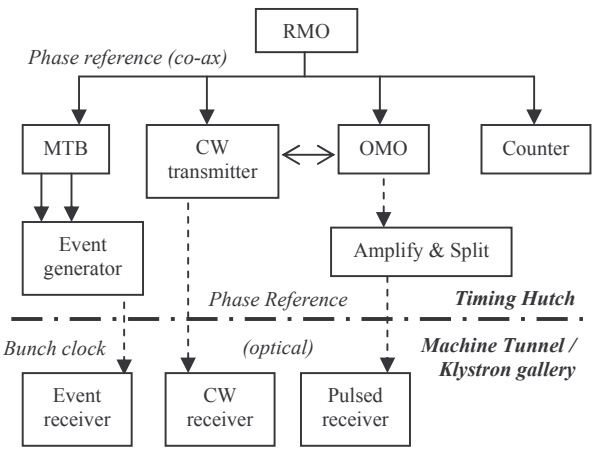

Figure 1: basic block diagram of the FERMI timing system. Solid lines indicate coaxial cables; dashed lines, optical fibres.

Primarily, the FERMI@elettra timing system generates and distributes throughout the facility the phase reference signal which all synchronized sub-systems (*timing clients*) are locked to. The frequency of the phase reference master oscillator is the same of the S-band accelerating structures in the linear accelerator (Linac). The phase reference information is transferred to the *clients*, either using an optical pulse train, generated in the Optical Master Oscillator (OMO) or a CW signal encoded onto an optical carrier (CW optical transmitter), actively stabilized fibre optics links being used for both systems.

The FERMI@elettra timing system also generates the bunch clock (up to 50Hz) and the laser *coincidence* clock (f_{COIN}=S-band÷38=78.895MHz) which is used to align the pulses from the different laser oscillators in the facility. The master time base (MTB) is implementing this task.

The bunch clock is then distributed throughout the whole facility, over fibre optics cables, by means of the *Event system* of Micro Research Finland Oy [7].

As a result, both the phase reference and the auxiliary signals are distributed using fibre optics (*copper free* timing system) which to our knowledge is a world premiere for synchrotron radiation facilities.

SIGNAL DELAY MEASUREMENT METHOD FOR TIMING SYSTEMS

M. Bousonville*, GSI, Darmstadt, Germany
J. Rausch, Technische Universität Darmstadt, Germany

Abstract

In this paper, a method for measuring the absolute signal delays of active optical transmission lines will be presented. This measurement method is an essential part of the timing system for FAIR (Facility for Antiproton and Ion Research).

To prevent interference of the timing signals whose delays are to be measured with the measurement signal sequence, the latter is transmitted on a separate optical carrier in the same fibre. By using a wavelength selective mirror at the end of the transmission line, the optical measurement signals are reflected and led back to the measurement unit. The measurement sequence consists of a number of sinusoidal signals with different frequencies that are modulated one by one on the optical carrier. For each frequency a phase comparison of the outgoing and returning signal is performed. In the last step, the absolute delay is calculated from the obtained phase values by using an algorithm.

It will be shown that this method enables cost efficient delay measurements with an accuracy of better than 100 fs.

INTRODUCTION

Different methods are used to provide phase stable reference signals e.g. for cavity synchronisation. All methods deliver one or more reference signals [1-12], mostly sinusoidal clock signals, to several points of the facility. To transmit the reference signal, standard single mode fibres (SMFs) are used. The transmission process should add as little as possible disturbances, like noise and variation of the signal delay, to the reference signals. Noise leads to fast phase fluctuations (jitter) and the variation of the signal delay causes slow phase shifts (drift) [13]. Many timing systems measure the delay changes and compensate them with phase shifter or delay devices, either optical [6-9] or electrical [10-12]. A common basic principle [6-12] is sketched in Fig. 1. For observation of the delay changes, a phase comparison of the outgoing and returning signal is performed.

A disadvantage of this functional principle is the high attenuation (about 15 dB [6], page 14), having effect on both the part of the signal that reaches the receiver (*Rx*) and the part of the signal that is reflected. Caused by the high attenuation, the signal power fed to the receivers is lower than in an optimal case [1], page 5. This results in a lower signal-to-noise ratio (SNR) and thus in more phase jitter. On the one hand, this affects the phase stability of the transmitted reference signal, on the other hand the phase comparison is less precise. The latter leads to disturbances while compensating the delay change in the fibre. These disturbances cause delay correction errors and therefore additional phase instabilities.

A further disadvantage is the fact that the signal for detection of the delay changes and the reference signal have the same frequency. Since the accuracy of the phase measurement, by approximation, is not depending on the frequency used, an accurate reading of the delay changes is more easily achieved with a higher frequency than with a lower one. Normally the frequencies of the reference signals are specified by other boundary conditions. Therefore within the basic principle of Fig. 1 it is not possible to increase the frequency to get a better delay observation.

DWDM

Relatively low frequencies (between 100 kHz and 200 MHz) are used in the FAIR timing system. Therefore the idea arose to determine the delay by other means. Using the *dense wavelength division multiplex* (DWDM) method, it is possible to transmit both signals on different optical carriers of different wavelengths over a shared fibre. In this way the two clock signals and the measurement signal can be sent independently of one another (Fig. 2).

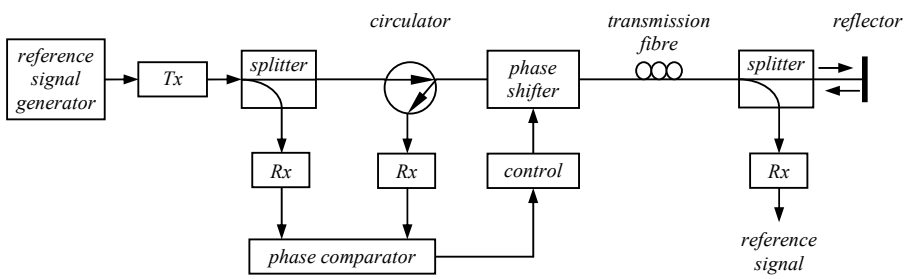

Figure 1: Basic principle of a frequently used timing system. High attenuation, reference signal = measurement signal.

*M.Bousonville@gsi.de

RELIABILITY TESTS OF THE LHC BEAM LOSS MONITORING FPGA FIRMWARE

C. F. Hajdu, B. Dehning, S. Jackson, C. Zamantzas, CERN, Geneva, Switzerland

Abstract

The LHC Beam Loss Monitoring (BLM) system is one of the most complex instrumentation systems deployed in the LHC. In addition to protecting the collider, the system also needs to provide a means of diagnosing machine faults and deliver a feedback of losses to the control room as well as to several systems for their setup and analysis. It has to transmit and process signals from almost 4'000 monitors, and has nearly 3 million configurable parameters.

In a system of such complexity, firmware reliability is a critical issue. The integrity of the signal chain of the LHC BLM system and its ability to correctly detect unwanted scenarios and thus provide the required protection level must be ensured. In order to analyze the reliability and functionality, an advanced verification environment has been developed to evaluate the performance and response of the FPGA-based data analysis firmware. This paper will report on the numerous tests that have been performed and on how the results are used to quantify the reliability of the system.

INTRODUCTION

The Beam Loss Monitoring system [1] is one of the most critical among the numerous systems installed for the protection of the LHC. It has to prevent quenches in the superconducting magnets and protect the machine components against damage. The system comprises nearly 4'000 detectors, ionisation chambers and secondary emission-based monitors, mounted onto the elements under supervision. The analogue output signal of the sensors is digitised by data acquisition cards [2], generally referred to as Current to Frequency Converter (CFC), installed in the tunnel. The data is then transmitted to the Threshold Comparators (TC) [3] via redundant broadband optical links. The TCs, installed in VME crates distributed in surface buildings around the LHC, collect and analyse the data. Their FPGA-based processing algorithm calculates integrals of the signals over different time windows, compares them to their respective abort thresholds and can trigger a beam abort as appropriate through the Combiner and Survey (CS) card installed in the same VME crate.

The integrity of the whole signal chain needs to be verified in order to ensure that the system provides the required level of protection. Firmware reliability in particular is a key issue. Due to the great complexity and sequential nature of the design, exhaustive testing – that is, verification by applying every possible sequence of input combinations to the design and checking its outputs – of the TC firmware is impractical [4]. Therefore, an effort has been made to lay the foundations of a comprehensive verification environment instead, implementing different approaches of verification, each of them focusing on different aspects of the system under test (see Fig. 1).

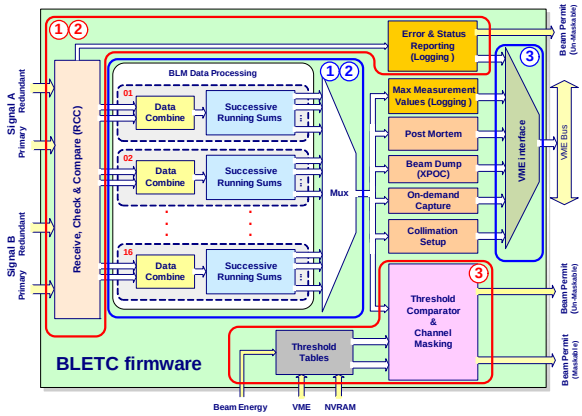

Figure 1: Block diagram showing the scope of the verification. Legend of the types of verification used: (1) Black box simulation, (2) Hardware-based approach, (3) Software-based approach.

Consequently, simulation testbenches, custom hardware and software suites have been designed and developed for the verification of critical blocks as well as to verify certain aspects of the behaviour of the installed system. The aim of this paper is to detail the implementation of these methods and the results obtained therewith.

SIMULATION

Functional simulation involves simulating the design description – in this case, in VHDL – to verify that the system meets the functional requirements stated in its

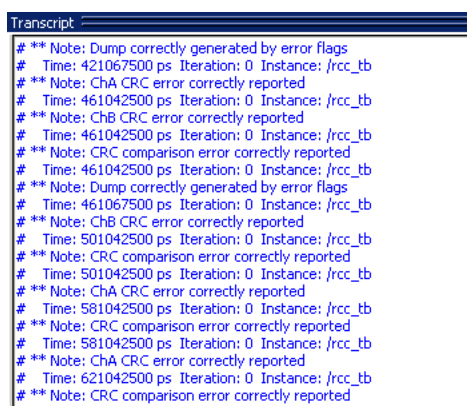

Figure 2: Excerpt of the output of the automatic checker for a test performed on the receiver part using ModelSim.

RESULTS OF BACKGROUND SUBTRACTION TECHNIQUES ON THE SPALLATION NEUTRON SOURCE BEAM LOSS MONITORS*

J. Pogge, S. Zhukov, SNS ORNL, Oak Ridge, TN 37831, U.S.A.

Abstract

Recent improvements to the Spallation Neutron Source (SNS) beam loss monitor (BLM) designs have been made with the goal of significantly reducing background noise. This paper outlines this effort and analyzes the results. The significance of this noise reduction is the ability to use the BLM sensors [1], [2] distributed throughout the SNS accelerator as a method to monitor activation of components as well as monitor beam losses.

OVERVIEW

Any study of the effects and causes of system noise must contain some identification of the nature of the system noise and its sources. We will identify the sources of noise in the BLM circuits and show the results of reduction techniques used to mitigate these noise sources.

Identifying Noise Sources

The SNS BLM sensors are primarily high-gain transimpedence amplifiers that collect the change in charge when particles or energy are incident on the sensor. The effects of noise associated directly with components used in high-gain transimpedence amplifiers are actually surprisingly low. The largest source of noise is induced currents and Electro Motive Interference (EMI) [3] on the long cables from the sensors located in the LINAC tunnel and the data acquisition system located in the instrument galleries. The distance between the sensors and the front end amplifier is large typically on the order of 100 meters. External influences such as electrical and electromagnetic sources make up the majority of the background noise seen at the front end amplifier (Fig. 1).

Design Approach

Having sufficiently determined the noise associated with the measurements, the BLM amplifier was designed to mitigate the bulk of the system noise in the design:

- Ultra low noise input bias current Op Amps were used in the transimpedence amplifier stage. A classic large-series resistor is used to ensure the voltage gain was low while the current gain was sufficiently large for the signal range.
- A second amplifier stage identical to the signal stage is attached to a second cable terminated in the LINAC tunnel and routed in juxtaposition to the signal cable.
- The signal and background input transimpedence amplifiers and the subsequent background subtraction stage have a bandwidth at least 4x the desired system bandwidth to decrease any phase error or effects in the signal subtraction.
- Post background subtraction low-pass filter is available, selected through software, to further smooth any noise effects present on the subtracted signal.

The resulting signal can be adjusted to not only remove a significant amount of EMI noise present on the signal wire, but also allows removal of the induced radio frequency (RF) pulse present on the signal and the subtraction cable. The resulting signal is a closer representation to actual loss of beam present during LINAC operations. This data is fed directly to the integrators used for the SNS Machine Protection System (MPS) [4] with no error caused by excess induction of non-loss noise sources. Additionally, the loss signal is available for digitization and analysis. Loss spectrum has been an interesting study to determine if the source of the losses can be identified, as has a study of methods to determine actual activation levels by monitoring the growth of non noise-related signals during periods of no beam or RF.

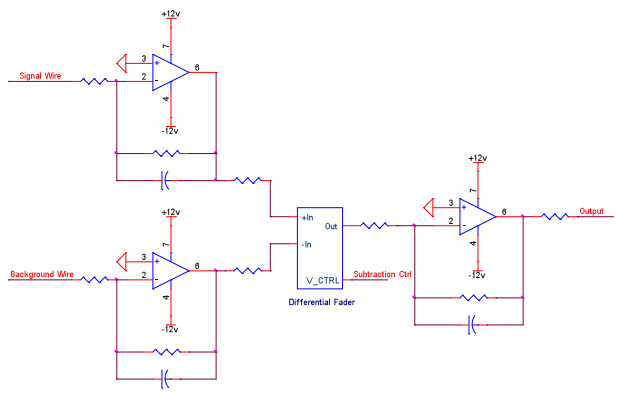

Figure 1: Front End Block diagram.

The new BLM amplifier module is a consolidation of four separate systems used on the current BLM design. This new circuit is a single-channel solution, including MPS, digital control and high-Voltage (HV) bias power supply. This new design helps to further reduce the noise associated with the Photo Multiplier Tube (PMT) and Ion Chamber BLM sensors by eliminating multiple sensors and allowing the digital, HV supply and amplifier to work

* ORNL/SNS is managed by UT-Battelle, LLC, for the U.S. Department of Energy under contract DE-AC05-00OR22725

MODELING THE OPTICAL COUPLING EFFICIENCY OF THE LINAC COHERENT LIGHT SOURCE BEAM LOSS MONITOR RADIATOR*

J. C. Dooling, W. Berg, and B.X. Yang, ANL, Argonne, IL 60439, USA
M. Santana Leitner, A. S. Fisher, and H.-D. Nuhn, SLAC NAL, Menlo Park, CA 94025, USA

Abstract

A large-solid-angle, Cherenkov detector beam loss monitor has been built and tested as part of the Linac Coherent Light Source machine protection system (MPS). The MPS is used to protect the undulator magnets by detecting high-energy electron beam loss. These electrons produce other forms of radiation that can lead to demagnetization of the undulator magnets. Cherenkov light is generated when primary electrons, lost from the beam, create a shower of secondary electrons that transit through the Cherenkov radiator medium. The radiator consists of an Al-coated plate of high-purity, fused-silica 12.77 cm wide, 6.29 cm high, and 0.64 cm thick, which is formed into a tuning fork geometry that envelopes the beam pipe preceding each undulator. The radiator transports Cherenkov photons via internal reflection through a tapered region and stem into the photocathode of a compact photomultiplier tube (PMT).

We calculate the optical efficiency of the radiator η_c, that is, the probability that a photon generated within the fused silica will reach the exit aperture adjacent to the PMT. A simple model based on line sources summed across image planes is compared for the case of normally incident electrons with a more detailed Monte Carlo random-walk simulation called RIBO[1]. Both analytical and numerical models show the efficiency to be relatively uniform over the full range of transverse locations in the radiator. This is encouraging for the MPS detection scheme, which seeks to protect the undulator magnets over their entire cross section. As we expect, both analyses show η_c to be a strong function of the surface reflectivity R_f; η_c ~0.0084 for R_f=0.95, but drops to 0.0033 for R_f=0.90.

INTRODUCTION

High-energy electrons lost from third- or fourth-generation light source beams can lead to the generation of star events, which are strongly correlated with the demagnetization of undulator magnets[2]. Cherenkov radiation provides a natural method to observe beam loss from these machines[3]. Cherenkov radiators fabricated from high-purity, fused-silica have several desirable characteristics for detection of high-energy electrons. First, they can withstand high levels of radiation without darkening or suffering degraded transmission[4]; second, they offer immunity to scintillation noise from lower-energy x-ray photons; third, Cherenkov radiation is produced at optical wavelengths that can be detected with high-gain photomultiplier tubes (PMTs) providing low electrical noise signals.

The Linac Coherent Light Source (LCLS) beam loss monitor (BLM) diagnostic for the free-electron laser (FEL) undulators is composed of a fused-silica radiator encased in an anodized aluminum housing. The BLM is part of the LCLS machine protection system; as such, the radiator seeks to cover a broad area of transverse space or large solid angle to fully monitor beam loss into the FEL magnets. The radiator is roughly in the shape of a “tuning fork” or “Y” where the re-entrant cutout of the fork is occupied by the electron beam vacuum vessel. The BLM is integrated with the beam finder wire diagnostic located just upstream of each undulator magnet. A cross section of the BLM is presented in Figure 1. The large parallel surfaces (z-planes) of the radiator are polished to optical grade flatness; whereas, the x- and y-planes edge surfaces are flame polished. The entire radiator is coated with a reflective layer of aluminum; the exceptions being the exit aperture facing the PMT detector and two small circular areas in the stem, one of which is used to introduce a ``heartbeat'' optical pulse.

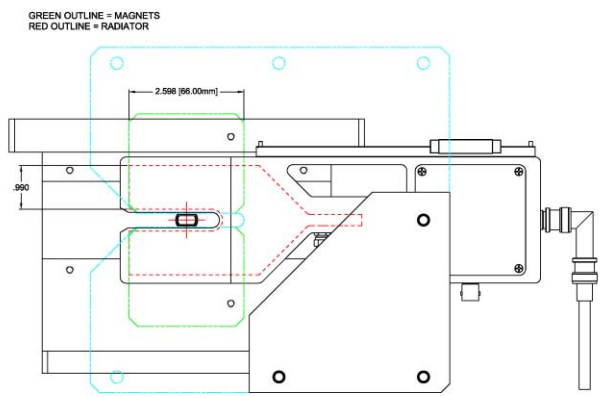

Figure 1: Cross sectional view of the beam loss monitor; view is looking upstream.

MODELING

The generation of photons from a super-luminal electron traversing a transparent medium of index of refraction n_r has been discussed in detail by a number of authors, for example[5,6].

*Work supported by the U.S. D.O.E. Office of Science, Office of Basic Energy Sciences, under contract numbers DE-AC02-06CH11357 and DE-AC02-76SF00515.

#dooling@aps.anl.gov

NEW ELECTRON BEAM DIAGNOSTICS IN THE FLASH DUMP LINE

N. Baboi*, D. Lipka, O. Hensler, R. Neumann, M. Schmitz, P. Smirnov, H. Tiessen, K. Wittenburg, DESY, Hamburg, Germany
A. Ignatenko#, DESY, Zeuthen, Germany

Abstract

Additional beam diagnostics has been installed in the dump line at FLASH in 2009. Its purpose is to prevent damage by long high current electron beam pulses, as happened in autumn 2008, when a vacuum leak occurred near the dump vacuum window. Beam position monitors (BPM), scintillator-based loss monitors and temperature sensors were installed so-far. Additional BPMs and loss monitors have meanwhile been installed. These include a magnetic coupled BPM placed after the vacuum window. Magnetic loops are used in order to prevent the influence of the ions on the pick-up signals. 4 ionization chambers, consisting of air-filled tubes, and 4 glass fibers have been installed parallel to the vacuum pipe, along the last 2 m of the beam pipe. Beam halo monitors were installed next to the magnetic BPM. These consist of 4 diamond and 4 sapphire sensors operating as solid state ionization chambers. The halo monitors are very sensitive to charged particles crossing the detectors. These additional diagnostic monitors have been commissioned in autumn 2009, when they have contributed to the successful run of long pulses with 3 to 9 mA current and up to 800 µs length. Their performance is summarized in this paper.

INTRODUCTION

FLASH (Free electron LASer in Hamburg) [1] is at the same time a user and a test facility. A laser light tuneable in the range 40 – 6.5 nm is produced for several user beam lines. During special studies periods, various experiments are scheduled, in order to make tests for various accelerator projects, in particular for the European XFEL (X-ray Free Electron Laser) [2] and the ILC [3] (International Linear Collider) study. These have similarities with FLASH, in particular the superconducting technology used for beam acceleration. Also, they all plan to use long bunch trains.

The long bunch trains at FLASH have to be safely sent into the dump at the end of the linac. Beam loss monitors (BLM) and charge monitors are primarily used for the machine protection. This paper shows the limitations of the dump diagnostics used so far, describes the modifications made and summarizes the results of the initial commissioning of the new devices.

The FLASH Facility

A schematic view of the FLASH linac is shown in Figure 1 as of September 2009. A photo-electric gun generates pulses of electron bunches with an energy of about 5 MeV. These are accelerated to up to 1 GeV by 6 accelerating cryo-modules, each containing 8 TESLA superconducting cavities. Two magnetic bunch compressors reduce the bunch length to less than 100 fs. A collimator section lowers the radiation losses in the undulators, by reducing the parasitic transported dark current. The beam properties are measured in two matching sections. While passing through the 30 m long undulators, the electron bunches produce FEL (Free Electron Laser) light through the SASE (Self-Amplified Spontaneous Emission) effect. The electrons are then sent to the beam dump, designed for about 100 kW power of a 2 GeV beam [4]. The FEL light goes to one of the user beam lines. A bypass line is used during test and commissioning periods in order to protect the undulators.

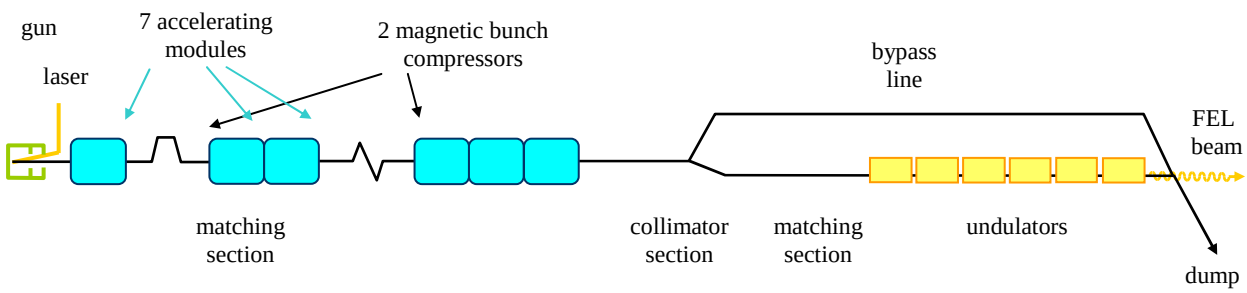

Figure 1 Schematic overview of FLASH (status 2009).

* nicoleta.baboi@desy.de
# On leave from NC PHEP BSU, Bogdanovich Str. 153, Minsk, Belarus

MULTI-CHANNEL MAGNET POWER-SUPPLY RAMP CONTROLLER FOR THE IUCEEM ALPHA SYNCHROTRON/STORAGE RING WITH CHANNEL ACCESS

Stanley Cohen, BiRa, Albuquerque, New Mexico, U.S.A.
Gary William East, Robert Ellis, IUCEEM, Bloomington, Indiana, U.S.A*

Abstract

A four-channel magnet-power-supply ramp controller has been designed and deployed at the new ALPHA (Advanced Electron Photon Facility) at the Indiana University Center for Exploration of Energy and Matter (IUCEEM). The first application is a power-supply controller. For all practical purposes, the system is a versatile arbitrary voltage-waveform-generator with full DAQ (data acquisition) capabilities that can be used in a variety of beam instrumentation settings. The real-time controller can generate four arbitrary independently-triggerable ramp profiles. A normalized wave-form vector is encoded as a Process Variable array and is uploaded and stored by the real-time controller as required. Each ramp array element is clocked out to a 16-bit DAC (Digital to Analog Converter) via a DMA FIFO and built-in FPGA. The duration of the waveform is programmable with a minimum time resolution of 20 µsec between profile values. Four bipolar DACs have an output range of +/- 10V. Eight digital I/O control bits are allocated for each control channel. Typically, these bits are used to monitor and control the power-supply operational state. The control-system interface uses the EPICS Channel-Access server accessible on Labview RT 2009.

ALPHA STORAGE RING

The Advanced eLectron PHoton fAcility (ALPHA) consists of an electron LINAC coupled to a storage ring which will provide the beam to a device test area[1]. Ultimately, it will provide a 20 MeV 68 mA electron beam. ALPHA is under construction at this time, commissioning is planned for the second quarter of 2010. There are a number of operating modes. In one mode of operation, the storage ring would modify the pulse structure to eliminate bunching of electrons emerging from the LINAC[2]. In another mode, the storage ring will capture bunches of electrons and compress their time width to provide high-intensity electron pulses. ALPHA will be capable of providing X-rays using high-efficiency Bremsstrahlung targets or by Inverse Compton Scattering.

This multi-mode operation requires beam management via sophisticated programmable power-supply control electronics.

The controller described below is an example of a system whose software and hardware architecture can be used as a versatile arbitrary voltage-waveform-generator with full DAQ (data acquisition) capabilities that can be deployed for a variety of beam instrumentation applications.

* Work supported by the Naval Surface Warfare Center-Crane division (NSWC-Crane) Contract No. N00164-08-C-GM03

POWER SUPPLY RAMPING AND CONTROL REQUIREMENTS

The ALPHA storage ring requires a number of magnets to ramp their magnetic fields in response to a timing pulse. Four main dipoles are wired in series and are excited by a single 20 kW power supply. Other magnets, such as correctors and quadrupoles have individual supplies controlled and monitored by the system that will be described.

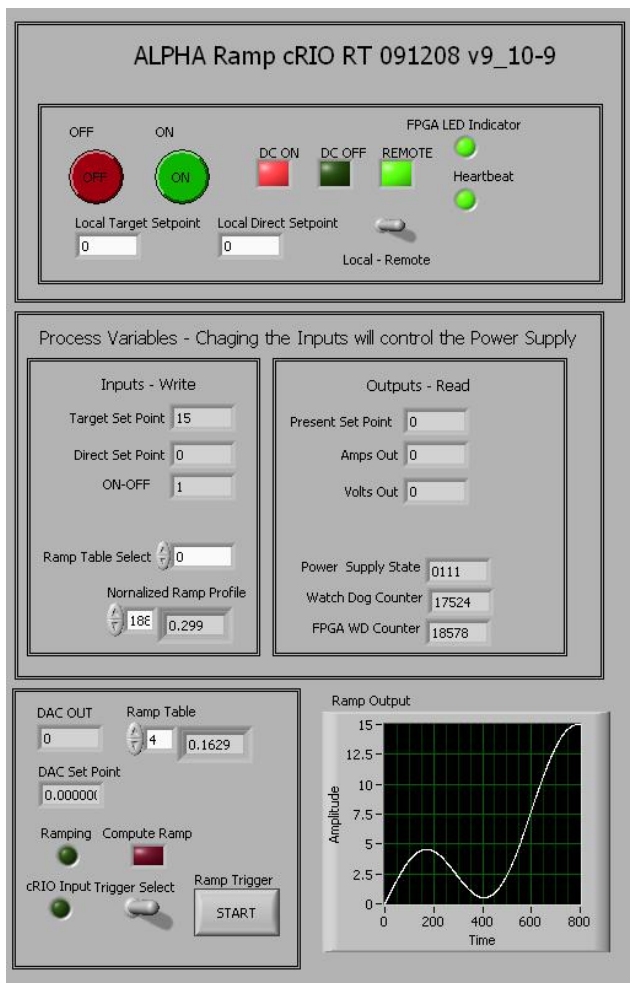

Figure 1: ALPHA ramping control panel.

FINAL FOCUS ION BEAM INTENSITY FROM TUNGSTEN FOIL CALORIMETER AND SCINTILLATOR IN NDCX-I*

S.M. Lidia#, F. Bieniosek, E. Henestroza, P. Ni, P. Seidl, LBNL, Berkeley, CA 94720, U.S.A.

Abstract

Laboratory high energy density experiments using ion beam drivers rely upon the delivery of high-current, high-brightness ion beams with high peak intensity onto targets. Solid-state scintillators are typically used to measure the ion beam spatial profile but they display dose-dependent degradation and aging effects. These effects produce uncertainties and limit the accuracy of measuring peak beam intensities delivered to the target. For beam tuning and characterizing the incident beam intensity, we have developed a cross-calibrating diagnostic suite that extends the upper limit of measurable peak intensity dynamic range. Absolute intensity calibration is obtained with a 3μm thick tungsten foil calorimeter and streak spectrometer. We present experimental evidence for peak intensity measures in excess of 400 kW/cm^2 using a 0.3 MV, 25 mA, 5-20 μsec K^{+1} beam. Radiative models and thermal diffusion effects are discussed because they affect temporal and spatial resolution of beam intensity profiles.

INTRODUCTION

The US Heavy Ion Fusion Science program is developing techniques for heating ion-beam-driven warm dense matter (WDM) targets [1-3]. Ion beams have several attractive features as drivers for generating WDM conditions:

- Precise control of local beam energy deposition *dE/dx*, nearly uniform throughout a volume, and not strongly affected by target temperature,
- Ability to use large sample sizes (~1 μm thick by 1 mm diameter),
- The ability to heat any target material: foams, powders, conductors, insulators, solids, gases, etc.

WDM conditions are obtained by combined longitudinal and transverse space-charge neutralized drift compression [3] of the ion beam to provide a hot spot on target with a beam spot size of ~1 mm, and pulse length from microseconds to nanoseconds. Local temperatures approaching 0.5 eV (~6000 K) have been observed in thin (50-150nm) foil targets of Au, Si, Pt, and C [4].

Beam profile measurements at the target plane are used to tune the beam transport system to optimize the beam intensity onto target foils. Alumina (Al_2O_3) scintillators are employed since they have a linear response over a large dynamic range and are relatively resistant to dose-related damage, at least at lower intensities. At higher intensities, greater than ~200kW/cm^2, saturation or other nonlinear effects may limit the upper range of measurable beam intensity. To address these issues, we have adapted our target diagnostic suite to examine the uses of thick foils for beam calorimetry measurements.

Tungsten has the highest melting temperature (3420°C) of the refractory metals from atmospheric pressure to ultra-high vacuum conditions. It is commonly used in high temperature applications (wire filaments, etc.) where high tensile strength is required.

The specific heat capacity, c_p, of tungsten (~24.4 J/mol/K) measures the temperature change expected from beam irradiation. Temperature-dependent values of the specific heat capacity can be found in standard references [5-6].

For beam calorimetry we use a 3μm thick solid tungsten foil, in which 300kV potassium ions deposit their energy within the first 100nm. The resolution of the optical system is ~11.4pixel/mm, or a pixel size of 88μm. On this length scale, the foil is thin compared to the resolution limit. The thermal diffusion length over a time *t* is given by

$$\delta_{th} = 2\sqrt{\kappa t}\,, \qquad (1)$$

*This work was supported by the Director, Office of Science, Office of Fusion Energy Sciences, of the U.S. Department of Energy under Contract No. DE-AC02-05CH11231.
#SMLidia@lbl.gov

ADC CONSIDERATIONS AND ANALYSIS FOR BAND PASS SAMPLING SYSTEMS

Alfred J. DellaPenna Jr., Brookhaven National Laboratory, Upton, NY 11973, U.S.A.

Abstract

With increasing demand of acquiring data at high speed with high resolution, more digitizers have become available for this purpose. With digitizers becoming faster and faster at higher data rates with higher resolutions, the factors in choosing the proper digitizer for a design is not just the number of bits. Deciding factors include jitter, maximization of the effective number of bits (ENOB) and linearity over the band of interest, and most importantly phase noise. Does the part you are evaluating match with the data sheet? If not, what is different in your test setup? (Your evaluation can only be as good as the equipment you are using to test the device.) With the availability of evaluation boards from almost any of the ADC vendors, a more in-depth evaluation can be performed fairly easily. Even the GUI interface is usually included with the evaluation board. So for a small investment on several choices, one can make a side by side comparison and see actual results.

INSTRUMENT SETUP

Our initial setup is illustrated in Figure 1. We used a single tone (500 Mhz) from a HP signal generator as the analog input. The digitizer clock, which requires the more stable (lower jitter) signal, was supplied by the Rohde & Schwarz SMA100A signal generator. Along with the evaluation boards a mating digital interface was purchased for each so we could utilize the graphical user interface that the vendor had created. The interface to the computer was through a USB cable. The software was downloaded from the vendor's website.

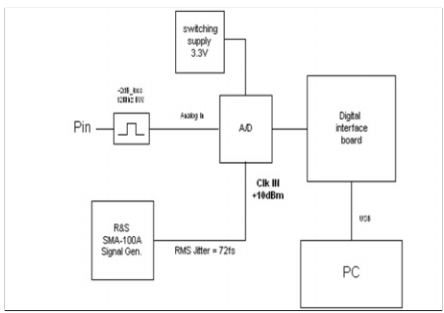

Figure 1: Digitizer setup. The analog input was from an Agilent N5181A. Software was downloaded from the digitizer vendor.

The onboard jumpers were usually set up at the factory; however, we did find that the evaluation boards allowed many different setup configurations. Choosing a setup that worked best for us took some time. Finally it was time to take some data.

We wanted to be sure it was a fair side by side evaluation of each digitizer. All of the evaluation boards had their analog input "protected" by limiting resistors; because of this, the same input signal did not use the same scale from one digitizer to another. This required us to either adjust the input to compare similar levels at the input to the digitizer, or modify the evaluation board itself (removing the limiting resistors). These modifications made the setup of all evaluation boards as close as possible, all running off the same supply and signal generators. Power sweeps were taken from -90 to +10 dBm and the associated plots were compared to each other. Figures 2-5 show the resultant Fast Fourier Transforms from each digitizer we were evaluating.

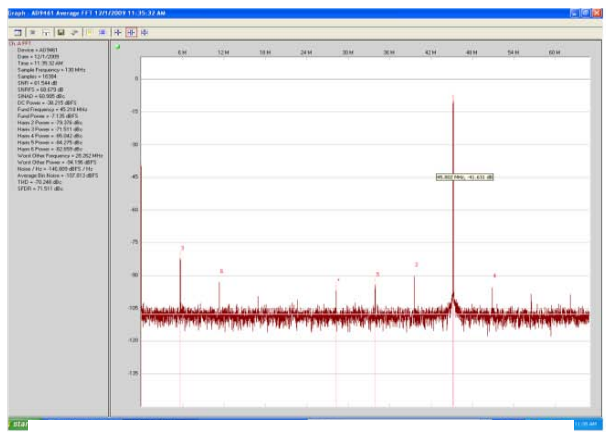

Figure 2: Analog Devices AF9461 FFT, power in +10 dBm.

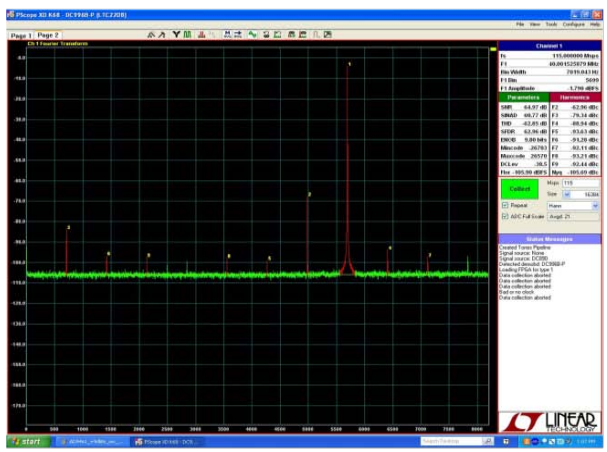

Figure 3: Linear Technology LTC2208 FFT, power in +10 dBm.

NSLS-II INJECTOR SYSTEM DIAGNOSTICS

D. Padrazo, O. Singh, I. Pinayev, R. Fliller, T. Shaftan, B. Kosciuk, R. Meier, Y. Hu
Brookhaven National Laboratory, Upton, NY 11973, USA

Abstract

The NSLS-II Injector System Diagnostics will provide instrumentation in the linac, Booster, Transfer Lines and Beam Dumps for measuring key beam parameters. These instruments will be adequate for staged commissioning of NSLS-II injectors, and will allow sufficient beam diagnostics for tune-up and top-up operations. This paper summarizes the status of the NSLS-II injector system diagnostics, focusing on those intended for the transfer lines, including the Linac to Booster (LTB) and Booster to Storage Ring (BSR).

INTRODUCTION

The NSLS-II is a state-of-the-art 3-GeV synchrotron light source being developed at Brookhaven National Laboratory. The injection system will consist of a 200 MeV linac, a 3 GeV booster synchrotron, and associated transfer lines. The instrumentation in the linac will provide sufficient beam diagnostics to determine bunch charge, length, transverse size, position, and beam losses. The LTB and BSR will include key instruments to be used for beam commissioning and tune-up, particularly the beam dumps and those diagnostics elements within the booster vault. Measurements of beam charge, bunch train, bunch charge, energy jitter, emittance, and energy spread can be achieved. Booster diagnostics will provide measurements for orbit correction, injection matching and transverse profile. In addition, elements are provided to measure beam current, bunch train pattern, tune and chromaticity. This paper will detail the implementation of these diagnostics components for the NSLS-II Injector System.

LINAC DIAGNOSTICS

A turn-key procurement, the NSLS-II linac is specified to have an output energy of 200 MeV, energy spread of 0.5%, bunch length of 20 ps, and normalized emittance of 55 mm-mmrad. The linac will be capable of operating in single bunch mode with a charge of up to 0.5 nC, or in multibunch mode with a bunch train of 80 to 150 bunches, separated by 2 ns with a charge per train of 22 nC. The linac will have a 100 kV electron gun with thermionic cathode, sub-harmonic pre-buncher, 3 GHz pre-buncher, 3 GHz buncher, and a 3 GHz acceleration section. Linac diagnostics will consist of a Wall Current Monitor (WCM) after the gun, and another before the buncher. There will be a WCM, FLAG, and Beam Position Monitor (BPM) before each LINAC tank. This will provide sufficient diagnostics to determine bunch charge, length, transverse size, and position. The WCMs will also provide a measure of the beam losses in the linac. Refer to the Diagnostics Table of Elements and the Plan View of Injector as shown in Table 1 and Figure 1 respectively.

Table 1: Gun and Linac Diagnostic Elements

System	Qty	Type	Abbrv.	Parameter Measured
Electron Source (Gun)	2	Wall Current Monitor	WCM	Intensity; longitudinal beam characteristics
Linac	3	Fluorescent Screens	FLAGS	Position; transverse profile
Linac	3	Wall Current Monitor	WCM	Bunch charge; intensity; beam loss
Linac	3	Beam position monitor	BPM	Beam position

BOOSTER DIAGNOSTICS

A turn-key procurement, the NSLS-II Booster is a 158 m combined-function-magnet synchrotron with an extraction energy of 3 GeV for top-up injection. The beam emittance will be damped below 50 nm-rad, with trains of up to 150 bunches. The bunch length will be 15 ps, and the energy spread will be 0.08% when fully damped. The expected total charge out of the booster is estimated at 10 nC when the linac is in multi-bunch mode. Booster diagnostics are chosen for commissioning and robust operation.

The booster will have 36 BPMs placed at strategic points in the ring to allow for robust orbit correction. Six flags will be located in the booster for commissioning, injection matching and transverse profile measurements. Beam current will be measured with a DCCT. An FCT will monitor the bunch train pattern. A pair of stripline kickers will be available for tune and chromaticity measurements, also serving in a beam cleaner system. Synchrotron light will also be used in conjunction with a streak camera to measure the bunch length. The diagnostic elements of the Booster are listed in Table 2.

BEAM INSTRUMENTATION REQUIREMENTS FOR THE HINS PROGRAM AT FERMILAB*

J. Steimel#, V. Scarpine, R. Webber, M. Wendt, FNAL, Batavia, IL 60510, U.S.A.

Abstract

A linear accelerator test facility called the High Intensity Neutrino Source (HINS) has begun operating at Fermilab. The goal of this program is to test new technology for the front end of an intensity frontier linac. Some of the new technologies that will be tested include: operation of multiple cavities from a single RF source using high-power vector modulators, round beam transport using superconducting, solenoidal focusing, accelerating beam with spoke cavities, and a transition to superconducting RF cavities at 10 MeV. The testing has been split into four different stages: 2.5 MeV beam from the RFQ alone, acceleration through six room temperature cavities with quadrupole focusing, acceleration through 18 room temperature cavities with solenoidal focusing, and acceleration through the room temperature section plus one cryomodule of superconducting spoke cavities. Each stage focuses on testing the beam quality with a particular new technology. This paper describes the instrumentation necessary to quantify the beam quality for each stage of the program.

INTRODUCTION

The Fermilab HINS program is building a low energy, linear, hadron, test accelerator for intensity frontier applications. Figure 1 shows one of the original proposed designs for HINS as the front end for an intense neutrino source [1]. The program has since been descoped to provide an accelerator that will be used as test bed to study novel, linear accelerator components and techniques. Successful designs and techniques will be utilized in the front-end design of ProjectX [2], a long-term plan to increase proton flux to MW levels for long baseline neutrino experiments at Fermilab.

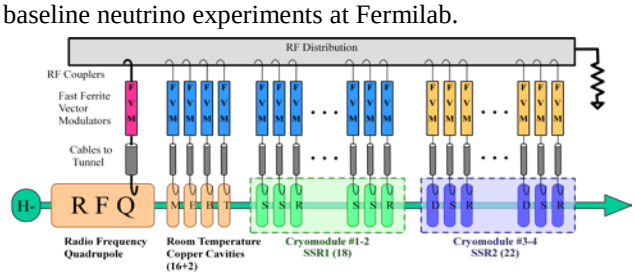

Figure 1: Original HINS proposal from 2006 showing a 90MeV beam line and four cryomodules.

There are four main concepts that the HINS program is currently prepared to test. First, it will test operation of multiple cavities from a single RF power source. One large RF power source is less expensive to procure and operate than many smaller sources. High power, ferrite vector modulators [3] (FVM) provide the fine amplitude and phase adjustments required for individual cavities. Second, it will test a lattice utilizing solenoidal focusing to propagate round beam. This lattice has been simulated to produce smaller beam halo at low energy than standard quad focusing [4]. However, the strength of the magnets needed for a practical solenoidal lattice require too much current for a normal conducting coil. These solenoid coils are superconducting. Third, the transition from normal conducting cavities to superconducting cavities will occur at 10 MeV. This is the lowest superconducting transition energy for any existing high-intensity hadron linac and is made possible by a spoke resonator cavity design [5]. This accelerator will also be the first to test any superconducting spoke resonator with beam. Fourth, the accelerator will be used to test advanced hadron linac instrumentation.

Testing of the different concepts will occur in four different stages based on resource availability. In the first stage, beam directly from the radio frequency quadrupole (RFQ) will be analyzed at 2.5 MeV. In the second stage, beam will be accelerated using six room temperature cavities with normal conducting quadrupole focusing. This will test beam operation with the FVMs. Once the cryogenic infrastructure is in place, the beam will be accelerated to 10 MeV using 18 room temperature cavities and superconducting solenoid focusing. This will test the beam halo and stability of the FVMs with many cavities. Once a spoke resonator cryostat is constructed, beam will be accelerated by the superconducting spoke cavities to test viability and stability of spoke cavity acceleration.

2.5 MEV RFQ

The 2.5 MeV beam line consists of a 50 keV proton source, a 2.5 MeV RFQ, a diagnostic line, and a beam dump. Figure 2 shows the layout of the 2.5 MeV diagnostic line. Beam studies on the RFQ were already performed with a simpler diagnostic line [6]. These studies verified the round beam profile from the RFQ. However, beam efficiency and beam energy were not precisely measured.

Ion Source

The HINS ion source is a duo-plasmatron, 50 keV, proton source [7]. The proton extractor is immediately followed by a low energy beam transport section (LEBT) consisting of two room temperature focusing solenoids, two dual plane dipole correctors, a beam stop, and a beam current toroid. Beam steering and emittance of the ion source are well characterized. The percentage of ions produced by the source that are protons is not as well

*Operated by Fermi Research Alliance, LLC under Contract No. DE-AC02-07CH11359 with the United States Department of Energy.
#steimel@fnal.gov

PHIL ACCELERATOR AT LAL – DIAGNOSTICS STATUS

J. Brossard#, F. Blot, S. Cavalier, A. Gonnin, M. Joré, P. Lepercq,
S. Letourneur, B. Mercier, H. Monard, C. Prevost, R. Roux, A. Variola,
LAL-CNRS-IN2P3/ Université Paris-Sud XI, bâtiment 200, 91898 Orsay, France.

Abstract

The "Photo-Injector at LAL" (PHIL : http://phil.lal.in2p3.fr/) is a new electron beam accelerator at LAL. This accelerator is dedicated to test and characterise electrons photo-guns and high-frequency structures for futur accelerator projects (like the next generation lepton colliders, CLIC, ILC). This machine has been designed to produce low energy (E<10 MeV), small emittance (ε # 10 π.mm.mrad), high current (charge # 2 nC/bunch) electrons bunch at low repetition frequency (ν_{rep}<10Hz) [1]. The first beam has been obtained on the 4th of november 2009. This paper will describe the current status and the futurs developpements of the diagnotics devices on this machine.

DESCRIPTION OF THE PHIL ACCELERATOR

PHIL is currently a 6 meters long accelerator with 2 diagnostics beam lines (see Figure 3). The direct beam line is mainly devoted to 2D transverse emittance and bunch length measurement. The deviate beam line is devoted to the mean and dispersion energy beam measurement. The injection in the deviated line is performed by a Tesla Test Facility (TTF) injector dipole.

The direct beam line is equipped with :

– 2 Beam Position Monitor (BPM).
– 1 phosphorescent transverse beam profile monitor.
– 1 Faraday Cup (FC).

One of the BPM is of the "button electrode" type, the other is of "re-entrant cavity" type. The beam profile monitor is a phosphorescent screen oriented at 45° from the beam axis. The screen is a cerium-doped yttrium:aluminium:garnet (YAG:Ce) crystal scintillator (300 µm thickness, 40 mm of diameter). Images have already been acquired on this first screen (located at 1925 mm from the photo-cathode). These preliminary measurements have shown that a millimeters size beam in both horizontal and vertical planes is already reachable (see Figure 2). The vertical and horizontal beam sizes are estimated using N differents images, after drak current substration (see Figure 1).

The FC is located at the end of the direct beam line.

The machine is also equipped with a false photo-cathode test pattern used to check the laser spot size and the position on the real photo-cathode.

Currently, the deviate beam line is only equipped with one Faraday Cup.

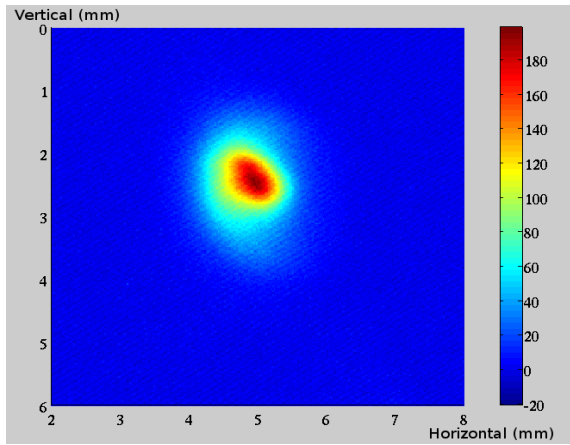

Figure 2: example of average transverse beam profile obtained at the first YAG:Ce screen station (1925 mm from the photocathode) using 10 images. For each images, the dark current has been substracted but not the jitter position.

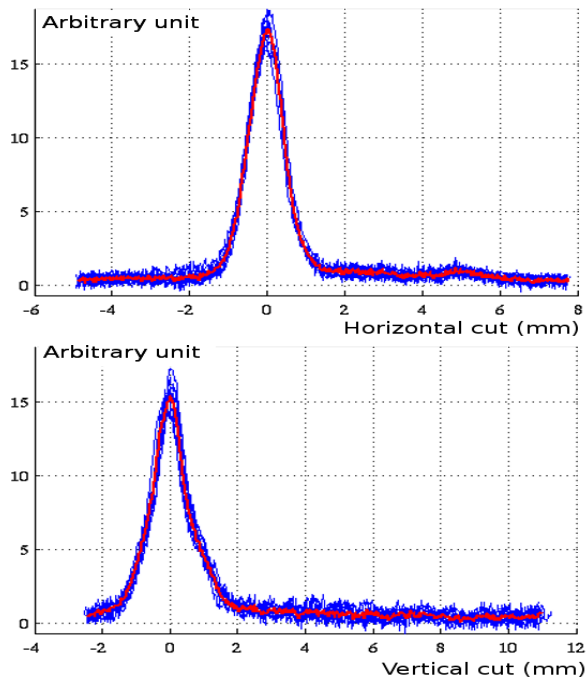

Figure 1: CCD intensity signal projected on horizontal and vertical axis (for 10 images) used for beam size estimation. The red curve is the average cut. On theses blues curves, the dark current and the jitter position have been substracted.

#brossard@lal.in2p3.fr

DESIGN STATUS OF THE DIAGNOSTIC SYSTEM FOR THE TAIWAN PHOTON SOURCE PROJECT

K.T. Hsu, C.H. Kuo, K.H. Hu, Jenny Chen, P.C. Chiu, C.Y. Wu, S.Y. Hsu

NSRRC, Hsinchu 30076, Taiwan

Abstract

The Taiwan Photon Source (TPS) is a 3 GeV synchrotron light source being built at the campus of NSRRC. Designs of various diagnostics are under way, and will be deployed in the future, to satisfy stringent requirements of TPS for commissioning, top-up injection, and operation. These designs, including beam intensity observation, trajectory and beam positions measurement, destructive profile measurement, synchrotron radiation monitors, beam loss monitors, orbit and bunch-by-bunch feedbacks, filling pattern, etc., are in the final design phase. Details of current status and implementation of the planned beam instrumentation system for the TPS will be summarized in this report.

INTRODUCTION

The TPS is a state-of-the-art synchrotron radiation facility featuring ultra-high photon brightness with extremely low emittance [1]. Civil construction was started from February 2010. The building will be finished in 2012. The campus of the NSRRC, which host the TPS and the existing 1.5 GeV Taiwan Light Source (TLS), is shown as Fig. 1. Machine commissioning is scheduled in late 2013. User service will start from 2014.

The TPS accelerator complex consists of a 150 MeV S-band linac, linac to booster transfer line (LTB), 0.15–3 GeV booster synchrotron, booster to storage ring transfer line (BTS), and 3 GeV storage ring. The latest generation diagnostic systems will help TPS to achieve its design goals. The storage ring has 24 double-bend achromat lattice cells with 6-fold symmetry. The main beam diagnostics related parameters for the booster synchrotron and the storage ring are summarized in Table 1.

Figure 1: Aerial view of the NSRRC campus. The upper left building is the existed TLS facility. The semi-underground building at upper right is the TPS facility.

Table 1: Major Parameters of the Booster Synchrotron and the Storage Ring

	Booster Synchrotron	Storage Ring
Circumference (m)	496.8	518.4
Energy (GeV)	150 MeV – 3 GeV	3.0
Natural emittance (nm-rad)	10.32 @ 3 GeV	1.6
Revolution period (ns)	1656	1729.2
Revolution frequency (kHz)	603.865	578.30
Radiofrequency (MHz)	499.654	499.654
Harmonic number	828	864
SR loss/turn, dipole (MeV)	0.586 @ 3 GeV	0.85269
Betatron tune ν_x/ν_y	14.369/9.405	26.18 /13.28
Synchrotron tune ν_s	-	0.00611
Momentum compaction (α_1, α_2)	-	2.4×10^{-4}, 2.1×10^{-3}
Natural energy spread	9.553×10^{-4}	8.86×10^{-4}
Damping partition $J_x/J_y/J_s$	1.82/1.00/1.18	0.9977/1.0/ 2.0023
Damping time $\tau_x/\tau_y/\tau_s$ (ms)	9.34/ 16.96 / 14.32	12.20/ 12.17 / 6.08
Natural chromaticity ξ_x/ξ_y	-16.86/-13.29	-75 / -26
Dipole bending radius ρ(m)	17.1887	8.40338
Repetition rate (Hz)	3	-

To get the benefits of the high brightness and small sizes of TPS sources, photon beams must be exceedingly stable, in position and in angle, to better than 10% of beam sizes and divergence. Table 2 gives the electron beam sizes and angular divergences for the selected TPS sources. The most stringent beam measurement and stability requirement will be for the vertical position at the 7 m straight for an insertion-device source (σ_y = 5.11 μm); this will require special consideration for measuring both electron and photon beams.

Table 2: The Electron Beam Sizes and Divergence

Source point	σ_x (μm)	$\sigma_{x'}$ (μrad)	σ_y (μm)	$\sigma_{y'}$ (μrad)
12 m straight center	165.10	12.49	9.85	1.63
7 m straight center	120.81	17.26	5.11	3.14
Dipole (1° source point)	39.73	76.11	15.81	1.11

LINAC DIAGNOSTICS

The TPS 150 MeV linac system was contracted to the RI Research Instruments GmbH (formerly ACCEL Instruments GmbH) [2]. The schedule for delivery and commissioning is early 2011 at test site. The linac will move to the TPS building in late 2012 after TPS building available. Beam instrumentation comprises five YAG:Ce screen monitors for beam position and profile observation,

DIAGNOSTICS UPDATE OF THE TAIWAN LIGHT SOURCE

C. H. Kuo, P. C. Chiu, Y. S. Cheng, Y. K. Chen, K. H. Hu, C. Y. Wu, Demi Lee, S. Y. Hsu, Jenny Chen, Y. T. Chang, C. J. Wang, Y.R. Pan, K.T. Hsu, NSRRC, Hsinchu 30076, Taiwan

Abstract

Diagnostics of the 1.5 GeV Taiwan Light Source (TLS) have been continuously upgraded since its operation started in 1993. The BPM electronics of the Taiwan Light Source (TLS) have been upgraded to Libera Brilliance in August 2008 to improve performance and functionality. Orbit feedback has also been migrated to a fast orbit feedback system to enhance orbit stability. Commercial photon BPM electronics were tested recently. A new-generation bunch-by-bunch feedback processor to improve beam stability was tested. Post-mortem diagnostic tools were gradually added to clarify reasons for beam trip. These upgrades contributed to improving beam quality and machine availability greatly.

INTRODUCTION

TLS was dedicated to the user in 1993. There have been several major upgrades recently, including a 2005 superconducting-RF upgrade and a 2008 BPM upgrade. The SRF system upgrade is improving beam quality and providing sufficient RF gap voltage for high current operation. Currently, the machine is operated at 1.5 GeV, 360 mA top-up injection. The BPM system upgrade also provides good diagnostics, which are essential to good quality machine operation. In the meanwhile, along with BPM upgrade, the orbit feedback system has also migrated to a fast orbit feedback system to enhance orbit stability, which is extremely important for a modern synchrotron light source.

To further improve beam availability, a beam trip event diagnostic has been deployed in the TLS. These diagnostic tools can clearly reveal and track causes of the beam trips and provide enough information to aid maintenance.

Libera Photon provides a good integration environment to correlate electron and photon beam motion. An earthquake detector has been installed lately as well, to record trip events caused by quakes. A new generation bunch-by-bunch feedback processor is also tested. All of these efforts above will be addressed respectively in the following sections.

CONTROL ENVIRONMENT ADAPTATION

The EPICS toolkits were chosen as the control system frameworks for the new 3 GeV synchrotron light source (Taiwan Photon Source, TPS). It has been decided that the control system for TLS should support both its existing control environment and EPICS as an upgrade-maintenance strategy to save resources and minimize development of the existing control system. New devices and/or replacement of the obsolete system are being considered to employ the EPICS directly. Gateways are implemented to exchange data between both environments and let them operate side by side. Modification for the control system has continuously proceeded during the last several years. New technology and improved maintenance are consequent advantages, along with manpower savings.

NEW BPM SYSTEM

Libera Brilliance [1] is employed to replace the existing BPM electronics for the TLS. Its integration started from 2007 until finished in August 2008 [2,3]. It was gradually deployed and performed without interfering with routine operation. There are 59 Libera Brilliances online, operating for more than one and half year. Adequate long-term reliability has been achieved.

Slow and Fast Data

New BPM system delivers high precision data at a 10 Hz rate for control system access with 0.1 μm resolution. The new BPM also delivers 10 kHz position data for fast orbit feedback applications and analysis applications with 0.2 μm resolution.

Turn-by-Turn Data and Post-mortem Data

Turn-by-turn data is also provided by Libera Brilliance. It is useful for accelerator physics study and helps to reveal fast beam motion such as beam excitation caused by the kicker and septum [2]. Post-mortem buffers as long as 256 kilosamples give turn-by-turn data before beam trip; this has proved to be a powerful diagnostic tool [2].

Some Observations by the New BPM System

The new BPM system unveils some effects that were not easily discovered systematically in the old BPM system. Several examples are summarized below.

A power supply with defects in its regulator might cause some 60 or 120 Hz strong perturbation. Fig. 1 is an example, showing a beam orbit motion that has 120 Hz power line noise. With the aid of the new BPM system, this perturbation was shown to come from a compensated corrector power supply of the insertion Device U9.

The leakage field of septum and kicker will also cause an orbit excursion and will have effects on the optical-radiation strength and precision. The experimental station should exclude the sampled data during injection by means of the provided gating signal. During the long shutdown of Spring 2010, mu metal was adopted to wrap the chamber and shield it from the field leakage. Figs. 2 and 3 show the orbit distortion caused by septum leakage before and after chamber shielding. The excursion is about half what it was before chamber shielding.

RECENT UPGRADE OF THE PITZ FACILITY*

J. W. Bähr[1], H. Al-Juboori, A. Donat, U. Gensch, H.-J. Grabosch, L. Hakobyan, M. Hänel, R. Heller, Y. Ivanisenko, L. Jachmann, M. A. Khojoyan, G. Klemz, W. Köhler, G. Koss, M. Krasilnikov, A. Kretzschmann, H. Leich, M. Mahgoub, J. Meißner, D. Melkumyan, M. Otevrel, M. Penno, B. Petrosyan, M. Pohl, S. Rimjaem, C. Rüger, M. Sachwitz, B. Schöneich, J. Schultze, A. Shapovalov, F. Stephan, M. Tanha, G. Trowitzsch, G. Vashchenko, L. V. Vu, T. Walther,† A. Brinkmann, K. Flöttmann, W.Gerdau, S. Lederer, L.Lilje, F. Obier, D. Reschke, S. Schreiber, DESY, Hamburg, Germany

J. Saisut, C. Thongbai, Chiang Mai University and Thailand Center of Excellence in Physics, Thailand

J. Knobloch, D. Richter, Helmholtz-Zentrum Berlin für Materialien und Energie GmbH, Berlin, Germany

P. Michelato, L. Monaco, C. Pagani, D. Sertore, INFN / LASA, Segrate MI, Italy

G. Asova, I. Bonev, L.Staykov, I. Tsakov, INRNE Sofia, Bulgaria

W. Sandner, I. Will, MBI Berlin, Germany

A.Naboka, V. Paramonov, RAS / INR Moscow, Russia

B. L. Militsyn, B. Muratori, STFC / DL / ASTeC, Daresbury, United Kingdom

M.Korostelev, The Cockroft Institute, Daresbury Laboratory, Warrington, United Kingdom

T. Vilaithong, Thailand Center of Excellence in Physics, Thailand

W. Ackermann, W.F.O. Müller, S. Schnepp, T. Weiland, TEMF, TU Darmstadt, Darmstadt, Germany

I. Ullmann,Universitaet Erlangen, Erlangen, Germany

J. Rönsch-Schulenburg, J. Rossbach, Universität Hamburg, Hamburg, Germany

Abstract

The Photo Injector Test facility at DESY, Zeuthen site (PITZ), is dedicated to develop and optimize high brightness electron sources for short wavelength Free-Electron Lasers (FELs) like FLASH and the European XFEL, both in Hamburg (Germany). Since October 2009 a major upgrade is ongoing with the goal to improve the accelerating components, the photocathode drive laser system and the beam diagnostics as well. The essential new feature in the running will be an in-vacuum 10 MW RF directional coupler to be used for the RF monitoring and control. In this context a significant improvement of the RF stability is expected. RF pulses of 800 microseconds with 10 Hz repetition rate will be used. The most important upgrade of the diagnostics system will be the implementation of a phase space tomography module (PST) consisting of three FODO cells each surrounded by two screen stations. The goal is an improved measurement of the transverse phase space at different charge levels. The upgraded facility will be described.

INTRODUCTION

High brightness electron sources for short wavelength Free Electron Lasers (FEL) are being developed and optimized at the Photo Injector Test facility at DESY, Zeuthen site [1]. In the recent running break major

* Supported by : EU contract: IASFS RII-CT-2004-506008

[1] Corresponding author:J.Baehr: juergen.baehr@desy.de

BEAM BASED MONITORING OF THE RF PHOTO GUN STABILITY AT PITZ

M. Krasilnikov*, F. Stephan, DESY, Zeuthen, Germany

Abstract

The stability of the photo injector is a key issue for the successful operation of linac based free electron lasers. Several types of jitter can impact the stability of a laser driven RF gun. Fluctuations of the RF launch phase and the cathode laser energy have significant influence on the performance of a high brightness electron source. Bunch charge measurements are used to monitor the stability of the RF gun phase and the cathode laser energy. A basic measurement is the so called phase scan: the accelerated charge downstream of the gun is measured as a function of the launch phase, the relative phase of the laser pulses with respect to the RF. We describe a method which provides simultaneous information on RMS jitters from phase scans at different cathode laser energies. Fluctuations of the RF gun phase together with cathode laser energy jitter have been measured at the Photo Injector test facility at DESY in Zeuthen (PITZ). Obtained results will be presented in comparison with direct independent measurements of corresponding instability factors. Dedicated beam dynamics simulations have been done in order to optimize the method performance.

INTRODUCTION

The stability of the phase in the RF photo gun is one of the most important specifications for the linac based FELs. The requirements on the RF phase stability are derived from the desired electron beam parameters such as bunch-to-bunch and pulse-to-pulse energy spread, the bunch compression in the injector, and the arrival-time of the beam at the undulators.

The RF systems in the injector of the XFEL require tight control of the RF field in the gun. The RF launch phase stability is expected to be in the order of 0.1 deg for the phase [1]. The shot-to-shot stability in energy of the cathode laser pulses is expected to be 2% (RMS) for single pulses and 1% (RMS) averaged over a pulse train [1]. This determines the stability of the bunch charge, which could be slightly better than the cathode laser one due to space charge related effects.

The photo injector test facility at DESY in Zeuthen (PITZ) develops electron sources for FELs like FLASH and the European XFEL at DESY in Hamburg. The stability of the electron source is one of the central issues of the research program at PITZ. This paper presents a method for precise monitoring of the gun stability, including RF phase and the cathode laser energy.

*mikhail.krasilnikov@desy.de

PHOTO INJECTOR IN ZEUTHEN

The PITZ photo injector consists of an L-band RF gun supplied with a cathode load-lock system and solenoids for space charge compensation. The cathode laser system is able to generate trains of electron pulses including temporal and transverse laser beam shaping. Further on the electron beam line contains a booster cavity and a big variety of beam diagnostics systems for the characterization of the electron beam at different energies.

The RF gun cavity is a 1½-cell normal conducting copper cavity, operated at a resonance frequency of 1.3 GHz with a peak power of up to ~7 MW. The RF power to the gun is supplied by a 10 MW multibeam klystron through two equal output ports. In front of the gun the RF pulses from both waveguides are combined using a custom T-shape combiner. No field pickups are available for the current gun cavity design. Before 2010 the control of the RF feed to the gun was realized via two directional couplers installed before the T-combiner. Cross-talking of both directional couplers under not well-known resonance conditions of the gun cavity made the control of the RF field in the gun practically impossible. So, no routine feed back was available and only the feed forward had been used. After the facility upgrade in spring 2010 a 10 MW in-vacuum directional coupler has been installed after the T-combiner. Measurements of the combined RF pulses should provide a possibility for better control on the field in the gun closing a feedback loop for the amplitude and phase stabilization.

The PITZ photo cathode laser system is developed by the Max-Born Institute (MBI, Berlin) and is capable to generate trains of flat-top pulses with up to 800 micropulses with 1 MHz frequency at 10 Hz repetition rate. An individual micropulse with a typical duration of ~20 ps (FWHM) and very short rise and fall time (~2 ps) has a wavelength of 257 nm, the pulse energy provides the possibility to emit high charge electron bunches (up to several nC) from Cs_2Te cathodes.

The master oscillator (MO) is one of the major components of the timing system at PITZ. Its fundamental frequency of 9.027775 MHz is used for timing and diagnostics and to generate harmonics for the synchronization of the low-level RF (144^{th} harmonics – 1.3 GHz) and the photo cathode laser system (3^{rd} , 6^{th} and 144^{th} harmonics – 27, 54 MHz and 1.3 GHz correspondingly).

A detailed description of the diagnostics available at PITZ can be found in [2, 3]. Most related to the subject of this work are bunch charge measurements, monitoring of the RF phase and amplitude in the gun and the laser pulse energy diagnostics. The bunch charge at PITZ can be measured using Faraday Cups (FCs) and Integrating

SLOW ORBIT FEEDBACK AT RHIC*

V. Ptitsyn, A. Marusic, R. Michnoff, M. Minty, G. Robert-Demolaize, T. Satogata, BNL, Upton, New York, U.S.A.

Abstract

Slow variations of the RHIC closed orbit have been strongly influenced by diurnal variations. These variations affect the reproducibility of RHIC operation and might have contributed to proton beam polarization degradation during past polarized proton runs. We have developed and commissioned a slow orbit feedback system in RHIC Run-10 to diminish these variations and improve energy ramp commissioning and tuning efficiency. This orbit feedback uses multiple dipole correctors and orbit data from an existing beam position monitor system. The precision of the orbit feedback system has resulted directly from application of an improved algorithm for measurement of the average orbit, from improved survey offsets and numerous measures taken to ensure deterministic delivery of the BPM data. Closed orbit corrections are calculated with an online model-based SVD algorithm, and applied by a control loop operating at up to 1 Hz rate. We report on the feedback design and implementation, and commissioning and operational experience in RHIC Run-10.

INTRODUCTION

The accelerator RHIC [1] at Brookhaven National Laboratory has been operating for eleven years providing collisions of heavy ion as well as polarized proton beams for experiments exploring quark-gluon matter and other specific features of Quantum Chromodynamics. The control of closed orbit of the circulating beam is especially important for the operation with polarized protons. The vertical orbit should be maintained with high precision, below 300 μm of the orbit rms value, in order to ensure the preservation of the proton beam polarization during the acceleration ramps to 250 GeV [2].

The development of the slow orbit feedback was motivated by several reasons. First, the feedback was expected to simplify and speed-up the process of acceleration ramp setup and development. Because of magnet realignments done quite regularly between the RHIC runs as well as because of different machine lattices used from year to year, and even in the course of the same RHIC run, the tuning of RHIC acceleration ramps has been a popular kind of control room work, which often could take more than one day. The orbit feedback, together with other developed feedbacks (tune, coupling, chromaticity) intended to shrink the time scale of the ramp development to less than one control room shifts.

The second reason for the feedback development was to make the closed orbit reproducible from one acceleration ramp to another. And the third reason was related with holding the closed orbit at required precision level during the course of the beam stores. The main problem for the reproducibility of the orbit on the ramps as well as for maintaining a constant orbit at the store was seen to be caused by diurnal slow orbit variations. Although these orbit variations were noted long ago until recently there has been no attempt to develop the feedback in order to tackle the problem. In 2009 RHIC has the first run for physics experiments with the proton beams accelerated to 250 GeV. A considerable polarization loss observed during the acceleration to 250 GeV stimulated the work towards better control of possible depolarization factors, including the control of the beam closed orbit both during the energy ramp and at store.

The additional appeal to address the problem of diurnal orbit variations came from a consideration to move the RHIC working point (betatron tunes) close to an integer value. The move of the working point can be advantageous for the polarization preservation as well as for improving the beam lifetime at the store energy. The closed orbit variation, however, would increase accordingly to the $1/\sin(\pi*Q)$ law as the betatron tune Q is pushed towards an integer value.

SLOW ORBIT VARIATIONS IN RHIC

Diurnal variations of the beam closed orbit in RHIC have been noted several years ago. An example of the variations observed during the stores of proton beams in 2005 is shown in Figure 1. Since this region (as well as the IR6 region) contains an experimental detector, the low-beta* optics is applied there, which effectively leads to enhancement orbit excursions in the quadrupole triplets surrounding the interaction point.

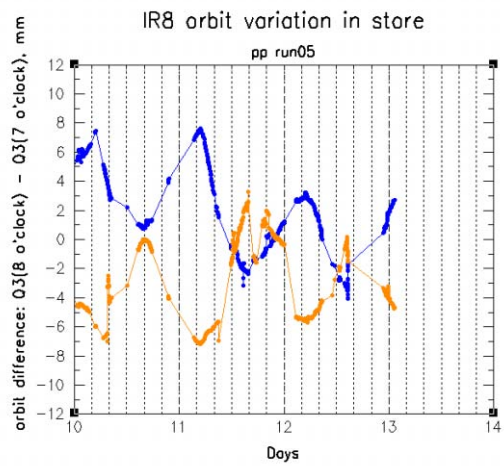

Figure 1: An example of the diurnal orbit variation is shown from RHIC Run-5. The difference of vertical orbit measured on left and right side of IP8 in Blue and Yellow RHIC rings is plotted.

* Work supported by Brookhaven Science Associates, LLC under Contract No. DE-AC02-98CH10886 with the U.S. Department of Energy.

NSLS2 TRANSVERSE FEEDBACK SYSTEM DESIGN

Weixing Cheng
NSLS-II, Brookhaven National Laboratory, Upton, NY 11973

Abstract

A diffraction-limited storage ring like NSLS2 requires stringent beam stability. Even with careful design of vacuum component to limit the geometric impedance, due to resistive wall impedance and fast-ion effect, transverse instabilities will happen at low current (~15mA). An active transverse feedback system has been designed to cure the coupled bunch instability. The system will have less than 200 micron seconds damping time at 500mA to suppress the fast-ion instabilities, which is severe in vertical plane due to small beam size.

INTRODUCTION

Bunch-by-bunch feedback systems have been proved effective to cure the coupled bunch instabilities. Third generation light sources and particle colliders need to run at high beam current to get the desired brightness and luminosity. Even with careful design of the vacuum chamber and other methods to cure the instabilities, there may be residual betatron oscillation or synchrotron oscillation. An active feedback system is straight forward to achieve the design current and required stability. Those methods to increase the tune spread by introduce non-linear field (like Chromaticity or Octupole magnets) may limit the dynamic aperture, which is not suitable especially at top-off operation. Active feedback has no side effect on the dynamic aperture and typically helps to suppress the injection transient.

Feedback systems are generally composed of three parts: RF front end to detect the transverse position error signal or longitudinal phase information; digitizer to sample and filter the error signals, as well as feedback gain control, phase adjustment etc; corrector module including high power amplifier and kickers. Shunt impedance of the kicker should be sufficient to kick the beam effectively with reasonable power. With the recent development of digital technology, especially the FPGAs (Field Programmable Gate Array), there is no reason to select digital feedback processors other than FPGA based. In a digital feedback loop, one can easily get rid of the DC offset as well as revolution harmonics by using digital filters. The digital delay adjustment avoids the use of long cables to do one-turn delay. The feedback digitizer itself is a powerful diagnostic tool with large memory to store the bunch-by-bunch position/phase information. Bunch oscillation and unstable modes can be revealed by transient measurements. The digitizer can be used to measure the tune of each individual bunch, or to clean unwanted bunches.

Treating the bunch as a rigid particle, the central motion of beam position/phase can be written as damped harmonic oscillation with external force. Eq (1) gives the oscillations in longitudinal plane, transverse plane is similar.

$$\ddot{\tau} + 2d_r\dot{\tau} + \omega_s^2\tau = f(t) = f^{wk} + f^{fb} \qquad (1)$$

Where

$$f^{fb} = -\frac{\alpha e}{E_0 T_0} V^{fb}(t)$$

with,

$$V^{fb}(t) = -jG^{fb}\tau \approx -\frac{G^{fb}}{\omega_s}\dot{\tau}$$

f^{wk} – wake force from the past bunches,
f^{fb} – kick force from the feedback system.

Beam stabilization requires the damping rate (radiation damping + feedback damping) be larger than the wake field excitation rate. Be aware that the wake field caused coupled bunch instability growth rate is proportional to the beam current. More feedback gain is needed for higher beam current. However, active feedback gain is not infinite, it's limited by the high power amplifier. Besides, with too much gain, the noise in loop might be amplified too much to excite the beam.

Instability growth rate has been estimated for the NSLS-II storage ring, see next section for more information. It shows that for transverse (especially vertical plane), feedback system is mandatory to achieve the designed goal of 500mA and preserve the low emittance < 1 nm.rad. Longitudinal instability in not expected to be a problem because of the use of superconducting RF cavity. The baseline design of NSLS-II will have feedbacks for horizontal and vertical planes. Some major parameters related to the transverse feedback are listed in Table 1.

Table 1, main parameters for NSLS-II feedback system

Parameter	Value	Unit
E	3	GeV
f_{rf}	499.68	MHz
h	1320	
f_{rev}	378.55	kHz
T_{rev}	2.64	μs
Q_X/Q_Y	33.36/16.28	
f_X/f_Y	136/106	kHz
$\varepsilon_x/\varepsilon_Y$	0.9/0.008	nm.rad
τ_x/τ_Y	54/54 (w/o DW)	ms
	23/23 (3 DW)	ms
Resolution	3	μm

SYNCHROTRON LIGHT MONITOR SYSTEM FOR NSLS-II

Weixing Cheng
NSLS-II, Brookhaven National Laboratory, Upton, NY 11973

Abstract

A visible synchrotron light diagnostic beam line has been designed at the NSLS2 storage ring, using the dipole radiation. The 'cold-finger' configuration has been selected to block the central x-rays. Beam power on the first mirror is less than 1W, no water cooling is required for the in-vacuum mirror. The beam line layout and major applications will be discussed in this paper. Two vacuum ports are reserved in the NSLS2 booster ring to monitor the transverse profile as well as bunch length measurement during ramping. There will be a synchrotron light port in the BTS transport line to observe the injection beam behavior during top-up operation.

INTRODUCTION

The ultra high brightness NSLS-II storage ring is under construction at Brookhaven National Laboratory. It will have 3GeV, 500mA electron beam circulating in the 792m ring, with very low emittance (0.9nm.rad horizontal and 8pm.rad vertical). The ring is composed of 30 DBA cells with 15 fold symmetric. Three damping wigglers will be installed in long straight sections 8, 18 and 28 to lower the emittance [1]. While electrons pass through the bending magnet, synchrotron radiation will be generated covering a wide spectrum. There are other insertion devices in the storage ring which will generate shorter wavelength radiation as well. Since the NSLS-II visible diagnostic beam line will use the radiations from bending magnet, we will discuss the dipole radiation only in this paper.

Synchrotron radiation has been widely used as diagnostic tool to measure the transverse and longitudinal profile. Three synchrotron light beam lines dedicated for diagnostics are under design and construction for the NSLS-II storage ring: two x-ray pin-hole camera beam lines with the source points from Cell 24 BM_A (first bending in the DBA cell) and Cell25 three-pole wiggler; the third beam line is using visible part of radiation from Cell 30 BM_B (second bending magnet from the cell). Pinhole beam lines designs can be found in the paper. [2] Our paper focuses on the design of the visible beam line. Synchrotron light monitors along the injector chain will be discussed as well.

Table 1 lists major parameters related to the NSLS2 storage ring

Parameter	Value	Unit	Comment
General machine parameters			
E	3	GeV	Energy
f_{rf}	499.68	MHz	RF freq.
h	1320		har. #
f_{rev}	378.55	kHz	
T_{rev}	2.64	μs	
C	791.96	m	
I	500	mA	
ε_x	0.9	nm.rad	with 3 DW
ε_y	0.008	nm.rad	
σ_E/E	0.09%		with 3 DW
Bending magnet parameters			
ρ	25.02	m	bending radius
B	0.4	Tesla	
E_c	2.4	keV	
λ_c	0.52	nm	
Bunch length related			
Vc	3.1	MV	
U0	287	keV	bend loss
	674	keV	total loss with 3DW
α	3.63E-4		
fs	3.32	kHz	
σ_t	15.66	ps	RMS bunch length
Beam size related			
β_x	2.7763	m	
β_y	19.5252	m	
η_x	0.1370	m	
σ_x	133.05	μm	
σ_y	12.50	μm	

SOURCE POINT

NSLS-II ring has 30 DBA cells, each cell has two bending magnets which bend the electron beam 6-deg each. Synchrotron radiation extracted from the beginning of bending magnets, with horizontal opening angle 0 to 4.25mrad. The nominal source point for user's beam line is 2.125mrad +/- 1.5mrad. To use the same extraction configuration is highly desired for the visible diagnostic beam line. Synchrotron radiation from the dipole has natural open angle depending on the radiation wavelength. With longer wavelength, the synchrotron radiation from dipole will have larger natural open angle. See Equation (1). For the 500nm green light, which will be used on the optic table for various measurements, the natural opening angle is ~1.2mrad. To avoid the bending magnet edge radiation, the diagnostic beam line horizontal aperture was selected from 1.25mrad to 4.25mrad. Edge radiation has been investigated and 1.25mrad is large enough to avoid the edge radiations at visible light range. On the other hand, edge radiations can be a useful diagnostic tool. We keep the option to move the aperture to intercept these kinds of radiations.

CONTINUOUS BUNCH-BY-BUNCH 16-BIT DATA ACQUISITION USING DDR2 SDRAM CONNECTED TO AN FPGA*

J. Weber, M. Chin, LBNL, Berkeley, CA, U.S.A.

Abstract

A hardware system that acquires and stores a large buffer of bunch-by-bunch 16-bit data has been realized. A high resolution (up to 16-bit) analog-to-digital converter (ADC), or bank of ADCs, samples the analog signal at the bunch frequency. The digitized data is fed into a Field Programmable Gate Array (FPGA), which contains an interface to a bank of Double Data Rate SDRAM (DDR) type memory. With appropriate data bus widths, the FPGA bursts the ADC data into the DDR fast enough to keep up with the bunch-by-bunch ADC data continuously. The realized system demonstrates continuous data transfer at a rate of 1GByte/sec, or 16-bit data at 500MHz, into a 64MByte DDR. This paper discusses the implementation of this system and the future of this architecture for bunch-by-bunch diagnostics.

INTRODUCTION

For many years, beam motion in particle accelerators has been understood well enough to design bunch-by-bunch feedback systems capable of stabilizing the beam. Until recently, these systems lacked the diagnostic capability to monitor the RMS motion of each bunch and store it continuously for an extended period. This information can be used to compute the various coupled bunch modes of oscillation. Monitoring the strength of each mode over time can provide valuable insight that could ultimately be used to better stabilize the beam. High bit resolution is desirable to increase the accuracy of the modal analysis.

One method of capturing long records of high resolution bunch-by-bunch data is digitizing the beam signal with one or several high resolution ADCs, sending the data to a high performance FPGA to pack into a buffer in a large DDR or bank of DDRs (see Figure 1). Only recently has the combination of ADC/FPGA/DDR technologies achieved the performance required to make such a measurement on an accelerator beam with a bunch rate of 500MHz or greater, such as at the Advanced Light Source (ALS).

A new transverse feedback system (TFB) is under development at the ALS that includes hardware capable of performing large bunch-by-bunch captures [1]. We have developed firmware for the FPGA that demonstrates the ability to capture up to 16-bit data at 500MHz and store it in a 64MB DDR, giving us the ability to capture over 15ms of continuous bunch-by-bunch data. This paper describes the hardware requirements and firmware options to achieve the measurement, as well as an example targeted for the ALS TFB and the NSLS-II RF BPM, and the future of this technology for bunch-by-bunch measurements.

* This work was supported by the Director, Office of Science, Office of Basic Energy Sciences, of the U.S. Department of Energy under Contract No. DE-AC02-05CH11231.

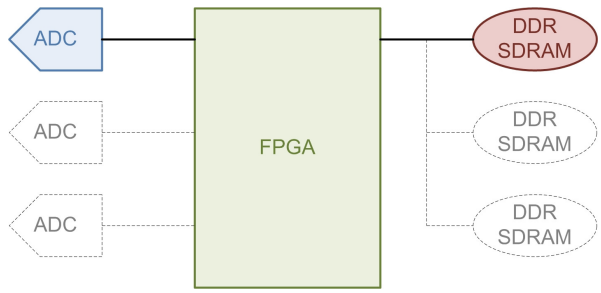

Figure 1: ADC-FPGA-DDR model for bunch-by-bunch data acquisition.

HARDWARE REQUIREMENTS

To capture bunch-by-bunch data, the effective sampling rate of the ADC circuit must match the maximum bunch rate of the accelerator. This can be accomplished by using a single ADC if the sampling rate and bit resolution are sufficient, or by time-interleaving samples from multiple ADCs. Ideally, a single ADC is used to eliminate sources of error caused by multi-ADC sampling, such as phase and amplitude mismatch and thermal drift. The ALS TFB system requires 12-bit resolution and 500Msps sampling, but at the time no single ADC was available that met those requirements. Instead, two 12-bit ADCs are used, each sampling at 250Msps and clocked 180 degrees out of phase to achieve an effective sampling rate of 500Msps.

The FPGA must be able to clock the related logic fast enough to process all the ADC data continuously. In a single ADC system, the FPGA must be clocked at the full bunch rate, unless the ADC has multiple parallel output data buses. In a multi-output ADC or multi-ADC system, the FPGA clock rate can be reduced since the data can be processed in parallel, although this uses additional logic resources. In practice, it is recommended to clock the FPGA well below its specified maximum clock rate since the amount of logic used in the FPGA is large enough that routing at such high frequencies becomes problematic or impossible. The ALS TFB uses a Xilinx Virtex-5 LX50 speed grade -1 FPGA clocked at 250MHz to match the ADC sampling rate, well below the FPGA maximum output clock frequency of 450MHz [2].

The FPGA provides the clock and control interface to the DDR chips, which all must be clocked synchronously and fast enough to transfer the ADC data continuously. At the basic level, the DDR theoretical bandwidth can be calculated by multiplying the maximum allowable DDR clock rate by 2, then by the data bus width. For the ALS TFB, which uses a DDR2 with maximum clock rate of 200MHz [3], the theoretical bandwidth is 200MHz × 2 ×

ACHIEVING HIGH-SPEED DATA ACQUISITION FOR REAL-TIME BEAM CONTROL AND MEASUREMENT

R. Soden, Y. Maumary, P-F. Maistre, Agilent Technologies SA, Plan-les-Ouates, Switzerland
S. Narciso, G. Hill, Agilent Technologies, Inc. Loveland, CO, U.S.A.

Abstract

Digital data acquisition in real-time applications falls into two categories: digitizing a stream of data without missing a single sample point, and capturing a stream of triggered events without missing a single trigger.

Maintaining these data streams over long periods requires an optimized combination of analog signal conditioning, precise digitization, digital data reduction and high-speed data transfer. This paper describes suggested methods to reduce the amount of measurement data required, reduce the amount of that data that is to be transferred to a measurement where possible, and then transferring this reduced data in the most rapid fashion. Our approach uses a combination of hardware, firmware and software elements that are designed to work together, optimizing performance and managing the data bottlenecks.

New hardware standards and architectures are discussed that improve the capabilities of today's technologies, providing access to higher data and measurement flux. Applications presented in this paper include high trigger rate capture for beam steering and fill pattern monitoring in charged particle accelerators.

THE KEY ASPECTS OF REAL-TIME MEASUREMENT

Measurement in real time requires a constant flow of accurate data. Maintaining the flow and the accuracy of the data transferred requires specific considerations to the techniques used.

Accurate measurement

Measuring once takes half the time of measuring twice! But to have confidence in a measurement means using equipment that is properly specified and meets those specifications.

These specifications need to go beyond the banner specifications of Bandwidth, Sampling rate, Resolution, and into the secondary specifications that talk of distortion and noise, which deteriorate signals and measurement.

Figure 1 shows the how noise and distortion are typically specified for high-speed digitizers. There are a number of surprising interactions between performance aspects that contribute to diminish the accuracy of the final acquisition. The effective number of bits (ENOB) antonymous to signal to noise and distortion (SINAD), provides a good measure of how all other performance aspects add up to the quality of the measurement of the final system.

Previous work has discussed noise and distortion in detail[1]. Unfortunately there is no simple answer to the question "Which digitizer should I use in my system?" Instead, each application and device must be reviewed on a case-by-case basis, with a view to optimizing the required measurement.

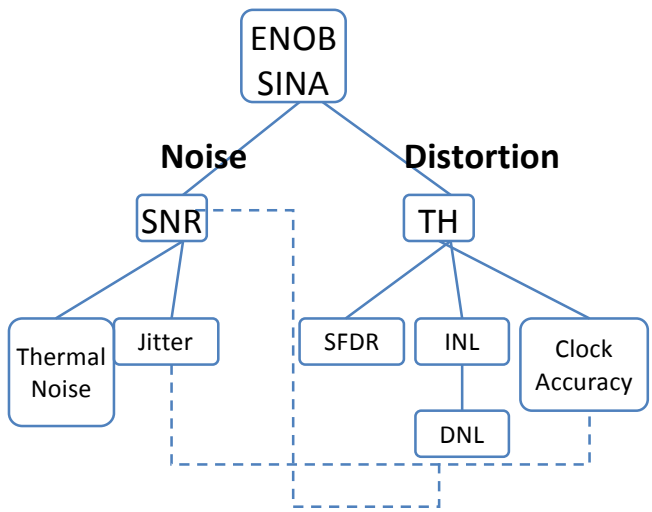

Figure 1: Noise and distortion specifications.

Data reduction

Smart handling of the acquired data on the card can reduce the amount of data that needs to be transferred to the system.

Segmented acquisition of only required data is the first step (trigger, delay, acquisition of pre-determined length vs, trigger, acquire), thus acquiring only the required data, not the preamble and post-acquisition data.

Data processing within on-board field programmable gate arrays (FPGAs) can be used on the module to reduce data down to a measurement.

Peak detection identifies peaks and troughs in data, outputting only peak heights and peak times, rather than the entire data waveform.

Waveform averaging captures repetitive signals and averages them to remove random noise.

Real time FFT processing reduces a temporal signal into its frequency power spectrum.

Data transfer

Optimized data transfer is achieved through the mix of how the data is transferred, and the bus over which the data is passed.

TUNING THE BEAM: A PHYSICS PERSPECTIVE ON BEAM DIAGNOSTIC INSTRUMENTATION *

M.S. Gulley#, Los Alamos National Laboratory, Los Alamos, NM 87545, U.S.A.

ABSTRACT

In a nutshell, the role of a beam diagnostic measurement is to provide information needed to get a particle beam from Point A (injection point) to Point B (a target) in a useable condition, with 'useable' meaning the right energy and size and with acceptable losses. Specifications and performance requirements of diagnostics are based on the physics of the particle beam to be measured, with typical customers of beam parameter measurements being the accelerator operators and accelerator physicists. This tutorial will be a physics-oriented discussion of the interplay between tuning evolutions and the beam diagnostics systems that support the machine tune. This will include the differences between developing a tune and maintaining a tune, among other things. Practical longitudinal and transverse tuning issues and techniques from a variety of proton and electron machines will also be discussed.

MOTIVATION

This is intended to be an 'end-user perspective', with the view that the accelerator operator and accelerator physicist are the primary users of beam diagnostic instrumentation. This is also intended to be a comparison of machines, not just a "LANSCE" talk. If this works, it will trace my experiences in going from an experimenter to an accelerator physicist to supervising operators to supervising beam diagnostic instrumentation personnel.

WHO IS THE TUNER?

To begin a discussion of this nature, one first must ask what is meant by a 'physics perspective'. As I struggled with this question, the first thing that I realized was that to understand such a perspective, one must begin by understanding the user.

Is there such a thing as a typical accelerator physicist? Of course not. However, there are certain commonalities. Let us start out with education. The education of most accelerator physicists comes from a couple of different areas. The first area is, of course, formal education and/or training in accelerator physics. This, actually, is not a common thing to find, at least in my experience. I performed an informal poll of my colleagues at and beyond the Los Alamos Neutron Science Center (LANSCE), which is where I work, and found a decided lopsidedness to the origins of many of the physicists there. Jeff Kolski is a graduate student from Indiana University working on his thesis performing studies of our Proton Storage Ring (PSR). So, he is developing the background one might expect from an 'accelerator physicist'; accelerator physics. Yuri Batygin, new to our Operations Physics Team, is also formally trained in accelerator physicst in the former USSR.

Now let's look at the other end of the scale, starting with me. I came from a background of accelerator-based atomic physics. Several of my colleagues, such as Larry Rybarcyk, Rod McCrady, Chandra Pillai, Glen Johns, and Thomas Spickermann all were experimental nuclear and/or particle physicists. Many of us landed at some point in our careers here at the accelerator to do experimental physics and eventually ended up moving over into the operation, design and modeling of accelerators. I have had numerous conversations where one of us would point to an area and make a comment about the first experiment we were involved in here.

The next question is "what, if anything, does this mean?" One thing that it means is that the odds are against the average physics graduate student walking into a physics program that has accelerator physics as a subject area. That is not surprising. I did an informal search for physics programs that included accelerator physics and found fewer than ten institutions in the US that offered programs of various types in fields of accelerator physics or beam physics. This is compared to institutions that number in the rough range of three hundred or so that offer graduate studies in physics.

The next question that can be asked is about the other major brand of accelerator tuner, the accelerator operator. Operators come from a different mold than the physicist does, typically. So, where does the typical operator come from? This question is as least as machine dependent as the first one. At LANSCE, many of the operators have a background of having served in the Navy's Nuclear Power School. This is the school that trains sailors and civilians for shipboard nuclear power plant operation and maintenance of naval nuclear ships and submarines. These 'navy Nukes' have several of the qualities needed for accelerator operation. They have experience with large, complex systems. They, in fact, have experience with large, complex systems that will kill you if you do not pay attention to what you're doing. They have experience with radiological environments. They have strong technical backgrounds.

LANSCE has also had some success with hiring operators with backgrounds in nuclear power plant operation. Another area that LANL has explored has been 'local talent'. What has been done is to go out and find qualified candidates who are in a local electrical/mechanical technician program and have them do an apprenticeship at the accelerator.

*Work supported by the Department of Energy (DOE) under Contract No. DC-AC52-06NA25396. (LA-UR-10-02861)
#gulley@lanl.gov

ION BEAM PROPERTIES AND THEIR DIAGNOSTICS FOR ECR ION SOURCE INJECTOR SYSTEMS

D. Leitner, LBNL, Berkeley, CA 94720, U.S.A

Abstract

Electron Cyclotron Resonance (ECR) ion sources are essential components of heavy-ion accelerators due to their ability to produce the wide range of ions required by these facilities. The ever-increasing intensity demands have led to remarkable performance improvements of ECR injector systems mainly due to advances in magnet technology as well as an improved understanding of the ECR ion source plasma physics. At the same time, enhanced diagnostics and simulation capabilities have improved the understanding of the injector beam transport properties. However, the initial ion beam distribution at the extraction aperture is still a subject of research. Due to the magnetic confinement necessary to sustain the ECR plasma, the ion density distribution across the extraction aperture is inhomogeneous and charge state dependent. In addition, the ion beam is extracted from a region of high axial magnetic field, which adds a rotational component to the beam, which leads to emittance growth. This paper will focus on the beam properties of ions extracted from ECR ion sources and diagnostics efforts at LBNL to develop a consistent modeling tool for the design of an optimized beam transport system for ECR ion sources.

INTRODUCTION

Because of their versatility, reliability, and their ability to produce ions throughout the periodic system ECR ion sources have become the injector of choice for many heavy ion facilities. Furthermore, the development and refinement of ECR ion sources over the last three decades has provided remarkable improvements in their performances. For example in 1974, the first ECR ion source Supermafios produced 15 eμA of O^{6+}, 30 years later in 2003 the VENUS (Versatile ECR ion source for Nuclear science) ECR ion source produced 2.8 emA of O^{6+}. These remarkable improvements were made possible by advances in permanent magnet strengths, and ECR design technology. The main driving components for improving the performance of ECR ion sources were formulated in Geller's famous ECR scaling laws, stating that higher magnetic fields and higher frequencies will increase the performance of ECR ion sources. Following these scaling laws a series of ECR ion sources were developed using normal conducting magnet technology and permanent magnets. In the last decade with advances in superconducting magnet technology, the next generation of high field superconducting sources has been developed utilizing frequencies of 24 to 28 GHz and magnetic confinement fields of several Tesla. These third generation superconducting ECR sources are now the injector of choice for next generation heavy ion facilities such as the Radioactive Ion Beams Factory (RIBF) at RIKEN, and the Facility for Rare Isotopes (FRIB) proposed to be built at Michigan State.

The magnetic fields in an ECR ion source serve both to confine the plasma and to provide a closed surface where the microwave can heat the electrons through electron cyclotron resonance. In most ECR ion sources the magnetic confinement fields are produced by combining a radial sextupole field with an axial mirror field, which provides a magnetic field increasing in both radial and axial directions. This "minimum-B" field configuration produces stable and dense plasmas. The magnetic field strength must be optimized for the selected ECR heating frequency to ensure efficient electron heating in addition to strong confinement. Ideally, the radial field strength should be twice the resonant field. The axial solenoid-mirror field-strength on the injection side of the ion source can be three to four times the ECR resonant field, while it is typically 2 times the resonant field at the extraction end. In case of the VENUS ECR ion source, which has been developed as prototype injector for Facility for Rare Isotopes FRIB and was designed for optimum operation at 28 GHz, the corresponding electron cyclotron resonance field strength is 1 T, but in order to achieve sufficient plasma confinement, the magnetic field at in injection are in the between of 3.5 to 4 T, at extraction 2 to 2.5 T and 2T radially at the plasma wall.

HEAVY ION INJECTOR BEAMS

In the last 10 years, the intensity and charge state requirements for the next generation nuclear science facilities have increased dramatically. For example for FRIB and RIBF, the intensities required for the heaviest ion beams are more than an order of magnitude higher than routinely used at currently operated heavy ion facilities. In particular, uranium beams are one of the most important and challenging beams for these facilities and will be used as an example to describe the characteristics of ion beams produced by ECR ion sources. For both facilities, about 0.5 mA uranium ion current is required from the front end of the driver LINAC (in the case of RIBF as a single charge beam of U^{35+} and in case of FRIB as combined current of U^{33+} and U^{34+}).

Of all currently operating ECR ion sources the fully superconducting ECR ion source VENUS at LBNL has produced the highest uranium intensities to date:

AN INSTRUMENTATION WISH LIST FOR HIGH POWER/HIGH BRIGHTNESS ERLS *

D. Douglas#, Jefferson Lab, 12000 Jefferson Avenue, Newport News, VA 23606, U.S.A.

Abstract

The advent of the energy recovering linac (ERL) brings with it the promise of linac-quality beams generated with near storage ring efficiency. This potential will not, however, be fulfilled without overcoming a number of technical and operational challenges. We will review the basics of ERL dynamics and operation, and give examples of idiosyncratic ERL behavior and requirements posing particular challenges from the perspective of diagnostics and instrumentation. Beam performance parameters anticipated in next-generation ERLs will be discussed, and a "wish list" for the instrumentation of these machines presented.

"TRADITIONAL" ACCELERATORS

Energy Recovering Linacs [1] comprise a class of electron accelerators using novel architecture to generate outstanding beam quality with high wall plug efficiency. Initially conceived almost half a century ago [2] and first realized a decade later in a reflectively symmetric geometry [3], contemporary ERLs are most easily understood as an evolution of the recirculating linac [4].

"Traditional" accelerators typically fall into one of two classes: synchrotrons (including storage rings and cyclotrons for the purposes of this discussion), or linear accelerators. In synchrotrons, the accelerated beam passes many times through a modest radiofrequency (RF) accelerating system, gaining a small amount of energy on each pass. Most of the accelerator consists of the transport system, which draws little additional power. Storage rings can therefore generate extremely high beam powers using modest wall plug power. In such systems, a few megawatts of RF drive and similar levels of DC power (for the transport system) can be used to generate gigawatts of beam power (e.g. 0.5 A at 2 GeV). As the beam is circulated many times, it is however susceptible to degradation from error sources and beam dynamical effects such as synchrotron radiation. Storage rings, though efficient, thus provide only limited beam quality.

In contrast, linear accelerators (linacs) accelerate the beam rapidly through multiple RF structures using only limited beam transport. Most of the required power is therefore devoted to RF drive; moreover, in conventional (normal conducting) linacs, the final beam power is typically limited by wall losses in the accelerating structures. For example, a linac with a megawatt of RF drive (with very modest DC power for additional beam transport use) will produce at most a megawatt of beam power (e.g. 50 μA at 20 GeV). Linacs are thus electrically inefficient - but as the beam is only in the machine for a single pass though the accelerator (and there is little or no bending) the beam quality does not degrade: performance is source limited. It is thus possible to generate very high quality beams – an advantage that outweighs the power inefficiency in many applications. The high beam quality (brightness) provided by linacs has motivated efforts to make them more cost effective. As a consequence, numerous methods are available to control cost, improve efficiency, and enhance the performance of these systems.

RECIRCULATION, SUPERCONDUCTING RF, AND ENERGY RECOVERY

Recirculation provides a simple means of controlling linac cost while maintaining final energy: simply "reuse" the linac accelerating structure multiple times, thereby reducing the required length. In a "recirculating" linac, the beam is transported from the end of the linac back to the front, and reinjected in phase with the RF fields for further acceleration. This approach leverages the low cost of beam transport relative to RF, so that the cost/performance optimum for a system lies somewhere between "straight" and "circular". The result [5] (Figure 1) is a system of lower cost than a conventional linac, but which provides better beam quality than a storage ring.

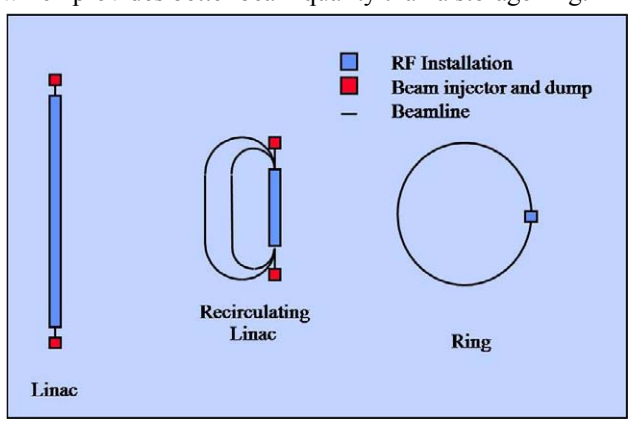

Figure 1: Evolution of conventional accelerator topology into that of the recirculating linac [6].

Superconducting RF (SRF) acceleration [7] provides a second means of linear accelerator cost/performance optimization. SRF cavities have essentially no wall losses and allow high gradient continuous-wave (CW) operation. This reduces the RF power required to reach a specific energy, increases average current, and significantly improves beam quality by avoiding the transients inherent in pulsed RF systems. The resulting reduction in RF power demand is sufficient to offset the cost of the

*Work supported by the Commonwealth of Virginia, the Air Force Research Lab, the Joint Technology Office, the Office of Naval Research, and by DOE Contract DE-AC05-060R23177.
#douglas@jlab.org

LANSCE BEAM INSTRUMENTATION AND THE LANSCE REFURBISHMENT PROJECT

R. C. McCrady, B. Blind, J. D. Gilpatrick, C. Pillai, J. F. Power, L. J. Rybarcyk, J. Sedillo, M. Gruchalla, Los Alamos National Laboratory, Los Alamos, NM 87544, U.S.A.

Abstract

The heart of the LANSCE accelerator complex consists of Cockroft-Walton-type injectors, a drift-tube linac (DTL) and a coupled-cavity linac (CCL). These systems are approaching 40 years of age and a project to re-establish high-power capability and to extend the lifetime is underway. Many of the present beam diagnostic systems are difficult to maintain, and the original beam position monitors don't provide any data at all. These deficiencies hamper beam tuning and trouble-shooting efforts. One thrust of the refurbishment project is to restore reliable operation of the diagnostic systems. This paper describes the present diagnostic systems and their limitations and the envisaged next-generation systems. The emphasis will be on the uses and requirements for the systems rather than the solutions and engineering aspects of the refurbishment.

INTRODUCTION

Figure 1 is a diagram of the accelerator complex at the Los Alamos Neutron Science Center (LANSCE). Presently protons and H^- ions are delivered to five experimental areas. The facility was originally designed for performing nuclear physics experiments with pions, muons and protons as probes with a primary beam power of 1MW. We currently produce about 125kW of beam power at one-half of the original duty factor due to a change of mission and aging of the system. The LANSCE-R (refurbishment) project aims to restore the higher-power operation and to ensure the on-going reliable operation of this accelerator facility.

One thrust of the LANSCE-R project is to extend the lifetime and restore reliable operation of the beam diagnostic systems in the linac. Some of the present systems are difficult to maintain, and the original beam position monitors (BPMs) do provide any data at all.

The large beam power and the various beam time-structures required at the experimental areas provide challenges in making diagnostic systems that can be used for production operations. The following sections describe the various beam conditions that drive the requirements for performance of the diagnostic equipment.

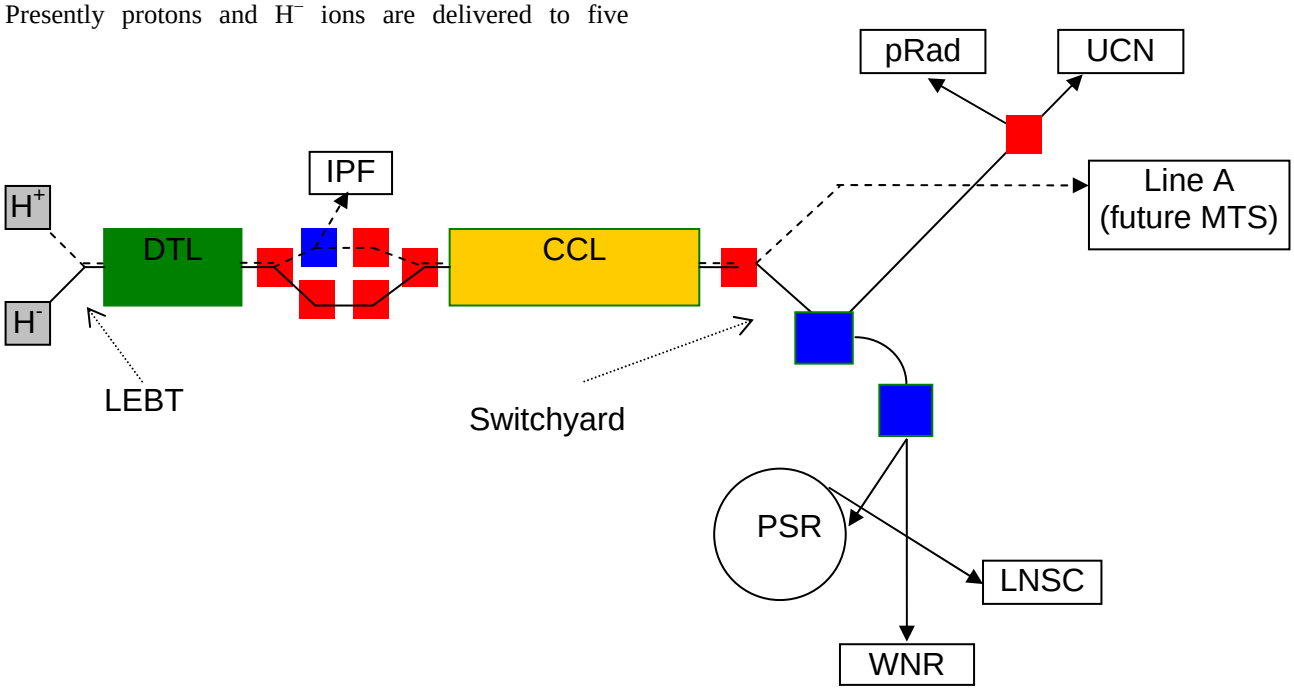

Figure 1: Schematic depiction of the LANSCE accelerator and experimental areas. Proton (H^+) beam lines are shown as dashed lines and H^- beam lines are shown as solid lines. The Low-Energy Beam Transport (LEBT) merges the two beam species and directs them into the linac. The beam switchyard, just downstream of the linac, directs beam to the various experimental areas. Blue squares denote pulsed magnets for switching beam delivery on a per macropulse basis. The experimental areas are: IPF: Isotope Production Facility; pRad: Proton Radiography; UCN: Ultra-Cold Neutrons; MTS: Materials Test Station (under development); LNSC: Lujan Neutron Scattering Center; WNR: Weapons Neutron Research. The beam to the LNSC is compressed in the Proton Storage Ring (PSR).

DEVELOPMENT OF BEAM CURRENT MONITOR WITH HIGH-Tc SQUID AT RIBF

T. Watanabe*, N. Fukunishi, Y. Sasaki, M. Kase, A. Goto and O. Kamigaito
RIKEN Nishina Center for Accelerator-Based Science, Wako-shi, Saitama 351-0198, Japan

Abstract

A highly sensitive beam current monitor with a high-critical-temperature (high-Tc) superconducting quantum interference device (SQUID) and a high-Tc current sensor, that is, a high-Tc SQUID monitor, has been developed for use in the radioisotope beam factory (RIBF) at RIKEN. As reported in the present work, the high-Tc SQUID monitor allows us to measure the DC of high-energy heavy-ion beams nondestructively in such a way that the beams are diagnosed in real time and the beam current extracted from the cyclotron can be recorded without interrupting beam user experiments. Both the high-Tc magnetic shield and the high-Tc current sensor were fabricated by dip-coating a thin layer of Bi_2-Sr_2-Ca_2-Cu_3-O_x (2223-phase, Tc=106 K) on a 99.9% MgO ceramic substrate. Unlike other existing facilities, all the high-Tc devices are cooled by a low-vibration pulse-tube refrigerator, enabling us to downsize the system. Last year, aiming at its practical use, the high-Tc SQUID monitor was installed in the RIBF. Using the monitor, a 1 μA Xe beam intensity (50 MeV/u) was successfully measured with 100 nA resolution. Here we report the present status of the facility, details of the high-Tc SQUID monitoring system and the results of the beam measurement.

INTRODUCTION

Accelerator complex of RIBF

The RIBF project to accelerate all elements from hydrogen to uranium up to an energy of 440 MeV/u for light ions and 350 MeV/u for heavy ions started in April 1997 [1]. Figure 1 shows a schematic layout of the RIBF facility. The research activities in the RIBF project make extensive use of the heavy-ion accelerator complex, which consists of one linac and four ring cyclotrons, i.e., a variable-frequency linac (RILAC), the RIKEN ring cyclotron (RRC), a fixed-frequency ring cyclotron (fRC), an intermediate-stage ring cyclotron (IRC) and a superconducting ring cyclotron (SRC). Energetic heavy-ion beams are converted into intense RI beams via the projectile fragmentation of stable ions or the in-flight fission of uranium ions using a superconducting isotope separator, BigRIPS [2]. The combination of these accelerators and BigRIPS is expected to greatly expand our knowledge of the nuclear world into the presently inaccessible region on the nuclear chart. We succeeded in accelerating a uranium beam to 345 MeV/u in March 2007, by which new RIs, the neutron-rich palladium isotopes of $_{125}$Pd and $_{126}$Pd, were discovered [3, 4].

In 2008, the RIBF succeeded in providing heavy-ion beams of $_{48}$Ca and $_{238}$U with particle currents of 170 pnA and 0.4 pnA, respectively, at an energy of 345 MeV/u. The search for new isotopes using in-flight fission of the 345 MeV/u uranium beam has continued. Consequently, fission fragments have been analyzed and identified using BigRIPS and we have observed 45 new neutron-rich isotopes. From the operational point of view, however, the intensity of the uranium beam should be greatly increased. Furthermore, RIBF research conflicts with ongoing research on the synthesis of super-heavy elements using a gas-filled recoil separator (GARIS), because both of them use the RILAC. To reconcile this conflict, a new additional injector linac for the RIBF (RILAC2) has been proposed and is now under construction. We have therefore constructed a superconducting electron cyclotron resonance (ECR) ion source that is capable of providing a microwave power of 28 GHz, a radio frequency quadrupole (RFQ) linac and three drift tube linacs (DTLs). The new injector, which will be ready in FY2010, will hopefully enable the independent operation of the RIBF experiments and research on super-heavy element synthesis [5].

Technical issues related to Faraday cups

It is essential to keep the beam transmission efficiency as high as possible, because the production of the RI beam requires an intense primary beam during beam user experiments. Furthermore, activation produced by beam loss should be particularly avoided. In this facility, to evaluate the beam transmission efficiency, about 50 Faraday cups are used. A Faraday cup is used in the conventional method of measuring the beam current. However, the beam cannot be used while it is being measured, and there is a danger of melting and activating the cup. Furthermore, it is difficult to completely suppress the high-energy secondary electrons that are produced by heavy-ion beams. When an accelerated particle collides with the surface of a Faraday cup, secondary electrons are always generated. If these electrons escape from the insulated cup area, the reading of the beam current is incorrect by the number of lost electrons. Thus, the suppression of secondary electrons is very important for measuring the beam current precisely. Normally, this can be achieved by applying a high negative voltage close to the entrance of the cup. However, since the electrical field on the beam axis is lower

* wtamaki@riken.jp

OVERVIEW ON E-XFEL STANDARD ELECTRON BEAM DIAGNOSTICS

D. Nölle, DESY, D-22607 Hamburg, Germany, for the XFEL Team

Abstract

The European XFEL is a 4th generation synchrotron radiation source, under construction in Hamburg [1,2]. Based on different Free-Electron Laser and spontaneous sources, driven by a 17.5 GeV superconducting accelerator, it will be able to provide several user stations with photons simultaneously. Due to the superconducting technology high average as well as peak brilliance can be produced. Flexible bunch pattern will allow for optimum tuning to the experiments demands. This paper will present the current planning of the electron beam diagnostics. An overview of the entire system will be given, as well as detailed insight into the main diagnostic systems, like BPM, charge and transmission diagnostics, beam size and beam loss monitor systems.

INTRODUCTION

The European XFEL (E-XFEL) is an international X-ray Free-Electron Laser user facility currently under construction close to DESY in Hamburg. The facility is constructed and will be operated by a limited liability company with shareholders from currently 12 counties.

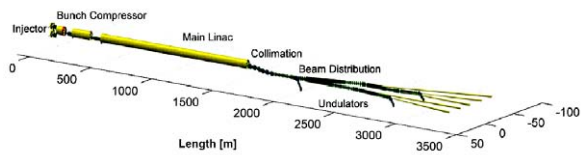

Fig. 1: Sketch of the layout of the E-XFEL.

DESY acts as the host laboratory and leads the accelerator consortium, that is in charge for the construction of the accelerator. Like FLASH [3] E-XFEL will be based on superconducting TESLA RF technology. Therefore, it can provide high duty cycles. Electron beams with pulse lengths up to 600 µs and a bunch repetition rates up to 4.5 MHz will be accelerated up to 17.5 GeV at a RF repetition rate of 10 Hz*. The shortest FEL wavelength will be 0.1 nm corresponding to photon energies of about 10 keV. To make optimum use of the high duty cycle, the long bunch trains can be distributed into 2 SASE undulator lines, which will be ramified into additional lines for "secondary undulators" that make use of the spent beam producing either FEL or spontaneous radiation. In a first phase up to 5 beam lines can be served simultaneously. The time structure of the beam can be adjusted independently for both main SASE undulators (SASE I and SASE II) by means of a kicker/septum scheme in the beam distribution system.

* At lower gradient even higher rep rates are possible.

Table 1: Design Beam Parameters of E-XFEL

Parameter	Value	Unit
Maximum energy	17.5	GeV
normalized emittance	1-2	mm mrad
typical beam sizes (RMS)	20-200	µm
bunch charge	0.1-1	nC
min. bunch spacing	222	ns
max. macro-pulse length	600	µs
bunches within macro-pulse	1 - 2700	
bunch pattern	arbitrary	
RF repetition rate	< 30	Hz

The facility starts at the DESY site. Close to the HERA cryo-plant that is going to be refurbished, the injector building and the entry shaft is under construction. From this building a tunnel, 6-20 m below surface, will head towards North West to the directions of Schleswig-Holstein. After about 2 km a shaft building is located, where the main tunnel splits up into the tunnels of the two main undulators, that further down split up into the 5 undulator and photon tunnels heading towards the experimental hall, located about 3.4 km after the gun.

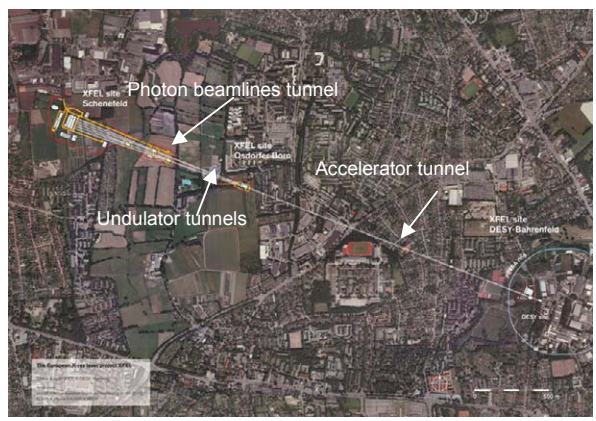

Fig. 2: Birds view of the E-XFEL site. DESY is marked by the PETRA III ring.

The current status of the facility can be described as follows: Groundbreaking for the civil construction took

ELECTRO OPTICAL SAMPLING OF COHERENT SYNCHROTRON RADIATION FOR PICOSECOND ELECTRON BUNCHES WITH FEW pC CHARGE

F. Müller, B. Steffen#, V. Schlott (PSI, Villigen, Switzerland)
Pavel Chevtsov (JLAB, Newport News, Virginia)

Abstract

Electro Optical (EO) sampling is a promising nondestructive method for measuring ultra short (sub-ps) electron bunches. The FEMTO slicing experiment at the Swiss Light Source modulates about 3 pC of the 5 nC electron bunch longitudinally. The coherent synchrotron radiation (CSR) emitted by this substructure was sampled by 100 fs long pulses from an Yb fiber laser in EO crystals of gallium phosphide. The broadening of this ps long structure over four turns of the synchrotron could be measured with sub-ps resolution.

INTRODUCTION

Femto slicing [1] is a technique to manipulate the temporal profile of a long (some 10 ps) electron bunch in a storage ring with a short pulse laser (100 fs). The very high electric field of the laser pulse (up to 10^9 V/m) modulates the energy of the electrons in a slice of the length of the laser pulse. After the first dispersive section this pure energy modulation is transferred into a longitudinally one. The resulting electron distribution consists of two humps containing the low and the high energy sliced electrons and a central dip, from where the sliced electrons have been removed (see Fig. 1). The dip will lead to an enhancement of synchrotron radiation in the millimeter wavelength range (THz) emitted at following dipole magnets of the storage ring.

To measure the time structure of synchrotron radiation pulses electro optical measurement techniques, developed for electron bunch length measurements, can be used. These techniques employ birefringence an electric field induces in an electro-optically active crystal like gallium phosphide (GaP) to transfer the time structure of the electric field onto a laser pulse which can be measured with fs accuracy. It has been shown that sub-ps electron bunches of some 100 pC charge can be measured with about 200 fs resolution applying the spectral decoding technique [2, 3] by using the Coulomb field of the relativistic electron bunch directly. By imaging and focusing the coherent radiation emitted from the electron bunch onto the crystal, the resulting field strength can be enhanced leading to larger EO signals [4].

In this paper we present results of the first direct measurements of coherent synchrotron radiation pulses from the sliced electron bunches at the Swiss Light Source (SLS) in time domain. We applied the technique of electro optical spectral decoding using a ytterbium fiber laser [5] which has been synchronized to the SLS rf master clock.

#present address: DESY, Germany, email: bernd.steffen@desy.de

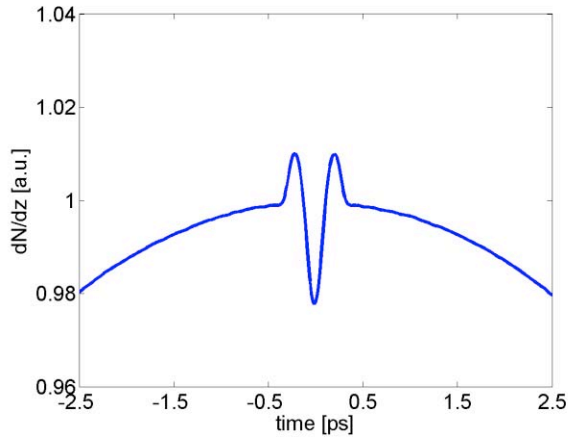

Figure 1: Charge distribution of the sliced electron bunch at the SLS right after the slicing.

FEMTO-SLICING AT THE SLS

The FEMTO slicing setup at the SLS is used to generate sub-ps hard x-ray pulses for pump-probe experiments at the μ XAS beam line. The slicing setup consists of a modulator (wiggler) for energy modulation, chicane dipoles for pulse separation, and a radiator (in-vacuum undulator).

A laser pulse from a regenerative Ti:Sa amplifier (30 fs rms, 2 kHz, 2.5 mJ, 800 nm) overlaps with the co propagating electron bunch in the modulator and induces an energy exchange between the laser pulse and the electron bunch. Depending on the relative phase between the two pulses, the electrons can either gain or loose energy. Since the electron bunch in the SLS storage ring is about 35 ps (rms) long, only a small number of electrons is energy modulated. According to simulations, a laser pulse energy of 2 mJ provides a maximum energy modulation of 1% (24 MeV) within this slice. The core bunch contains 5 nC and the slicing efficiency is about $6 \cdot 10^{-4}$ which leads to a charge of the modulated particles of approximatly 3 pC.

The chicane between modulator and radiator induces a spatial (±2 mm) and angular (±0.5 mrad) horizontal offset of the sliced beam at the radiator center which is used to separate the fs x-ray pulse for the ps background in the μ XAS beam line. Additionally the chicane is a dispersive element which transfers the pure energy modulation in to a longitudinally one which is slightly broader than the initial modulation. X-ray diffraction measurements on high-amplitude phonon dynamics of photoexcited

BEAM HALO IMAGING USING AN ADAPTIVE OPTICAL MASK*

H. D. Zhang, R. B. Fiorito#, A. G. Shkvarunets, S. Bernal, I. Haber, R. A. Kishek, P. G. O'Shea,
University of Maryland, College Park, MD, USA
S. Artikova, MPI- Heidelberg, Heidelberg, Germany
C. Welsch, Cockcroft Institute, University of Liverpool, Liverpool, UK

Abstract

We have developed a technique that employs a digital micro-mirror array to produce an image of the halo of an electron beam with an enhanced dynamic range. Light produced by the beam intercepting a phosphor screen is first imaged onto the array; an adaptive mask is created and applied to filter out the beam core; and the result is reimaged onto an intensified CCD camera. We describe the optics used, the masking operation and preliminary results of experiments we have performed to study beam halo at the University of Maryland Electron Ring.

INTRODUCTION

Beam halo in intense beams is a phenomenon typically caused by parametric resonances or nonlinear forces due to space charge. It can lead to a number of undesirable effects, such as nuclear activation, emission of secondary electrons, and increased noise in the detectors. For high average power machines, halos can be damaging even if the number of particles in the halo is orders of magnitude below that in the core of the beam [1].

Halo can be observed by imaging visible light emitted by beam particles interacting with various types of screens, e.g. phosphor, YAG, OTR; or with optical synchrotron or edge radiation. However, there is usually an extreme contrast between beam core and halo; the ratio of halo to core intensity can be 10^{-5} or less. Therefore, a high dynamic range imaging system is required to view the details of the halo distribution. Also in any real optical system diffraction and scattering in the lenses due to the high core intensity can contaminate the halo image observed.

To solve these problems, several approaches have been considered. One is to allow the core intensity to saturate the camera. However, with sensitive CCD's and especially intensified CCD's, blooming and possible damage problems exist. Other methods are: passive spatial filtering, e.g. coronagraphy [2]; use of a high dynamic range (28 bit) camera such as the Spectra-Cam CID [3]: and, recently [4], an mask technique based on a digital micro-mirror array (DMA).

The DMA method has the advantages that the mask is adaptive to any shape beam and that a high dynamic range (DR) is achievable with a low cost camera; a DR~10^5 has been previously measured with a laser and a standard 8 bit CCD camera [4]. However, it has also been observed that the DMA produces a cross like diffraction pattern when illuminated by the laser; i.e. the DMA acts like a 2D grating. Since this may have a negative effect in an actual optical system used to image the beam, it is important to test the DMA in such a system.

We have developed an imaging method using a DMA to measure the halo of the electron beam at the University of Maryland Electron Ring (UMER) [5]. UMER is suitable machine to do halo experiments and test the theory of halo formation in space charge dominated beams. The beam is low energy (10 keV) but high current (10's of mA) with a variable pulse length (20-100 ns) and repetition rate (20-60 Hz). Radiation exposure is of minimal concern so that experiments can be easily set up and run *in situ*. Moreover, the beam is quite reproducible and stable over long time periods (hrs).

In the following sections, we will describe the optics system we have developed to image the beam with a DMA, the algorithm to spatially filter the image of the beam, our measurements of the dynamic range and optical performance of the system and finally preliminary beam halo images obtained with an adaptive mask.

EXPERIMENT SETUP

Digital micro-mirror array

The DMA we use is the DMD Discovery 1100 manufactured by Texas Instruments Inc. [6]. This type of device which is widely used in projectors and digital TV's is made up of hundreds of thousands of microscopic mirrors. A segment of the array and a mechanical drawing of one element are shown in Fig. 1(a) and 1(b) [6]. Each mirror on the chip can be individually addressed and rotated to either +12° or -12° with respect to the normal, when a voltage is applied to electrodes situated underneath the corners of each micro-mirror. When the voltage to the DMA is zero, all the mirrors are in a nominally flat, floating state.

Light from an external source can be reflected from mirrors in one state, e.g. $+12^0$, along a desired optical path, while the light reflected by mirrors in the opposite (-12^0) state will be directed 48^0 away from this optical path. When incorporated into an imaging system the device can be used as a spatial light modulator. The parameters of the device are shown in Table 1 [6].

*Work supported by the US Office of Naval Research, the Joint Technology Office and the US Department of Energy.
#rfiorito@umd.edu

DITANET CONTRIBUTING TO STATE-OF-THE-ART DIAGNOSTICS DEVELOPMENTS

C.P. Welsch

University of Liverpool and the Cockcroft Institute, UK

on behalf of the DITANET consortium

Abstract

DITANET is the largest-ever EU funded training network in beam diagnostics. The network members - universities, research centers and industry partners - are developing diagnostics methods for a wide range of existing or future particle accelerators, both for electron and ion beams. This is achieved through a cohesive approach that allows for the exploitation of synergies, whilst promoting knowledge exchange between partners. In addition to its broad research program, the network organizes schools and topical workshops for the beam instrumentation community.

This contribution gives an overview of the Network's research portfolio, summarizes the main research results from the first two years of DITANET and presents past and future training activities.

INTRODUCTION

The DITANET project officially started on 1.6.2008 and consists of ten network beneficiary partners and presently 17 associated and adjunct partners. The training network brings together Universities, research centres, and the industry sector with the aim to jointly train the next generation of young scientists in beam instrumentation.

A core idea of DITANET is that all network members interact and collaborate closely, promote the exchange of trainees and staff within the network, and jointly organize training events, workshops and conferences open also to external participants.

The participation of industry is an integral part of the training within DITANET and all partners from industry are included as members of the supervisory board to ensure that industry-relevant aspects are covered in the different projects carried out within the network and to enhance knowledge transfer. In addition, they offer internships to the students from the network to complement the scientific training and thus actively contribute to building the bridge between the academic and the industrial sector.

RESEARCH

DITANET covers the development of diagnostic methods for a wide range of existing and future accelerators. The developments target beam profile, current, and position measurement. This section presents some of the research outcomes to date.

The Ultra-low Energy Storage Ring

The international Facility for Antiproton and Ion Research (FAIR), to be located at the site of the GSI Helmholtz Centre for Heavy Ion Research in Darmstadt, Germany comprises a series of rings to provide intense beams of antiprotons, unstable exotic nuclei and highly charged ions.

The Facility for Low-energy Antiproton and Ion Research (FLAIR) is based on the need for high-brightness high-intensity low-energy antiproton beams. Antiprotons from the new experimental storage ring (NESR) will be injected into the Low energy Storage Ring (LSR) at an energy of 30 MeV. They will then be cooled and further decelerated to 300 keV energy. The Ultra-Low energy Storage Ring (USR) [1], presently being developed by the QUASAR Group, will provide electron-cooled beams of antiprotons in the energy range between 300 and 20 keV.

These boundary conditions put challenging demands on the USR beam instrumentation. Some important beam parameters are summarized in Table 1.

Table 1: USR beam parameters

Energy	300 keV → 20 keV
Relativistic β	0.025 → 0.006
Revolution frequency	178 kHz → 46 kHz
Revolution time	5.6 µs → 21.8 µs
Intensity	1 µA → tens of fA
RF frequency (h = 10)	1.78 MHz → 459 kHz
Bunch repetition time (h = 10)	560 ns → 2.2 µs
RF bucket length (h = 10)	4.4 m
Charge per bunch (h = 10)	0.3 pC ($2 \cdot 10^6$ pbars)

Depending on whether slow or fast extraction will be applied, the beam intensity and the time structure of the extracted beam will vary in a wide range.

*Work supported by the EU under contract PITN-GA-2008-215080.
#carsten.welsch@quasar-group.org

BEAM LOSS MONITORS (BLMS): PHYSICS, SIMULATIONS AND APPLICATIONS IN ACCELERATORS

A. Zhukov, ORNL, Oak Ridge, TN, U.S.A.

Abstract

Beam loss monitors are common devices used in hadron and lepton accelerators. Depending on accelerator specifics, BLMs could be just diagnostics or could play an essential role in the machine protection system (MPS). This tutorial discusses different types of BLMs and their applicability to different accelerators. It covers traditional BLMs like ionization chambers and scintillator-based devices, and also less common techniques like those based on fiber optics and avalanche diodes. The tutorial gives an overview of the underlying physics involved in beam loss detection, and recent advances in computer simulation of particle interaction with matter helpful for BLM modeling. Options for signal processing electronics are described, as well as interfaces to both the control system and the MPS.

INTRODUCTION

Definition

First we want to define a beam loss and a beam loss monitor. Charged particles are accelerated in accelerators and supposed to follow design trajectory along the beam line. Some of the particles deviate from the prescribed path and hit the beam pipe. They then interact with media and create radiation. So the beam loss is *unintentional* interaction of beam particles with media causing radiation. A beam loss monitor is intended to detect this radiation. Sometimes the particles interact with materials by design; good examples of that are Faraday cups, wire scanners, collimators, scrapers and other insertable devices. The presence of such devices complicates analysis of BLM signals since they add significantly to radiation field around them. In addition, there are other sources of radiation that do not involve direct interaction of primary particles with materials. These sources include synchrotron radiation and cavity X-rays. An ideal BLM should be sensitive to radiation caused by loss and insensitive to other sources of radiation. While one can imagine a beam loss detector that is not a radiation detector we won't discuss such devices in this paper.

BLM Purpose

The ultimate goal of a BLM system is to identify the loss level and if possible, the loss's location and time structure. This could result in a beam abort if the loss level endangers equipment (for example, by burning a hole in a drift tube or quenching a superconducting magnet). It also can provide feedback for better beam tuning. Residual activation is a big problem for high power hadron machines; the BLMs can help to limit that.

General BLM-specific considerations

While beam loss monitors are commonly used as beam diagnostics devices, beam loss is a somewhat standalone topic of beam instrumentation. This is probably due to the nature of the physics processes the BLMs rely on. Other diagnostics devices usually are directly coupled with Accelerator physics and electrodynamics principles. BLMs involve many different parts of physical science, such as: electrodynamics, high-energy particle detectors, nuclear physics, radiation protection, neutron physics, etc. Due to this fact, beam diagnostics overview papers typically mention the physics processes inside BLMs briefly and interpret a BLM as a black box with known parameters and detector response function. We will try to give an overview of radiation detector physics here and refer to corresponding literature for more in-depth information [1,2,3].

The other important fact to consider is the sensitivity of loss monitors to real world geometry. Usually, a BLM is a radiation detector which is placed in an accelerator tunnel in the vicinity of the beam pipe; almost everything that is located nearby could potentially influence the BLM by attenuating (or in some cases increasing) the radiation field measured by the detector. This fact makes detailed analytic calculations of losses almost impossible in any non-ideal case. Fortunately many computer codes exist to address this problem. These codes account for both the vast distribution of involved physics and the complex physical layout of modern accelerators.

BLM PHYSICS ASPECTS

Electromagnetic interaction of charged particles with a medium

As we will see later the interaction of charged particles with materials is the most important thing to consider while designing a BLM. When a charged particle passes through matter, it loses its energy by ionization and atomic excitation. These processes are dictated by the EM interaction between atomic electron and incident charged particle.

The Bethe-Bloch equation is the main formula governing this process:

$$-\frac{dE}{dx} = 0.31\,\frac{MeV}{g/cm^3}\,z^2\,\frac{Z}{A}\,\frac{1}{\beta^2}\left(\ln\frac{2m_e c^2\gamma^2\beta^2}{I} - \beta^2 - \frac{\delta}{2}\right), \quad (1)$$

where Z/A is the ratio of atomic charge and the atomic mass number, z is the charge of the incident particle (in units of electron charge), m_e is the electron's rest mass and I is the ionization potential – a property of the atom; all other variables denote standard relativistic quantities.

HIGHLIGHTS FROM DIPAC 2009

V. Schlott, PSI, Villigen, Switzerland

Abstract

The 9th European Workshop on Beam Diagnostics and Instrumentation for Particle Accelerators (DIPAC 2009) was hosted by Paul Scherrer Institute (PSI) and took place at the Hotel Mercure Conference Center in Basel, Switzerland from May 25th – 27th 2009. A record number of 210 registered participants contributed to an exciting scientific program with ten invited talks, fourteen contributed orals and 118 poster contributions. In this talk, I will provide an overview of the various fields of beam instrumentation, which have been discussed during the workshop. A number of highlights from the scientific program have been selected, illustrating some of the outstanding achievements in accelerator diagnostics, which have been presented at DIPAC 2009.

INTRODUCTION

The DIPAC workshop series represents the European pendant to the biannual Beam Instrumentation Workshop in the US. The 9th DIPAC edition [1] was held by Paul Scherrer Institut (PSI) at the Hotel Mercure Conference Center in Basel, Switzerland from May 25th – 27th 2009. As a strong increase in the number of participants could already been observed at DIPAC 2007 in Venice (189 participants), DIPAC 2009 reached a record number of 206 registered participants presenting 142 contributions (10 invited, 14 contributed talks and 118 poster presentations). Since the workshop duration of 2½ days needed to be kept due to organizational reasons, the program committee decided to omit the parallel discussion sessions in favour of an additional (third) poster session, while providing sufficient time for discussions during the 7 plenary oral sessions. An industrial exhibition, a workshop dinner in Schloss Bottmingen and an optional visit of the accelerator-based large research facilities at PSI completed the workshop program. The scientific program of DIPAC 2009 could be divided into the following categories:

- diagnostics overviews and commissioning experience
- BPM systems and position stability / stabilization
- transverse profile and emittance measurements
- beam charge and loss monitors
- longitudinal diagnostics, timing & synchronization

The vast majority of the presentations were of excellent quality and almost all of the presenters submitted their papers by the end of the workshop, so that the proceedings could be made available over JACoW [2] and in a printed hard copy within 4 months after the event.

For this paper, I have selected highlights from each of the above categories, trying to spread the choices over the different accelerator types and particle species at the same time. Still, the list of the quoted contributions is of course not complete and my personal interest and present field of work has certainly influenced the selection.

COMMISSIONING EXPERIENCE

Almost 20 contributions presented an overview of diagnostics systems for specific accelerators and reported about the first commissioning experiences with their beam instrumentation.

First Experiences with LHC Beam Diagnostics

Rhodri Jones reported on the first results from LHC beam diagnostics, which could be obtained during injection tests and the subsequent days of circulating beam in LHC [3]. Thanks to years of planning, testing, hardware commissioning and excellent collaborations with internal and external groups, all LHC diagnostics devices were available and operational from the very beginning. Injection and the first turn in LHC could be observed on a 1 mm thick alumina screen by the LHC beam observation (BTV) system on 10/9/2008.

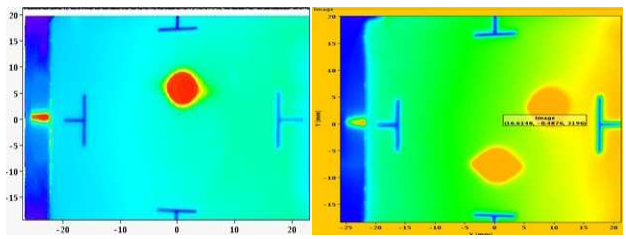

Figure 1: First injection into LHC (left side) and first full turn in LHC (right side) as recorded by the BTV system. Courtesy of Rhodri Jones.

The signal to noise level of the beam loss monitor (BLM) system, consisting of over 4000 N_2 filled ionisation chambers and secondary emission monitors, is 2 orders of magnitude lower than the signal from the pilot bunch ($2x10^9$ protons). This should be sufficient to allow safe and quenchless injection with a total intensity up to $5x10^{11}$. Likewise, the high sensitivity of the beam charge monitors (~ $7x10^8$ protons or 1.3 μA and a dynamic range from $2x10^9$ to $5x10^{14}$) allowed the observation of the first circulating beam in ring 2.

The 1054 BPMs in combination with the powerful on-line optics software provided in the beam threading mode first turn position data to allow for checks of BPM polarity and machine optics errors. The BPM system resolution of ~ 5 μm in orbit mode with a single pilot bunch confirmed the lab sensitivity measurements. Still, electronics drifts induced by air temperature variations could be observed in some locations.

The availability of the tune, chromaticity and coupling measurements at an early stage, being capable of measuring tunes with only a few turns allowed to adjust